Superseded TTR-1420

~~CONFIDENTIAL~~

UNCLASSIFIED

WT-1420

MASTER

This document consists of 144 pages.

No. 130 of 163 copies, Series A

OPERATION

PLUMBBOB

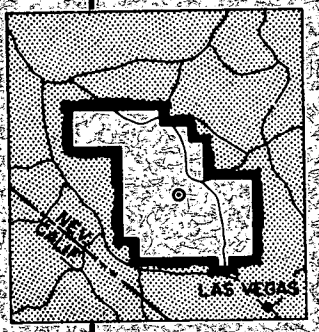

NEVADA TEST SITE

MAY–OCTOBER 1957

Project 3.1

BLAST LOADING AND RESPONSE OF UNDERGROUND CONCRETE-ARCH PROTECTIVE STRUCTURES (U)

Issuance Date: June 5, 1959

HEADQUARTERS FIELD COMMAND
DEFENSE ATOMIC SUPPORT AGENCY
SANDIA BASE, ALBUQUERQUE, NEW MEXICO

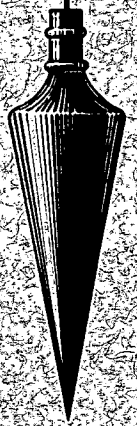

~~CONFIDENTIAL~~

UNCLASSIFIED

DISCLAIMER

Inquiries relative to this report may be made to

Chief, Defense Atomic Support Agency
Washington 25, D. C.

When no longer required, this document may be destroyed in accordance with applicable security regulations.

DO NOT RETURN THIS DOCUMENT

AEC Technical Information Service Extension
Oak Ridge, Tennessee

WT-1420

OPERATION PLUMBBOB — PROJECT 3.1

BLAST LOADING AND RESPONSE OF UNDERGROUND CONCRETE-ARCH PROTECTIVE STRUCTURES (U)

W. J. Flathau, Project Officer
R. A. Breckenridge
C. K. Wiehle

U. S. Army Engineer Waterways Experiment Station
Corps of Engineers
Vicksburg, Mississippi

and

U. S. Naval Civil Engineering Laboratory
Port Hueneme, California

ABSTRACT

The purpose of this project was to evaluate the effects of a kiloton-range nuclear airburst on buried reinforced-concrete arch structures located in the high overpressure region. Since these were to be considered as personnel protective structures, they were evaluated for their resistance to blast, radiation, and missile hazards.

Four structures, with the top of the arch crown 4 feet below ground surface, were positioned at three different overpressure ranges for the Priscilla Shot, a 36.6 kt, 700-foot-high burst. All four arches were semicircular in cross-section, with an inside span of 16 feet and an arch thickness of 8 inches. Three of the structures were 20 feet long and the fourth was 32 feet long. A 20-foot-long structure was placed at each of the predicted ground-surface air overpressure levels of 50-, 100-, and 200-psi, while the 32-foot-long structure was placed at the predicted ground-surface air overpressure level of 50 psi. It was specified that all structures be designed to withstand a 50-psi peak blast overpressure using 3,000-psi concrete. The four structures were instrumented for measurements of air overpressures, earth pressures, deflections, accelerations, strains, radiation, and missiles.

The four structures received actual air overpressures of 56, 124, and 199 psi and suffered only minor damage, all remaining structurally serviceable. The structure at the 199-psi pressure level exhibited obvious cracking of the floor slab and minor tension cracking of the arch intrados; however, even though the damage was slight, the peak floor slab acceleration of 13.4 g may have been physiologically hazardous to personnel.

It was observed that the earth loading around the arch surface was not uniform and that the arch itself underwent appreciable bending. The passive pressure exerted by the soil on the arch surface aided in developing the transmission of the compressive load.

Subsequent analysis, allowing for the actual concrete strength of 4,500 psi, showed that the capacity of the structures at the time of the Priscilla Shot exceeded the specified design capacity of 50-psi ground-surface air overpressure. Consequently, the data obtained are not sufficient for more than tentative conclusions about the ultimate capacity of the structure. A retest at higher overpressures should furnish the additional data needed.

The entranceway of the shelter was designed to exclude air overpressure only, therefore considerable radiation was admitted; however, this entranceway could easily be modified to greatly reduce the amount of radiation transmitted through it to the interior of the structure. Also, the entrance is of the emergency type, for economy, and would be secondary to a rapid access entrance in an actual protective shelter. There were no missile and apparently no dust hazards in any of the structures.

This test showed that an underground reinforced-concrete arch is an excellent structural shape for resisting the effects of a kiloton-range nuclear air burst.

FOREWORD

This report presents the results of one of the 43 projects comprising the Military Effects Program of Operation Plumbbob, which included 28 test detonations at the Nevada Test Site in 1957.

For overall Plumbbob military-effects information, the reader is referred to the "Summary Report of the Director, DOD Test Group (Programs 1–9)," WT–1445, which includes: (1) a description of each detonation, including yield, zero-point location and environment, type of device, ambient atmospheric conditions, etc.; (2) a discussion of project results; (3) a summary of the objectives and results of each project; and (4) a listing of project reports for the Military Effects Program.

PREFACE

This project was a joint, coordinated effort between the U. S. Army Engineer Waterways Experiment Station (WES), Corps of Engineers, Vicksburg, Mississippi, and the U. S. Naval Civil Engineering Laboratory (NCEL), Port Hueneme, California. The project was under the general direction of E. P. Fortson, Jr., F. R. Brown, and G. L. Arbuthnot, Jr.; Captain R. L. Hunt, Corps of Engineers, was in direct supervision of the project, with W. J. Flathau designated as the project officer. Special recognition is given to Captain E. S. Townsley who contributed valuable technical support and assistance during the preparation of the final report. NCEL participation in the project was under the general direction of Dr. W. M. Simpson and S. L. Bugg, with C. K. Wiehle and R. A. Breckenridge designated as co-project representatives. Other engineers making substantial contributions to this project were W. A. Shaw and J. O. Rotnem, NCEL, and Sp 3 J. D. Laarman and Pfc R. A. Sager, WES.

Special credit is due Major James Irvine, Jr., USA, and Captain C. A. Robertson, USA, formerly assigned to the Office, Chief of Engineers, and CAPT A. B. Chilton, USN, assigned to the Bureau of Yards and Docks, for their efforts during the initiation of this project.

Consultation with Dr. N. M. Newmark of the University of Illinois and Dr. C. H. Norris of the Massachusetts Institute of Technology provided valuable information in formulating the project. Their advice and assistance are gratefully acknowledged.

CONTENTS

FIGURES

TABLES

Chapter 1
INTRODUCTION

1.1 OBJECTIVE

The general objective of Project 3.1 was to determine the suitability of underground concrete arches for use as protective shelters as well as their resistance in the high overpressure ranges (50 to 200 psi) from a kiloton-range air burst.

The specific objectives of the project were to: (1) compare the response of four underground concrete-arch structures when subjected to controlled loading ranging from design load through failure load; (2) determine the load distribution on a buried arch due to a nuclear blast; (3) gain a better understanding of the basic response of that portion of the arch element which is in no way affected by restraint or support from the end walls; (4) determine to what extent the end walls of an underground arch affect its response; (5) study the interaction of the soil and the structure in order to establish an idealized soil-structure system that can be adapted to analytical treatment; (6) determine the amount of protection from radiation provided by the structure; and (7) gain information of direct use in establishing design criteria for a prototype cast-in-place concrete personnel shelter.

1.2 BACKGROUND

Previous nuclear-blast-effect tests on underground structures have been limited in number and have indicated principally the ability of the structures to withstand the applied loads, as illustrated by the test of the Federal Civil Defense Administration underground group shelter during Operation Teapot (Reference 1).

Full-scale tests by the Bureau of Yards and Docks, Department of the Navy, on arch structures located aboveground during Operations Greenhouse (Reference 2), Upshot-Knothole (Reference 3), and Teapot (Reference 4) demonstrated the potential advantages of arch-type protective structures, and indicated that added benefits might result if such structures were located below the ground surface and equipped with properly designed end walls and entrances.

Prior to Operation Plumbbob, there was no substantiated design criteria for a blast-resistant, underground, reinforced-concrete arch structure. It was expected that a full-scale test would furnish information on the response of such a structure that would be directly applicable to the design of rigid-arch structures of various spans and lengths.

1.3 THEORY

To test the suitability of the design procedures pertaining to buried arches set forth in EM 1110-345-413 to 421, entitled "The Design of Structures to Resist the Effects of Atomic Weapons," (Reference 5) prepared for the Corps of Engineers by the Massachusetts Institute of Technology (MIT), a contract was negotiated with the firm of Ammann and Whitney, New York, to design a structure to be tested in this project using the methods outlined in that manual.

Another contract was negotiated with the firm of Holmes and Narver, Inc., Los Angeles, California, to analyze the structure designed by Ammann and Whitney using methods other than

those set forth in Reference 5. The analysis was performed to predict pressure ranges from ground zero where (1) failure of the structure would not be expected (actual design level), (2) probable failure would be expected, and (3) total failure (collapse) would be expected.

The MIT design method (Reference 5) is based on the assumption that the overpressure transmitted to an underground arch is uniform over the entire surface of the arch (see Figure 1.1.a). This type of pressure distribution results in pure compression throughout the arch. If it is assumed that the overpressure transmitted to an underground arch is not uniform, (see Figure 1.1.b), then the arch is subjected to combined bending and compression. Under this assumption, a secondary loading is produced by the resistance of the earth to the outward deflection of the arch. The analysis made by Holmes and Narver was based on an assumption of the latter type.

1.3.1 Uniform Overpressure Distribution. The following excerpts from Section 421 (Reference 5) set forth the general principles used in the design of the underground arch structure for this project:

> "Page 11-7: The design of each element of the structure for the static plus dynamic earth overpressure is preceded by a preliminary design of that element for the static load stresses to which it would normally be subjected. The static design should follow accepted design procedures and specifications.
>
> "Page 11-15: Arches, domes, and circular elements are loaded practically uniformly throughout by the earth overpressures and because of their great stiffness under this type loading the design is based upon a dynamic load factor of unity.... It is assumed for design purposes that the load over the entire surface of the arch, dome, or circular section is uniform and equal to the air-blast overpressure on the ground surface above the structure. The earth overpressure load curves on plane surfaces bounding the shell surfaces, such as end walls of an arch or the top of a circular tank, are computed as for a similarly located element of a rectangular structure.
>
> "Page 11-16: Design the main arch, dome, or circular element to support the static loading... Investigate the resistance of these elements to the static plus the dynamic load to which they are subjected. The maximum dynamic load is handled as an additional static load and no dynamic analysis is involved. It is assumed that the dynamic load is uniformly applied and that the element is very rigid under this type of loading so that a dynamic load factor of unity is used."

1.3.2 Non-uniform Overpressure Distribution. For a vertically applied dynamic overpressure, previous tests in Nevada indicated that the horizontal pressure on the vertical surface of a relatively rigid rectangular structure is approximately 0.15 of the vertical pressure (References 6 and 7).

Should the findings of References 6 and 7 be substantiated for an underground semicircular arch, then such an arch would be subjected to bending, and its ultimate load-carrying capacity would be influenced by its flexibility. A load applied to the arch through the overlying earth mass would produce a downward deflection of the crown and an outward deflection of the haunches. This outward deflection would be resisted by the soil mass and a passive pressure would be developed. The exertion of the passive earth pressure would be beneficial, since a more favorable pressure distribution on the arch might result, depending on the flexibility of the structure and the compressibility of the soil. However, one requirement for such structural behavior is that the arch permit the deflection and still remain serviceable.

Some assumption must be made relative to the distribution of the initial horizontal overpressure. For example, it could be assumed to be a horizontal overpressure equal to some fraction of the vertical overpressure, or it could be a trapezoidal loading with the overpressure at the crown being equal to the vertical overpressure, and with the overpressure at the spring line being equal to some fraction of the vertical overpressure. Holmes and Narver made assumptions that are shown in Figure 1.2.

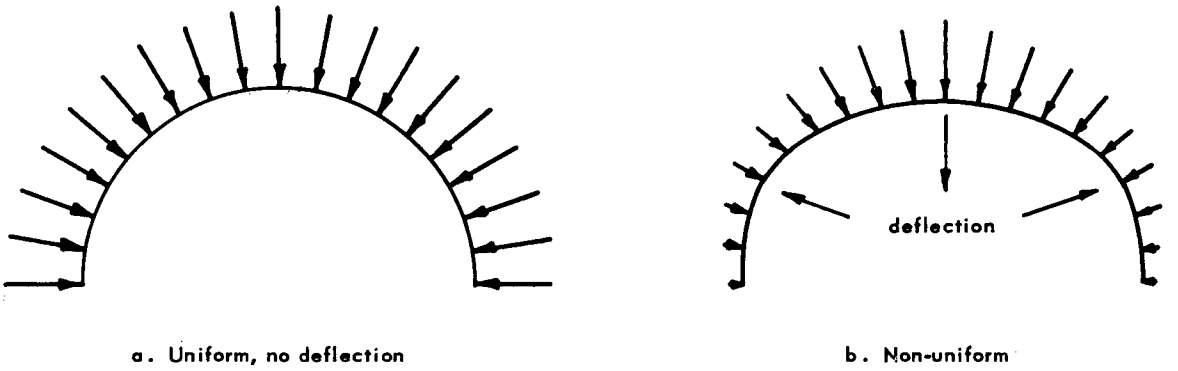

a. Uniform, no deflection

b. Non-uniform

Figure 1.1 Assumed overpressure distributions on underground arches.

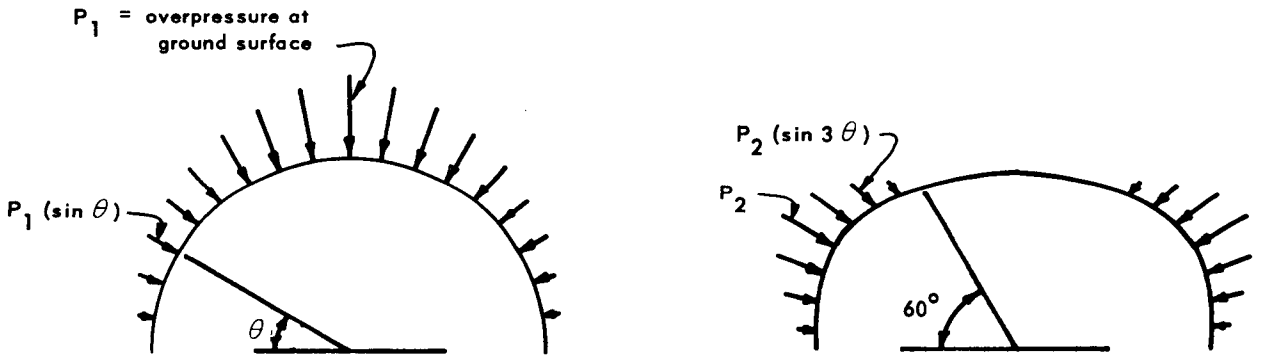

P_1 = Radial overpressure distribution following sinusoidal variation

P_2 = Resulting deflection develops passive earth pressure

Figure 1.2 Loadings assumed by the firm of Holmes and Narver, Inc.

The following excerpts from the Holmes and Narver report (Reference 8) set forth the general principles used in their preshot analysis of this project's underground structure:

> "In the case of semicircular arches, the load due to overpressure is assumed to act radially, following a sinusoidal variation, with a maximum intensity at the crown equal to the overpressure at the ground surface, and with zero intensity at the base. In addition to this 'primary' p_1 loading which might be regarded as being the load pattern which would apply to a very rigid structure, a 'secondary' p_2 load pattern is considered, intended to approximate the load due to passive earth pressure developed in the region of outward deflection of the arch. This is assumed as a radial sinusoidal loading with maximum intensity p_2 at $\theta = 30°$, zero intensity at $\theta = 60°$, and zero intensity at the base of the arch where $\theta = 0°$.
>
> "The stabilizing effect of the p_2 loading is a function of the unknown soil characteristics and the flexibility of the arch."

It was further stated that:

> "Several types of arch failure are possible (see Reference 9). An upper limiting value of the collapsing load would be obtained on the assumption that the loading is a uniform radial pressure. [The assumption made in Section 421 of Reference 5.] Failure would then occur either by elastic instability, or by a compression failure in the material.
>
> "A second type would be failure due to unsymmetrical loading resulting in high bending stresses accompanied by minimum thrust.
>
> "A third type of failure would be a symmetrical loading condition producing a much lower bending stress in conjunction with a high thrust.
>
> "The first type of failure implies complete absence of bending stresses, giving a collapsing pressure that is too high. The second type of failure is not critical because of its extremely transient nature. This leaves the third type as the critical loading condition.
>
> "The load pattern assumed to represent the critical loading condition is the sinusoidal type previously described.
>
> "Under the loading, yield 'hinges' are assumed to occur in sufficient number to reduce the structure to a mechanism at failure. In calculation of the static yield resistance, allowance is made for the effect of axial thrust and the tributary earth mass on the period of vibration..."

These Holmes-Narver assumptions concerning the loading were used in their preshot analysis and have been refined in their postshot analysis. The refinements are presented in Appendix A.

Chapter 2
PROCEDURE

2.1 TEST STRUCTURES

Four reinforced-concrete arch structures were tested during Shot Priscilla, all placed underground with the top of the crown 4 feet below the ground surface. The four arches were semicircular in cross section, with an inside radius of 8 feet and a thickness of 8 inches. Three of the structures were 20 feet long, while the fourth was 32 feet long. The 32-foot-long structure was included to assure an unrestrained section of arch essentially free of end-wall effects, so that it could be determined how far and to what extent end walls affect arch action. This added length provided a favorable length-to-span ratio of two to one.

The 32-foot-long structure (3.1.n) and one of the 20-foot-long structures (3.1.a) were placed in an area for which a ground-surface overpressure of 50 psi was predicted; the other two structures were placed in areas for which overpressures of 100 psi (3.1.b) and 200 psi (3.1.c) were predicted. The general location and shot geometry for the structures are shown in Figure 2.1; Figure 2.2 shows the plan and cross section of a typical structure.

For clarity, the following definitions pertaining to arches are presented as used in this report. Also see Table 2.1.

Springing line: Formed by the intersection of the arch with the floor slab.
Crown: The topmost part of the arch.
Haunch: The sides of an arch between the springing line and the crown.
Intrados: The inside surface of the arch.
Extrados: The outside surface of the arch.
Arch span: Horizontal distance from springing line to springing line.

2.1.1 Design. The structural design was accomplished by the firm of Ammann and Whitney under Contract No. DA-22-079-eng-195. This contract stipulated that: (1) the structure be buried so that the crown would be 4 feet below the natural ground surface; (2) the arch be semicircular; (3) the structure be designed to resist the effects of a 50-psi ground-surface air overpressure resulting from the detonation of a 30-kt device 500 feet aboveground; (4) the compressive strength of the concrete be 3,000 psi; and (5) the principles set forth in EM 1110-345-414 to 421 (Reference 5) be followed. The results of the design accomplished by Ammann and Whitney are contained in Reference 10.

The procedure in the manual dictated a very thin arch to resist the transient load, but in order to provide a structure suitable to resist both static and transient loads, a thicker arch was selected. The final structure was intended to be a standard-type structure that could be used by the armed services if it proved satisfactory in a full-scale test.

Although Section 421 of Reference 5, which concerns below-ground structures, specifies a dynamic load factor of one, Ammann and Whitney elected to use a dynamic load factor of two, basing their decision on the discussion in Section 420 of Reference 5, which concerns aboveground arches.

Ammann and Whitney computed the overpressure load per linear foot of arch length by multiplying: design overpressure times dynamic load factor times arch span.

$$\text{Total load} = 50 \times 2 \times 144 \times 16.67 = 240{,}000 \text{ lb/ft}$$

The load at each reaction would then be:

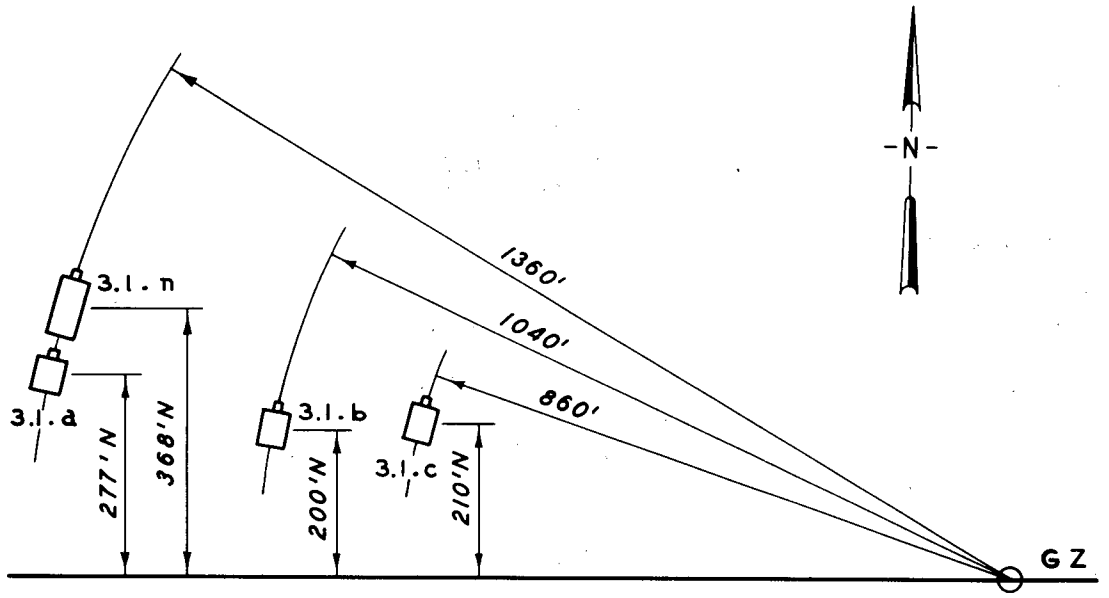

PLAN

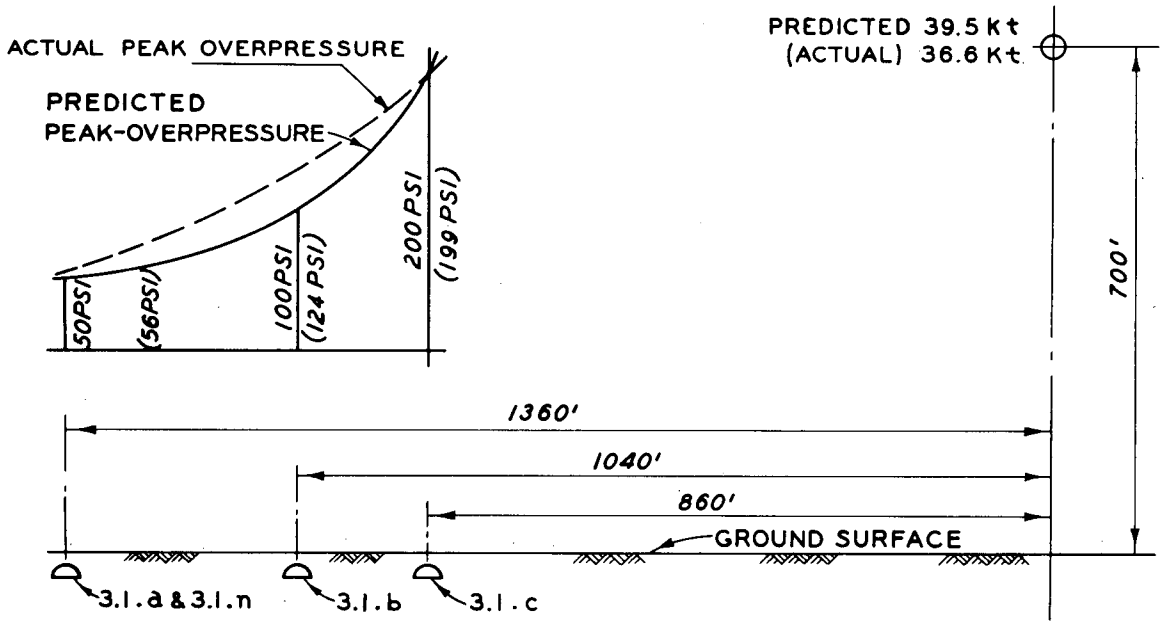

ELEVATION

Figure 2.1 Project plot plan.

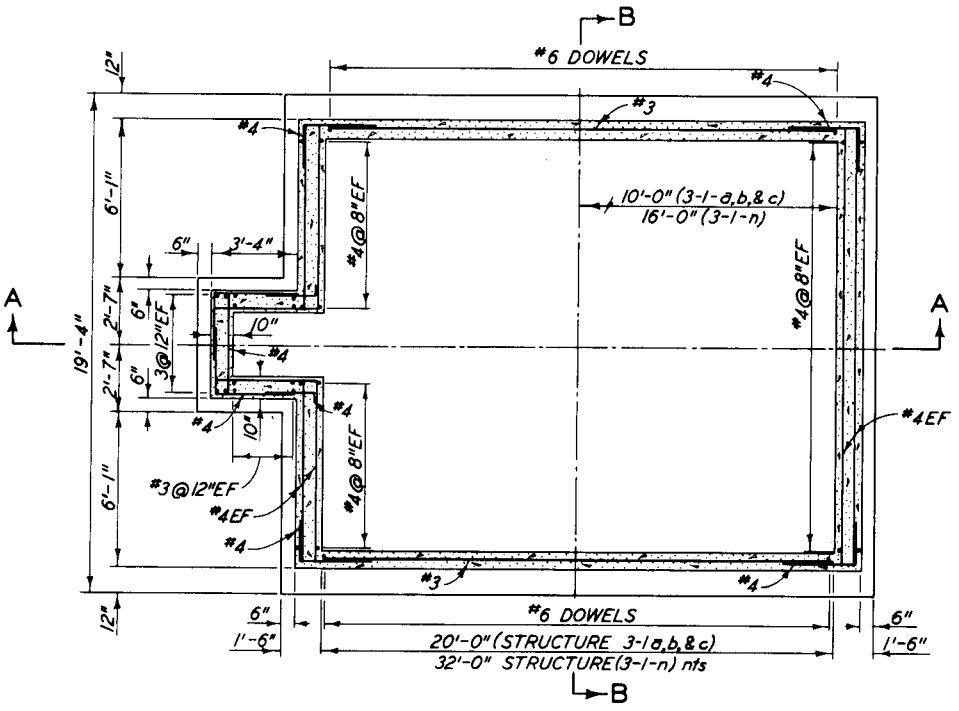

FLOOR PLAN

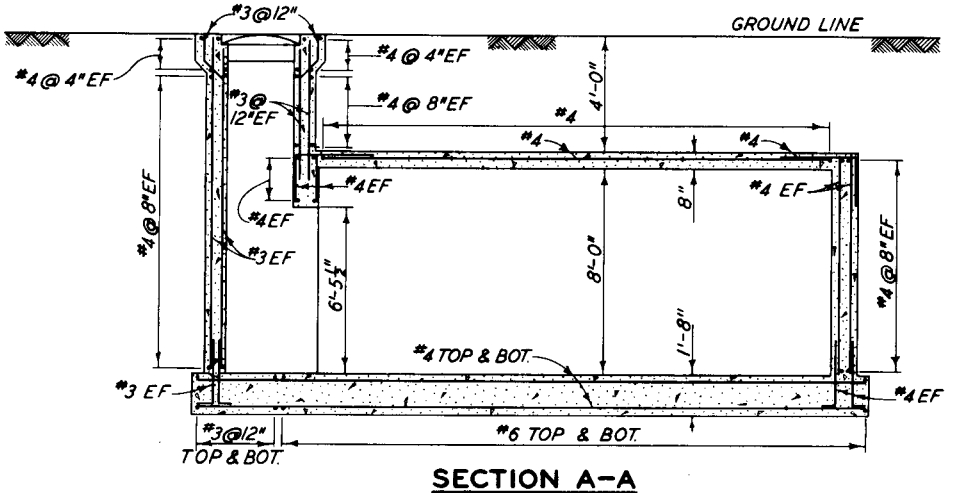

SECTION A-A

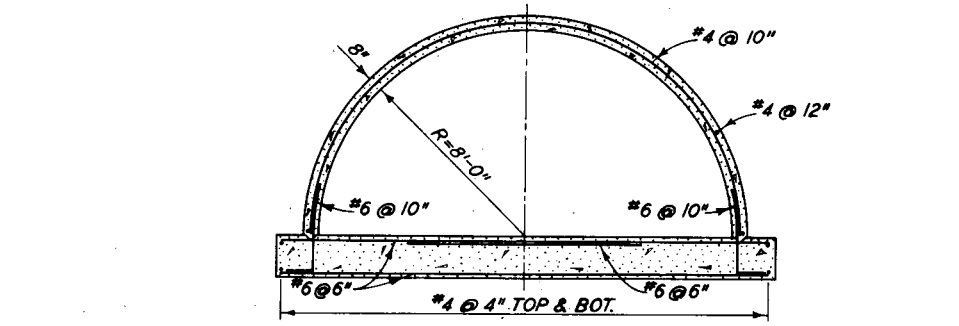

SECTION B-B

Figure 2.2 Plan and elevation of typical structure.

$$\text{Reaction} = \frac{240{,}000}{2 \times 12} = 10{,}000 \text{ lb/in}$$

Inasmuch as Reference 5 assumes a uniform loading, there would be no bending, and thus the thickness needed to resist the blast would be determined by dividing the reaction by the ultimate dynamic compressive strength of the concrete:

$$\text{Required thickness} = \frac{10{,}000}{3{,}000 \times 1.3 \times 0.85} = 3 \text{ inches, where}$$

the ultimate static compressive strength is 0.85 × 3,000 psi, and the 30-percent strength increase is assumed for dynamic (blast) loads. However, to meet the American Concrete Insti-

TABLE 2.1 EXPECTED DEFLECTIONS

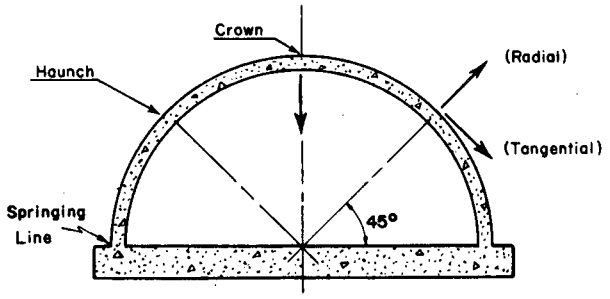

Structure	Crown Deflections		Haunch Deflections	
	Radial (inward)	Tangential	Radial (outward)	Tangential (downward)
	inches	inches	inches	inches
3.1.a	0.5 to 0.9	0	0.3 to 0.6	0.2 to 0.4
3.1.b	0.9 to 17.0	0	0.6 to 10.0*	0.4 to 7.0*
3.1.c†	17.0	0	10.0	7.0

* Passive earth pressures will probably reduce the upper values noted above.
† Collapse is anticipated. Maximum deflections cannot be established.

tute (ACI) code requirements for the specified 3,000-psi concrete, an arch thickness on the order of 8 inches (depending upon specific design) was found to be the practical minimum for static loads alone. This minimum value was established by means of a cracked-section analysis.

The final design included No. 4 reinforcing bars ($\frac{1}{2}$-inch diameter), spaced at 10-inch centers transversely and at 12-inch centers longitudinally, placed at the center of the concrete-arch section.

2.1.2 Damage Prediction. Before Operation Plumbbob, very little was known regarding the response of buried arches to blast forces from nuclear weapons. However, it was necessary to predict the response and establish the locations of the structures in this experiment. These predictions were also to be used to establish the range of the instruments involved and to set the channel sensitivity of each electronically recorded measurement. To this end, the firm of Holmes and Narver performed a preshot analysis of the arch structure as designed by Ammann and Whitney, using methods other than those prescribed in Reference 5. The Holmes and Narver report (Reference 8) predicted that: (1) failure of the structure was not to be expected at the 50-psi ground-surface air-overpressure level; (2) probable failure of the structure would occur at the 100-psi level; and (3) failure (collapse) of the structure would occur at the 200-psi

level. The estimated displacement along the center portion of the arches of the structures at the three pressure levels is shown in Table 2.1.

The general principles used in the Holmes-Narver preshot analysis were given in Section 1.3.2. An important conclusion reached by Holmes and Narver was that:

> "In the case of the arch-type structures, it is evident that soil characteristics have an important effect on ultimate strength and that proper compaction of the backfill around the sides of the arch is essential for maximum strength."

To obtain a better understanding of the behavior of a buried arch in the plastic range and to determine the ultimate mode of failure of the arch, three one-eighth-scale models of the arch used in this project were tested at the U. S. Naval Civil Engineering Laboratory (NCEL). Geometric similitude was maintained between the model and the prototype; however, because of the small scale, no attempt was made to maintain similitude of the unit weight of the concrete. Graded sand was used in the concrete mix for the model, and the design strengths of the concrete were the same as had been specified for the prototype. Small steel wires were used to simulate the reinforcing steel. Soil cover was provided by sand which had been passed through a No. 10 sieve.

For convenience, the width of the arch segment was limited to 4 $\frac{1}{2}$ inches. A reinforced plywood box housed the model and the sand cover. Static loads were applied to the sand cover by a hydraulic jack and steel beam, as shown in Figure 2.3. In order to reduce the frictional resistance of the sand on the plywood during loading, two layers of plastic-impregnated paper (well greased) were placed on all inner surfaces of the plywood box.

Three arch segments were tested, one with floor slab and two without floor slab. Soil-pressure gages placed at the springing line indicated that the loss of vertical pressure through the soil mass varied from approximately 55 percent at 20-psi applied load, to 45 percent at 50-psi load, and 30 percent at 130-psi load. This loss was presumably a transfer of pressure to the sides of the box through friction and was not considered of much importance in qualitative tests of this type.

Figure 2.4 shows the arch segment with the floor slab, after sustaining an applied static load of 175 psi. The crown of the arch and the floor slab cracked at 50-psi applied load. The initial compression failure of the concrete arch occurred at one springing line at about 110 psi, and at the opposite springing line at 130 psi. Failure of one side occurred at 140 psi and failure of the other side at 170-psi applied load; extreme cracking and spalling of the concrete accompanied these failures. It should be emphasized that these loads were applied to the surface of the sand, and that the actual loads on the arch segment were probably less than the above-mentioned values.

The arch deflection at maximum load was approximately $\frac{3}{4}$ inch; permanent set after removal of the load was $\frac{1}{2}$ inch.

Based on a static analysis of the structure (assuming a nonuniform pressure distribution) and on results of the model tests, the NCEL prediction of structural behavior of the arch section up to the design load (50 psi) was as follows:

At a dynamic overpressure of approximately 10 to 15 psi, the moment-carrying capacity of the arch will be exceeded at the springing line. Since the reinforcing steel will be stressed beyond the yield point, there will, in effect, be plastic hinges formed at the springing line. During the next phase the structure will act as a two-hinged arch, and because of the stiffness of the arch the deflection will be small. At approximately 25- to 35-psi overpressure, assuming a symmetrical loading, additional plastic hinges will form at the crown and at the haunches, resulting in a 5-hinged arch mechanism. Failure of the structure is prevented by the buttressing effect of the soil against the outward deflection of the haunches. At the 50-psi design overpressure level the arch will show evidence of permanent deflection due to the plastic deformation at the critical sections. On the intrados of the arch, tension cracks will be apparent at the crown, and compression failure will be apparent at a point on the arch about 25 degrees up from the springing line. Although the arch will be serviceable after receiving a blast load of 50 psi, plastic hinges will have formed at the five critical sections. It is evident that considerable plas-

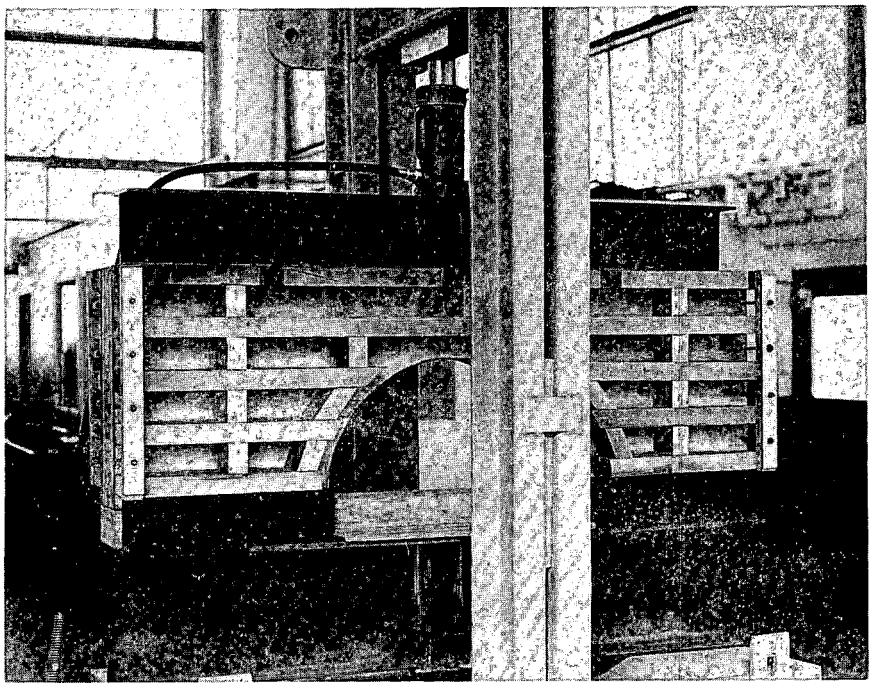

Figure 2.3 Loading of model arch.

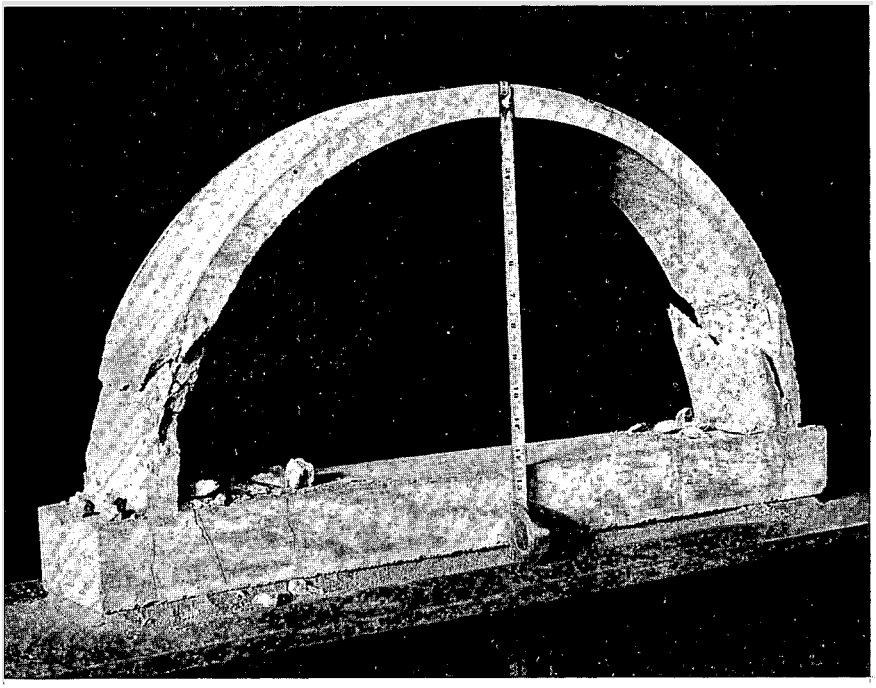

Figure 2.4 Model arch after test.

tic deformation will occur before a uniform pressure distribution can be realized. With an asymmetrical loading of any great magnitude on the arch, considerable structural damage could occur during this test because of the small steel ratio of one-half of one percent.

2.2 CONSTRUCTION AND MATERIALS

The four structures were constructed by the general contracting firm of Lembke, Clough, and King of Las Vegas, Nevada. Holmes and Narver acted as the architect-engineer for the Atomic Energy Commission and provided construction-inspection services for all projects. The entire construction time for this project was about three months. The excavation for the four structures was completed early in March 1957, the structures were completed by 12 April 1957, and the backfill operation was completed by 4 June 1957. (See Appendix G for specifications and associated design drawings used in conjunction with the construction program.)

2.2.1 Soil Properties. Prior to the field operation, laboratory tests were performed as a part of Project 3.8, Soils Survey, on both undisturbed and remolded samples of soil obtained from the general vicinity of the site where the structures were to be located. The soil in the area had a uniform appearance and texture, and can be generally classified as clayey-silt. The results of compaction tests, Atterberg limits tests, and mechanical analyses on the natural soil at various depths are shown in Figure 2.5.

In an attempt to duplicate the compressibility characteristics of the natural soil, a series of tests were performed on samples of remolded soil of various water contents, using three different compaction efforts. Test specimens were prepared from the mold samples, and a confined compression test was performed in a consolidometer apparatus. A tangent modulus of deformation was established from the test data; based on analysis of the data, the backfill material was recommended to be placed at 100 percent standard AASHO density, with a water content 3 percent less than optimum. The resulting recommended and as-placed values of dry density and water content for the backfilled soil necessary to duplicate the modulus of compressibility are given in Table 2.2 along with values for the undisturbed natural soil located adjacent to the backfill areas.

Shortly after the backfilling operation was completed, undisturbed soil samples were obtained from both the backfill and the adjacent natural soil at depths of 4 and 10 feet at the four stations. Samples were obtained in the backfill after the shot also, but no strength tests were made since the results from the preshot and postshot density and water-content tests showed no significant change and thus no change in the postshot strength characteristics of the material (see Table 2.2). The compressibility of the compacted backfill was about equal to that of the natural undisturbed soil when compared by means of similar tests, i. e., consolidation tests, constant ratio of applied stress triaxial tests, and soniscope tests, as shown in Table 2.3. The compressive modulus for the compacted backfill as determined by the soniscope test is lower than that for the natural soil, which may be due to test conditions. The natural soil samples were encased in 3-inch-diameter steel tubes when subjected to soniscope tests whereas the undisturbed record samples were encased in 6-inch-diameter cardboard tubes. The difference in tubes may have had a marked effect on the transmission characteristics of the samples. (For a detailed description of the various soil properties and associated tests, see the report of Plumbbob Project 3.8, Reference 11.)

2.2.2 Construction-Material Properties. Type II portland cement was used in the construction of the concrete arches. The aggregate was pit run, screened, and stockpiled at the Frenchman Flat area; the maximum size of coarse aggregate was approximately 2 inches. A mechanical analysis of the sand indicated that the grain sizes ranged from a No. 4 to a No. 200 U. S. standard sieve size. A summary of the proportions used in the concrete mix design for the four structures is shown in Table 2.4.

Thirty standard concrete cylinders (compressive strength specimens) and ten concrete beams (flexural strength specimens) were obtained from each structure for laboratory tests which es-

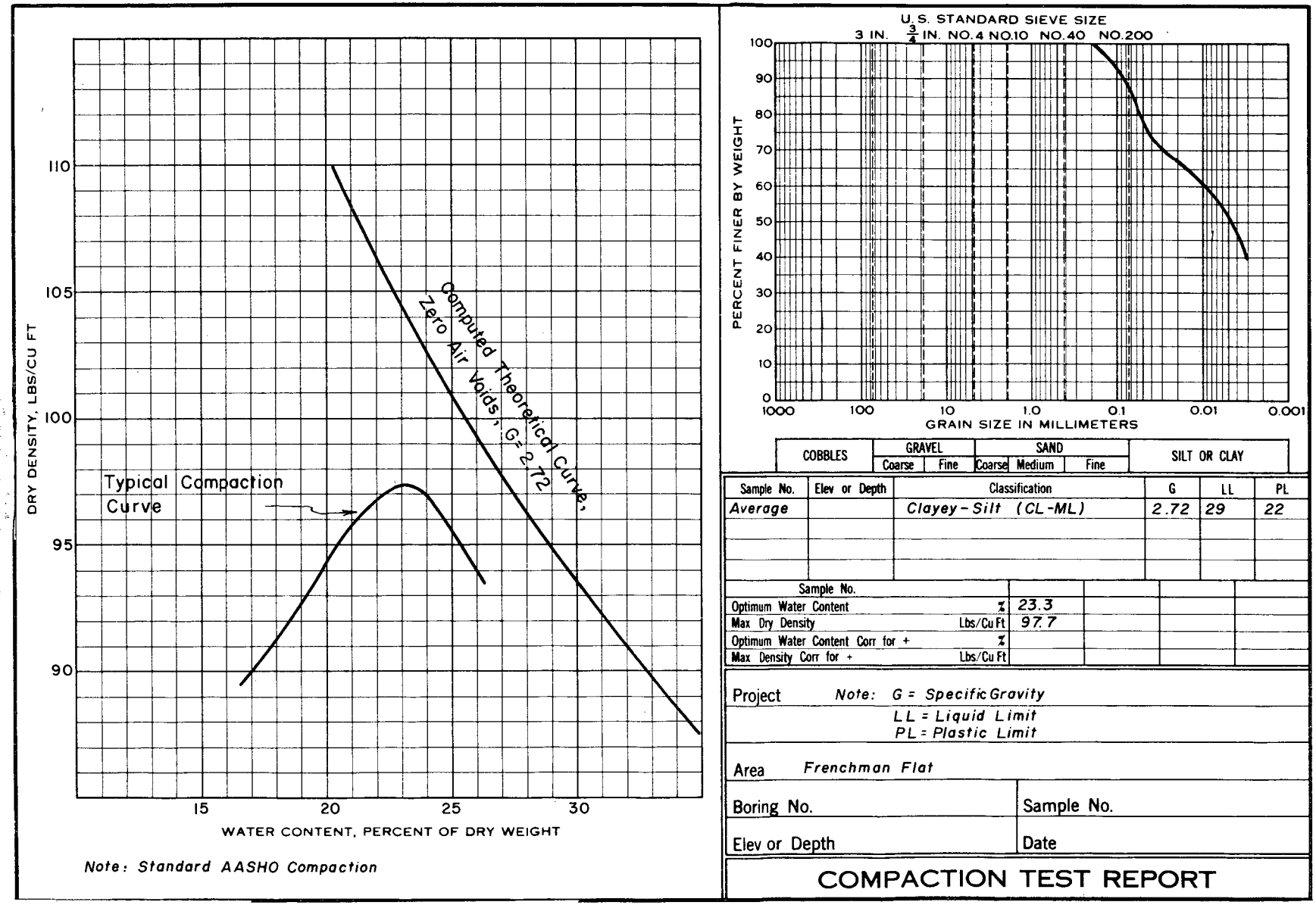

Figure 2.5 Typical backfill material of the 3.1 structures.

TABLE 2.2 DENSITY AND WATER CONTENT OF SOIL

	Water Content, pct			Dry Density, pcf		
	Ranged			Ranged		
	From	To	Average	From	To	Average
Undisturbed Natural Soil	9.4	15.1	12.8	73.5	86.3	79.0
Recommended for Backfill	20.0	23.0	21.5	94.7	99.4	97.1
Control Tests during Backfill*	17.5	24.0	20.7	88.0	107.0	96.7
Preshot, 4 ft below Surface of Backfill	16.3	22.1	19.2	90.4	104.2	99.9
Postshot, 4 ft below Surface of Backfill	16.8	20.8	18.5	90.2	106.1	99.2

* Average of 40 samples per structure.

TABLE 2.3 COMPARISON OF COMPRESSIBILITY CHARACTERISTIC OF NATURAL SOIL WITH COMPACTED BACKFILL

	Natural Soil (psi)			Compacted Backfill (psi)		
	Ranged			Ranged		
	From	To	Average	From	To	Average
Modulus of deformation (consolidated tests at applied stress = 50 psi)	2,410	6,080	4,130	3,200	6,950	5,300
Modulus of compression (triaxial tests)	1,500	12,000	6,450	3,850	14,000	7,600
Compressive modulus (soniscope tests)	223,580	734,050	506,000	130,440	146,340	135,800

TABLE 2.4 CONCRETE DESIGN MIX PER CUBIC YARD

Standard mix prescribed for all structures

Material	Weight	Absolute Volume
	lb	ft^3
Gravel	2,000	12.03
Sand, 1,188 lb (dry)	1,188	7.70
Free Water in Sand, 4.35 pct or 52 lb	52	0.84
Water Added, 28.5 gal	237	3.80
Cement, 5.5 sacks	517	2.63
Totals:	3,994	27.00

tablished 7-day, 28-day, and shot-time strengths. The tops of the cylinder specimens were covered immediately after they were prepared. All the exposed surfaces of the specimens and structures were sprayed with Hunt's curing compound. The various specimens were placed on the ground surface near the appropriate structure.

Shortly after the forms were stripped from the various structures, half of the specimens to be tested at shot time were removed from the molds and allowed to cure in the open. When the structures were backfilled, the specimens that had been removed from the molds were covered with the same backfill material in an attempt to simulate the curing condition experienced by the various structures. The remaining specimens (7-day, 28-day, and the remaining shot-time specimens) were removed from the molds in the testing laboratory. All of the shot-time specimens were sent to the testing laboratory one month prior to the Priscilla event.

The laboratory tests, conducted by the Nevada Testing Laboratory, Ltd., Las Vegas, Nevada, consisted of determining the compressive strengths, flexural strengths, and static moduli of elasticity of the concrete specimens at various times after the structures were poured. In addition to these tests, values of the dynamic modulus of elasticity at shot time were determined for several of the specimens by personnel of the Concrete Division of the Waterways Experiment Station (WES). Tests to determine the static modulus of elasticity were performed on the cylinder specimens, while the dynamic tests (nondestructive) were performed on the beam specimens in order to take advantage of the additional length—thus increasing the reliability of the results. Dynamic modulus of elasticity was calculated by using procedures outlined by the American Society for Testing Materials (ASTM Designation C215-55T). Several specimens were tested at the end of seven days to determine if the concrete had attained sufficient strength to allow the removal of forms. The other specimens were tested at 28 days and at the time of the Priscilla event. The results of all tests indicating the compressive strength values with respect to age for each structure are shown in Figure 2.6. Four curves of average stress versus strain for the concrete specimens obtained from the various arch sections and tested at shot time are shown in Figure 2.7. The results of the concrete strength tests at the time of the Priscilla event are shown in Table 2.5.

In addition to the above specimens, NCEL personnel prepared three compressive and three flexural strength specimens from both the base slab and the arch of Structure 3.1.n. These specimens were removed from the molds when the forms were stripped from Structure 3.1.n, stored on the floor slab for curing purposes, and tested at shot time. The results of these NCEL tests are included with the strength results shown in Figures 2.6 and 2.7.

Intermediate-grade billet steel was used exclusively as the reinforcing material in the various structures. Ten sample reinforcing bars of 18-inch length were taken for each of the three sizes used (Nos. 3, 4, and 6). All bars from each group were tested for ultimate strength, percentage of elongation, and stress versus strain into the plastic range. The tests on the reinforcing-bar specimens were performed at NCEL; results of these tests are shown in Table 2.6.

2.2.3 Construction Methods. A backhoe was used to excavate the four areas. The soil properties were such that the contractor could utilize vertical excavations, thereby necessitating a minimum of excavation effort. The sides of the excavation were approximately 2 feet from the sides of the base slabs of the various structures, and the floor of the excavation was level to within $\pm \frac{1}{4}$ inch.

Concrete materials were combined in a portable, central batching plant adjacent to Water Well 5b (Frenchman Flat), $2\frac{1}{2}$ miles from the construction area. Bulk cement was used and was stored in a portable hopper that weighed the amount of cement required per batch of concrete. A portable batching plant (Travel Batcher) was used to hold and weigh the cement, sand, and gravel. The cement, aggregate, and water were poured into the mixing trucks (5-cubic-yard capacity) simultaneously.

The base slabs for all of the structures were poured first. The steel in the base slab was placed according to plan, except that the top reinforcing bars were inadvertently placed one inch lower than was specified. (See Figure 2.8 for typical placement of reinforcing steel in a

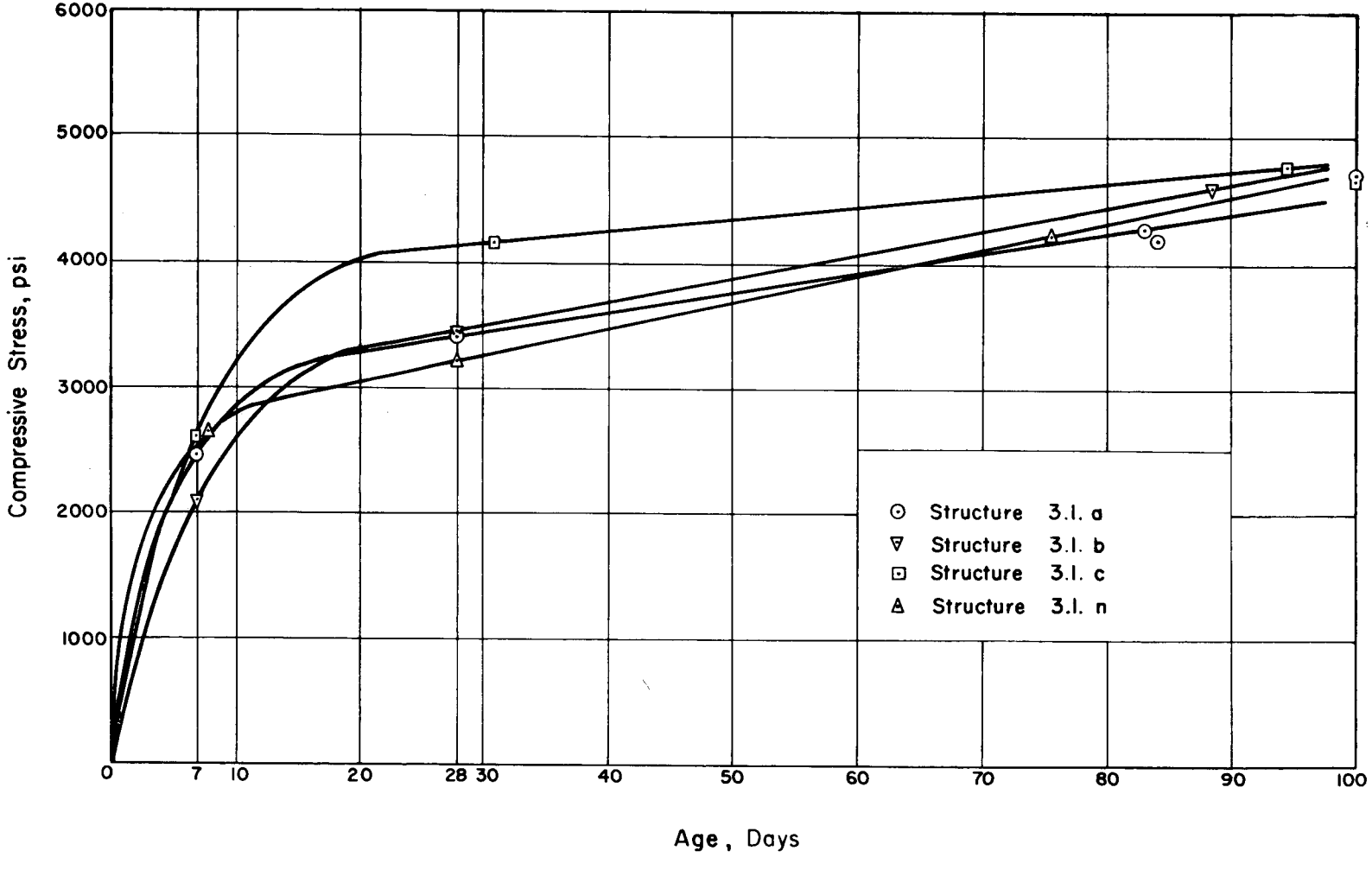

Figure 2.6 Compressive strength of concrete versus age.

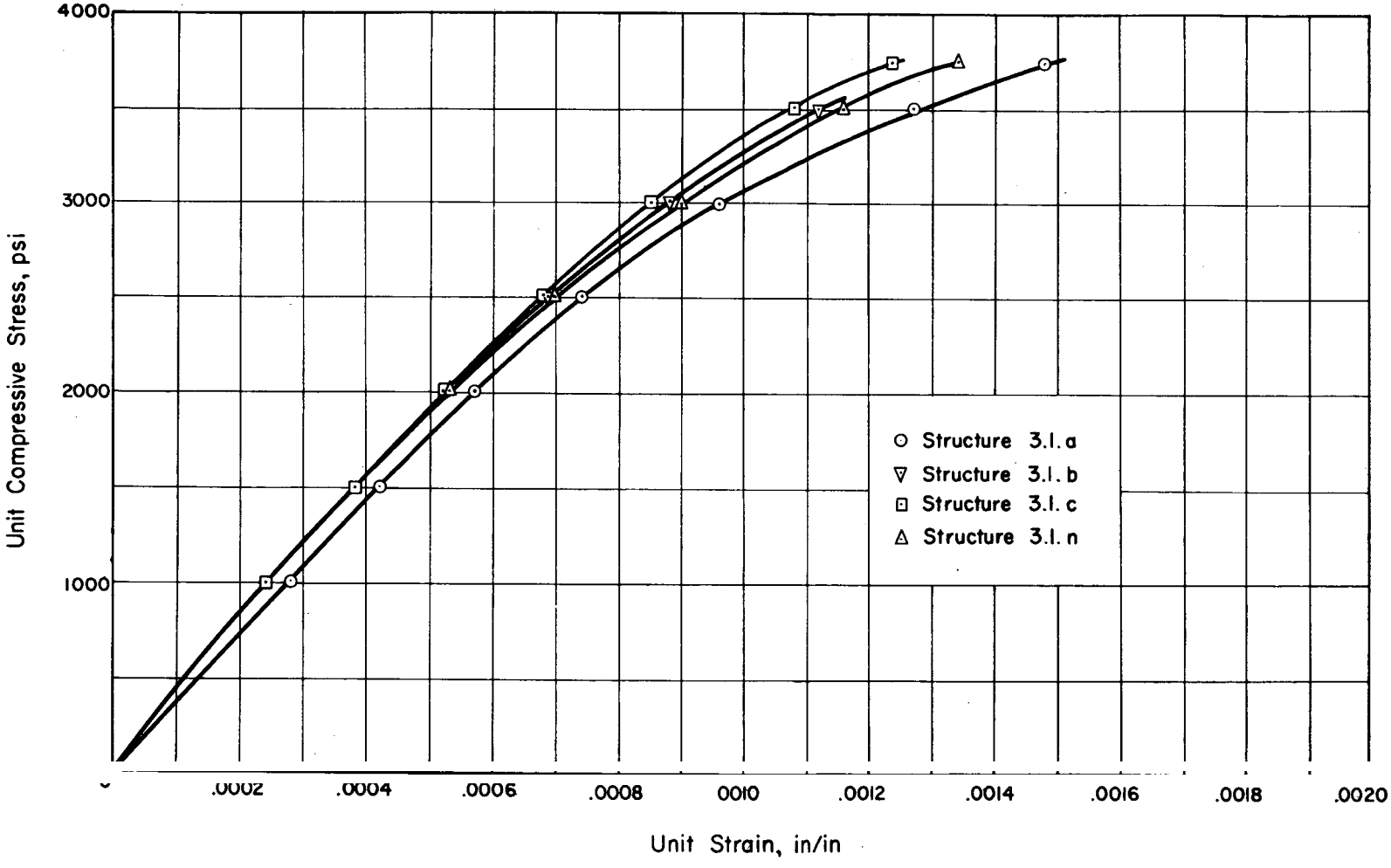

Figure 2.7 Stress-strain curve for concrete at shot time.

base slab.) Concrete was placed by a hydraulic crane with a drop-bottom bucket (½-cubic-yard capacity) and was compacted by electrical vibrators. After the concrete had attained its initial set, the exposed surfaces were sprayed with Hunt's curing compound.

The upper portion of the structures (the arch, end walls, and the entrance shaft) was poured monolithically and placed in the manner described previously. The intrados of the various structures were formed by placing Universal-type forms (1 by 4 feet) on semicircular wood supports fixed on 4-foot centers along the floor slabs. The extrados forms, seven rows on 1-foot

TABLE 2.5 CONCRETE STRENGTH CHARACTERISTICS

Specimens tested at the time of the Priscilla event

Structure	Compressive Strength, Ultimate	Modulus of Rupture	Modulus of Elasticity E				Modulus of Rigidity, G	Poisson's Ratio, r	
			Static*	Dynamic					
	psi	psi	10^6 psi	10^6 psi			10^6 psi	Dimensionless	
				A†	B†	C†	D†	E†	F†
3.1.a	4,270 (83 days)	539	3.44	4.65	4.40	5.30	1.93	0.21	0.14
3.1.b	4,610 (88 days)	524	3.74	4.65	4.49	5.22	1.94	0.20	0.16
3.1.c	4,780 (94 days)	548	3.82	4.42	4.54	5.24	1.94	0.20	0.17
3.1.n	4,210 (76 days)	490	3.44	5.01	4.73	5.47	2.01	0.23	0.16
Average	4,470	525	3.61	4.68	4.54	5.31	1.95	0.21	0.16

* Values obtained from 6- by 12-inch cylinders; all other values obtained from 6- by 6- by 24-inch beams.

†A. Obtained from flexural resonant frequency by vibrating transversely in the horizontal plane.
B. Same as above by vibrating transversely in a vertical plane.
C. Obtained from longitudinal resonant frequency.
D. Obtained from torsional resonant frequency.
E. Poisson's ratio, $r = E/(2G) - 1$, using E value from Column A.
F. Same as above, using E value from Column B.

centers, were placed on the bottom half of the arch, leaving the remaining surface adjacent to the crown to be screeded. The exposed concrete was sprayed with Hunt's curing compound after the concrete had attained its initial set. (See Figure 2.9 for details of form and steel placement in the arch section of the structures; a completed structure is shown in Figure 2.10.)

Prior to the placement of the backfill, controlled amounts of water were thoroughly mixed with the backfill material in order to establish the desired water content. The material was

TABLE 2.6 REINFORCING STEEL PROPERTIES

Bar Size Number	Yield Point	Ultimate Strength	Elongation in 8 inches	Modulus of Elasticity
	psi	psi	percent	10^6 psi
3	52,200	73,400	21.3	29
4	47,500	73,200	21.3	31
6	47,100	75,600	22.3	30

then spread in 4-inch lifts and compacted with mechanical and pneumatic tampers. The soil immediately around the earth pressure cells located on the various structures was carefully hand tamped to attain the same degree of compaction as the surrounding backfill material. Personnel from Project 3.8 took samples during the backfill operation to ensure that proper compaction was obtained. (See Section 2.2.1 for soil properties.)

Shortly after the backfill operation was completed, the top layer of soil developed a polygonal cracking pattern, the cracks penetrating the top lift of the compacted backfill. To prevent fur-

ther cracks in the soil and the subsequent loss of moisture, the backfill areas were sprayed with water and covered with a loose layer of dry soil over which tarpaulins were placed.

2.3 MEASUREMENTS

Determination of the load applied to a structure is a requisite in proper design. However, up to the present time, no reliable experimental information has been available concerning the load distribution on an underground arch structure subjected to a nuclear blast. Obtaining a true picture of the pressure-time distribution for an underground arch under these conditions is complicated by various factors, such as the flexibility of the arch and the compressibility of

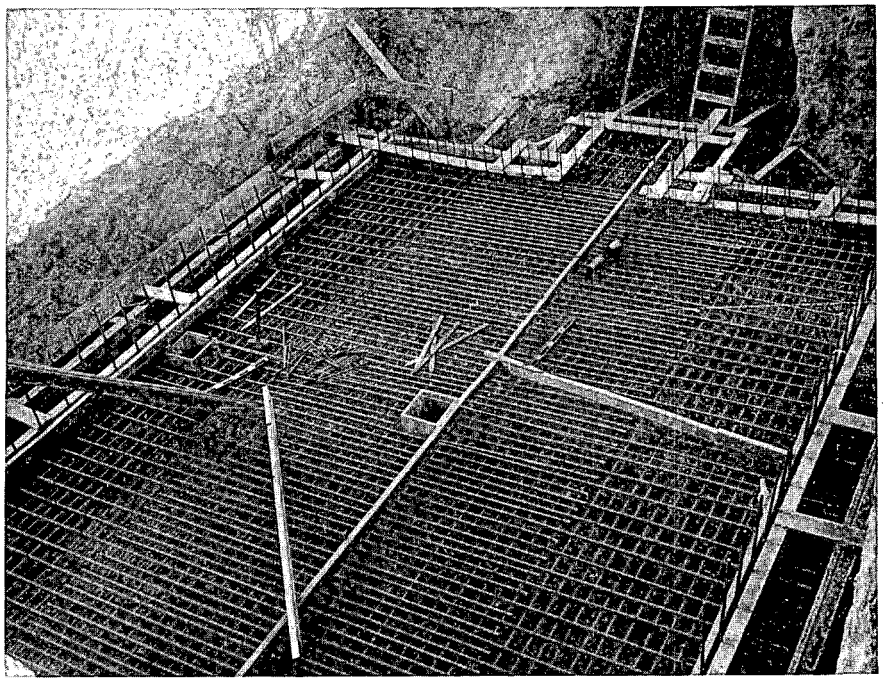

Figure 2.8 Floor slab prior to pouring concrete, Structure 3.1.c.

the soil. Previous reports (References 6 and 7) indicate that for Nevada Test Site soil the average lateral pressure on a vertical wall of an underground rectangular structure subjected to a nuclear blast is approximately 15 percent as great in magnitude as the pressure applied at the top surface of the soil for depths of earth cover of up to 8 feet. This information is not directly applicable to arch structures, however, since the arch deflection affects the soil pressure. Therefore, attempts were made in this investigation to determine the load distribution on the arch.

In addition to a knowledge of the loading conditions, proper design of a structure depends on an understanding of its structural behavior under the applied loads. Since information on the response of an underground arch structure subjected to blast loading is meager, response measurements were also obtained for these structures.

2.3.1 Instrumentation. Instrumentation of the four structures of this project included both electronic (remote-recording) and mechanical (self-recording) systems. Electronic measurements were made of transient air overpressures, deflections, accelerations, earth pressures, and strains; mechanical measurements were made of air overpressures and deflections. The Ballistic Research Laboratories (Project 3.7) accomplished the instrumentation for Structures 3.1.a, b, and c; for a detailed description of this work refer to Appendix B. The NCEL accom-

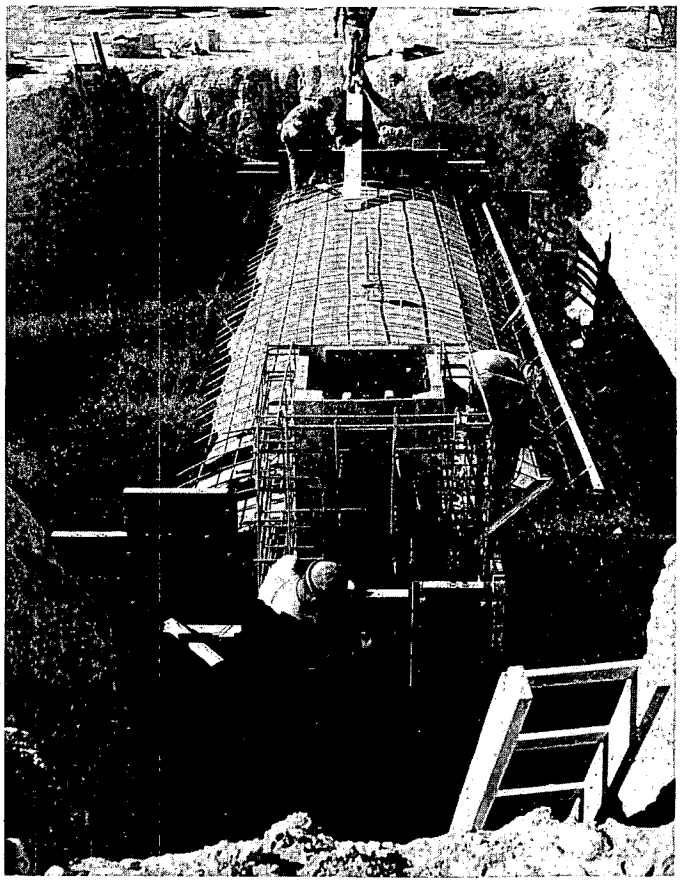

Figure 2.9 Reinforcing steel and forms in place for arch, Structure 3.1.n.

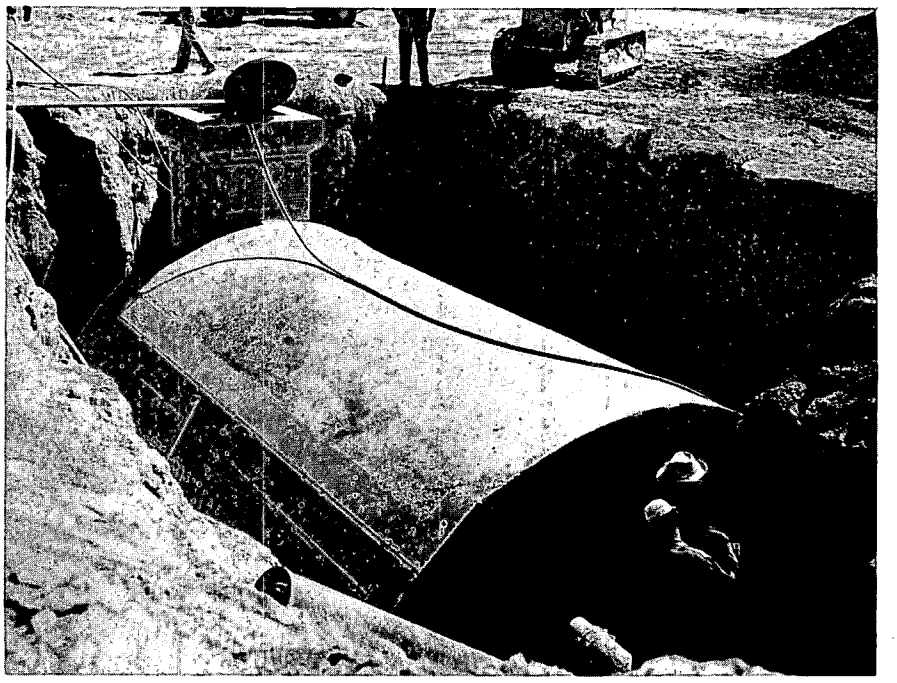

Figure 2.10 Completed structure prior to backfilling, Structure 3.1.a.

plished the instrumentation for Structure 3.1.n; for a detailed description of this work refer to Appendix C. The general instrumentation layout, including gage identification for the four structures, is shown in Figures 2.11 and 2.12.

In order to determine the degree of radiation protection afforded, all four structures were instrumented with gamma film badges and neutron chemical dosimeters by the Chemical Warfare Laboratory (Project 2.4). A description of this work is presented in Appendix D.

A possibility existed that the severe ground shock would spall the inside surfaces of the structure, thereby creating missile (chips or fragments of concrete) hazards. To determine the quantity and size of these missiles, Styrofoam missile traps were installed in all of the structures by the Lovelace Foundation (Project 33.2). In addition, dust collectors were placed in the four structures to determine if the ground shock would cause dust on and within the concrete walls to spill into the structure. A description of this work can be found in Appendix E.

The instrumentation utilized is listed in Table 2.7. Figures 2.13 through 2.16 show the overall layout of the recording instruments in the four structures, as well as a view of the interior of the structures.

To determine the effect of irradiation on different types of photographic paper and film used in electronic recording, four types of recording paper and one type of film were exposed to various intensities of radiation. Results are presented in Appendix F.

2.3.2 Damage Survey. The damage survey consisted of level and transit surveys, photographs, and a visual inspection.

A level and transit survey was performed after the structures were completed, and prior to the backfilling. Identical surveys were also performed both prior to and after the shot in order to determine the relative permanent deflections and movements caused by the ground-surface air overpressure.

Photographs and visual inspections of the structures were made before and after the shot to record visible damage and also to aid in the interpretation of instrumentation results.

2.3.3 Methods of Data Analysis. The methods of reducing the records obtained from the various gages are presented in Appendices B and C. Presented below are two methods in which the final records shown in Appendices B and C were used to determine: (1) transient deflection by means of double-integration of acceleration records; and (2) transient moment and thrust from strain records.

Method Using Acceleration Records. Since transient deflection records for the base slab were not available, the acceleration records for Structures 3.1.a, b, and c were double-integrated by the β method, originated by Professor N. M. Newmark, to yield the transient deflections. This method is a numerical integration process in which various values of β can be selected to represent variations of accelerations in the time interval, h. It is particularly adaptable to computer solution.

Equation of motion: The equations of velocity and displacement take the following form:

$$X_{n+1} = X_n + V_n h + (\tfrac{1}{2} - \beta)\,\alpha_n h^2 + \beta \alpha_{n+1} h^2$$

and

$$V_{n+1} = V_n + \frac{h}{2}(\alpha_n + \alpha_{n+1})$$

Where: X = deflection
V = velocity
α = acceleration
h = time interval
β = variable

When β is assigned a value of $\frac{1}{6}$, the variation of acceleration is linear in the time interval h,

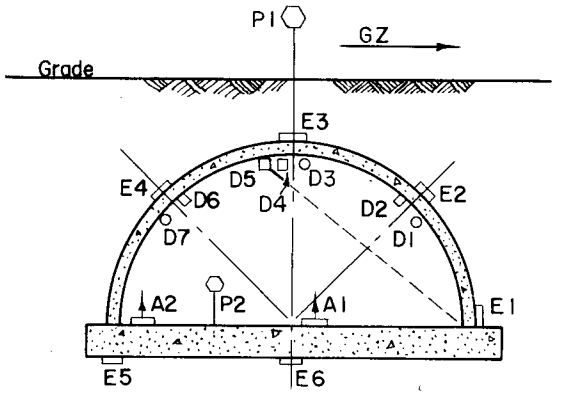

SECTION C-C

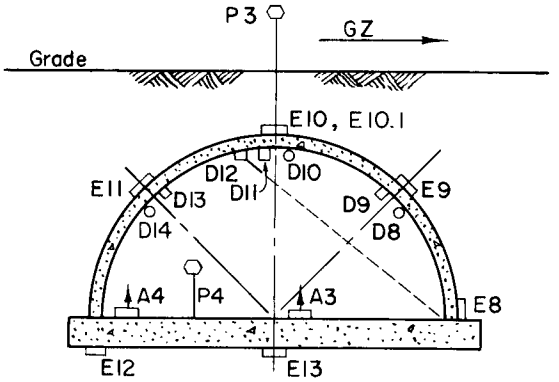

SECTION B-B

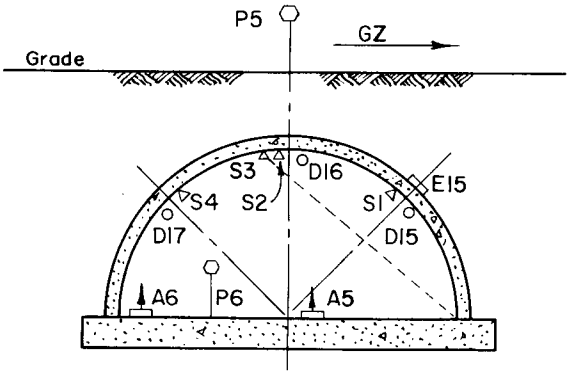

SECTION A-A

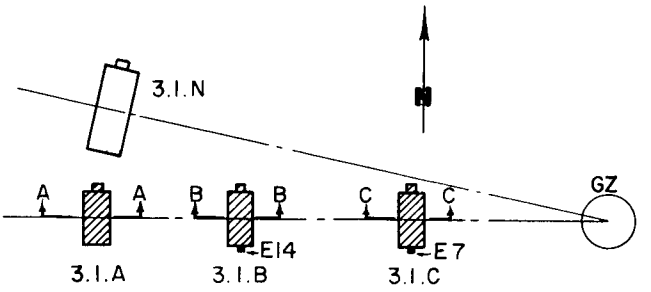

KEY PLAN

LEGEND

ELECTRONIC RECORDING

(E) Earth Pressure/Time

(D) Deflection/Time (Radial)

(A) Acceleration (Vertical)

SELF RECORDING

(P) Air Pressure

(D) Deflection

Radial

Angular

(S) Scratch Gage

Figure 2.11 Instrumentation layout, Structures 3.1.a, b, and c.

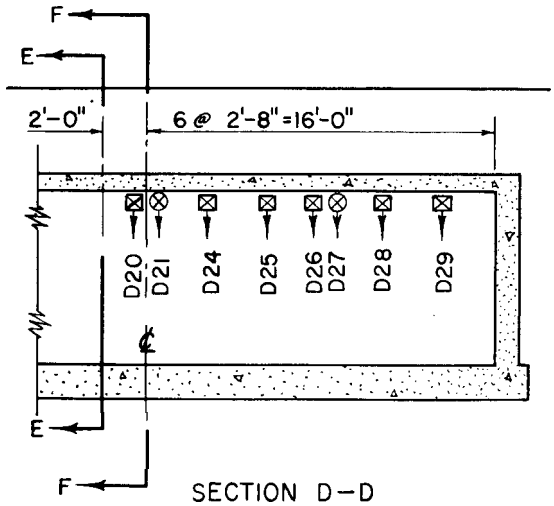

SECTION D-D

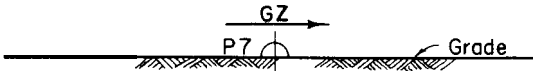

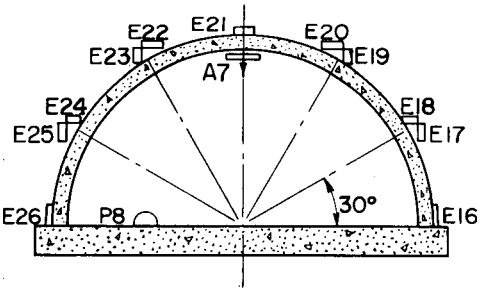

SECTION E-E

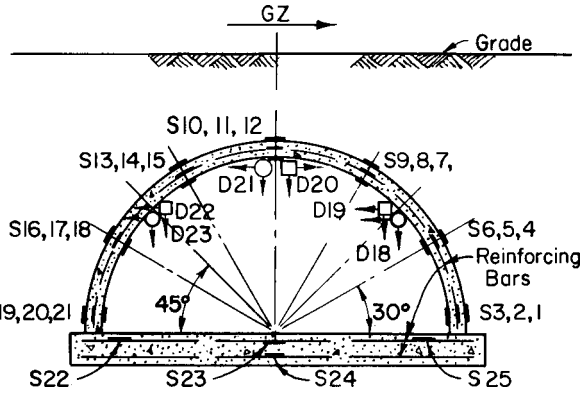

SECTION F-F

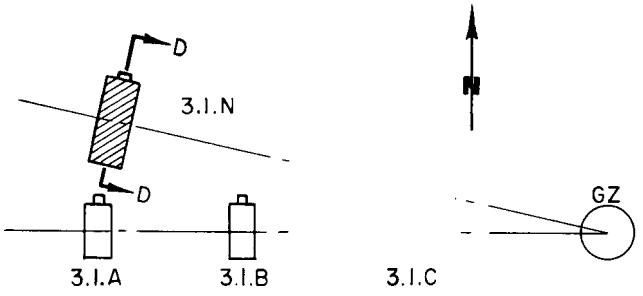

KEY PLAN

LEGEND

ELECTRONIC RECORDING

(E) Earth Pressure/Time

(P) Air Pressure/Time

(D) Deflection/Time

Horizontal

Vertical

(A) Acceleration (Vertical)

(S) Strain

SELF RECORDING

(D) Deflection

Horizontal

Vertical

Figure 2.12 Instrumentation layout, Structure 3.1.n.

TABLE 2.7 INSTRUMENTATION SUMMARY

Type	Quantity	Type	Quantity
Electronic-recording Gages:		Radiation Measuring Devices:	
Earth pressure/time	26	Gamma film badges	20
Displacement/time	17	Neutron chemical dosimeters	20
Acceleration/time	7	Neutron threshold devices	2
Air pressure/time	2	Total	42
Strain/time	16		
Total	68	Missile Measuring Devices	4
		Electrical Strain Gages (static readings only)	9
Self-recording Gages:		Mechanical Strain Gage Stations	39
Scratch type (peak deflection only)	4		
Deflection/time	24		
Air pressure/time	6		
Total	34		

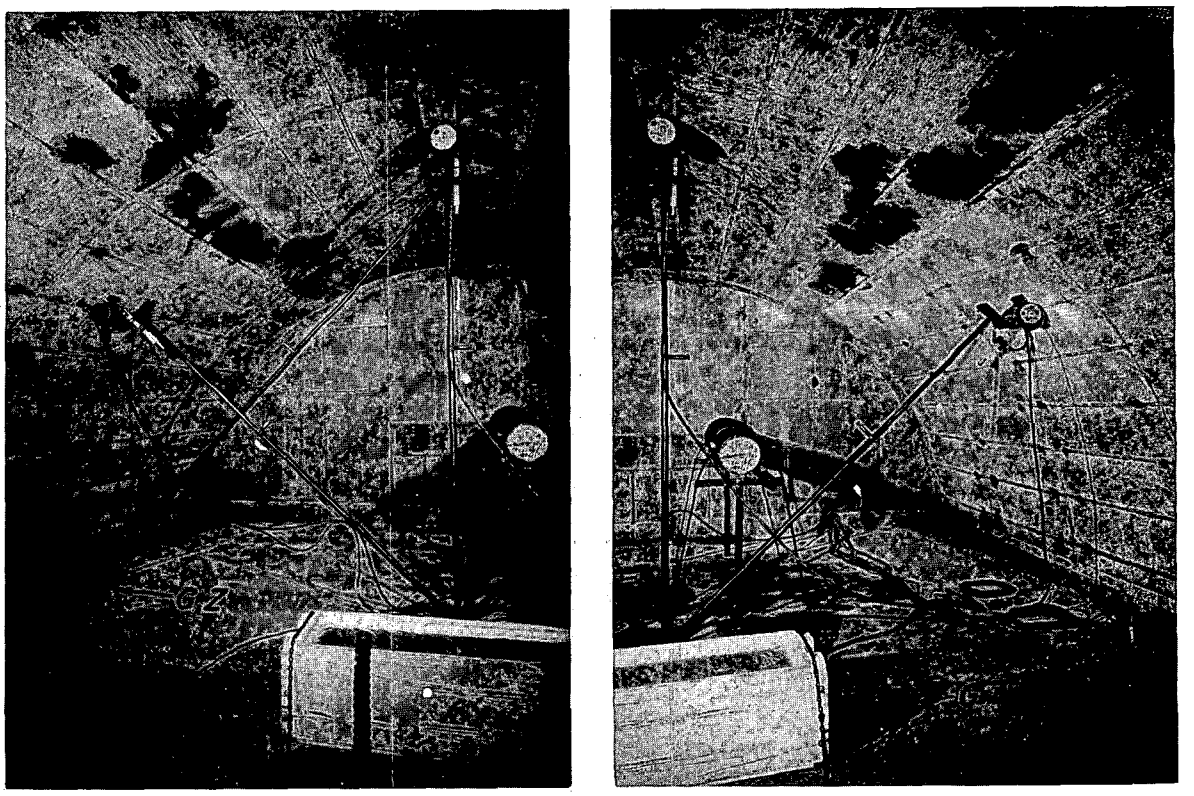

Figure 2.13 Interior views, Structure 3.1.a.

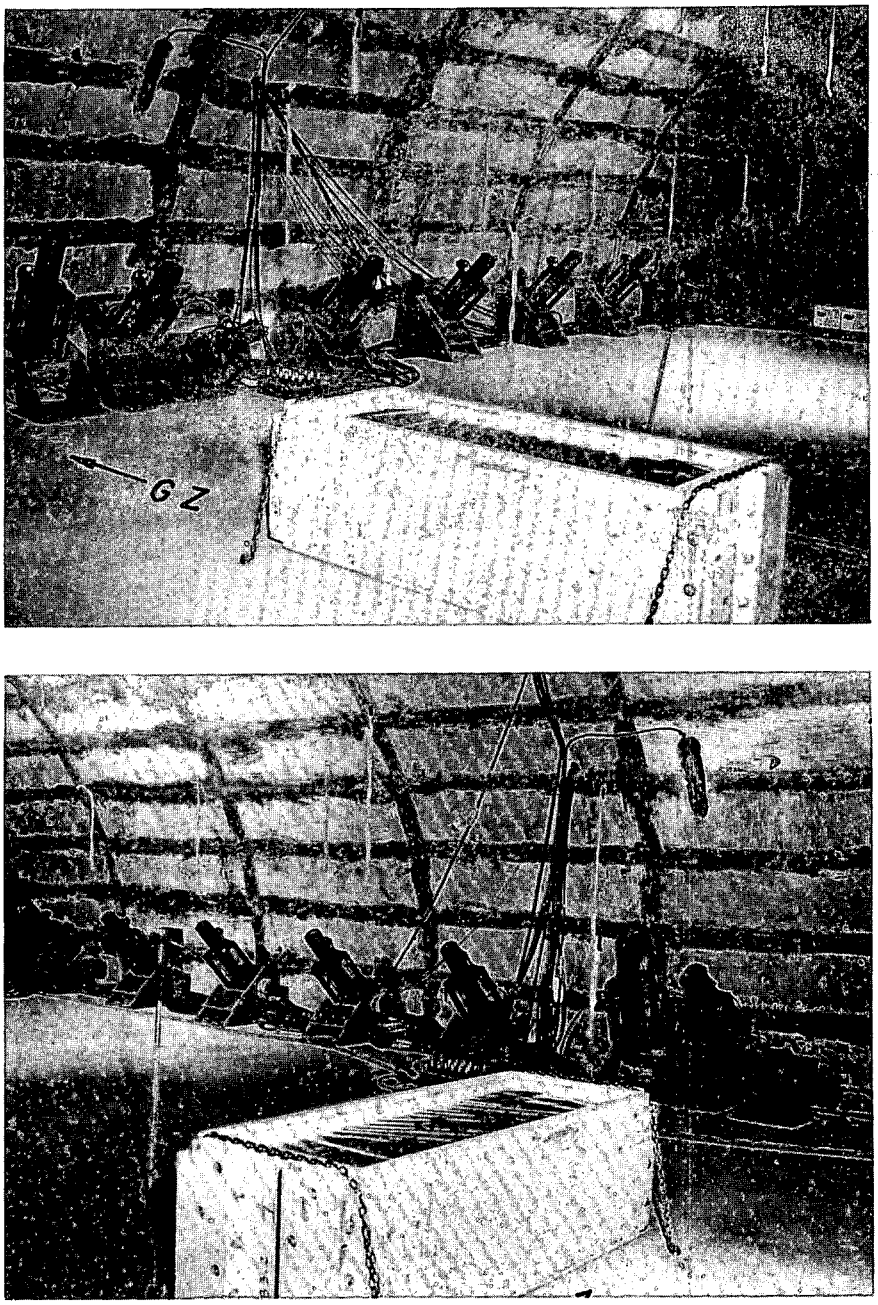

Figure 2.14 Interior views, Structure 3.1.n.

and the deflection equation becomes

$$X_{n+1} = X_n + V_n h + \tfrac{1}{3}\alpha_n h^2 + \tfrac{1}{6}\alpha_{n+1} h^2$$

Since records from accelerometers are subject to baseline shifts, the records shown in Appendix B were corrected using a method suggested by D. C. Sachs of Stanford Research Institute. This method assumes that no acceleration for underground structures occurs after t_d (t_d is time at which the positive air pressure phase ends) and therefore that the velocity remains constant thereafter. Since the accelerometer was found stationary, this constant velocity must have been

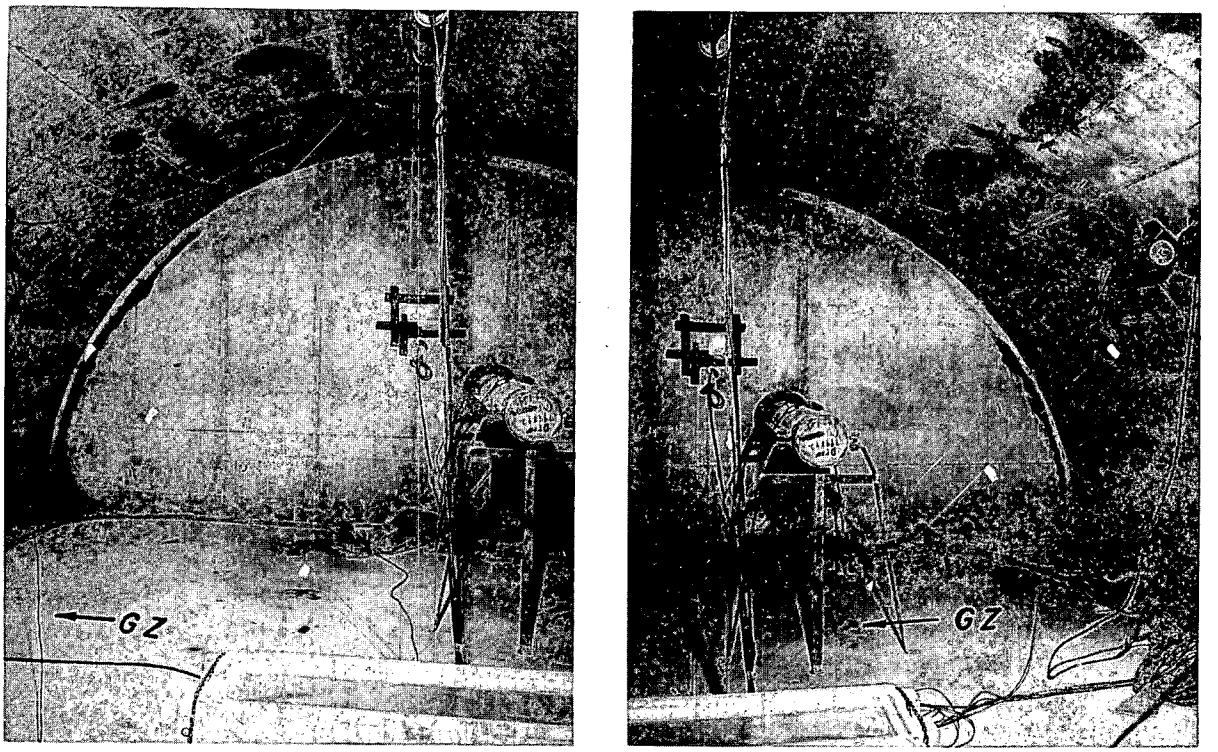

Figure 2.15 Interior views, Structure 3.1.b.

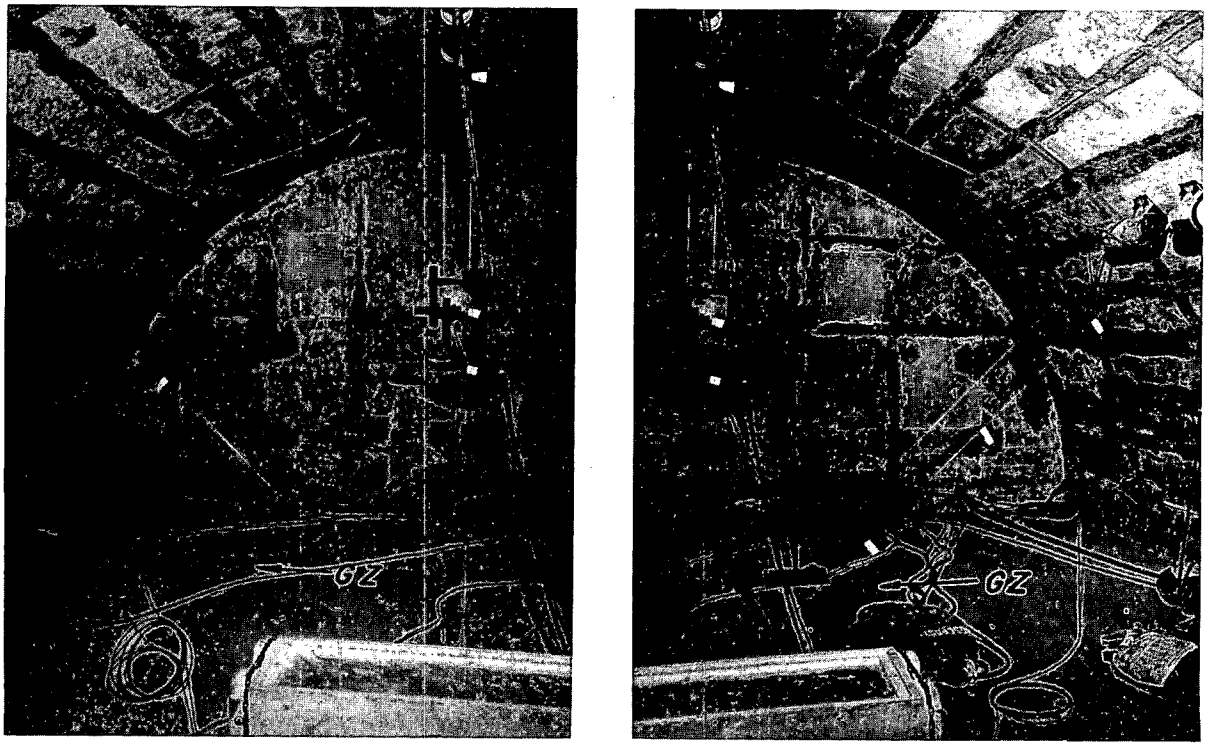

Figure 2.16 Interior views, Structure 3.1.c.

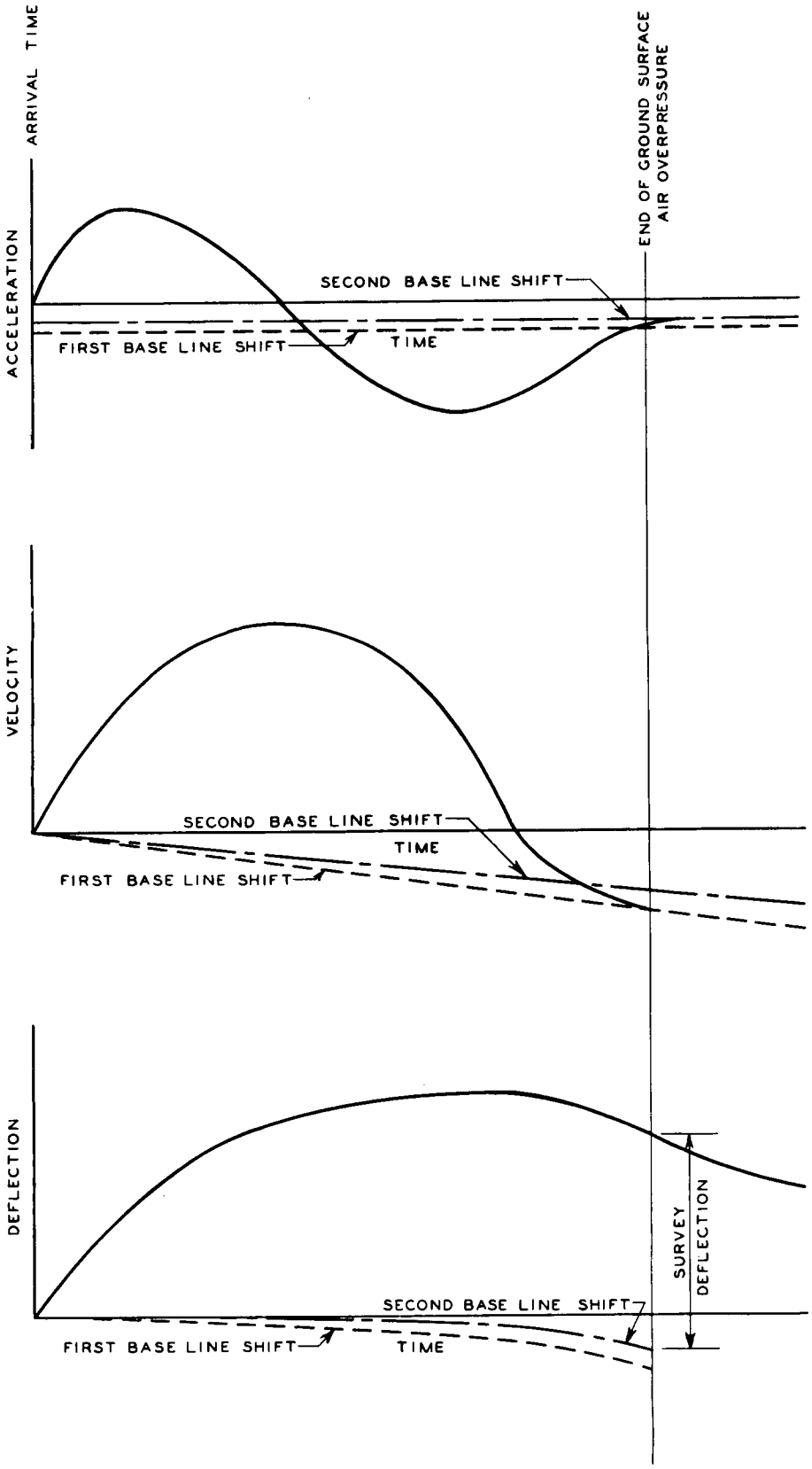

Figure 2.17 Sample plot for double integration of acceleration record.

zero. If the first integration of the acceleration record did not give a zero velocity at t_d, the axis of the acceleration record was shifted to obtain the desired zero velocity (see Figure 2.17).

This revised acceleration record was then double-integrated to obtain displacement. Since from the above discussion both the acceleration and velocity are zero after t_d, it follows that the displacement at t_d must be the permanent displacement. Accordingly, a second shift of the acceleration record axis was made so that the computed displacements at t_d were equal to the surveyed permanent displacement (see Figure 2.17).

This twice-revised acceleration record was then considered valid, and was used as the source of displacement time data.

Method Using Strain Records. The major purpose of instrumenting Structure 3.1.n with strain gages was to determine the moment and thrust at various points throughout the arch, and how this moment and thrust varied with time. In particular, it was desired to ascertain these reactions at the springing line.

With this purpose in mind, strain gages were placed on the outside surface, inside surface, and the steel reinforcing (neutral axis of uncracked section) at seven different points around the arch. There were, however, insufficient channels to record all of these gages during the blast. It was therefore decided to record the strains at both springing lines, at the crown, and at the 30- and 60-degree points of the ground-zero side. In addition, the measurements at the three latter points could be recorded only for two of the three gages. Since concrete cracks at tensile strains of about 100 to 200 microinches per inch, gages on the tension side would not give worthwhile data at strains greater than this. Therefore, the gage on the steel and the gage thought most likely to be on the compression side were the two gages used for recording purposes.

In order to simplify the reduction of strain to moment and thrust, it was assumed that: (1) the variation of strain across a given section was linear; (2) as long as the structure remained elastic, a constant value could be used for the modulus of elasticity; (3) the concrete was cracked at tensile strains greater than approximately 100 microinches per inch; and (4) the effect of the steel in the arch could be neglected.

With the above assumptions, the strains at any given section could be separated into the strain due to moment and the strain due to thrust. The strain due to moment would be equal to one half the algebraic difference of the strains in the extreme uncracked fibers. The strain due to thrust would be equal to one half the algebraic sum of the strains in the extreme uncracked fibers.

The thrust would then be determined by multiplying the strain due to thrust by the modulus of elasticity and area of the concrete. The moment would be determined by multiplying the strain due to moment by the modulus of elasticity and the section modulus of the concrete.

One strain gage was placed on the top reinforcing steel of the floor slab near each springing line. To determine the horizontal reaction at the springing line, it was necessary to make the assumption that the moment in the floor slab at this point was equal to the moment in the arch at the springing line. A moment that placed the intrados in compression at this point would also produce a compressive strain in the subject gage. An outward movement of the arch would produce a tensile strain in the gage. Therefore, to determine the strain due to the horizontal thrust, the bending strain had to be algebraically subtracted from the recorded strain. The strain due to horizontal thrust was then used in the manner described previously to calculate the horizontal thrust in the base slab. This was assumed to be equal to the horizontal reaction of the arch at the springing line.

Chapter 3
RESULTS

All four of the structures withstood the effects of the Priscilla Shot and remained in usable condition. Even though none of the 3.1 structures failed, valuable information was obtained from the test. The buried concrete arches proved very effective in resisting the blast effects from a nuclear weapon.

This chapter presents only the peak values of transient and permanent measurements. The variations of earth pressure, deflection, acceleration, etc., with time are presented in Appendices B and C.

3.1 AIR OVERPRESSURE

The actual air overpressures received at the three ranges were 56, 124, and 199 psi compared to the predicted values of 50, 100, and 200 psi. The project plot plan (Figure 2.1) shows that Structures 3.1.a and 3.1.n received the lowest loading of 56 psi, Structure 3.1.b next with 124 psi, and Structure 3.1.c received 199 psi, the highest loading. The closeness of the predicted values to the recorded values indicated that load-input conditions in this test were satisfactory.

The ground-surface air-overpressure values measured by the self-recording pressure gages appear reliable, since these values compare favorably with the blast-line data. The blast line was located approximately 250 feet from the above gages.

Measurements showed no increase in air pressure within any of the four structures during the test.

3.2 EARTH PRESSURE

The peak transient earth pressures on Structure 3.1.b (see Figure 3.1) show that in several instances the earth pressure exceeded the ground-surface air overpressure. Even though the values of pressure were recorded to the nearest one psi, some of the values could not be accurately determined because either the range of the calibration or the range of the amplifying equipment was exceeded. This was especially true for gages E10 and E10.1, at the crown of Structure 3.1.b. These gages were placed next to each other in order to determine what effect the method of mounting had on earth-pressure measurements (see Appendix B). Only the peak earth-pressure values for the precursor phase could be compared since the peak values for the main shock phase were beyond the calibrated range of the gages.

A comparison of pressure values from gages E9 and E11 shows that the loading was asymmetrical. The peak pressure for gage E9, located on the ground-zero side, was 60 percent higher than for gage E11, located on the lee side of the arch.

It should be pointed out that the earth pressures being discussed are transient pressures resulting from ground-surface air overpressure and that the static earth pressures (dead load) existing at the time of the shot are not included. Negative values would indicate reductions in the existing static earth pressures.

The geometry of the earth-pressure gage mounting at the 30- and 60-degree positions on Structure 3.1.n (see Figure C.1) adversely affected the measurements. The projection of the mounts into the soil apparently caused an increase of pressure on the gages measuring vertical pressures and, possibly because of arching, a decrease on the gages measuring horizontal pressure. The

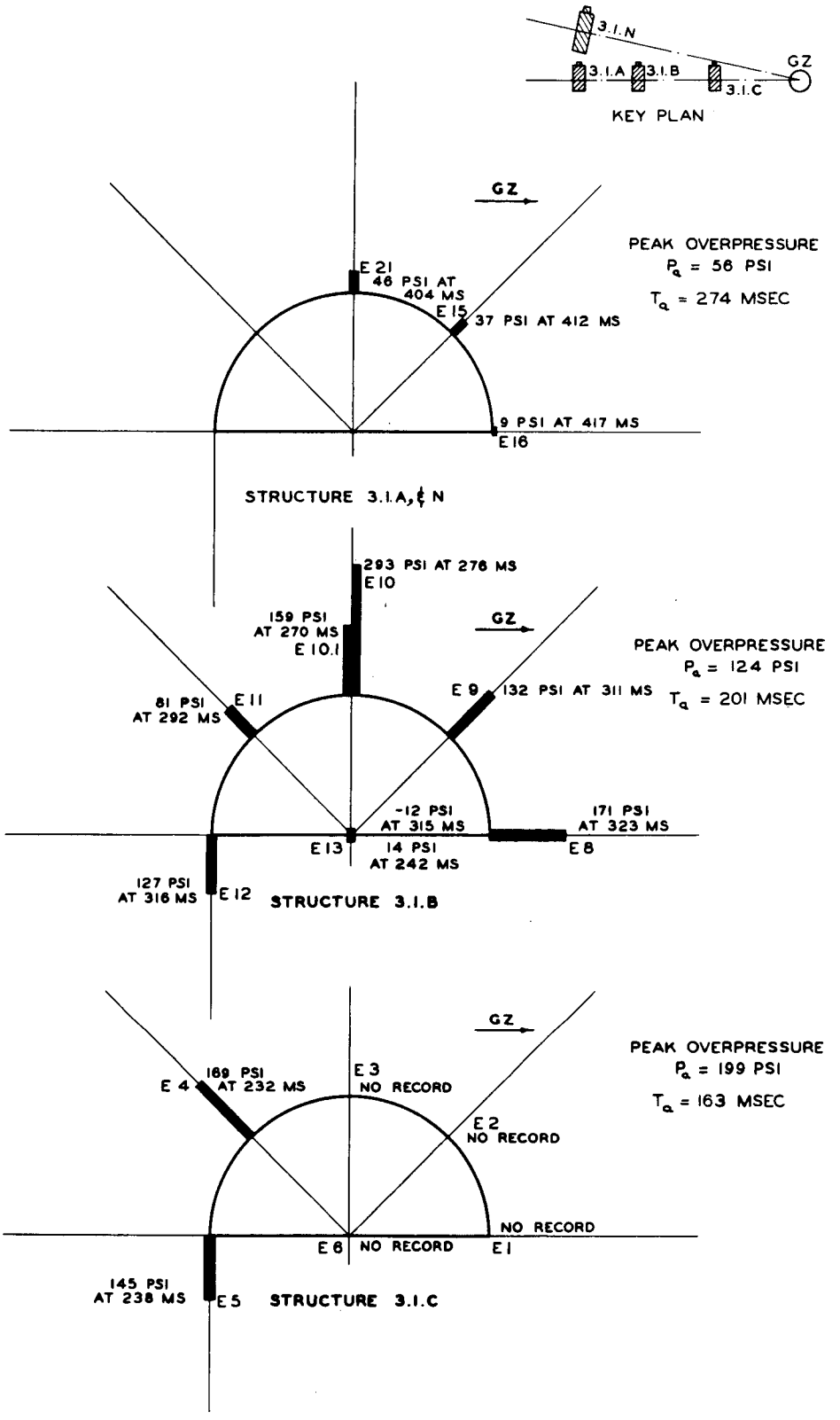

E – EARTH PRESSURE GAGE

NOTE ZERO TIME IS TAKEN AS THE TIME OF DETONATION OF THE DEVICE

Figure 3.1 Peak transient earth pressure, Structures 3.1.a, b, c, and n.

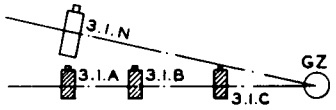

KEY PLAN

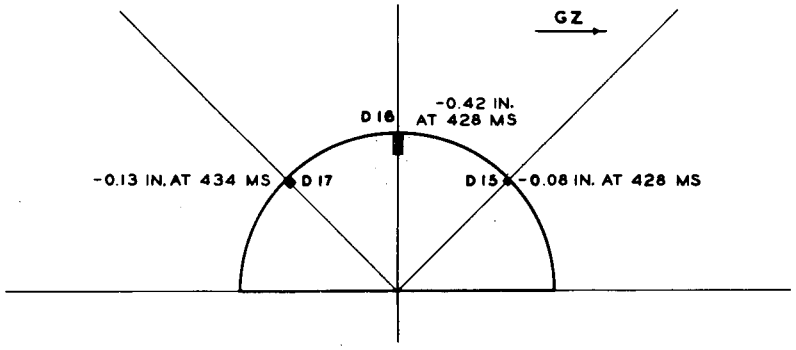

STRUCTURE 3.1.A

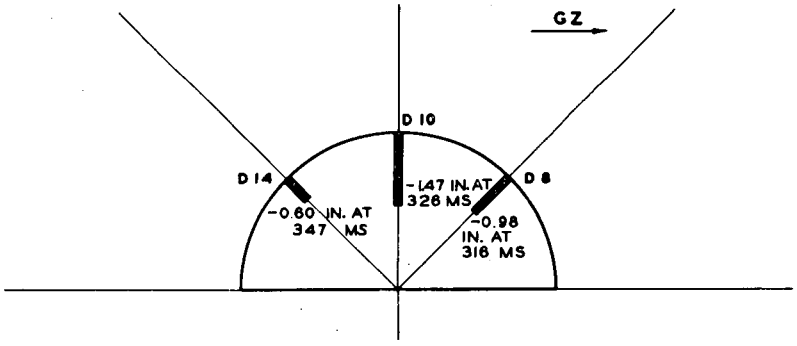

STRUCTURE 3.1.B

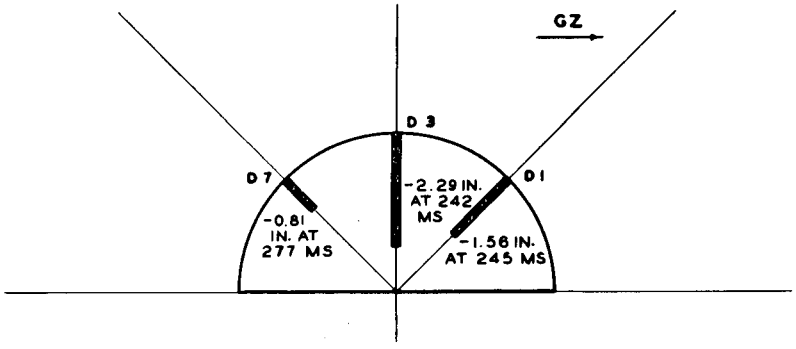

STRUCTURE 3.1.C

D-ELECTRONIC DEFLECTION GAGE

NOTE ZERO TIME IS TAKEN AS THE TIME OF DETONATION OF THE DEVICE

Figure 3.2 Peak transient deflection, with respect to the center of the floor slab, Structures 3.1.a, b, and c.

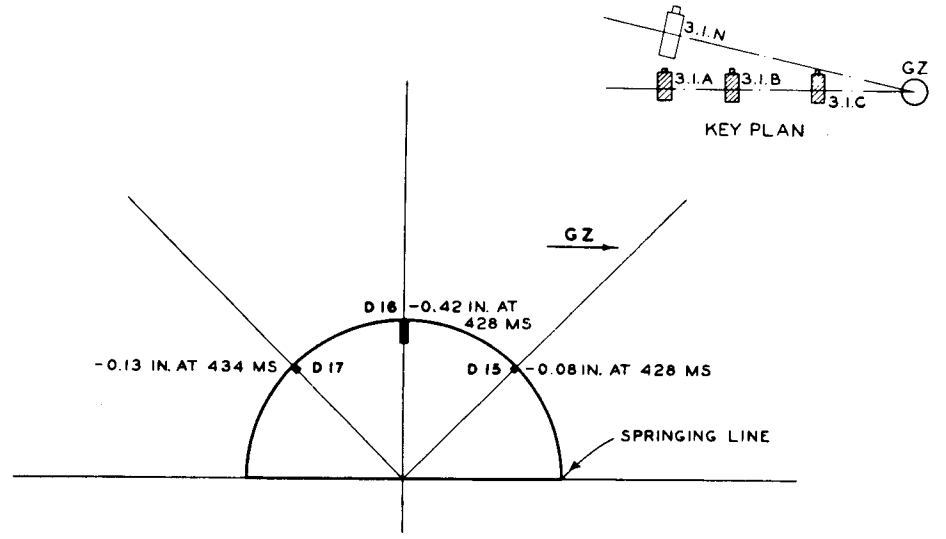

NOTE: ZERO TIME IS TAKEN AS THE TIME OF DETONATION OF THE DEVICE

Figure 3.3 Peak transient deflection with respect to the springing line, Structures 3.1.a, b, and c.

gages at the crown and springing line, however, were flush-mounted and gave what appear to be reliable measurements, which are included in Figure 3.1.

3.3 DEFLECTION

The peak transient radial deflections of the arch with respect to the center of the floor slab for Structures 3.1.a, b, and c are shown in Figure 3.2. These values are the actual recorded maxima, as read from the deflection-gage records. However, the floor slab itself underwent differential deflection as indicated by comparing the integrated acceleration records (see Figures 3.7 and 3.8). Therefore, the plots of peak transient radial deflections of the arch were adjusted,

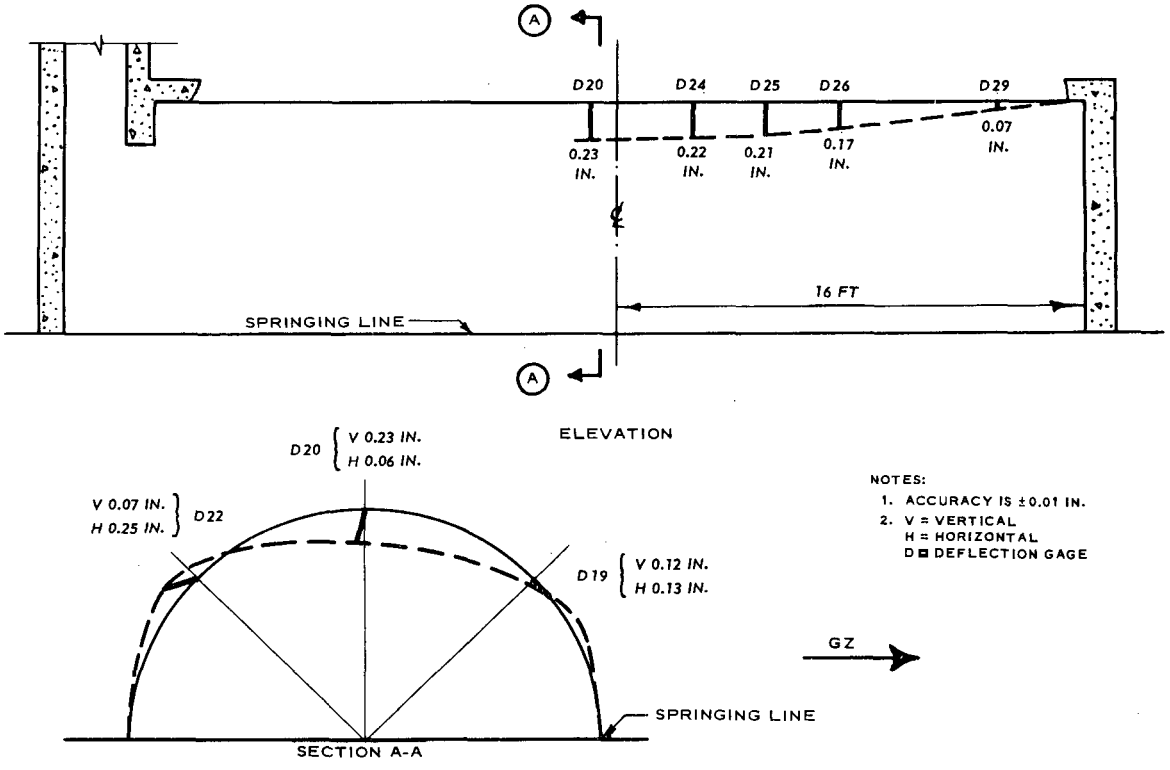

Figure 3.4 Peak transient deflections with respect to the springing line, Structure 3.1.n.

taking into consideration the movement of the floor slab. These corrected values are used in Figure 3.3, which shows the peak transient radial deflections of the arch and center of the floor slab with respect to the springing line.

The record from the accelerometer located at the center of the floor slab for Structure 3.1.a was not suitable for double integration and could not be used in determining deflections of the slab. Therefore, since the acceleration of the slab was small, it was assumed for Figure 3.3 that there was no differential deflection in the floor slab. However, by comparing the combined transient deflection of 0.42 inch for Structure 3.1.a with the crown deflection of 0.23 inch for Structure 3.1.n (Figure 3.4), it might be assumed that the peak transient downward deflection for Structure 3.1.a ranged from 0.20 to 0.30 inch and that the upward deflection of the center of the base slab was approximately 0.20 inch, all values being relative to the springing line.

The corrected plots (Figure 3.3) show the outward movement of the haunch, which was not evident in Figure 3.2. Since electronic instrumentation channels in the field were at a premium, only one gage was located at each of the three points on the arches, even though it requires two gages to describe the excursion of a point. It was hoped that the two self-recording (backup) gages

would describe both the horizontal and vertical movement of the crown; however, none of the self-recording deflection gages functioned.

The peak transient deflections of the 3.1.n arch with respect to the springing lines are shown in Figure 3.4. In this structure two gages were used at each point to trace both the horizontal and vertical movements. Section A-A of Figure 3.4 shows the maximum excursion of three points on the intrados near the center of the structure. These deflections show that the structure underwent bending with the crown moving downward and the haunches outward. It can also be observed that the bending was slightly asymmetrical with some movement away from ground zero. The elevation view shows the deflections of the crown along the longitudinal center line of the arch. The deflections of this structure were not large enough to definitely establish the distance to which the end walls affected arch action. This was indicated, however, by the pattern of the cracks discussed in Section 3.8.

The permanent deflection of the crown with respect to the springing line for Structure 3.1.a, b, and c is compared in Figure 3.5, again showing the influence of the end walls in restraining

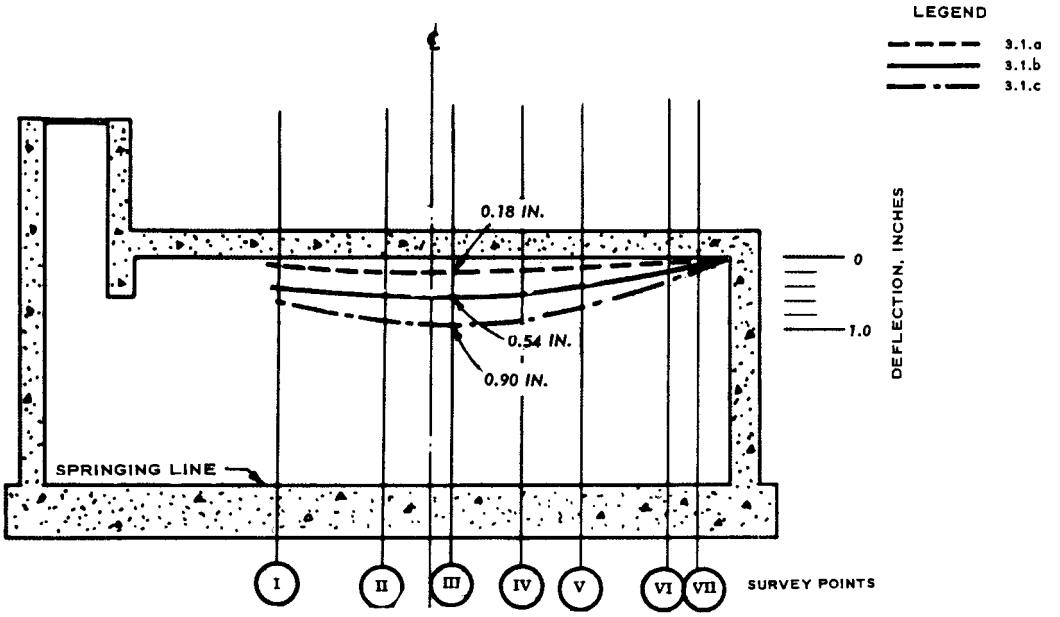

Figure 3.5 Permanent crown deflection with respect to the springing line of the arch, Structures 3.1.a, 3.1.b, and 3.1.c.

arch deflection. The permanent deflection of the crown with respect to the springing line for Structure 3.1.n measured less than 0.05 inch. The permanent deflections determined from a level survey are given in Tables 3.1, 3.2, 3.3, and 3.4.

3.4 ACCELERATION

The peak transient accelerations of the floor slabs are shown in Figure 3.6. The largest acceleration was a 13.4 g at the springing line of Structure 3.1.c. This acceleration had a duration of approximately 25 milliseconds. It is interesting to compare this peak floor-slab acceleration of 13.4 g with the peak free-field acceleration of the soil. The top of the floor slab was 12 3/4 feet below the ground surface. At a depth of 10 feet and at the same range as Structure 3.1.c, References 12 and 19 show free-field accelerations of 16.5 g and 17.1 g, respectively. It is also interesting to observe how the acceleration increases as the overpressure increases. The same references indicate that by increasing the ground-surface air overpressure from 200 to 300 psi the peak acceleration at a depth of 10 feet would be increased from

TABLE 3.1 PERMANENT DEFLECTION, STRUCTURE 3.1.a

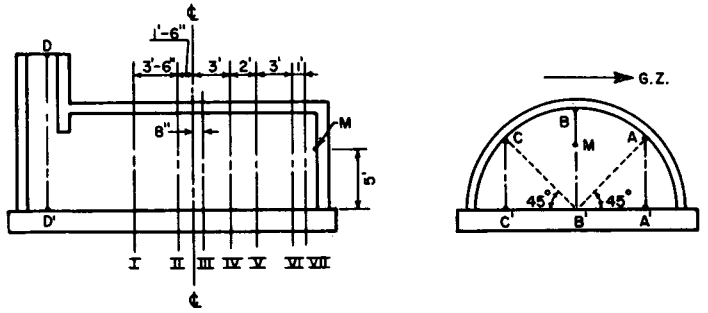

Points M, D, and D' moved 0.47 inch down.

Vertical deflections are actual residual movement.

The horizontal movement of the arch relative to the floor slab was within the least reading of this survey.

These measurements were taken with level and plumbbob and are accurate to within 0.06 inch.

Section	Vertical Deflection (inches)								
	C	C'	C to C'	B	B'	B to B'	A	A'	A to A'
I	0.60↓	0.48↓	0.12	0.60↓	0.48↓	0.12	0.60↓	0.48↓	0.12
II	0.60↓	0.48↓	0.12	0.60↓	0.48↓	0.12	0.60↓	0.42↓	0.18
III	0.48↓	0.48↓	0	0.66↓	0.42↓	0.24	0.66↓	0.48↓	0.18
IV	0.54↓	0.48↓	0.06	0.66↓	0.48↓	0.18	0.54↓	0.48↓	0.06
V	0.54↓	0.42↓	0.12	0.60↓	0.48↓	0.12	0.54↓	0.54↓	0
VI	0.54↓	0.48↓	0.06	0.54↓	0.48↓	0.06	0.54↓	0.48↓	0.06
VII	0.54↓	0.48↓	0.06	0.60↓	0.48↓	0.12	0.60↓	0.48↓	0.12

TABLE 3.2 PERMANENT DEFLECTION, STRUCTURE 3.1.n

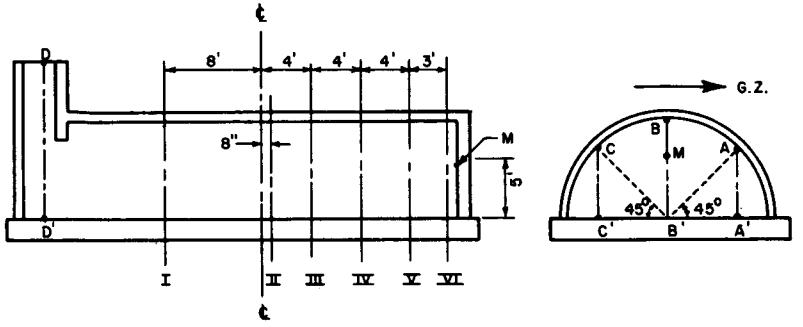

Points M, D, and D' moved 0.34 inch down.

Vertical deflections are actual residual movement.

These measurements were taken with level and plumbbob and are accurate to within 0.06 inch.

The horizontal movement of the arch relative to the floor slab was within the least reading of this survey.

Section	Vertical Deflection (inches)								
	C	C'	C to C'	B	B'	B to B'	A	A'	A to A'
I	0.34↓	0.28↓	0.06	0.34↓	0.15↓	0.19	0.34↓	0.28↓	0.06
II	0.34↓	0.28↓	0.06	0.34↓	0.15↓	0.19	0.34↓	0.15↓	0.19
III	0.34↓	0.28↓	0.06	0.34↓	0.15↓	0.19	0.34↓	0.22↓	0.12
IV	0.34↓	0.22↓	0.12	0.34↓	0.22↓	0.12	0.34↓	0.28↓	0.06
V	0.34↓	0.28↓	0.06	0.34↓	0.22↓	0.12	0.34↓	0.22↓	0.12
VI	0.34↓	0.28↓	0.06	0.34↓	0.34↓	0	0.34↓	0.28↓	0.06

TABLE 3.3 PERMANENT DEFLECTION, STRUCTURE 3.1.b

Refer to Table 3.1 for location of points.

Points M, D, and D' moved 0.84 inch down. Point D moved 0.25 inch west.

Vertical deflections are actual residual movement.

Horizontal deflections are movements of the arch relative to a point directly below on the floor slab.

These measurements were taken with level and plumbbob and are accurate to within 0.06 inch.

Section	Vertical Deflection (inches)								
	C	C'	C to C'	B	B'	B to B'	A	A'	A to A'
I	1.02↓	0.66↓	0.36	1.08↓	0.54↓	0.54	0.96↓	0.60↓	0.36
II	1.02↓	0.66↓	0.36	1.08↓	0.36↓	0.72	1.02↓	0.60↓	0.42
III	1.02↓	0.42↓	0.60	0.96↓	0.30↓	0.66	1.02↓	0.42↓	0.60
IV	0.96↓	0.66↓	0.30	1.02↓	0.42↓	0.60	0.96↓	0.54↓	0.42
V	1.02↓	0.60↓	0.42	1.02↓	0.48↓	0.54	0.96↓	0.60↓	0.36
VI	0.96↓	0.78↓	0.18	0.96↓	0.66↓	0.30	0.90↓	0.66↓	0.24
VII	1.02↓	0.84↓	0.18	0.90↓	0.72↓	0.18	0.84↓	0.72↓	0.12

Section	Horizontal Deflection (inches)		
	C to C'	B to B'	A to A'
I	0.09↖	0.19←	0.22←
II	0.03←	0.16←	0.22←
III	----	0.19←	0.25←
IV	0.03←	0.09←	0.22←
V	0.06←	0.19←	0.19←
VI	0.03←	0.12←	0.16←
VII	0.06↖	0.19←	0.12↖

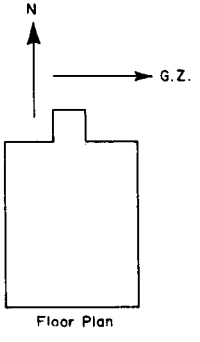

TABLE 3.4 PERMANENT DEFLECTION, STRUCTURE 3.1.c

Refer to Table 3.1 for location of points.

Points M, D, and D' moved 1.38 inches down.

Vertical deflections are actual residual movement.

Horizontal deflections are movements of the arch relative to a point directly below on the floor slab.

These measurements were taken with level and plumbbob and are accurate to within 0.06 inch.

Section	Vertical Deflection (inches)								
	C	C'	C to C'	B	B'	B to B'	A	A'	A to A'
I	1.68↓	1.20↓	0.48	1.86↓	0.90↓	0.96	1.92↓	1.26↓	0.66
II	1.74↓	1.14↓	0.60	1.92↓	0.72↓	1.20	1.92↓	1.20↓	0.72
III	1.80↓	1.14↓	0.66	1.98↓	0.84↓	1.14	1.98↓	1.02↓	0.96
IV	1.86↓	1.32↓	0.54	2.04↓	1.02↓	1.02	1.86↓	1.26↓	0.60
V	2.04↓	1.32↓	0.72	1.98↓	1.14↓	0.84	1.86↓	1.26↓	0.60
VI	1.86↓	1.50↓	0.36	1.86↓	1.38↓	0.48	1.80↓	1.44↓	0.36
VII	1.80↓	1.62↓	0.18	1.80↓	1.56↓	0.24	1.80↓	1.50↓	0.30

Section	Horizontal Deflection (inches)		
	C to C'	B to B'	A to A'
I	0	0.22↙	0.16←
II	0	0.16←	0.19↙
III	0.06↙	0.09←	0.19↖
IV	0.06←	0.19↖	0.25↖
V	0.09↖	0.19↖	0.19←
VI	0.03↖	0.22↖	0.16↖
VII	0.06←	0.22↖	0.12↖

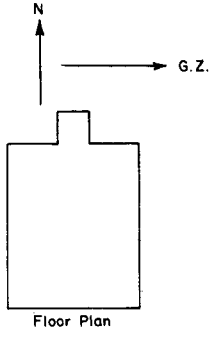

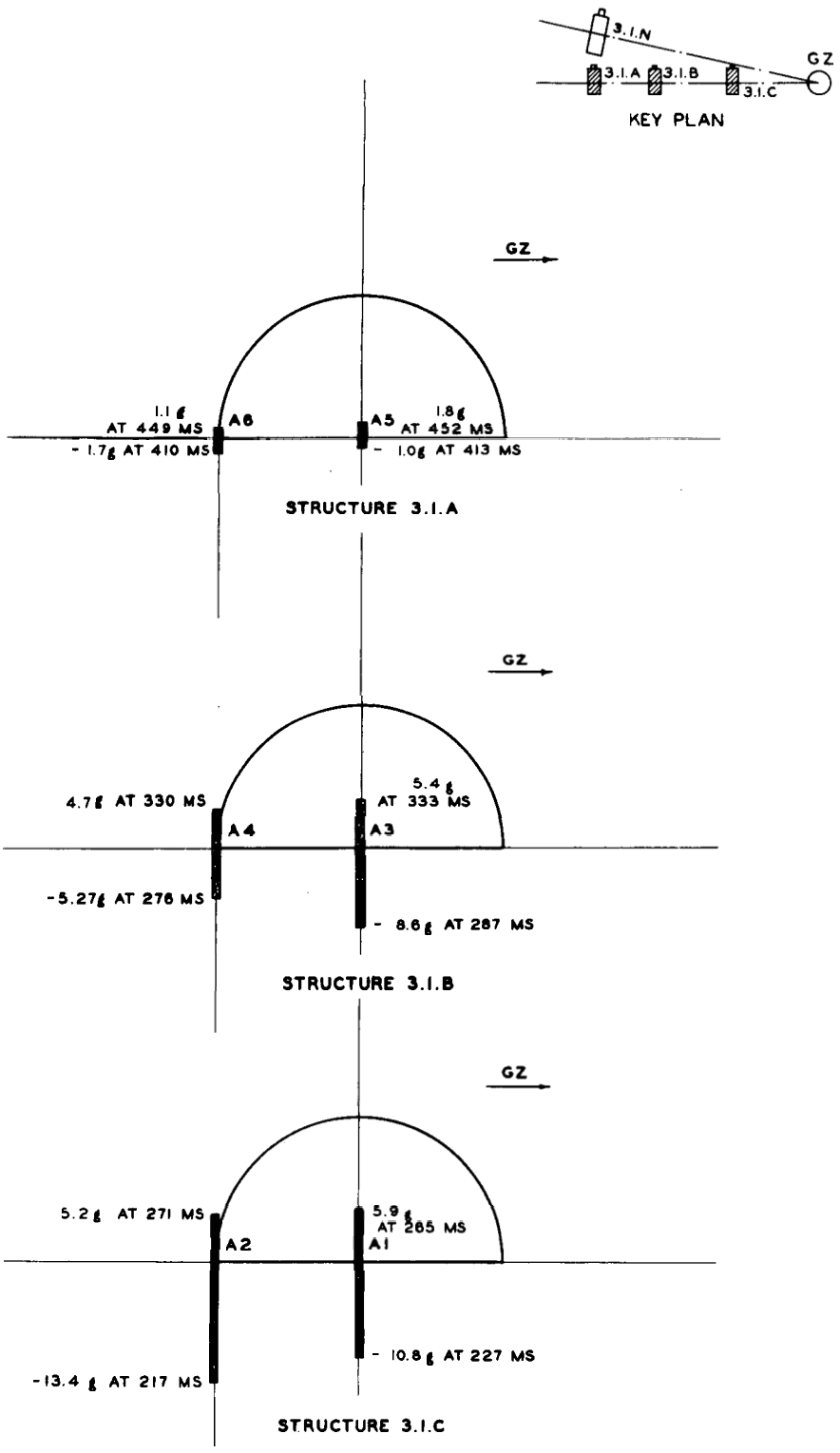

A - ACCELEROMETER

NOTE: ZERO TIME IS TAKEN AS THE TIME OF DETONATION OF THE DEVICE

Figure 3.6 Peak transient acceleration, Structures 3.1.a, b, and c.

an average of 16.8 g to an average of about 150 g. These high values of acceleration would most probably be physiologically hazardous to personnel (Reference 31).

The adjusted double-integrated acceleration records (see Section 2.3.3 for the method used in integrating records) for gages A-3 and A-4 of Structure 3.1.b, and 1AV-10 of Reference 12 are shown in Figures 3.7, 3.8, and 3.9, respectively. The deflection history of the base slab and free-field measurements as shown in the three figures was used in the preparation of a transient history of earth pressure and deflection for Structure 3.1.b shown in Figure 4.2 of the next chapter. Figures 3.7 and 3.8 were also used in preparing Figure 3.3. The adjusted records for Structures 3.1.a and c are not shown.

3.5 STRAIN

Strain-versus-time records were taken at 16 points on Structure 3.1.n. Peak transient values of strain approximately 150 milliseconds after the arrival of the blast wave at the structure are shown in Figure 3.10. The three strains at the springing line on the ground-zero side plot into essentially a straight line for any given time. At all other gage sections only two strain values were recorded. A straight line was drawn through each set of values. Strains were not recorded on any of the other test structures.

It was assumed that the concrete cracked at tensile strains greater than about 100 microinches per inch. Based on this assumption, it is believed that the concrete was cracked to a depth of greater than 3 inches in some places.

The largest recorded concrete strain was 575 microinches per inch, at the crown on the extrados. A concrete modulus of elasticity of 4.5×10^6 psi would give a resulting stress of about 2,600 psi. The largest recorded steel strain was 1,000 microinches per inch in tension. It was in the top steel in the center of the floor slab. When multiplied by a steel modulus of elasticity of 30×10^6 psi, the resulting steel stress was 30,000 psi in tension.

The values of residual or permanent concrete strains were low, as can be seen in Figure 3.11. Large tensile strains indicate cracks, as can be seen by comparing with Figure 3.17.

3.6 MISSILES

No missiles (concrete fragments) were found in the missile traps in any of the structures.

3.7 RADIATION

A summary of the total radiation dose within the four structures and the total amount at the ground surface (free-field radiation dose) is shown in Figures 3.12 through 3.15. These four figures show that the entranceways admitted the major portion of the radiation dose into the structures. Although no special effort was made to attenuate radiation at the entranceways, examination of the figures shows that radiation was attenuated greatly with distance.

3.8 DAMAGE SURVEY

Structure 3.1.a. Visual inspection of the interior of this structure indicated minor damage in the form of small hairline cracks located mainly in the floor slab. The location of these cracks is shown in Figure 3.16.

Structure 3.1.n. Visual inspection of the interior of this structure indicated minor damage in the form of small hairline cracks located in the floor and intrados. The location and size of the cracks are shown in Figure 3.17. The restraint of the end walls on the arch action is graphically illustrated by these cracks, even though the cracks are of insignificant widths. The crack pattern indicates that the end walls affected the arch for a distance of about 11 feet, or slightly less than $1\frac{1}{2}$ times the arch radius.

Structure 3.1.b. Visual inspection indicated minor damage in the form of small- to medium-size cracks. The width of cracks in the floor slab varied from hairline to $\frac{1}{16}$ inch; the cracks

(Text continued on Page 59)

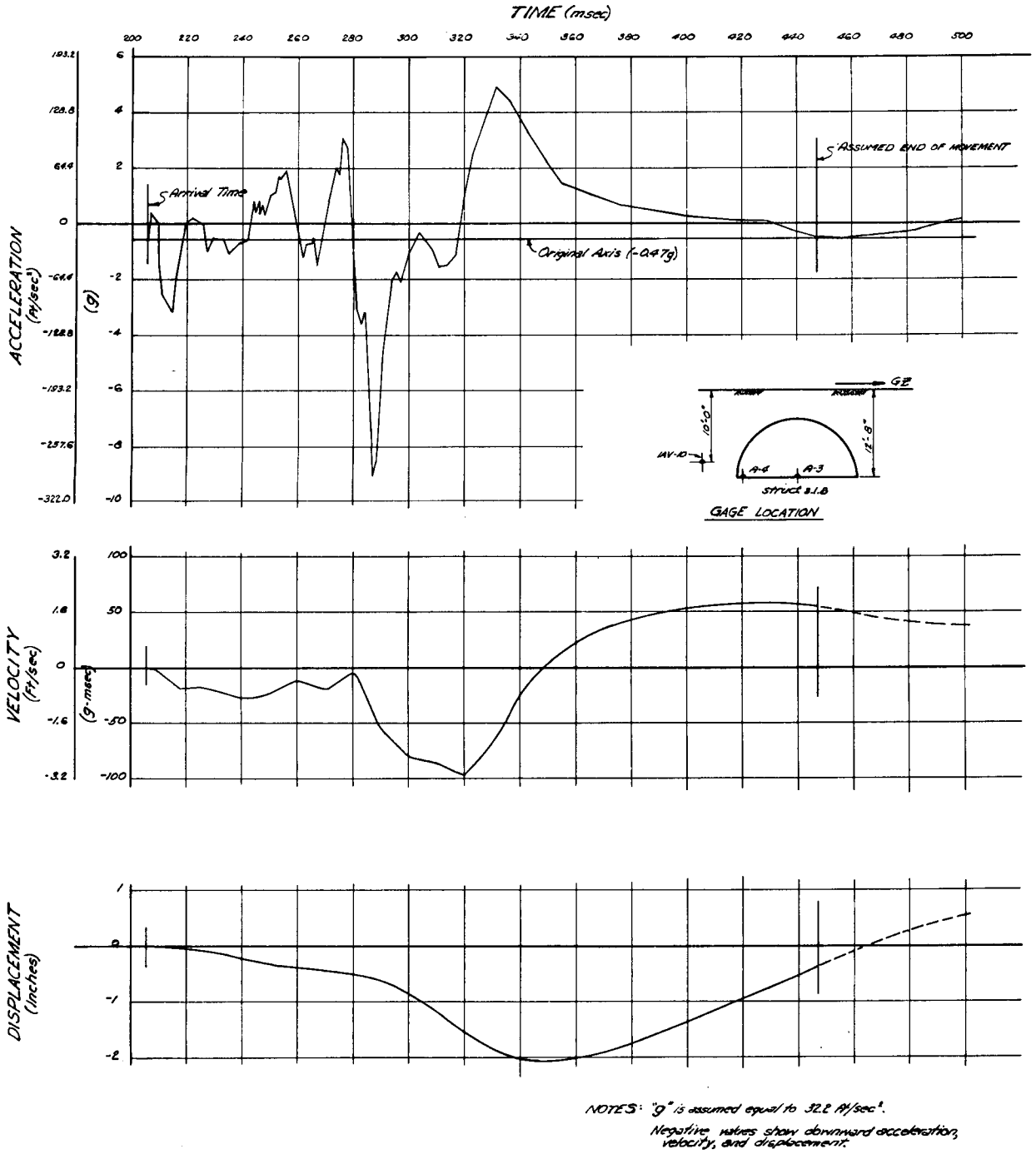

Figure 3.7 Adjusted double-integration of Record A-3, Structure 3.1.b.

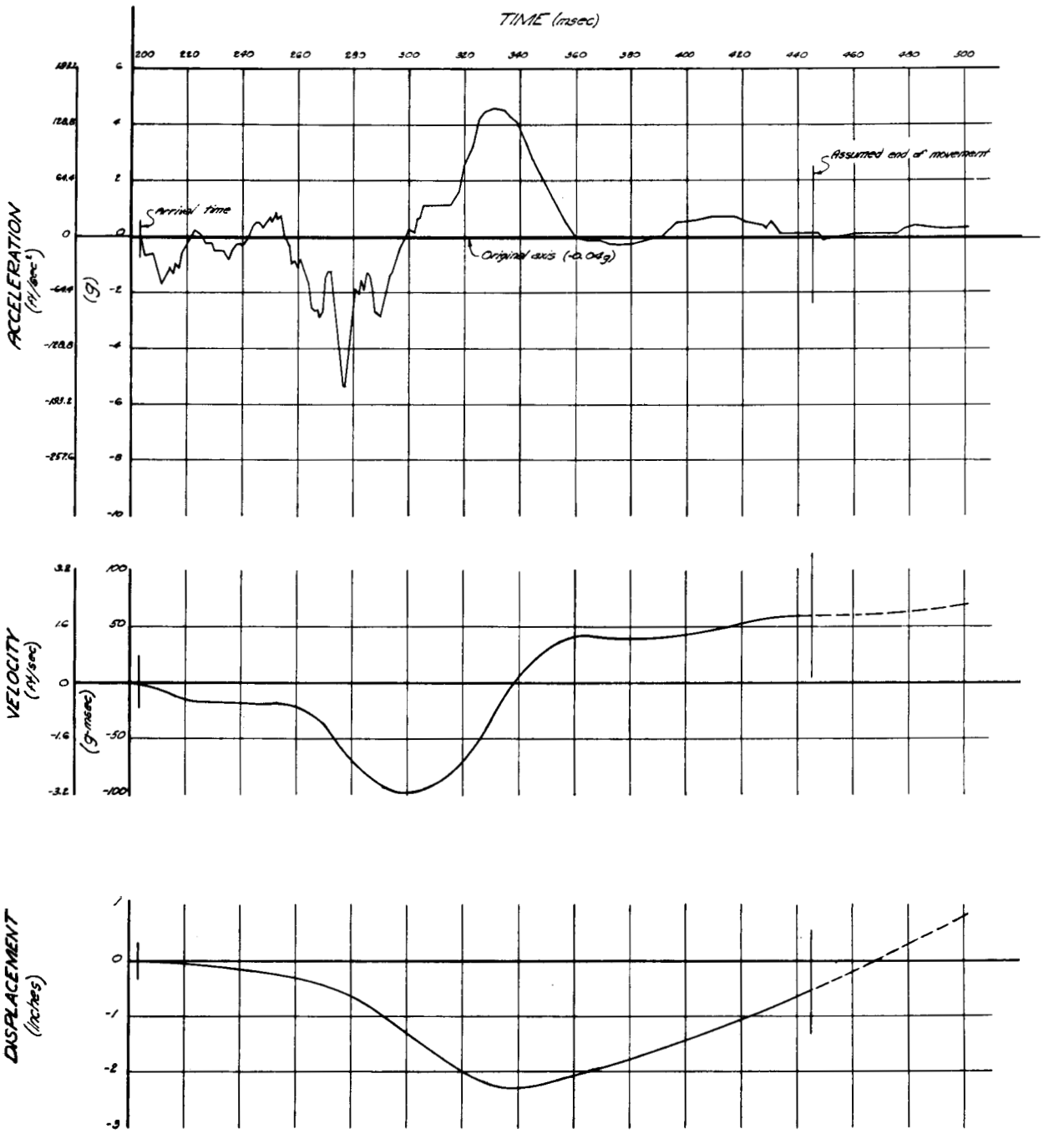

Figure 3.8 Adjusted double-integration of Record A-4, Structure 3.1.b.

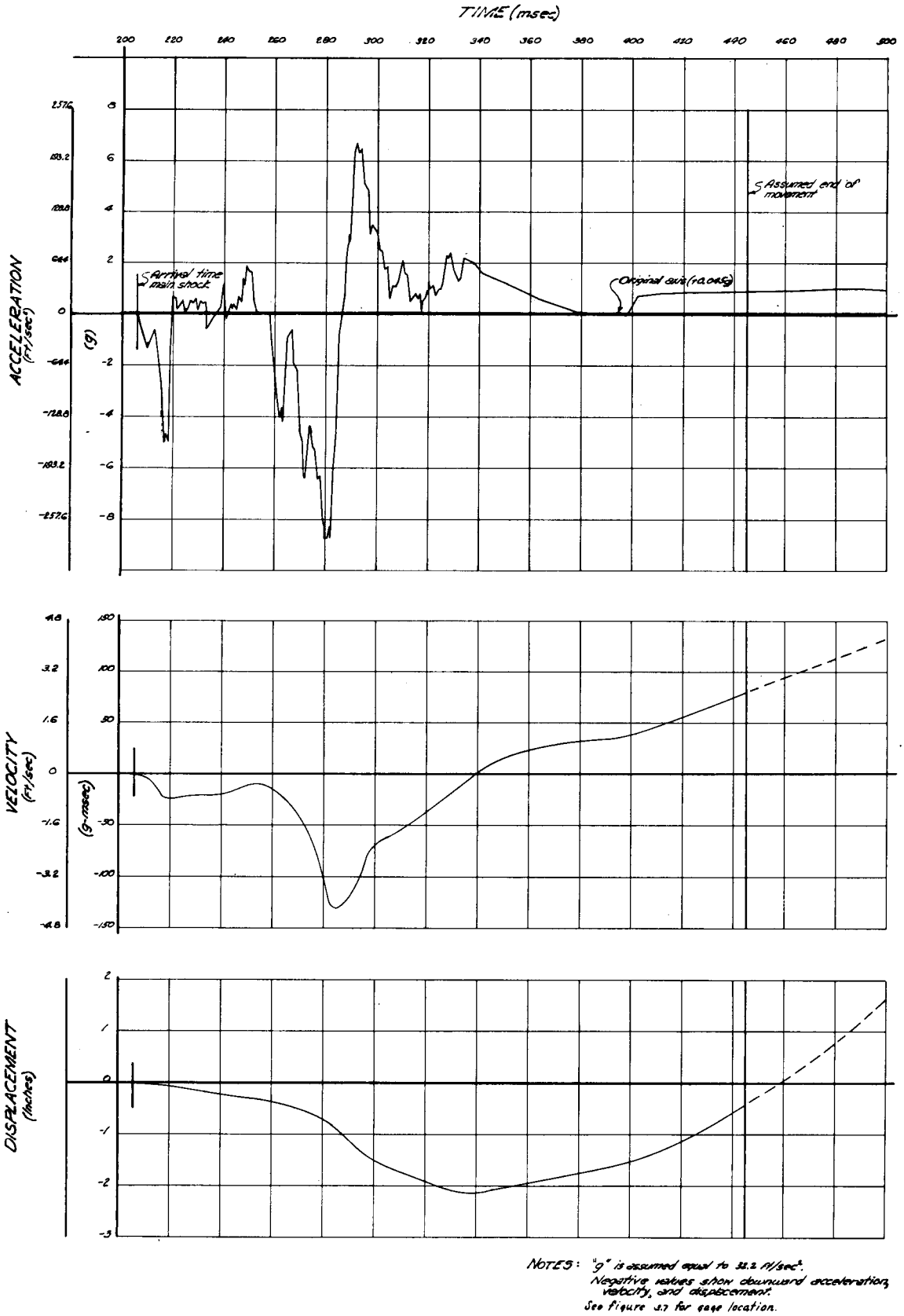

Figure 3.9 Adjusted double-integration of Record 1AV-10 (free-field), Reference 12.

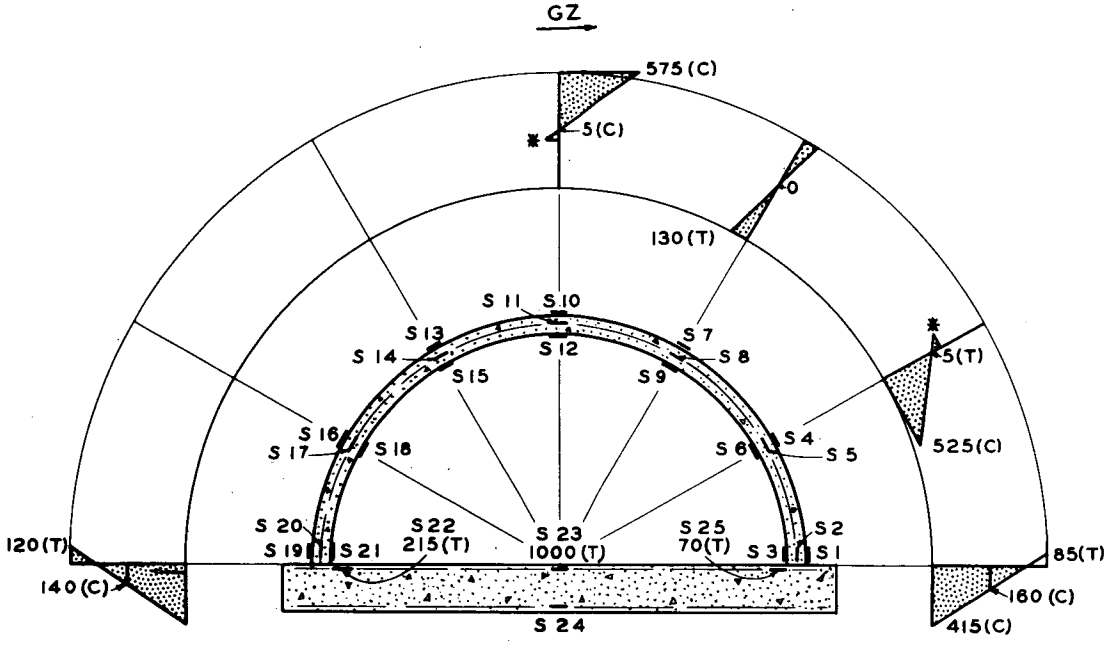

STRAIN, STRUCTURE 3.1.n, MICROINCHES PER INCH

NOTES:

1) * ASSUMED MAXIMUM CONCRETE TENSION OF APPROXIMATELY 100 MICROINCHES PER INCH

2) T = TENSION AND C = COMPRESSION

3) ABOVE STRAINS OCCURRED APPROXIMATELY 150 MILLISECONDS AFTER BLAST WAVE FIRST REACHED STRUCTURE 3.1.n

4) GAGES S4, 7, 12, 13, 14, 15, 16, 17, 18, USED FOR STATIC READINGS ONLY

5) GAGES S21 AND S24 - NO TRANSIENT RECORDS

Figure 3.10 Peak transient strains, Structure 3.1.n.

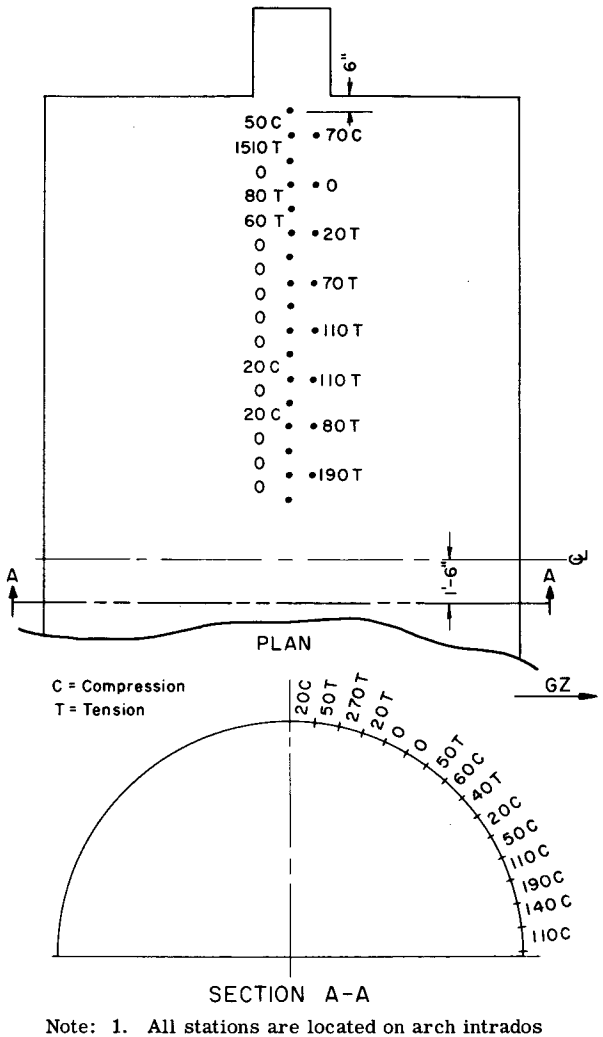

Note: 1. All stations are located on arch intrados at 10-inch centers.
2. Readings are in microinches per inch.

Figure 3.11 Permanent concrete strains, Whittemore gages, Structure 3.1.n.

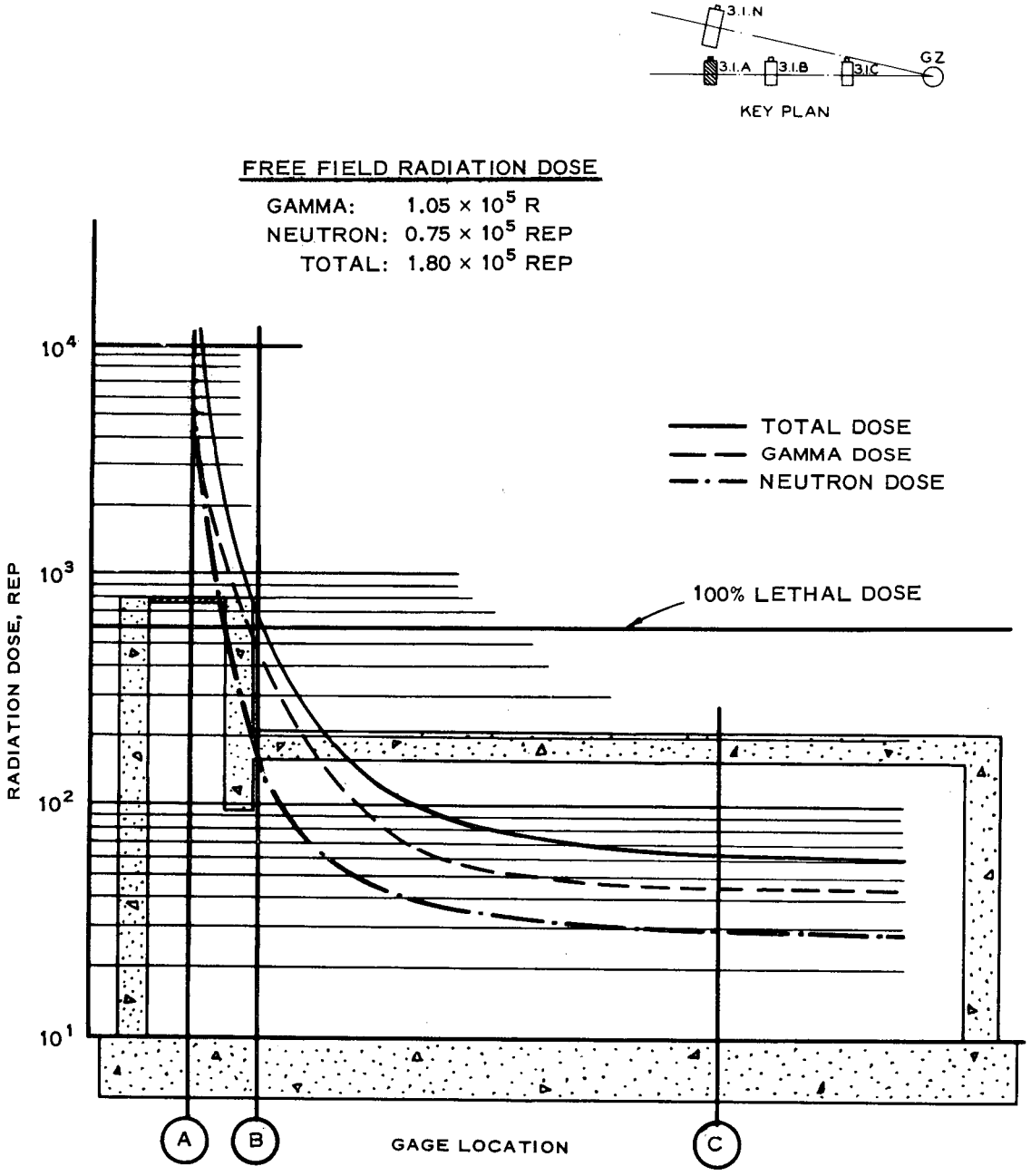

Figure 3.12 Total nuclear radiation dose profile, Structure 3.1.a.

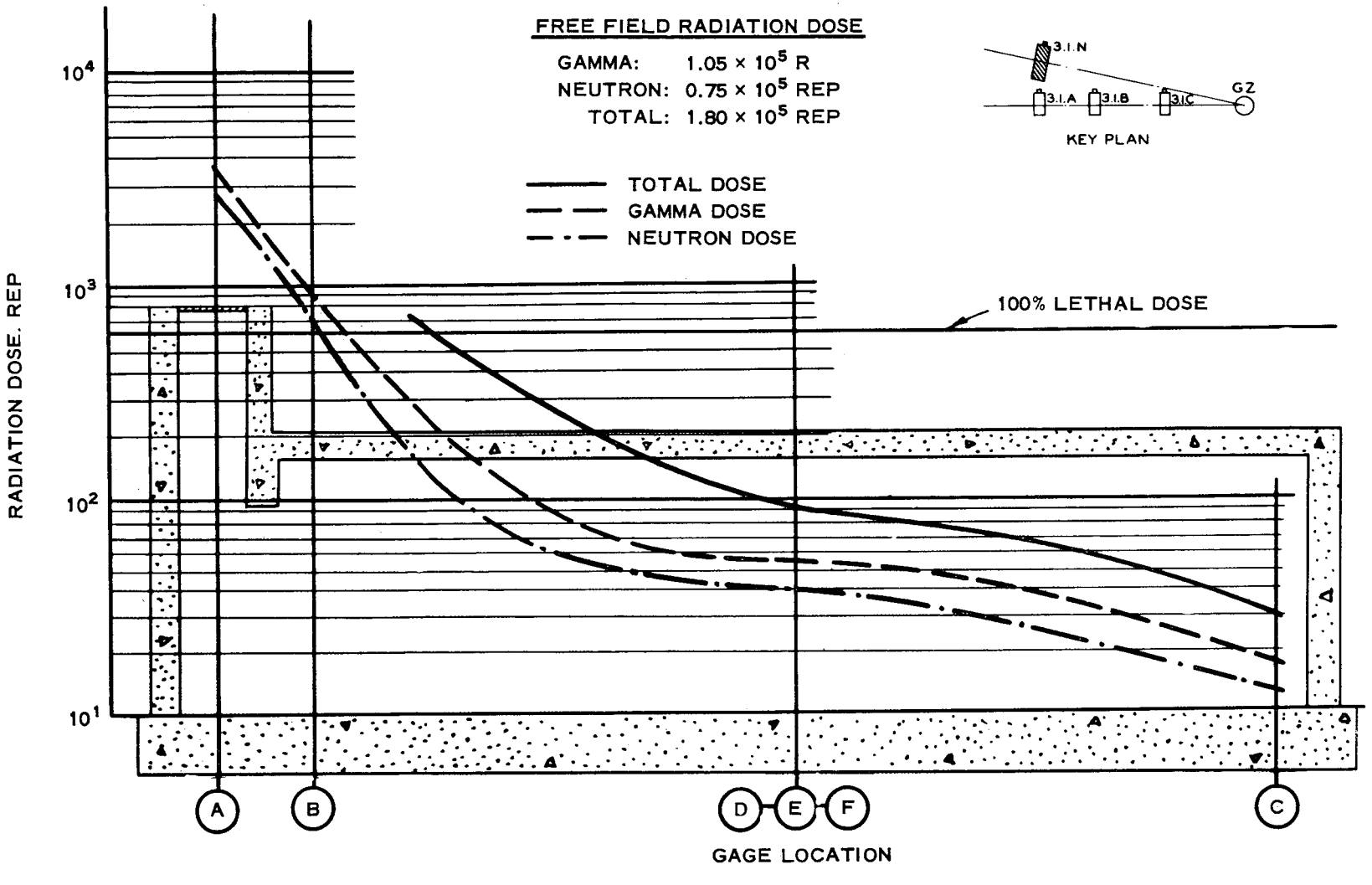

Figure 3.13 Total nuclear radiation dose profile, Structure 3.1.n.

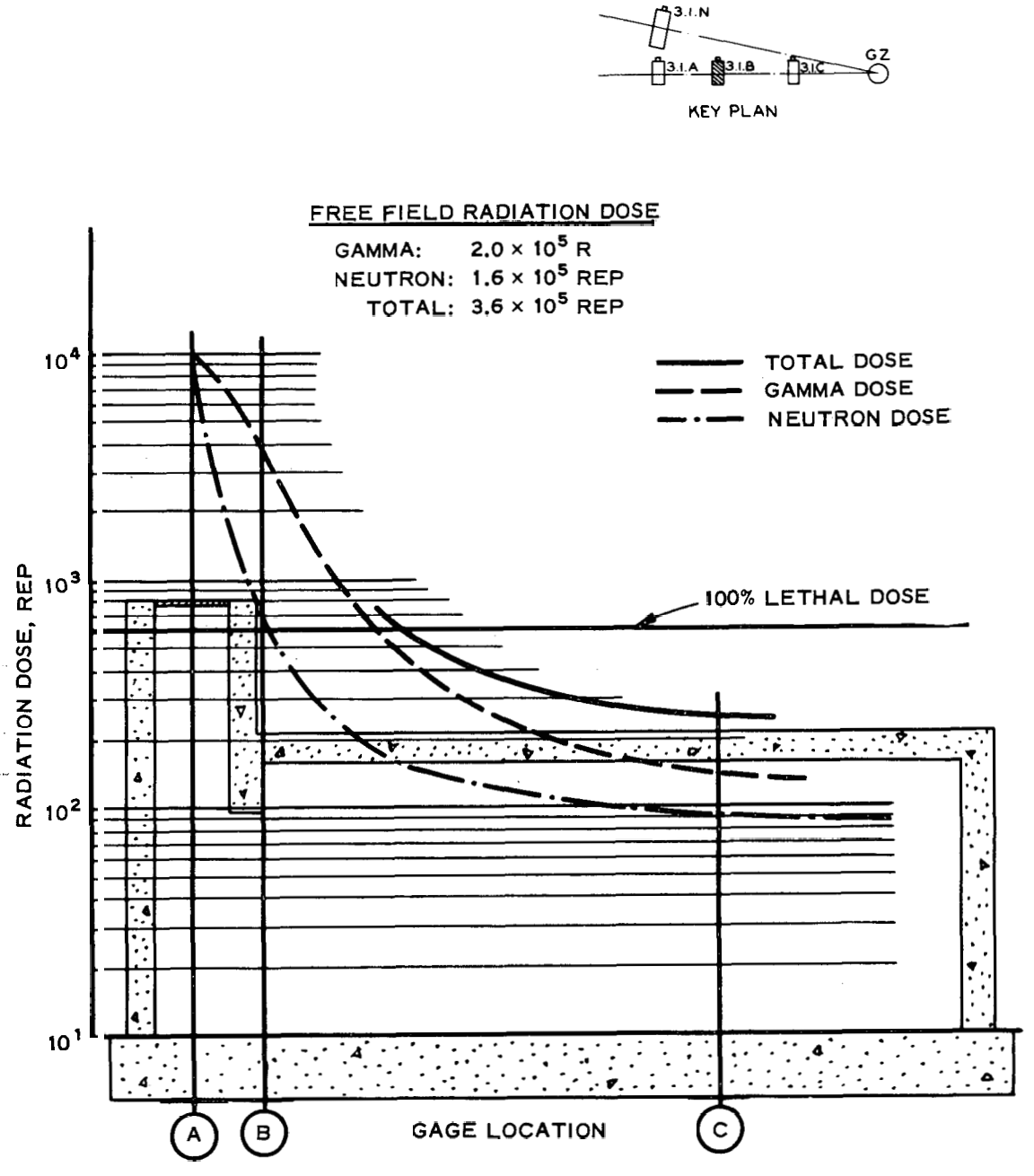

Figure 3.14 Total nuclear radiation dose profile, Structure 3.1.b.

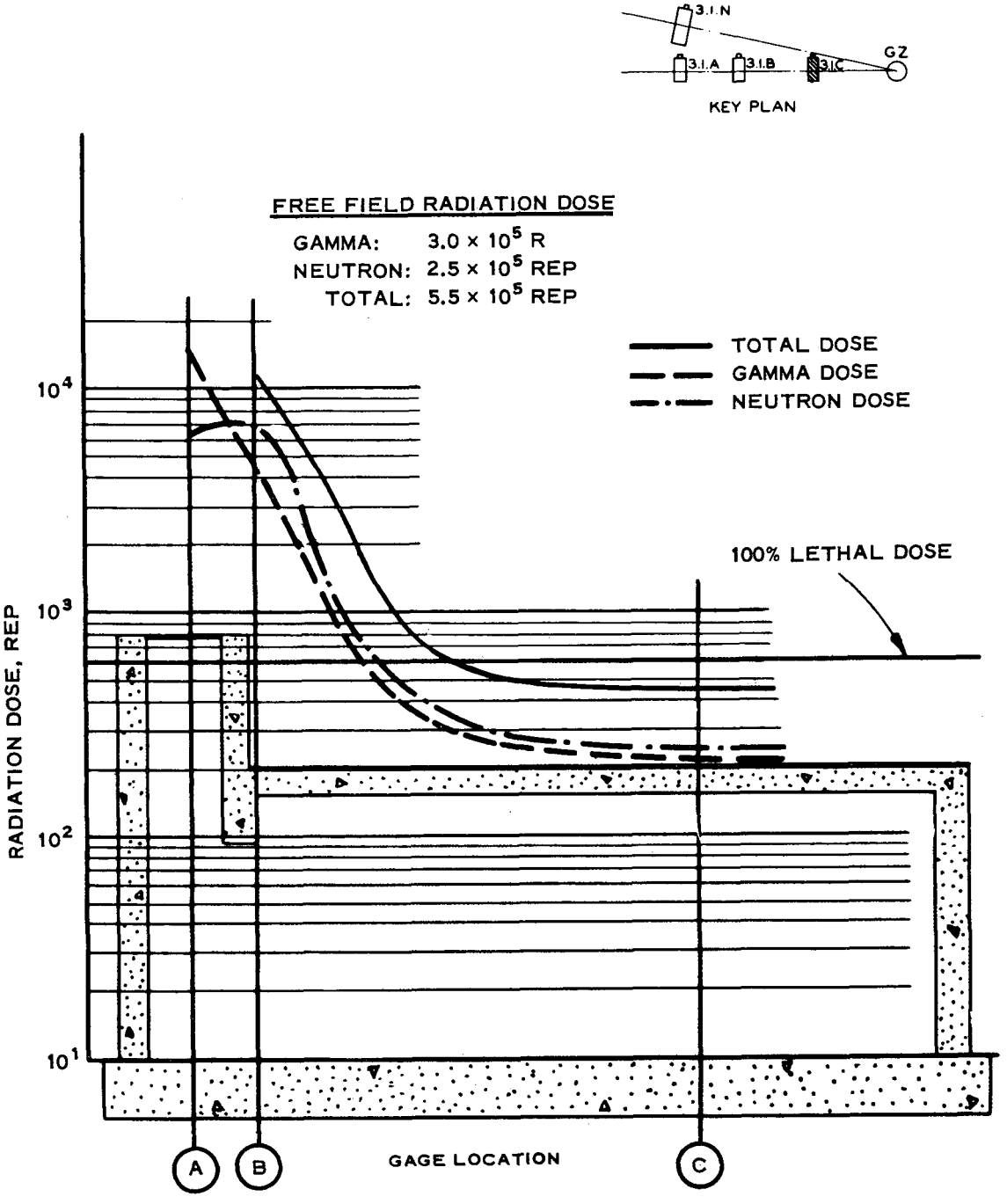

Figure 3.15 Total nuclear radiation dose profile, Structure 3.1.c.

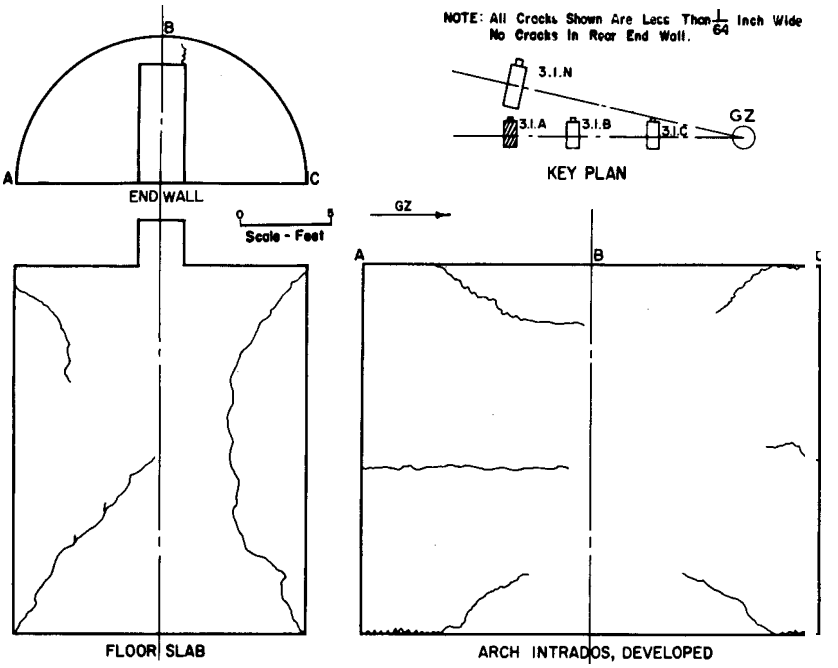

Figure 3.16 Postshot crack survey, Structure 3.1.a.

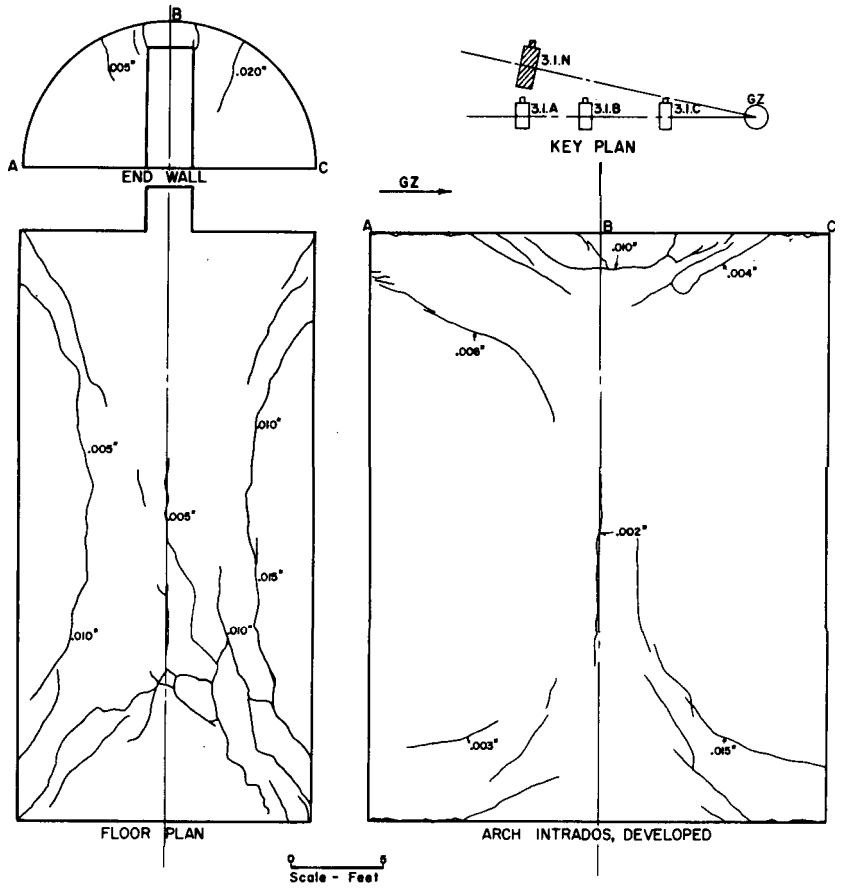

NOTE: No Cracks In Rear End Wall.

Figure 3.17 Postshot crack survey, Structure 3.1.n.

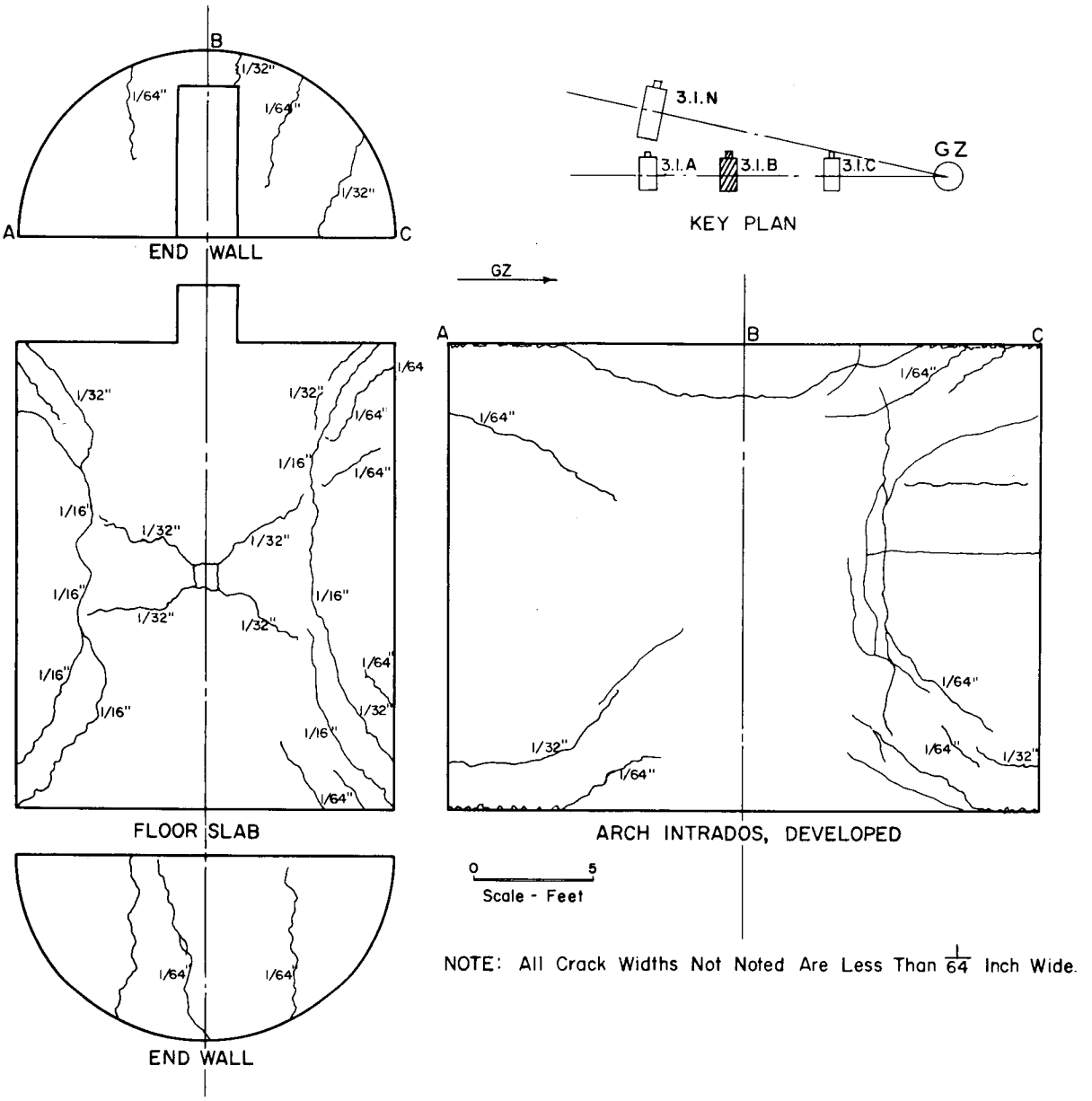

Figure 3.18 Postshot crack survey, Structure 3.1.b.

in the intrados varied from hairline to $1/32$ inch. It is apparent that the floor slab underwent bending, with the top of the floor slab in tension. Horizontal hairline cracks located 7 feet above the plane of the springing lines on the ground-zero side of the intrados show that the arch also underwent bending. Figure 3.18 shows the results of the postshot crack survey of this structure.

Structure 3.1.c. A large number of cracks developed in the floor slab, intrados, and end walls of this structure. The width of the cracks in the floor slab varied from hairline to $3/16$ inch,

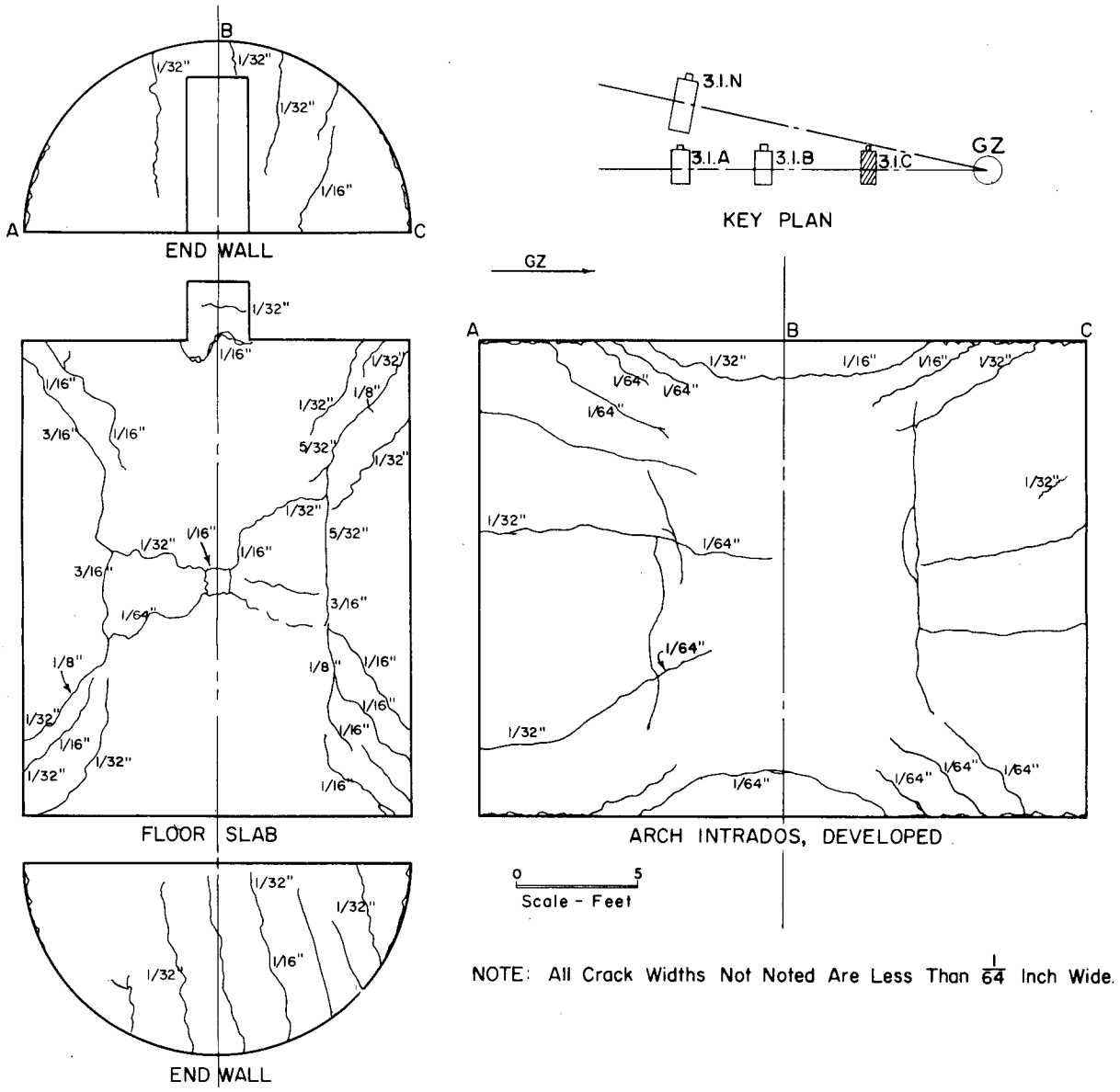

Figure 3.19 Postshot crack survey, Structure 3.1.c.

while the cracks in the intrados varied from hairline to $^1/_{32}$ inch in width. The results of the postshot survey of cracks are shown in Figure 3.19. Cracks in the floor slab are visible in the two interior views of Structure 3.1.c, shown in Figure 3.20. Figure 3.21 shows one of the diagonal cracks in the floor slab (the loose material on the floor is grout, not structural concrete). The general crack pattern around the grout-filled hole through which an earth-pressure gage was placed under the center of the floor slab is shown in Figure 3.22.

Minor compressive spalling of the concrete was observed over a 2-foot length on the ground-zero side of the intrados, near the center of the structure and approximately 2 feet above the

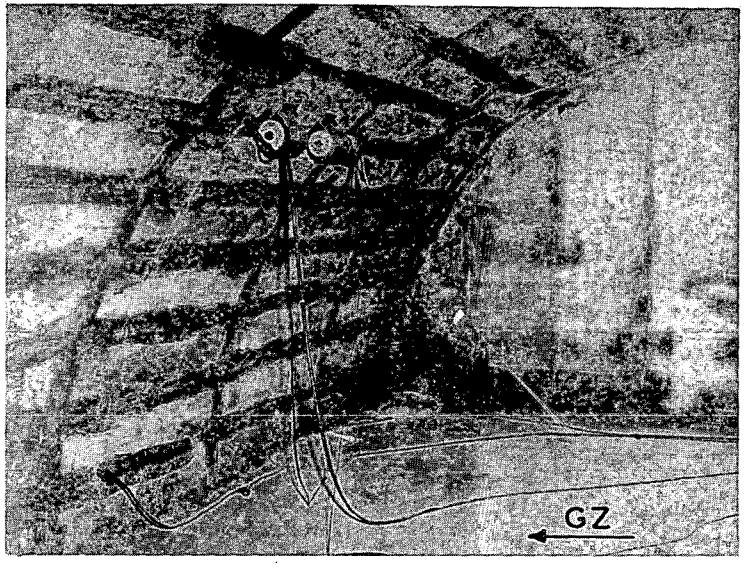

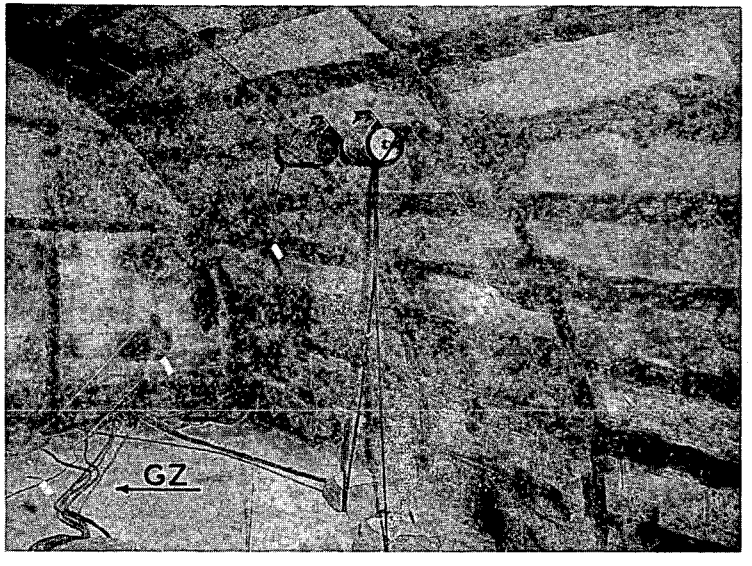

Figure 3.20 Interior views, Structure 3.1.c, postshot.

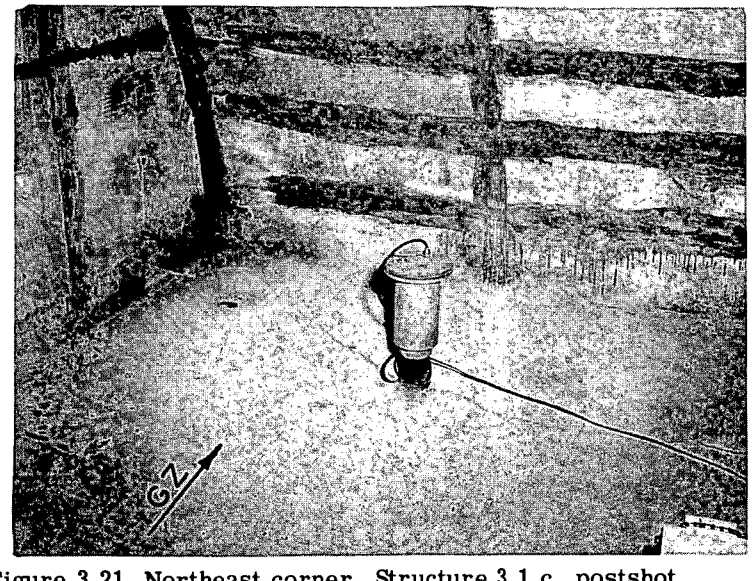

Figure 3.21 Northeast corner, Structure 3.1.c, postshot.

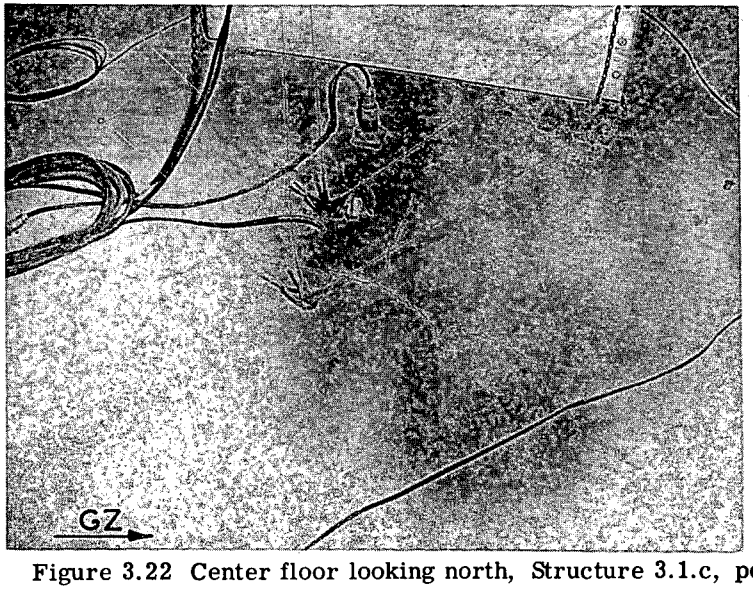

Figure 3.22 Center floor looking north, Structure 3.1.c, postshot.

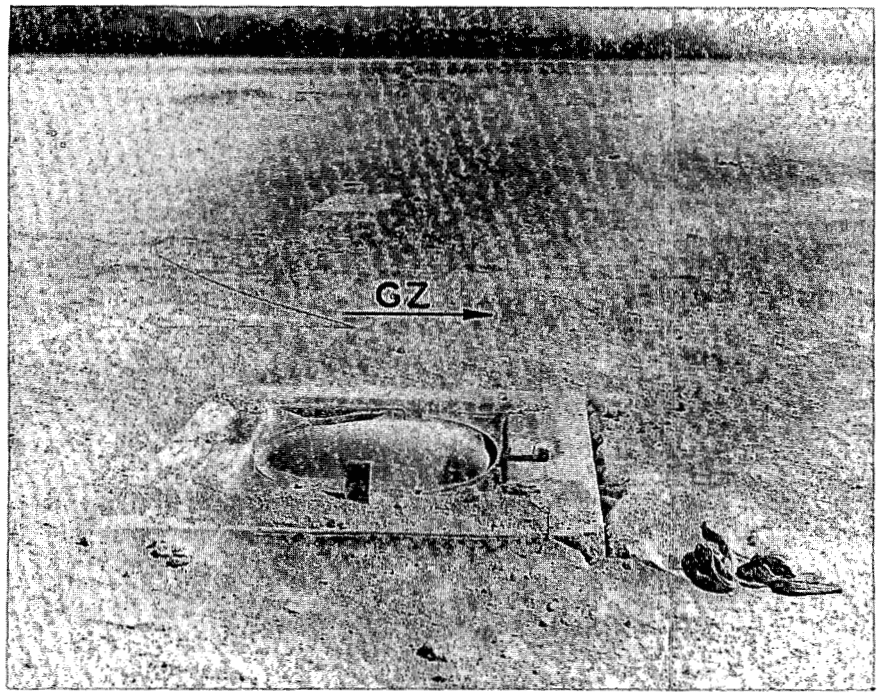

Figure 3.23 Hatch cover, Structure 3.1.c, postshot.

springing line. Horizontal cracks 7 feet up from the plane of the springing lines on the intrados of both the ground-zero and leeward side of the arch indicated that the arch was subjected to bending.

The entranceway hatch cover and the surrounding ground surface prior to the initial re-entry of the structure are shown in Figure 3.23. Some scouring of the earth was observed on the ground-zero side. The entranceway had been moved away from the earth on the ground-zero side, creating a vertical crack between the concrete surface of the entranceway and the earth backfill.

Chapter 4
DISCUSSION of RESULTS

4.1 CONSTRUCTION MATERIALS

In a field test in which the load is generated by an atomic weapon, it is just as important that the actual strength of the materials involved (i.e., the concrete, reinforcing steel, and soil) closely approximate their design strength values as it is for the actual blast pressure to closely approximate the design blast pressure. The degree of proximity of the actual values of material strength and blast pressure to the predicted values dictates the degree of success of the experiment.

4.1.1 Concrete Strength. The average concrete compressive strength of the four structures at the time of the Priscilla Shot was approximately 4,500 psi, or 50 percent greater than the design strength of 3,000 psi. Therefore, the structural capacity of the arch structures to resist overpressure loadings was accordingly greater. The average concrete strength for Structure 3.1.c (199-psi air-overpressure level) at shot time was 4,800 psi, which was 60 percent greater than the design strength. If it is assumed that resistance to failure depends on ultimate concrete strength, then the ultimate load (ground-surface overpressure that would cause collapse) for the 4,800-psi concrete would be appreciably greater than that for the 3,000-psi concrete.

If a uniform radial loading (Figure A.1, Loading A) is used and 3,000-psi and 4,800-psi concrete strengths are assumed, the calculated collapsing air overpressures for Structure 3.1.c for these two strengths would be 280 psi and 450 psi, respectively.

4.1.2 Backfill Material. In tests of buried structures, knowledge of backfill material is important since it is through this medium that the air-induced ground shock must pass in order to act upon the structures.

The degree to which the load is diverted from the structure (the arching action of soil) is a difficult quantity to evaluate and no attempt is made in this report to determine the arching characteristics of the soil surrounding the test structures. However, the backfill was placed and controlled so that the modulus of compressibility would be the same as that of the adjacent natural soil; thus, a given overpressure would cause equal deflections in the backfill and in the natural soil. (See Table 2.2 for a comparison of moduli of compressibility.) In order to attain this duplication of the moduli of compressibility, it was necessary that the density and the water content of the backfill material be greater than that of the natural soil. Because of the duplication of the compressive moduli, the test structures were surrounded by soil having nearly the same load-carrying capacity as that of the natural soil.

By comparing the density and water-content samples prior to and after the shot, it was found that no change in water content or density of the backfilled soil occurred at depths of 4 feet below the ground surface at the three pressure levels.

The depth of the backfill over the arches was not changed by the effects of the shot. The measured depth of earth cover over the crown of Structures 3.1.a, b, c, and n was 4.3, 4.1, 4.1, and 4.2 feet, respectively.

The strains and deflections measured on Structure 3.1.n during backfilling were small. Approximately 250 strain readings were taken, none of which were greater than 50 microinches per inch. The deflection readings showed that during backfilling the maximum upward deflection of the crown was about 0.01 inch and the maximum inward deflection of the haunch midway be-

tween the springing line and crown was about 0.01 inch. At the completion of the backfilling, the crown was deflected downward about 0.02 inches and the haunch was deflected outward about 0.01 inch.

4.2 ARCH RESPONSE

The crack pattern of the model arch (Figure 2.4) tested by the U. S. Naval Civil Engineering Laboratory (NCEL) was geometrically similar to the crack patterns (Figures 3.16 through 3.19) that developed in all four prototype structures. The compressive spalling of concrete observed in Structure 3.1.c occurred 2 feet above the springing line, which corresponds closely to the geometrically equivalent location of compressive failure in the model arch. On the basis of geometric similitude only, the predicted load to produce failure for Structure 3.1.c by using the values obtained from the model arch is calculated as follows:

$$p_p = \frac{p_m \times f_p}{f_m}$$

Where: p_p = Failure load, prototype. (Assume that the dynamic load is carried as a static load and that the concrete strength, f_c, is increased for dynamic capacity, Reference 5).

p_m = Static failure load, model. (**Section 2.1.2: Failure on one side** occurred at 140 psi and the other at 170 psi; however, the effective load on the arch must be computed by reducing the pressures by 28 and 25 percent, respectively, to account for the load loss to the walls of the test container. The effective loads are therefore 101 and 128 psi, respectively, the average being 115 psi.)

f_p = Concrete strength, prototype. (4,780 psi from Table 2.5 multiplied by a dynamic increase factor of 0.85 × 1.30 equals 5,300 psi.)

f_m = Concrete strength, model (3,000 psi).

Then:

$$p_p = \frac{115 \text{ psi} \times 5{,}300 \text{ psi}}{3{,}000 \text{ psi}} = 203 \text{ psi}$$

If a value of plus or minus 10 percent is assumed for the variance of concrete strength, then the pressure to cause failure would range from approximately 180 to 220 psi. The effect that the end walls of the prototype structure had in supporting part of the overpressure load is not included nor is the magnitude of that load known. **These crude calculations coupled with the evidence** of compressive spalling indicate that the arch may have been very close to failure.

It was found that the four structures underwent a gross transient and permanent downward displacement, as well as relative deflections of the arch and floor slab with respect to the springing lines of the arches. The total permanent downward displacements of the four test structures, referenced to a survey point located on the top of the entranceway of each structure, is presented in Figure 4.1, showing that the displacement caused by the blast increased linearly with air overpressure up to the 200-psi level.

4.2.1 Transient Response to Earth Pressure. To represent graphically the transient response of the arch to the earth pressure or ground shock, sequential plots of earth pressure and deflections (Structure 3.1.b) with respect to time, along with the respective ground-surface air overpressures, are shown in Figure 4.2. In the sequential plots, the base (line AB) has been removed from the arch proper, thus giving two distinct plots (i. e., arch and base slab) of earth pressure and deflection. The radial arch deflections are plotted with respect to the springing line, whereas the base slab not only shows the relative deflection of the center of the base slab

with respect to the springing line but also shows the transient gross displacement of the springing line as well. In addition, based on data obtained in Project 1.5, (Reference 12), free-field soil displacement determined at the same air-overpressure range (see Figure 3.9) also is shown in Figure 4.2. Even though the free-field data were taken at a depth of 10 feet and the top of the

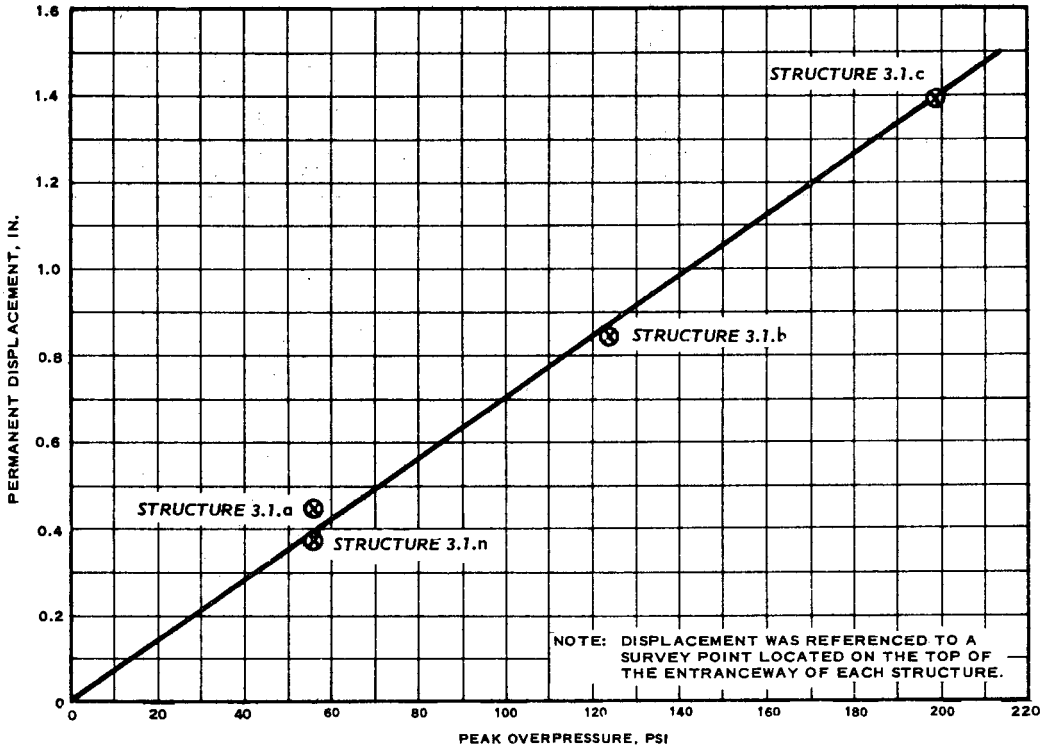

Figure 4.1 Permanent downward displacement of the 3.1 structures.

slab of the test structure described herein was located 12 feet 8 inches below the ground surface, the free-field data were referenced to the original location of the base slab (line A_oB_o) so that a direct comparison of displacement could be made.

The air-induced ground shock arrived approximately 200 msec after zero time (time of detonation). The first visible effects of earth pressure on the crown of the arch occurred at 205 msec. The following is a description of the response of the arch structure at the times of the various plots shown in Figure 4.2.

At 210 msec: The entire structure began moving downward (gross movement) as a rigid body; the free-field point had not yet started to move.

At 230 msec: The earth pressure was nearly uniform over the entire arch surface and base slab. The free-field point moved downward 0.14 inches while the base slab moved downward 0.11 inches.

At 250 msec: The precursor wave was nearly terminated and the decrease in earth pressure could be observed. In addition to the gross displacement of the structure as a whole, the arch began to deflect with respect to the springing line.

At 260 msec: The main shock arrived. Here again, the crown, by virtue of its position, was subjected to load before the free-field point, which explains why the downward movement of the base slab caught up with the downward displacement of the free-field point. Apparently the arch deflection had not yet responded to the main shock. It was also observed that the pressure at the 45-degree lines increased slightly, while the pressure at the springing line was essentially zero. This fact was also observed during the initial precursor build-up at 210 msec.

At 270 msec: The earth pressure was rapidly building up around the arch with the greatest pressure at the crown. The pressure on the base slab at the center was decreasing,

(Text continued on Page 74)

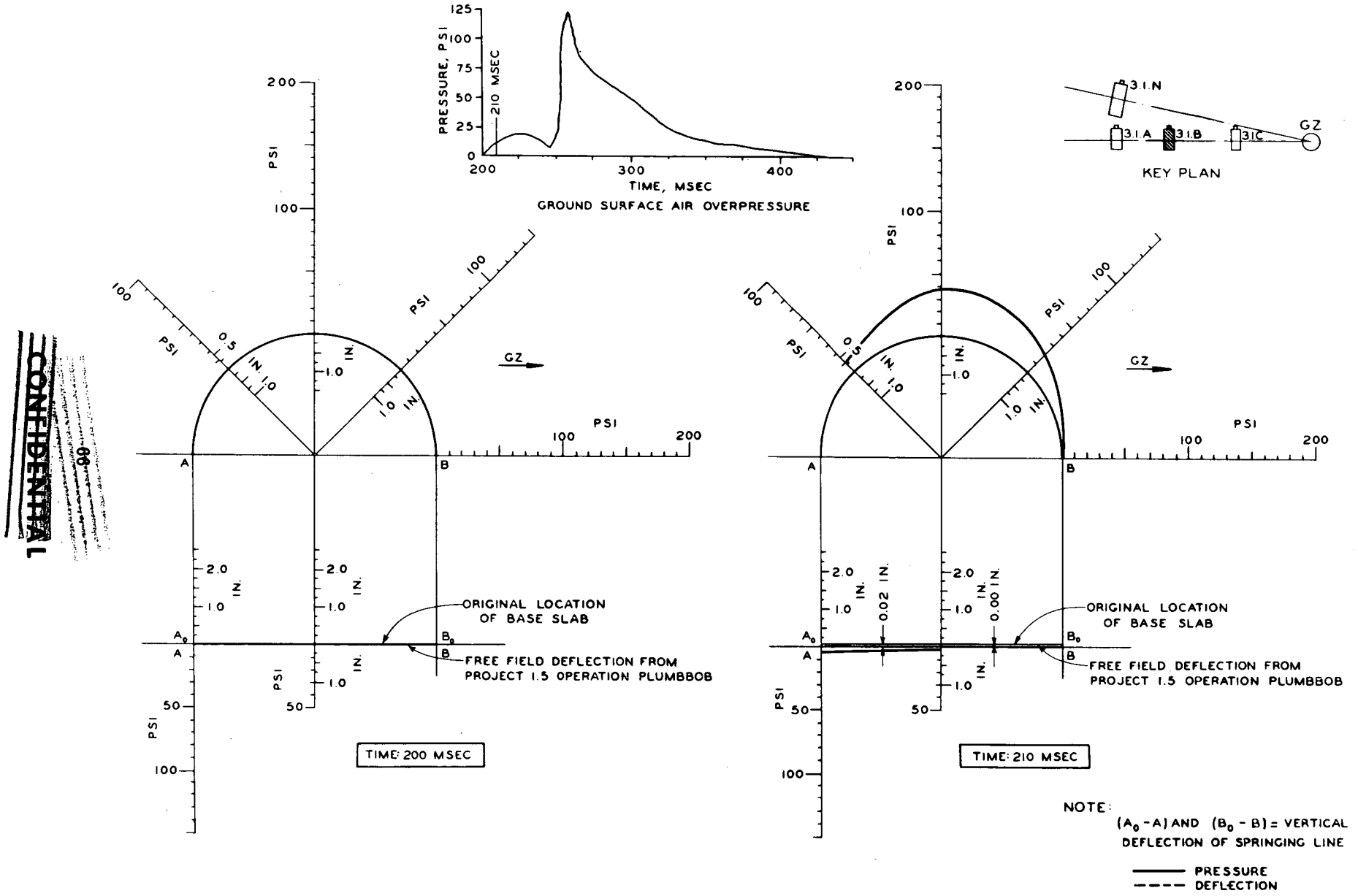

Figure 4.2 Sequential plot of earth pressure and deflection, Structure 3.1.b.

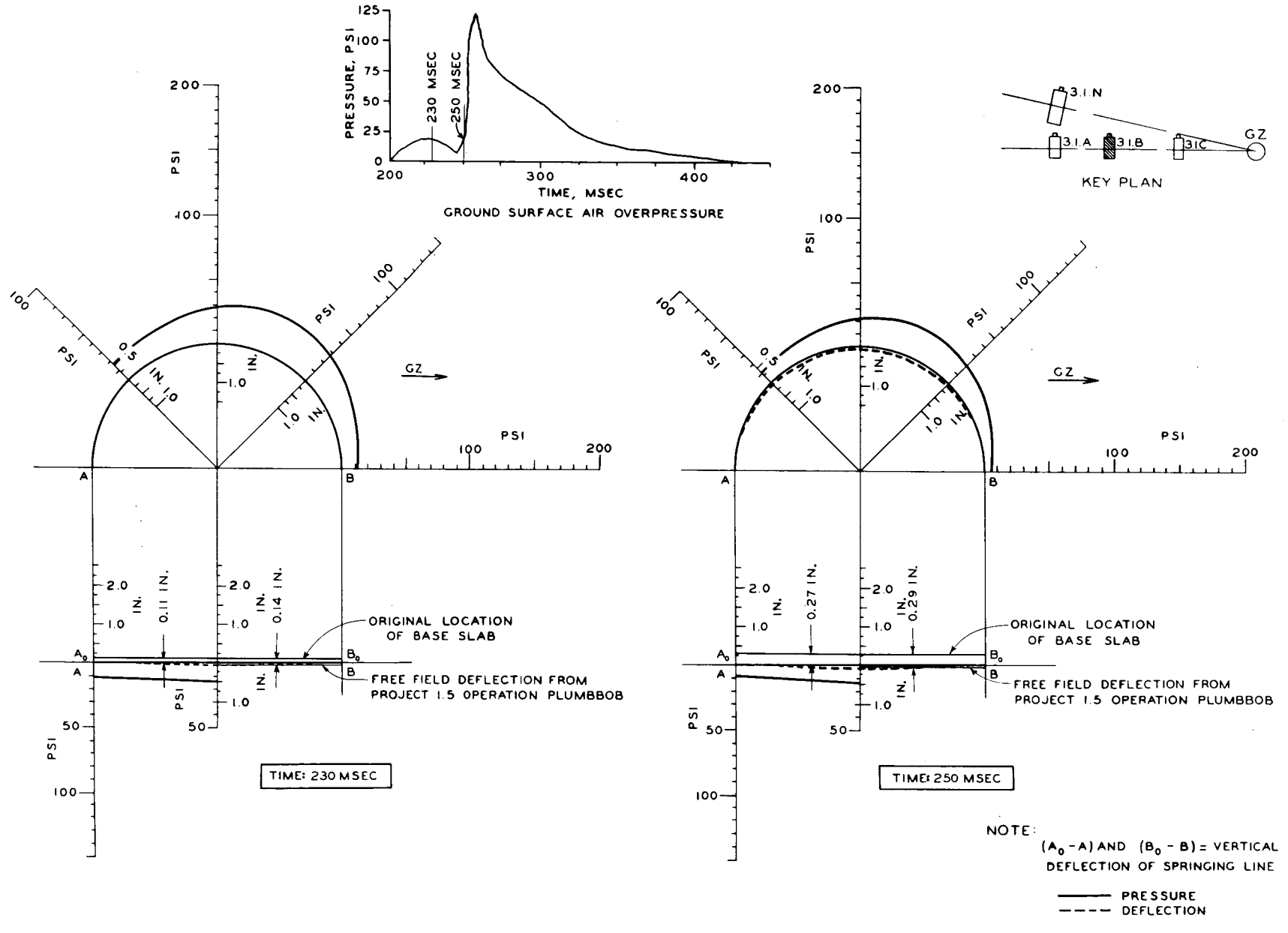

Figure 4.2 Continued.

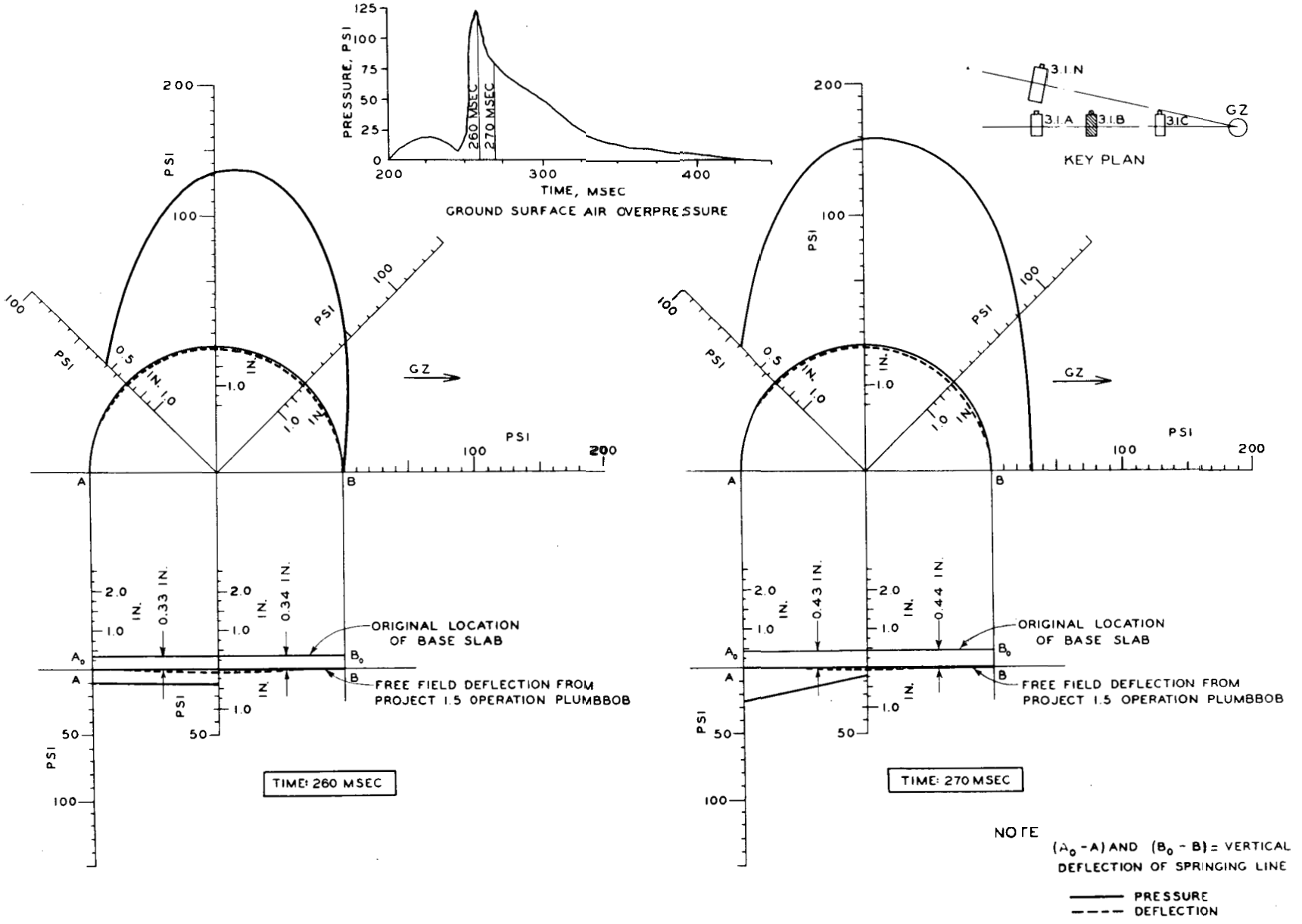

Figure 4.2 Continued.

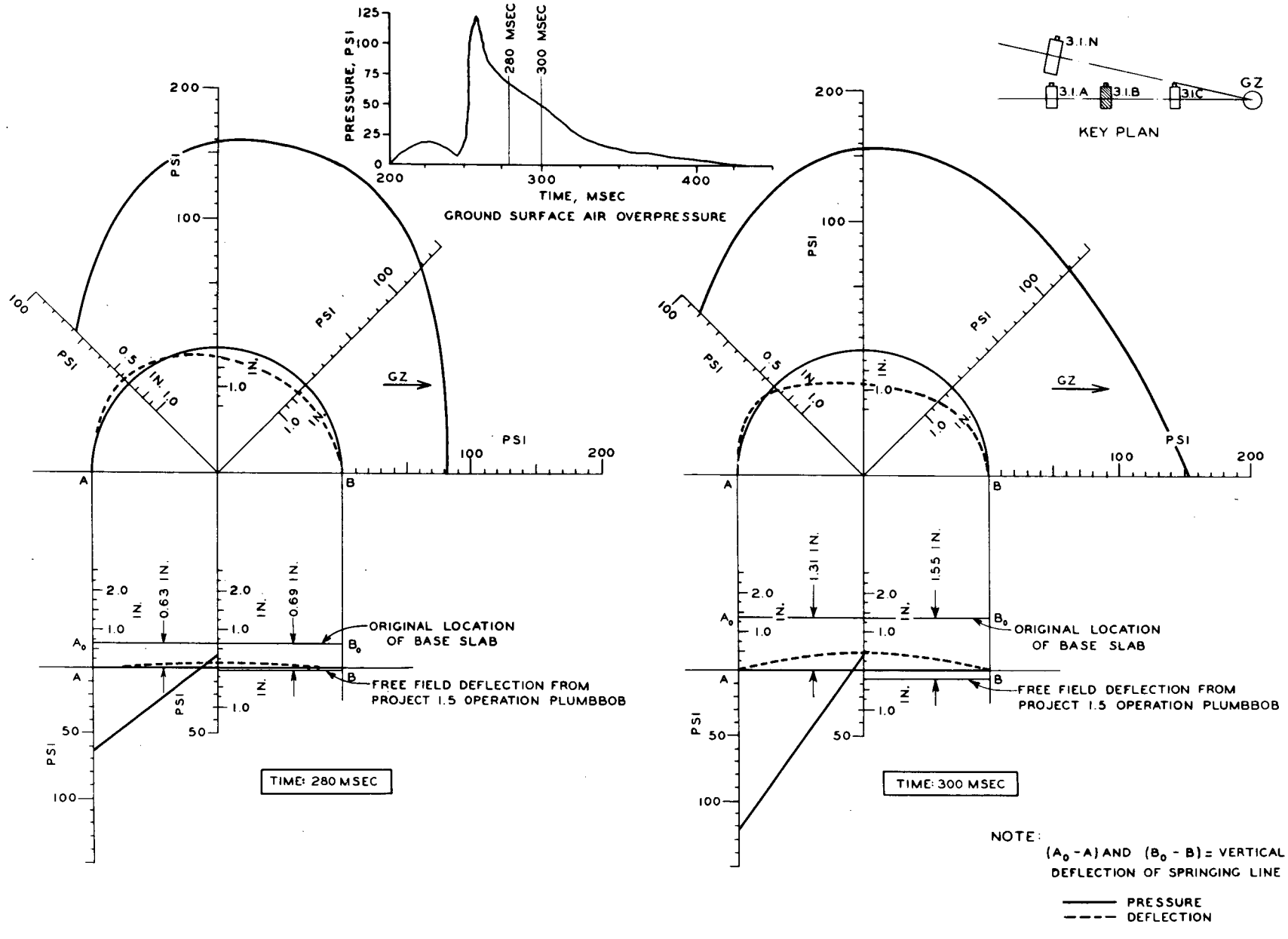

Figure 4.2 Continued.

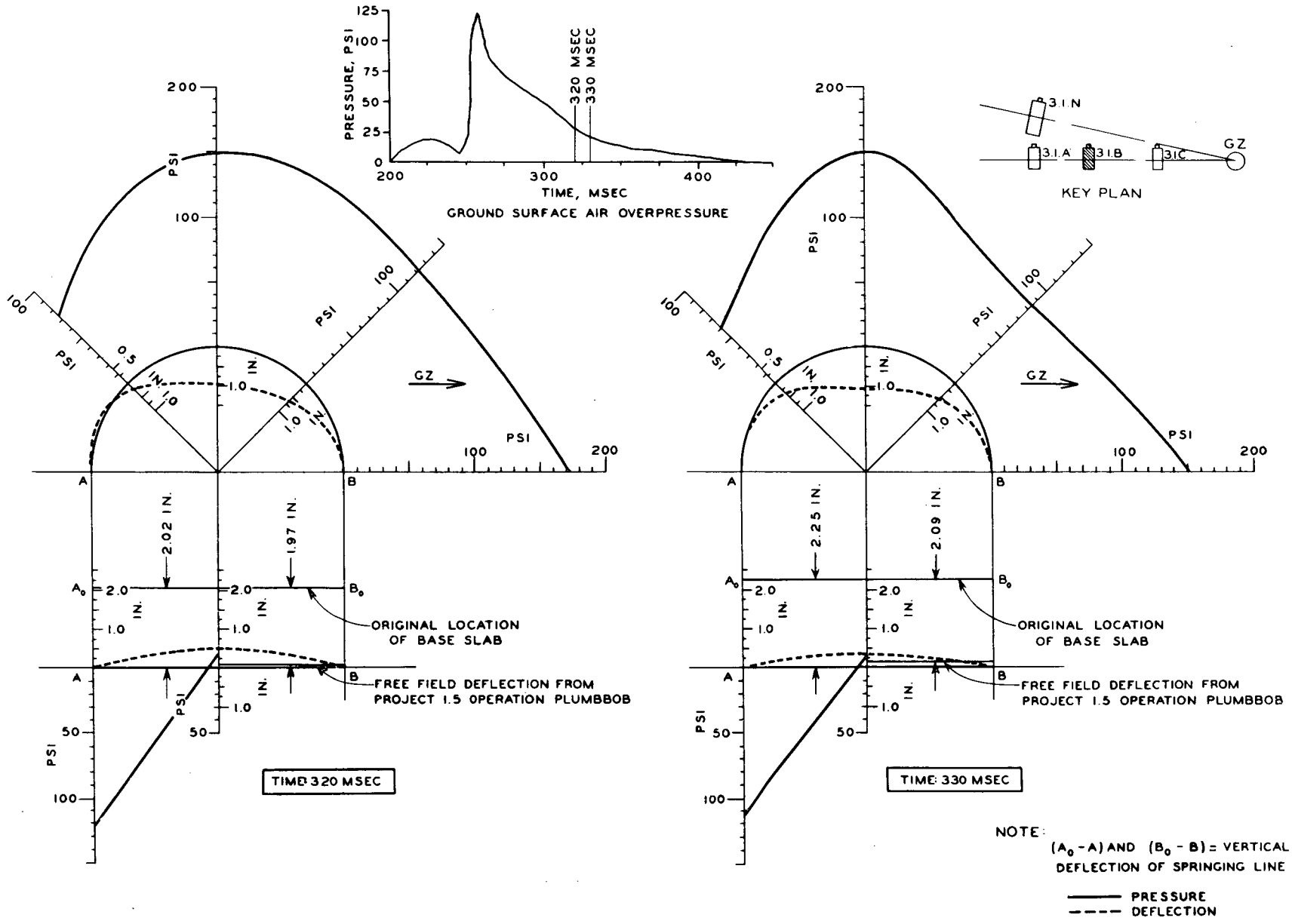

Figure 4.2 Continued.

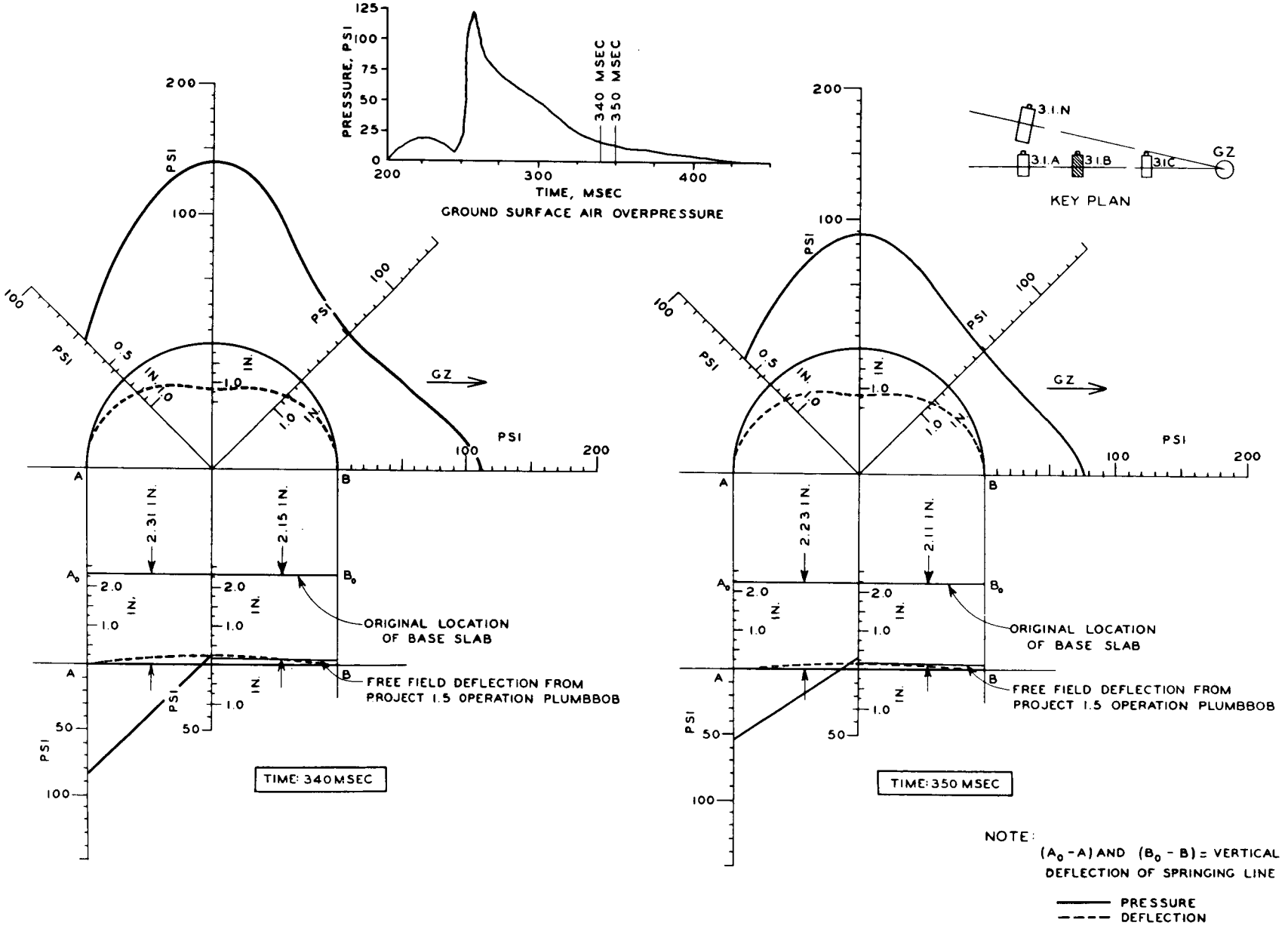

Figure 4.2 Continued.

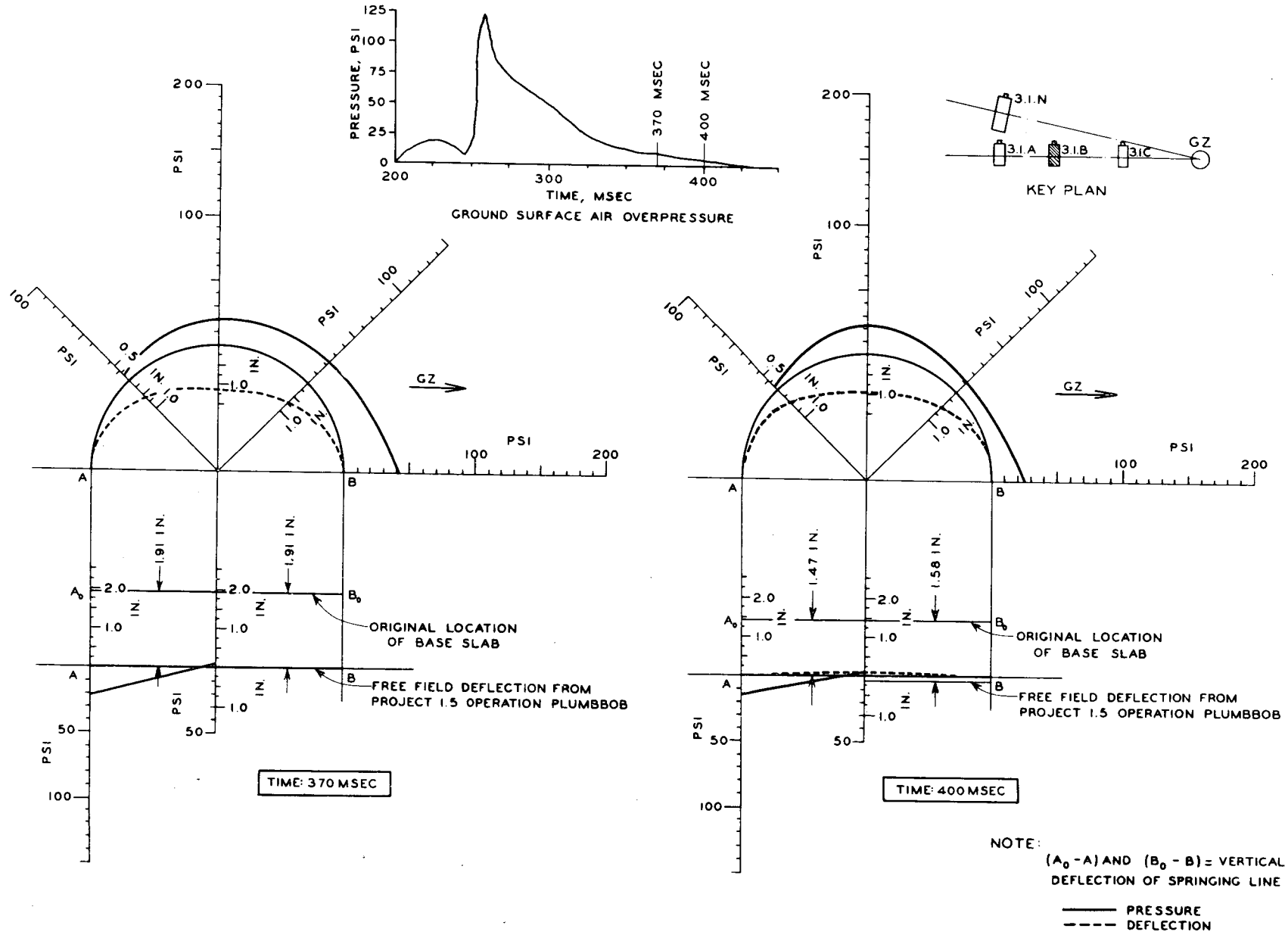

Figure 4.2 Continued.

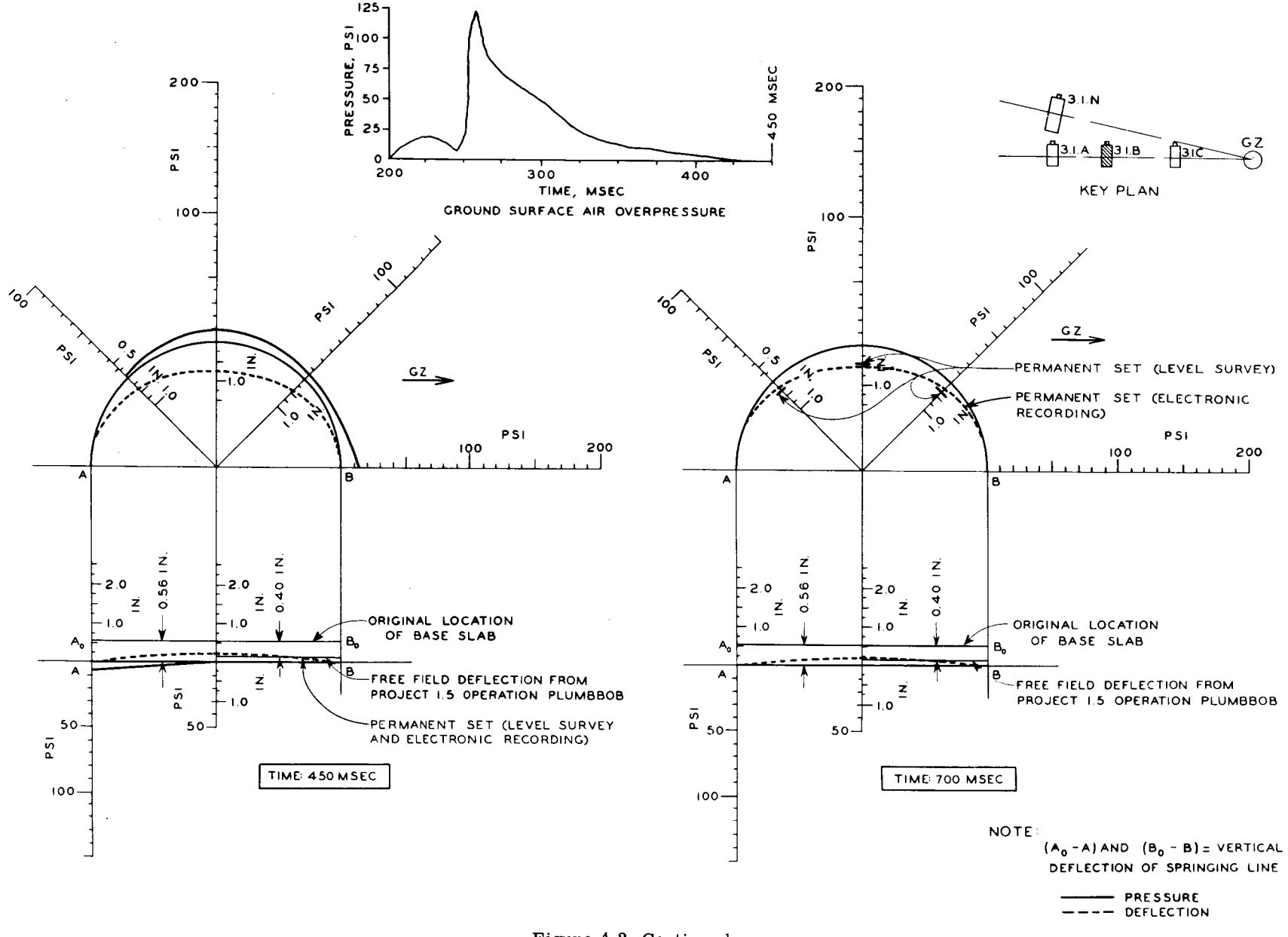

Figure 4.2 Continued.

while the pressure at the end was increasing, indicating redistribution of pressure and the initiation of cracking in the base slab.

At 280 msec: The ground-surface air overpressure was approximately 70 psi and decreasing rapidly. The earth pressure continued to build up around the arch, increasing greatly at the springing line. The pressure on the slab at the center was negative, while the pressure build-up at the end was considerable, thus indicating that by now the slab had cracked through (see Figure 3.15 for crack pattern) and that the central portion of the slab was no longer capable of carrying loads transmitted by the arch. The slab under each springing line was now acting as a wall footing, carrying the load transmitted by the arch. Rather than attempt an intuitive interpretation of the pressure distribution on the base slab, the pressure distribution is shown to be triangular although the actual pressure distribution most likely was not triangular. The relative movement of the slab was greater at the center than at the ends, thus showing that the cracked slab (footings) was being punched into the soil. The arch was beginning to respond to the main shock, showing asymmetrical deflection; the haunch on the ground-zero side moved inward while the opposite haunch moved outward.

At 300 msec: The earth pressure at the springing line increased with respect to the other earth pressures around the arch ring. This might be explained as being the at-rest pressure while the other observed pressures are active pressures being reduced by arching in the soil. On the other hand, this may be due to an outward movement at the springing line and thus be a passive earth pressure. There are not sufficient data to determine if there was any movement at the springing line, although such movement would be consistent with the general inward deflection of the arch ring. The displacement of the free-field point became greater than the displacement of the base slab.

At 320 msec: The relative increase of the springing line earth pressure continued. The relative deflection (0.5 inch) of the center of the slab with respect to the springing line reached a maximum. The springing line gross displacement exceeded that of the free-field point.

At 330 msec: The deflection curve showed an inward bending of the crown.

At 340 msec: The gross downward movement of the springing line reached a maximum value of 2.31 inches. By comparison, the peak transient downward displacement of Structure 3.1.c was 3.36 inches.

At 350 msec: The earth pressure decreased greatly while the arch deflections reached a maximum. The displacement of the base slab and the free-field soil point began to decrease.

At 370 msec: The earth pressure decreased greatly. There was no differential deflection between the center of the floor slab and the ends.

At 400 msec: The crown and ground-zero-side haunch were returning to the permanent set at a faster rate than the leeward-side haunch. The free-field point gross displacement exceeded that of the springing line.

At 450 msec: The permanent set of the floor slab is shown. The last trace of earth pressure was recorded at 500 msec.

At 700 msec: The permanent set of the arch ring is shown and is compared with the values obtained from a level survey.

The peak transient and permanent deflections of the crown with respect to the springing line are shown in Figure 4.3. The permanent deflections in this case were approximately one half the magnitude of the maximum transient deflections. These plots indicate the possibility of compiling a set of failure criteria based upon ultimate permanent set.

4.2.2 Arch Reaction. The strain information was used to determine reactions, i.e., moments, thrusts, etc., for Structure 3.1.n. A sequential plot of moment and thrust for the arch is shown in Figure 4.4. An interaction diagram of moment and thrust (using the data from Figure 4.4) for the springing line and crown is shown in Figure 4.5 along with interaction curves for the working stress of 1,350 psi for 3,000-psi concrete, the working stress of 1,900 psi for 4,210-psi concrete (actual average cylinder strength for Structure 3.1.n, Table 2.4), and the diagram for ultimate moment and thrust (Reference 15) using the dynamic strength value for 3,000-psi concrete. The diagram for ultimate moment and thrust using the dynamic value of

the measured concrete strength is not shown. The figure shows that the arch underwent appreciable bending action.

Plots of moment, vertical reaction, and horizontal reaction at the springing line for Structure 3.1.n are shown in Figure 4.6. All three plots show that the response at each springing

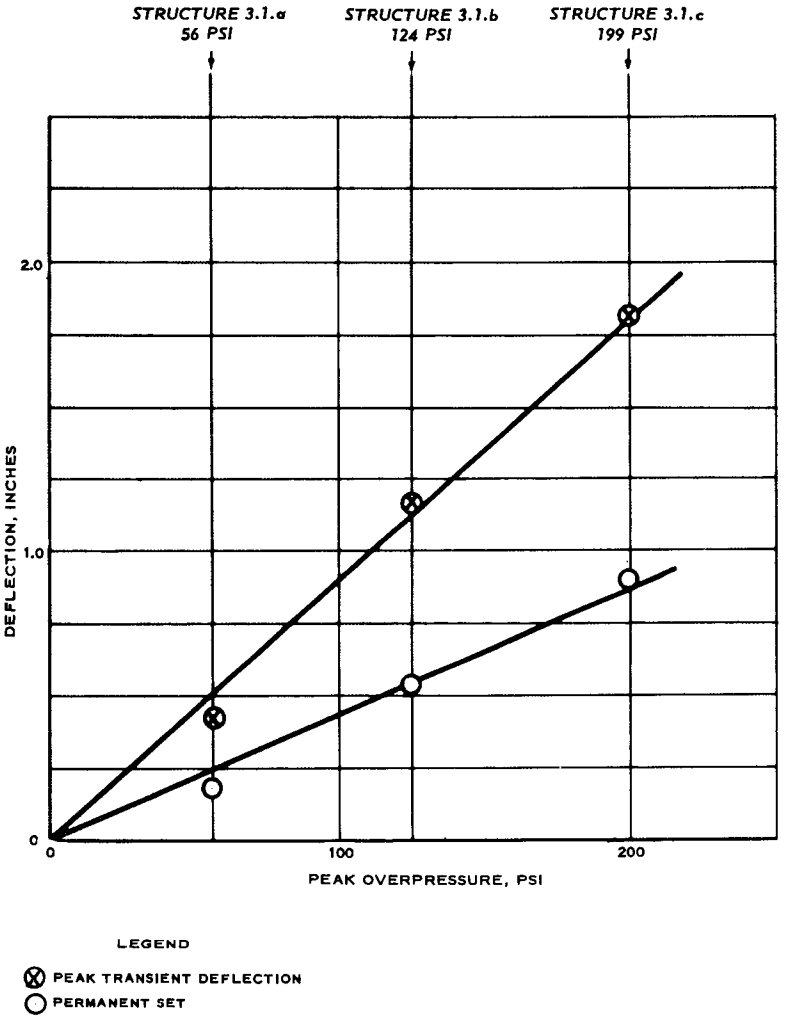

Figure 4.3 Peak transient and permanent deflections of crown with respect to springing line, Section III, Structures 3.1.a, b, and c.

line was approximately the same and that the time lag for the response at each springing line was negligible. The vertical reaction at the springing line, assuming that the ground-surface air overpressure (56 psi) is projected vertically, is as follows:

$$\text{Reaction} = \frac{56 \text{ psi} \times 12 \text{ in/ft} \times 100 \text{ in}}{1{,}000 \text{ lb/kip}} = 67 \text{ kips/ft}$$

The average value of the maximum vertical reaction for each springing line (Figure 4.6) is 65 kips per foot, which approaches the value calculated from the ground-surface air overpressure.

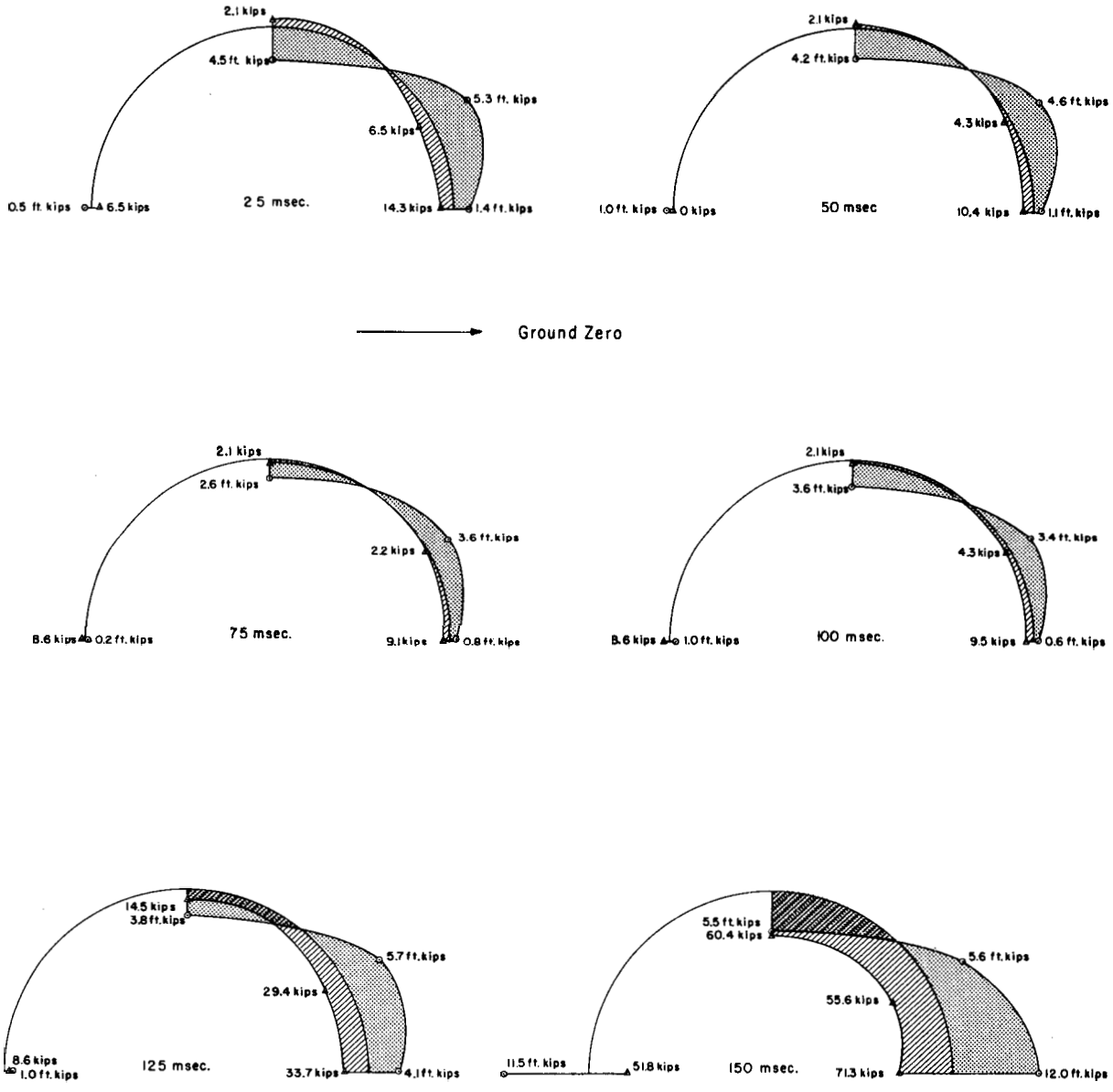

⊙= Moment, ft.-kips per ft. (Plotted on tension side).

▲= Axial Thrust, kips per ft. (Values plotted on inside are compression).

Time is after arrival of blast wave at Structure 3.1.n (T_o = 274 milliseconds)

Figure 4.4 Transient moment and thrusts, Structure 3.1.n.

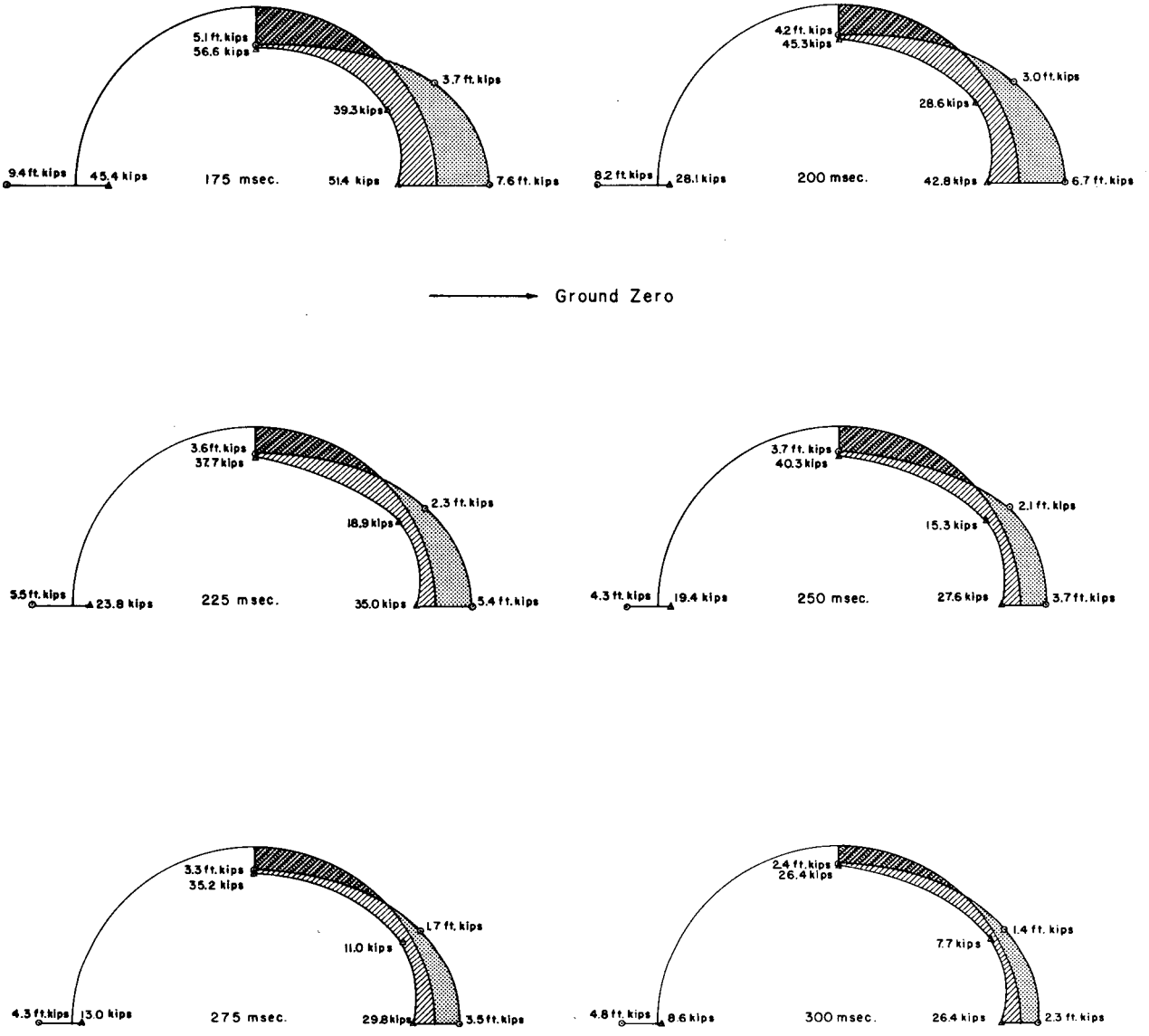

Figure 4.4 Continued.

A comparison of this average value and calculated value indicates that the vertical component of earth pressure on the structure is, for practical purposes, equal to the ground-surface air overpressure directly above the structure.

4.3 RADIATION

A method of predicting gamma radiation within buried structures (presented in Reference 13) was used to predict the average radiation within the four structures. The method assumes that radiation will follow the path of least resistance, and thus it is assumed that the radiation experienced right-angle turns as illustrated in Figure 4.7. It is also assumed that one right-angle turn attenuates radiation by a factor of $1/15$ or (6.7×10^{-2}) and that two right-angle turns attenuate

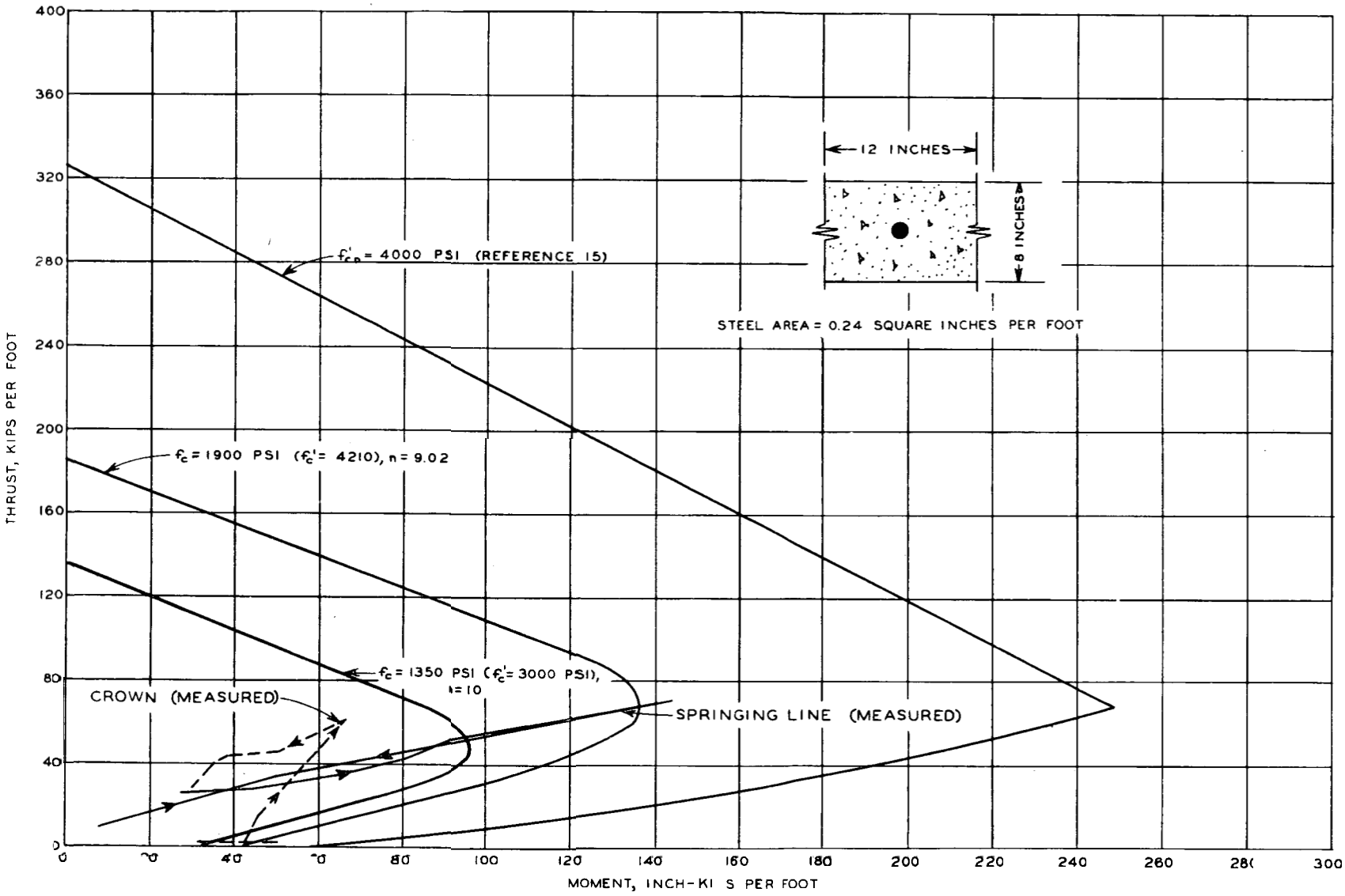

Figure 4.5 Interaction diagram for measured, design, and ultimate values of moment and thrust, Structure 3.1.n.

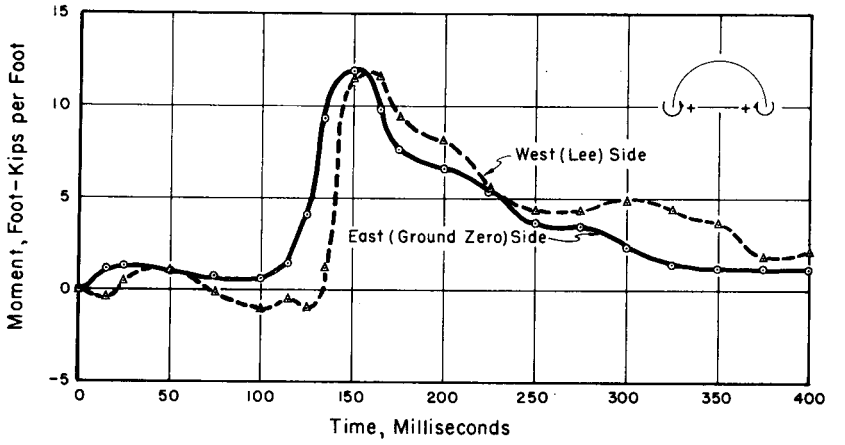

Moment versus Time

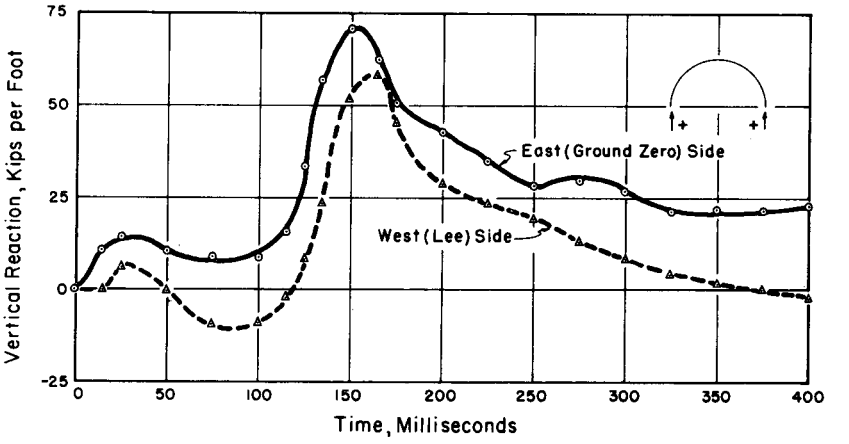

Vertical Reaction versus Time

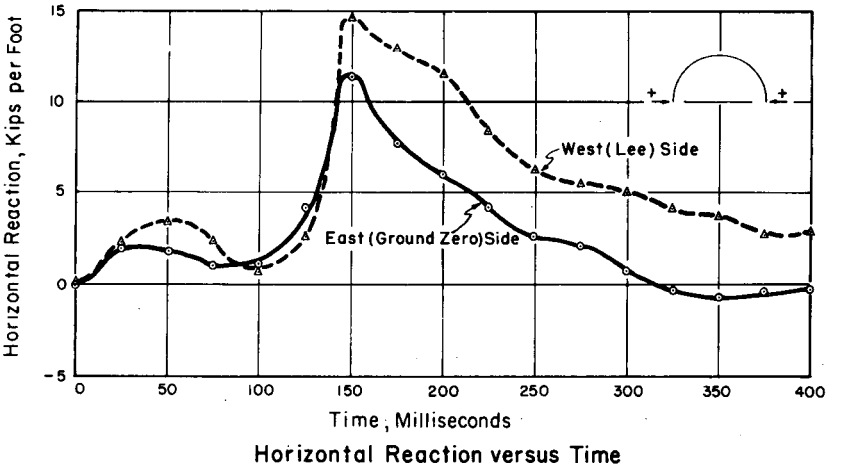

Horizontal Reaction versus Time

Note: Curves start when blast wave first hit Structure 3.1.n, at zero + 274 milliseconds.

Figure 4.6 Transient springing line reactions for Structure 3.1.n.

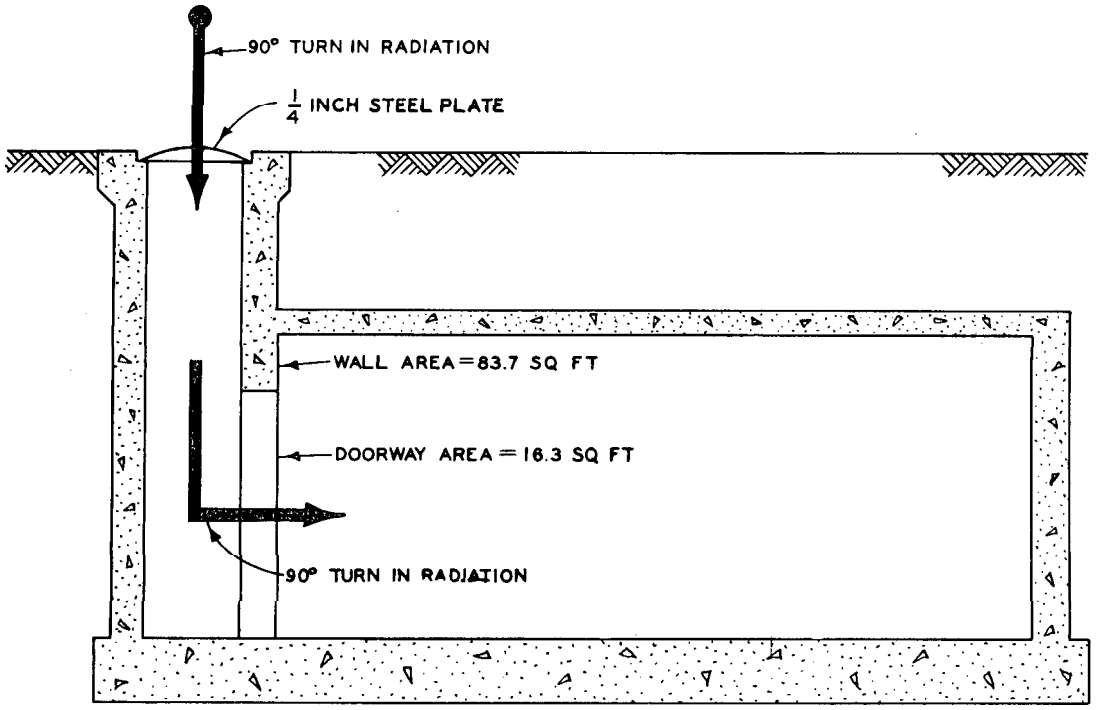

a. TRANSMISSION THROUGH ENTRANCEWAY

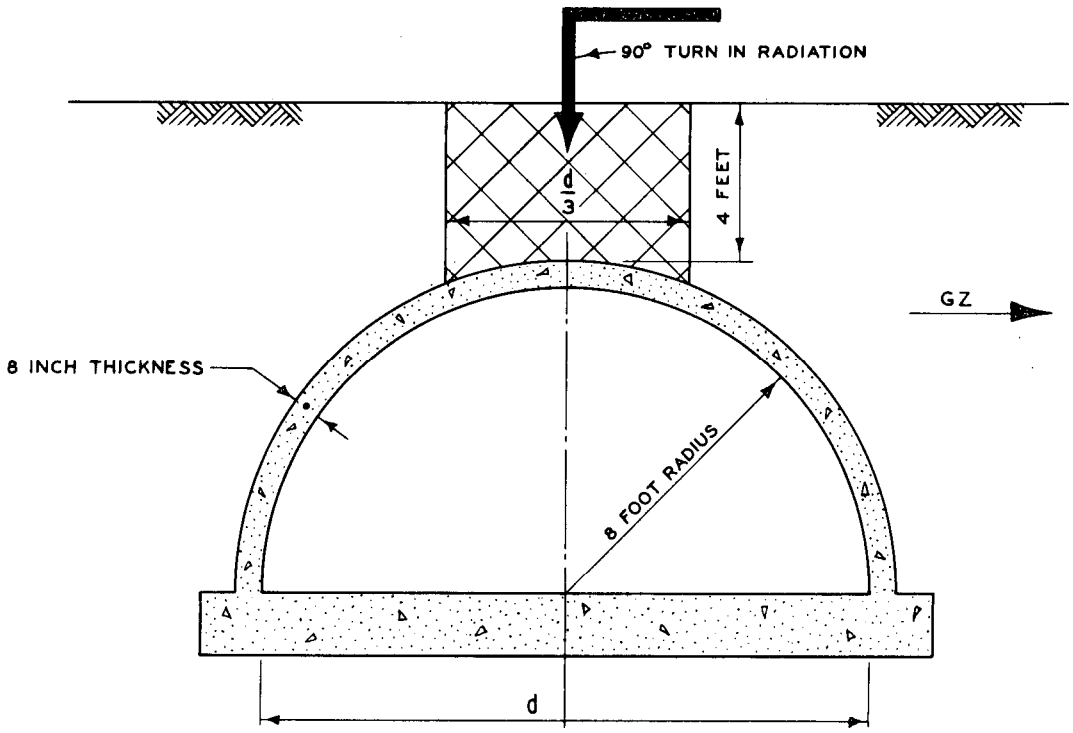

b. TRANSMISSION THROUGH EARTH COVER AND CONCRETE

Figure 4.7 Assumed transmission of gamma radiation into the 3.1 structures.

it by a factor of $1/200$ or (5×10^{-3}). In addition, it is also assumed that radiation is attenuated by the ratio of entranceway area to wall area. The attenuation factors for materials such as concrete, steel, etc., are determined in Reference 14.

Since radiation enters structures of the 3.1 type in two ways, (1) through the entranceway, and (2) through the earth cover and concrete arch section, the attenuation factors for the two paths of radiation must be determined. The calculations are as follows:

The attenuation factor (A_t) for entranceways can be determined by means of the following formula:

$$A_t = A_d \times A_s \times A_a$$

In this formula, A_t = total attenuation factor

A_d = attenuation caused by two right-angle turns in radiation transmission = 5×10^{-3}

A_s = attenuation factor for $1/4$-inch steel plate = 9×10^{-1}

A_a = attenuation effect determined by the ratio of entranceway area to wall area = $16.3\ ft^2 \div 83.7\ ft^2 = 2 \times 10^{-1}$

Thus, A_t is determined to be 9×10^{-4}.

The attenuation factor (A_t) for earth cover and concrete arch can be determined by means of the following formula:

$$A_t = A_d \times A_e \times A_c \times A_a$$

In this formula, A_t = total attenuation factor

A_d = attenuation caused by one 90-degree turn in radiation transmission = 6.7×10^{-2}

A_e = attenuation factor for 48 inches of soil = 5×10^{-3}

A_c = attenuation factor for 8 inches of concrete = 3.5×10^{-1}

A_a = area effect = $1/3\ d^* \div d = 3.3 \times 10^{-1}$

Thus, A_t is determined to be 3.9×10^{-5}.

The attenuation factors, as calculated above, were used to predict the radiation within the structures and the resulting values are shown in Table 4.1 along with measured radiation values taken near the center line of the structures. It is interesting to note that the predicted values of internal gamma radiation intersect the curves shown in Figures 3.12 through 3.15 at distances of 5 to 8 feet from the entranceway.

4.4 ACCOMPLISHMENT OF OBJECTIVES

The general and specific objectives listed in Chapter 1 are repeated here along with a statement regarding how well they were accomplished.

General Objective. "To determine the suitability of underground concrete arches as protective shelters as well as their resistance in the high-overpressure ranges (50 to 200 psi)

---

* The use of a "radiation-window" width of d/3 is arbitrary. It represents an attempt to find a correlation between the increase of "window" width and an increase in attenuation due to increased soil thickness.

TABLE 4.1 COMPARISON OF PREDICTED WITH MEASURED GAMMA RADIATION DOSE WITHIN THE STRUCTURES

Structure	Free Field Gamma Dose	Predicted Internal Gamma Dose			Measured Gamma Dose*
		Attenuation Factors			
		Entranceway (9×10^{-4})	Soil and Concrete (3.9×10^{-5})	Total	
	r	r	r	r	r
3.1.a and n	1.05×10^5	95	4	99	45
3.1.b	2.0×10^5	180	8	188	125
3.1.c	3.0×10^5	270	12	282	210

* Measured 13.3 feet from door in 3.1.a, b, and c, 16 feet from door in 3.1.n.

from a kiloton-range air burst." The resistance of the 3.1-type structures to high overpressures was proved to be adequate.

Specific Objectives.

1. "To compare the response of four underground concrete arch structures when subjected to controlled loading ranging from design load through failure load." Even though the close-in structure did not fail, the comparisons of the responses of the structures at the three overpressure levels has provided valuable data concerning the behavior of such structures under three loads.

2. "To determine the load distribution on a buried arch due to a nuclear blast." The load distribution was determined and compared to the ground-surface air overpressure even though the magnitude of certain earth-pressure records was questionable.

3. "To gain a better understanding of the basic response of that portion of the arch element which is in no way affected by restraint or support from the end walls." Analysis of the data showed that the response of the arch was significant in both bending and compression. From the available data it is not known to what degree the end walls restrained arch action at the central portion of the structures.

4. "To determine to what extent the end walls of an underground arch affect its response." It was found that the end walls restrain the arch for a distance ranging from approximately one to one and one half times the arch radius.

5. "To study the interaction of the soil and the structure to establish an idealized soil-structure system that could be adapted to analytical treatment." Although the magnitude of certain earth-pressure values is questionable, the interaction of the soil and structure was compared. The sum of the vertical reactions at the springing lines for Structure 3.1.n was essentially equal to the total air-overpressure load directly above the structure. The value of the horizontal component of earth pressure is of paramount importance since it can greatly increase the structural resistance of the arch by providing an opposing reaction. Test results indicated that the ratio of horizontal to vertical earth pressure is closer to 0.5, which is much greater than the previously accepted value of 0.15 (References 6 and 7). A more accurate knowledge of the horizontal to vertical pressure ratio must be known before any idealized system can be developed.

6. "To determine the amount of protection from radiation provided by the structure." The protection was determined and is graphically presented in this report. It is evident that the additional protection from several half-value layer thicknesses of material located between the hatch cover and interior of the structure would reduce the gamma dose to a tolerable value even at the 200-psi air-pressure range.

7. "To gain information that will be of direct use in establishing the design criteria for a prototype cast-in-place concrete personnel shelter." Several methods of loading have been presented (Figures 1.1a, 1.2 and A.1) but the final selection of loading criteria cannot be made until failure is produced in one of the structures during some future test.

Chapter 5
CONCLUSIONS and RECOMMENDATIONS

5.1 CONCLUSIONS

The following conclusions are based on the behavior of the soil-structure combination described herein and are limited to similar combinations subjected to similar loads.

The 3.1-type structure proved to be an adequate shelter for resisting air overpressure of up to 200 psi, thereby showing that an underground reinforced-concrete arch is an excellent type structure for use in providing protection against nuclear-blast effects.

A reasonable design method for underground arches cannot be developed until more is known about the dynamic properties of soil-structure combinations. In this case it was observed that the earth pressure distribution around the relatively stiff arches were nonuniform and slightly asymmetric, thus causing the arch to undergo appreciable bending. The transient earth pressures exerted on structures of this type were greater at some points than the ground-surface air overpressure. This seems to be due to a combination of reflected and passive earth pressures.

The earth-overpressure distribution around a relatively rigid arch structure is nonuniform and the arch element undergoes appreciable bending.

The horizontal earth pressure resulting from ground-surface air overpressure is apparently greater than had been previously anticipated.

Displacement of the 3.1 structures as a whole, as well as the relative deflection of the crown, is directly proportional to the overpressure. During transient loading, a test structure buried in the Frenchman Flat soil moved at approximately the same rate and magnitude as the free-field surrounding soil.

The end walls affect arch action for a distance of about $1\frac{1}{2}$ times the arch radius.

Strain gage measurements of the test structure at the 56-psi level yielded valuable information for determining moments and thrusts in the arch. Plane sections before loading remained plane during loading. The vertical reactions at the springing line were approximately equal to the ground-surface air overpressure times the vertical projection of the arch structure. The largest moments and thrusts occurred near the springing line, and this would be the probable location of any failure.

The simple entranceway used for the structures sealed out the air pressure. It was not designed to attenuate radiation and thus did not provide adequate radiation protection for personnel.

At high-pressure levels (greater than 100 psi), floor slabs that are monolithic with the arch receive relatively high magnitude loads and accelerations, which may make it necessary to use shock-mounted flooring in order to reduce possible adverse physiological effects.

5.2 RECOMMENDATIONS

It is recommended that the use of footings be investigated for arch-type structures. The floor slab of the structure could be made much thinner and poured separately, then joined to the footing with some type of flexible water seal. This method of connection would most likely reduce the induced acceleration to the floor slab caused by the air-induced ground shock. The design method as shown in Reference 5 may continue to be used until refinements to the procedure are determined or a new procedure is presented. The significant bending measured in Structure 3.1.n points out that the procedure which is based on compression solely from the dynamic load may not be as conservative as believed previously. The entranceway should be modified for actual

use to reduce the radiation admitted to the interior of the structure. This could be accomplished in several ways, depending on the intended use of the structure: one method would be to use the existing entranceway but add baffle walls within the structure; another would be to utilize an entranceway separated from the structure by at least one 90-degree, horizontal turn.

The 3.1-type structures should be exposed to much higher overpressures during future tests. Deflection measurements to determine outward movement of the springing line should be made, in addition to determinations of the excursions of points located at 30, 45, 60, and 90 degrees on the arch intrados. The apparent success of using strain gages in determining reactions shows the usefulness of this type of gage for use in future tests.

The results of the simple model tested in the laboratory points up the possibility of this type test in determining: failure modes, deflection patterns, the effect of various soil types on the ultimate load-carrying capacity of structural elements, and the verification of design methods. It is recommended that a model testing program be initiated and also that full-scale tests be conducted to verify the predicted values obtained in the model tests. Since the cost of building and testing models is small compared to the cost of prototype structures, a large number of model tests could be performed so that statistical results for a wide variety of test conditions can be obtained.

Appendix A[1]
IDEALIZED LOADING CRITERIA

Further analytical development and tests resulting in structural failures will be required to verify the adequacy of any method of calculating the overpressure required to cause collapse of a buried arch. In the interim, any recommendations for loading criteria must be considered to be tentative.

Further analytical development and tests resulting in structural failures will be required to verify the adequacy of any method of calculating the overpressure required to cause collapse of a buried arch. In the interim, any recommendations for loading criteria must be considered to be tentative.

A.1 DISCUSSION

It is possible to develop analyses accounting for the contribution of passive soil pressure to the resistance of the arch which are rigorous to the extent of providing a soil reaction in the region of outward movement which is proportional to the radial deflection. Reference 8 presented a less sophisticated attempt to account for this passive soil pressure by use of an inward acting soil loading at the haunches. A correlation of either method with test results to provide worthwhile loading criteria does not appear to be practical at this time.

Serious consideration was also given to the possibility of using a simple variable to express the influence of arch flexibility and soil properties. This approach was found to be impractical in the present state of the art, due to the impossibility of assigning a definite numerical value to this variable.

Methods which fail to account for arch flexibility and soil properties may not result in optimum design of arches with large rise to span ratios. However, until the variables involved can be properly isolated these methods seem to be necessary, and are probably adequate provided that (1) sufficient ductility is provided in the arch to permit large deflections without collapse, and (2) suitable backfill, properly compacted, is used. For arches with high rise to span ratios requirement (1) seems more important than providing a high moment capacity.

The concept of modal loadings (References 16 and 17) is a reasonable way of providing the necessary resistance against several possible types of failure. Some of these modes may not be critical for a given arch shape or span, but, nevertheless, should be included to avoid overlooking a critical condition in other cases.

To be acceptable, any criteria presented should include one or more loadings producing bending in the arch in order to provide a minimum flexural strength which might otherwise be lacking. The difficulty lies in determining just what this minimum should be. There appears to be no alternative to basing this esti mate on a guess as to the collapsing overpressure for these arches.

Three loadings, designated A, B, and C, are presented (Figure A.1), the first being identical with Loading (1a') of Reference 16. Loading B alters Loading (1b') of Reference 16, reducing its severity by limiting the amount of thrust to be considered in combination with the bending moment. This gives a result more nearly in accord with the conclusion, based on the permanent deformation pattern of Structure 3.1.c, that failure will not occur in an antisymmetrical mode. Loading C is a variation of loading (1c') of Reference 16, modified to predict the anticipated collapsing overpressure for this arch. Provisions are included for considering the transient nature of Loadings B and C.

In the case of semicircular arches the bending moment from Loading C is very much less than that which would be obtained with the same peak overpressure uniformly distributed over the horizontal projection of the arch. Most of this reduction is attributable to the buttressing action of the soil around the haunches. In the case of flatter arches this action may not be developed to the degree attained in a semicircular arch. On the other hand, as the rise to span ratio decreases, the bending moment from Loading C begins to approach, and finally exceeds, that which would be obtained with the peak overpressure uniformly distributed over the horizontal projection, so that the influence of buttress action becomes relatively less important with decreasing rise to span ratios. This creates an uncertain situation that would require further study, and probably tests, for clarification. Because of this, applicability of the criteria given here to arches having rise to span ratios of less than about $\frac{1}{4}$ may be questionable.

In establishing the resistance of the arch for blast loading conditions ultimate strength methods should be used which account for redistribution of moment due to formation of yield hinges. Increased yield stresses

[1] Using the data from Appendix B, the firm of Holmes and Narver, Inc., performed a postshot analysis for WES (Reference 15). The most significant results were the idealized loading criteria contained in Chapter 5, which has been reproduced here as Appendix A.

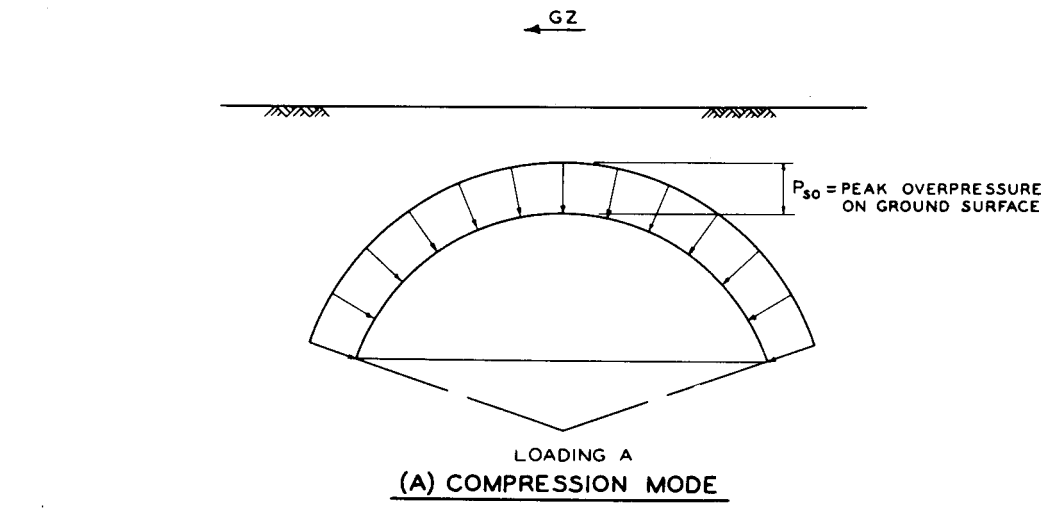

(A) COMPRESSION MODE

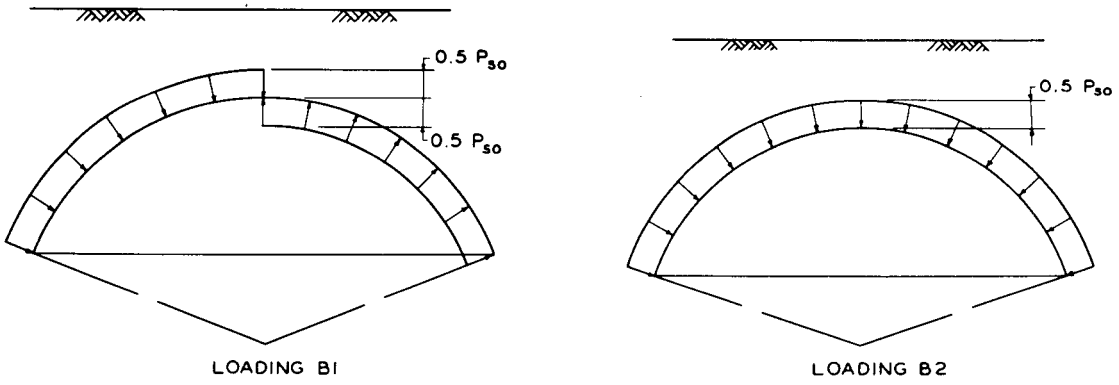

(B) DEFLECTION MODE

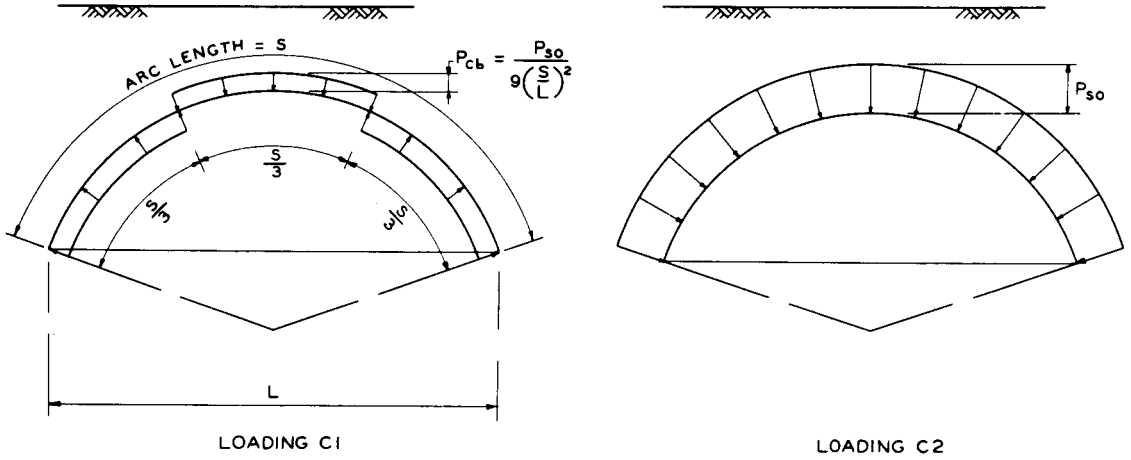

(C) COMPRESSION-BENDING MODE

Figure A.1 Recommended idealized loadings.

appropriate to dynamic loading should also be used. If the proportions of the structure indicate appreciable shell action, this should be accounted for in the design, and the structure should be reinforced as required to carry shell stresses in addition to those resulting from arch action.

It should be emphasized that in practice this loading criteria, or any other aimed at predicting the collapsing overpressure, may not control the design. Depending on the occupancy or function, the structure may become unserviceable at an overpressure much less than that corresponding to total collapse.

A.2 RECOMMENDED LOADS

The following three load conditions are recommended for design of completely buried reinforced concrete arches.

Loading A (Compression Mode): A static uniform radial load acting inward with an intensity equal to the peak overpressure at the ground surface (Figure A.1a).

Because the period of vibration of the arch in this type of loading is relatively short compared to the rise time of the overpressure, the overpressure should be regarded as a steady state load rather than a transient load. The factor of safety against buckling should not be less than 1.0 and the axial thrust should not exceed the yield capacity of the arch section.

Loading B (Deflection Mode): A combined loading (Figure A1b) consisting of parts B1 and B2 as follows:

1. A uniform radial load acting inward on the side adjacent to the blast, acting simultaneously with a uniform radial load of the same intensity acting outward on the far side. The intensity of the load should be equal to 50 percent of the peak overpressure acting at the ground surface.

2. In combination with load B1, a uniform radial load acting inward over the entire periphery with an intensity equal to 50 percent of the peak overpressure acting at the ground surface.

With negligible error, the load B1 can be assumed to decay linearly from the initial peak value to zero in the time required for the shock wave to travel across the structure, and the load B2 can be considered as a steady state load.

The required resistance should be computed by considering loading B1 as a dynamic rather than a static load. For analysis purposes the period of vibration of the arch for this loading condition can be calculated as that of a beam with a length equal to the developed length of the arch from springing line to crown. Consider the beam to be hinged at the end corresponding to the crown of the arch and to have the same support condition at the other end as that existing at the base of the arch. The period of vibration should allow for the weight of earth cover over the arch between crown and springing line, and for the effect of axial thrust.

When the relative amounts of thrust and moment place the arch section in the compression regime, the gross concrete section should be used in computing the period of vibration.

Due to the short duration of this load condition, buckling may be ignored.

Loading C (Compression-bending Mode): A combined loading (Figure A.1c) consisting of parts C1 and C2 as follows:

1. A uniform radial load acting inward, and over the central one third of the length of the arch axis, with a uniform radial load acting outward on the outer thirds. The intensity, P_{cb}, of the load on the central one third of the arc should be varied as a function of the length, s, of the arch axis, and the span, L, according to the formula:

$$P_{cb} = \frac{P_{so}}{9\left(\frac{s}{L}\right)^2}$$

2. In combination with load C1, a uniform radial load acting inward over the entire periphery with an intensity equal to the peak overpressure at the ground surface.

The load C1 should be considered to have the same variation with time as that of the overpressure on the ground surface. In lieu of this, an equivalent linear approximation of the variation with time may be used. The load C2 can be considered as a steady state load.

The required resistance should be computed by considering loading C1 as a dynamic rather than a static load.

The period of vibration for this loading condition should be computed as that of a simply supported beam with a span equal to one third of the total length of the arch axis, and should allow for the weight of earth over this portion of the arch, and for the effect of axial thrust.

Only the central portion of the arch should be investigated, assuming simple support at the points of load reversal. The effect of thrust from load C2 on moment capacity and buckling of the arch should be considered.

If the relative amounts of thrust and moment place the arch section in the compression regime the gross concrete section should be used in computing the period of vibration and the critical buckling load.

The resistance of the outer thirds of the arch should not be less than that provided in the central portion.

Application of this loading criteria, neglecting

shell action, gives the following results for these arches:

Loading	Approximate Collapsing Overpressure (psi)
A	450
B	520
C	310 to 370

[The above collapsing overpressures for the 3.1 arch structures are based on a concrete strength of 4,800 psi and a dynamic increase factor of 33 percent. The stresses due to dead load are neglected.]

Loading C gives the critical condition for these arches, and probably would control in nearly all other cases. The upper limit for Loading C is obtained by, (1) using a low value for the estimated effective duration of the overpressure, (2) using the gross concrete section in calculating moment capacity, neglecting the steel, and (3), neglecting buckling. Neglecting buckling may be realistic for a short span semicircular arch, but it is believed that buckling should be considered for longer spans.

The lower limit for Loading C is obtained by, (1) using a higher estimated value for the effective duration of the overpressure, (2) using the cracked section in calculating moment capacity, and (3) considering buckling.

Loading C predicts a substantial decrease in collapsing overpressure under a long duration pulse.

Appendix B'

INSTRUMENTATION of STRUCTURES 3.1.a, b, and c

B.1 QUANTITY AND LOCATION

Two general types of gages were used: electronic recording and mechanical self-recording. A total of 16 electronic earth-pressure gages, 6 electronic accelerometers, 9 electronic deflection gages, 6 self-recording pressure gages, and 8 self-recording deflection gages were employed. Table B.1 lists the ranges and positions of these gages. Figure 2.11 shows the actual locations of gages on the structures.

B.2 GAGES

B.2.1 Accelerometers. Acceleration measurements were made with Wiancko Type 3 AAT accelerometers (see Figure B.1). The sensing element consisted of an armature bonded at its center to the vertex of a V-shaped spring member and held in close proximity to an E-coil (see Figure B.2). The E-coil was composed of two windings wound on the extreme legs of an E-shaped magnetic core. As the armature rotated, it decreased the reluctance of the magnetic path defined by the armature, the center leg, and one extreme leg of the E and increased the reluctance of the other, similar path. A weight, the size of which depended upon the range of the accelerometer, was attached to one end of the armature so that an acceleration in a direction normal to the armature caused it to rotate about the vertex of the spring. With the windings of the E-coil connected into a full-impedance bridge, an unbalance voltage roughly proportional to the applied acceleration could be obtained.

The accelerometer was also sensitive to rotational accelerations — it could not be used where these were present. The stiffness of the spring was such that linear accelerations were measured only in the desired direction. The accelerometers were oriented in the vertical direction for these structures.

The natural frequency of a 5 g accelerometer was approximately 70 cps; of a 100 g accelerometer, approximately 450 cps. The gages were damped to 0.70 of critical at a temperature of 80 F.

The accelerometers were mounted on the floors spaced from the concrete by a $\frac{3}{8}$-inch-thick lead washer to dampen out unwanted high-frequency components. Three properly spaced threaded studs were fixed into the concrete. The gage was positioned so that three holes drilled in a flange around one end of the gage case were fitted over the studs. Thus, the gage was mounted with its sensitive axis (the axis of the cylindrical case) lying parallel to the direction of the acceleration that was being measured.

B.2.2 Soil Pressure Gages. The earth-pressure measurements were made with a Wiancko Type 3-PE footing stress gage (see Figures B.3 and B.4). The sensing mechanism was formed by two inflexible circular plates separated by a spring seal around their edges. One of the plates was bored concentrically and the hole was covered by a flexible diaphragm flush with the outside surface of the plate. Thus, two adjoining chambers were created: one formed by the volume between the two circular plates and a smaller one formed by the volume of the drilled hole. The chambers were filled with fluid so that when pressure was applied squeezing the two plates together, the flexible diaphragm was bulged outward. This motion was coupled to an armature (see Figure B.4) and caused it to rotate near an E-coil of the type described in Paragraph B.2.1. The bored plate was the base for the gage and was placed against the footing. As pressure was applied, the motions of the solid plate and the the flexible diaphragm were in the same direction, but the amplitudes of their motions were in inverse proportion to their respective areas.

Two methods of mounting the earth-pressure gages were employed. In each, provision was made for allowing a solid, flat surface for support of the gage base plate and an even distribution of pressure over the sensitive plate. Where measurements underneath a structure were to be made, a square hole was left in the concrete floor slab so that after calibration the gage could be lowered into the hole with its sensitive face directly flush against the ground. Reinforcing bars were welded to existing bars in the walls of the holes; thus, when concrete was poured into the hole, the gage was cast into a block which was essentially a part of the structure. The ground under the sensitive plate was prepared to allow even distribution of pressure; the concrete incased the base plate firmly.

Where measurements were made on the sides or the top of the structures, a hole the size of the housing of the gage-sensing mechanism was cast in the wall of the structure. The gage was then set against the structure, with the sensing-mechanism housing

[1] By H. S. Burden, Project 3.7, Ballistic Research Laboratories, Aberdeen Proving Ground, Maryland.

fitting into the hole and the base plate resting squarely on the structure surface. A length of pipe, threaded over the gage cable, was screwed into the sensing-mechanism housing so that it extended through to the inside of the structure. Over this pipe, the following were placed in sequence: a washer having diameter greater than that of the hole in the wall, a helical spring, and a nut which screwed onto the end of the pipe to compress the spring. The force produced in the compressed spring held the gage firmly against the outside surface of the wall. A fairing of Calseal grout (a plaster-of-Paris-type material) was applied around the gage to smooth the contours of the installation (see Figure B.10). During the backfill operation, a square box was placed over the gages and removed when the level of the backfill was above the gage. Backfill soil was placed into the resulting void in 2-inch lifts and carefully hand-tamped until the void was completely filled.

An additional gage, E10.1 in Structure 3.1.b, was installed on the top of the structure using a mounting method similar to that used for the other gages on the tops of the structures, except that the grout fairing was omitted. This gage was placed adjacent to gage E10 of the same structure. A comparison of the records may be found in Figure B.12.

allowed the spring to be wound to and held at a high value of torque prior to installation of the wire; releasing the ratchet applied tension to the wire.

Modulation of the voltage applied to the gage was obtained by two methods.

The first method, for gages with a range greater than 1 inch, was a continuous-rotation wire-wound potentiometer connected to the pulley shaft. The housing of this potentiometer, rather than being permanently fixed to the gage casing, could be rotated by a knob with a calibrated scale. By rotating this knob in a direction opposite to the expected rotation of the deflection-gage pulley, the pulley rotation could be exactly simulated, and by means of the calibrated scale, the magnitude of the corresponding deflection determined. This procedure was followed in calibrating the recording channels used with this gage (see Section B.4); the potentiometer was then locked in place.

The second method, for gages with a range of 0 to 1 inch, used a linearly variable differential transformer as a variable-impedance element. The hollow, cylindrical armature of this transformer was threaded over the gage wire and clamped in place; the solenoid winding of the transformer, inside which the armature moved axially, was held by a rigid frame. Thus the

TABLE B.1 GAGE RANGES AND POSITIONS

Structure	Gage Type	No. of Gages	Ranges
3.1.a	Accelerometer	2	25 g, 10 g
	Earth Pressure	1	25 psi
	Deflection	3	0-1 in.
	Self-recording Pressure	2	50 psi, 25 psi
3.1.b	Accelerometer	2	50 g, 25 g
	Earth Pressure	8	100 psi
	Deflection	3	1-6 in.
	Self-recording Deflection	4	1-6 in.
	Self-recording Pressure	2	100 psi, 25 psi
3.1.c	Accelerometer	2	100 g, 50 g
	Earth Pressure	7	200 psi
	Deflection	3	1-6 in.
	Self-recording Deflection	4	1-6 in.
	Self-recording Pressure	2	200 psi, 100 psi

B.2.3 Electronic Deflection Gages. The deflection gages were mounted on the inside surface of the structures. Referenced to a point on the floor by means of hardened steel wires, the gages measured the relative displacements between the points of attachment.

The wire was wrapped around a pulley mounted on a shaft supported by journals in each end of the gage case (see Figure B.5). A heavy coil spring inside the case applied torsion to the pulley shaft so that the wire was held in tension and would wind on or off the pulley as the surfaces moved. A ratchet on the pulley shaft

gage sensed directly the linear motion of the displacement, and the pulley arrangement served only to produce tension in the wire.

The coil was not permanently fixed to its support, but to simulate a motion of the armature, the coil could be moved with respect to the stationary armature by a calibrated vernier provided for that purpose. This device was used in calibration (see Section B.4.3); after calibration, the coil was locked into position.

The tension in the steel wire was about 60 pounds, and the gage was able to follow a deflection rate of 25

ft/sec. The gages were mounted on embedded plates anchored to the inside surfaces of the structure.

B.2.4 Self-Recording Deflection Gages. These gages used a spring-loaded pulley and wire system identical to that used for the electronic deflection gages (Figure B.5). The potentiometer in the electronic gages was, however, replaced by a machined screw which converted the rotary motion of the deflection gage pulley to a small linear motion of a stylus. The stylus scratched a record of its excursions on an aluminized glass disk which was rotated by a precisely governed, battery-operated motor (Figure B.6), producing a record of deflection versus time. The maximum amplitude was proportional to the screw pitch and inversely proportional to pulley diameter.

Response characteristics and mounting of these gages were identical to those for the electronic deflection gages. Initiation of the disk-motor operation was by means of Edgerton, Germeshausen and Grier (EG&G) timing signals received 5 seconds before detonation time.

B.2.5 Self-Recording Pressure Gages. The principal element of this gage is a pressure capsule which expands as pressure is applied to its interior. A record of the expansions is scratched on an aluminized disk as it is rotated by an accurately governed motor.

This capsule is, basically, a chamber formed by welding together at their edges two diaphragms, each of which is impressed with a series of concentric corrugations. Pressure is transmitted to the inside of the element through an inlet port which passes through a heavy brass mounting flange. In operation, the element is mounted on the inside of the gage baffle plate with the inlet port of the element lining up with the pressure hole in the baffle plate. Thus the blast pressures are transmitted to the inside of the element, while the outside is held at the constant pressure sealed inside the gage casing. This causes the element to bulge and move the stylus out from the element mount a distance dependent on the pressure.

Without the concentric corrugations, elements of this type display severe nonlinearity of deflection versus pressure. In a corrugated element, however, each of the sections bounded by one of the corrugations is sensitive to essentially one small range of pressures and responds linearly over that range. Over the total range of the element, which is the sum of the ranges of all the sections, the response is therefore practically linear. The actual value of linearity is ±0.5 percent.

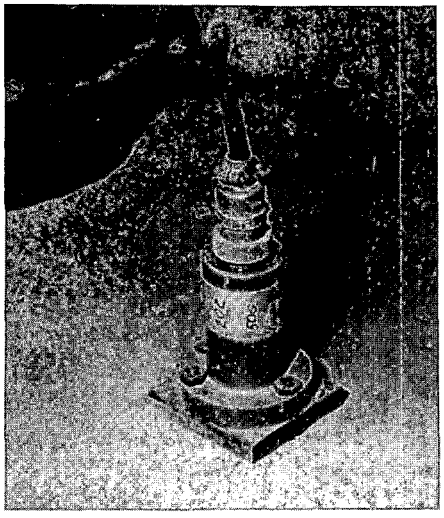

Figure B.1 Wiancko accelerometer.

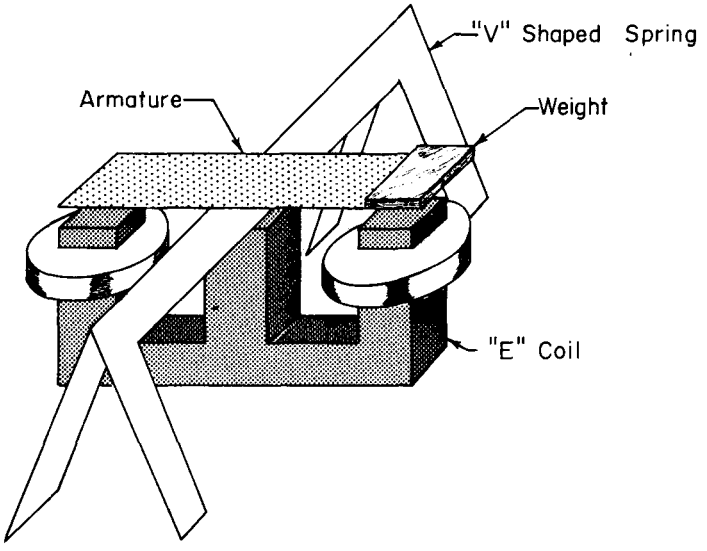

Figure B.2 Schematic drawing of accelerometer sensing mechanism.

B.3 METHODS OF RECORDING DATA

B.3.1 Electronic Recorders. Each electronic unit recorded twenty channels of information on a magnetic tape 35 mm wide. For each channel, a phase-modulated information signal and a reference signal were supplied. Phase modulation was obtained by combining the 3,750-cps amplitude-modulated output signal from the gage with another signal of 3,750 cps but 90 degrees different in phase. The reference signal (7,000 cps) was mixed with the information signal; the two were simultaneously amplified and then recorded on the same magnetic track. Thus, the reference signal was subjected to exactly the variation in amplifications or tape characteristics experienced by the information signal, and their relative phase was maintained unchanged.

Also, a sharp, amplitude-modulated detonation-time marker was recorded on one magnetic track set aside for this purpose.

The playback separated the reference and the in-

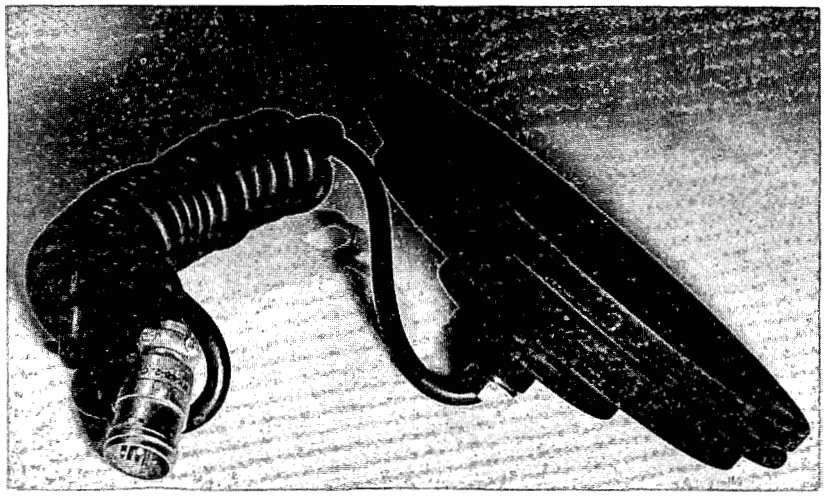

Figure B.3 Wiancko-Carlson soil pressure gage.

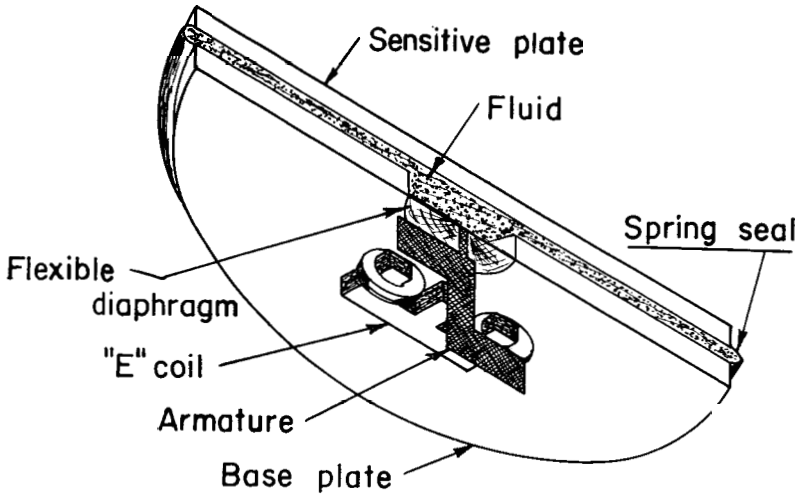

Figure B.4 Schematic drawing of soil pressure-sensing mechanism.

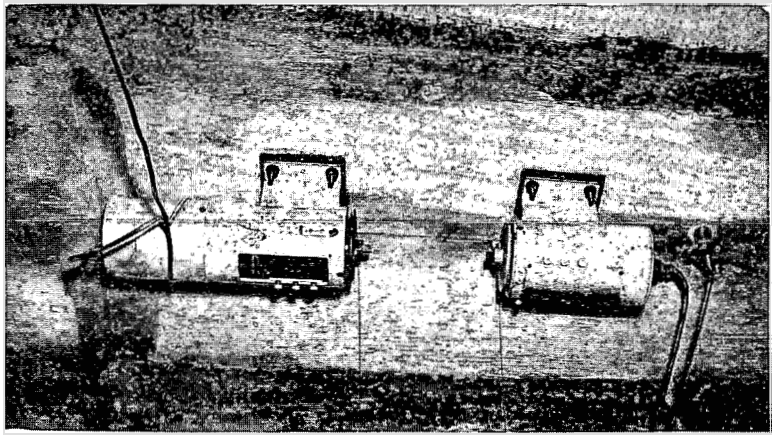

Figure B.5 Deflection gages: self-recording type to left; electronic type to right.

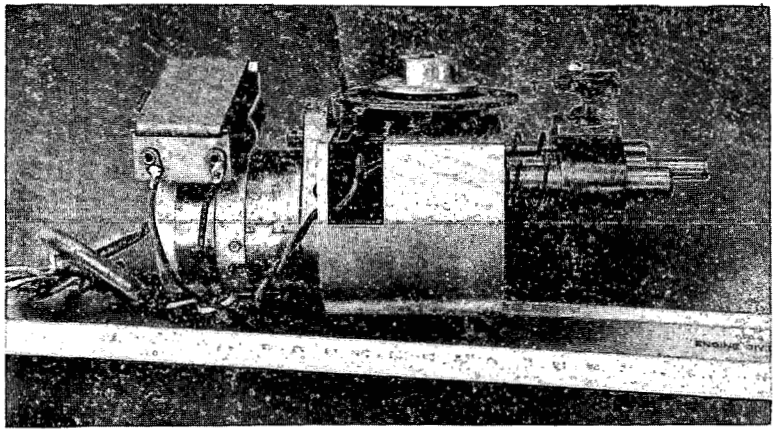

Figure B.6 Self-recording deflection gage recording unit.

formation signals, and applied them to a phase discriminator which produced an output voltage proportional in magnitude to the tangent of the measured variable. Operation is normally in the linear portion of the curve of q versus the tangent (where q is the measured variable), so that output is proportional to the measured variable. Also, timing pulses were derived from the 7,000 cps reference signal. The signal, the timing pulses, and the detonation-time marker were then recorded on a photographic paper recorder to produce a final record.

B.3.2 Self-Recording Mechanisms. The self-recording displacement-gage mechanism is shown in Figure B.6. A metal block supports the governed motor which drives the turntable through a bevel gear. A machined screw, mounted in ball bearings, moves the stylus carrier linearly along a radius from the center of the turntable. Spring loading of the stylus carrier minimizes backlash as it moves along the carrier guide pins.

In these gages, a precisely governed battery-operated motor which rotated an aluminized glass disk was placed in operation by visible or thermal radiations from the detonation. A stylus attached to a compact metal bellows element traced on the rotating disk a record of the dilations of the bellows as they were subject to the pressures of the blast wave, giving a time-dependent record of the blast pressure.

The thermal initiator consisted of a heavy spring-loaded plunger held cocked by a thermal-line: two brass strips soldered together with low-melting-point solder and painted black. The absorption of thermal radiation caused the links to part and the plunger to close a motor starting switch. This method was used in conjunction with the visible-radiation initiator.

The visible radiation initiator used a cadmium sulfide photocell, a transistor amplifier, and a high-speed electrically latching relay. The voltage produced in the photocell by a transient light pulse was amplified and closed the relay. For these gages located inside the structures, the photocell was placed outside and connected to the gage by a shielded cable.

Two motor speeds were used: for Structure 3.1.c, 10-rpm motors were installed in the gages; for the other structures, 3-rpm motors were employed. Because of inertia and the time needed for establishment of proper phase relationships in the motor speed governor, the motors do not reach a stable speed immediately. The 3-rpm motors reach their rated speed in 90 msec, but oscillate about that value for an additional 300 msec; the 10-rpm motors reach their speed gradually and without instability in 400 msec.

B.4 CALIBRATION

B.4.1 Acceleration. The accelerometers were given static calibrations on a spin-table accelerator before their installation (see Figure B.8). The spin table was a disk which was rotated at a speed determined accurately by an electronic tachometer. The accelerometer was mounted on the disk with its sensitive direction parallel to the radius of the disk. Connections to the recorder cable were made through slip rings on the spin-table shaft. An accurate knowledge of the distance of the accelerometer sensing element from the center of the disk and the rotational velocity of the disk were used to find the radial acceleration produced in the sensing element. The disk velocity was varied to produce accelerations 20, 40, 60, 80, 100 and 150 percent of the expected maximum. Spin table acceleration values could be computed with an accuracy of 2 percent.

B.4.2 Earth Pressure Gages. These gages were generally calibrated in pairs or groups of four before being placed in their mounts (see Figure B.9). Two gages were placed with their sensitive faces separated by a layer of blotting paper. An aluminum ring, slotted to allow exit of the gage cable, was placed against each base plate to protect the protruding section of the gage containing the sensing element (see Section B.2.2). This sandwich was then placed, with a Baldwin SR-4 load cell, between the jaws of a portable hydraulic press. The force applied through the aluminum rings to the base plate was measured by the load cell to an accuracy of better than one percent. The blotting paper allowed an even distribution of load over the sensitive faces of the gage sandwich. Where convenient, a pair of such sandwiches could be impressed simultaneously. After calibration, the gages were installed and the cables buried.

B.4.3 Electronic Displacement Gage. Calibration of these gages was done after their installation. The calibration of the large-displacement model was performed by rotating the housing of the sensing element potentiometer (see Section B.2.3). Calibration for a displacement in a given sense was obtained by rotating the potentiometer housing in a direction opposite to the corresponding rotation of the gage pulley. A full-scale rotation from the center position of the calibrated knob attached to the housing corresponded to one half turn in the opposite direction by the gage pulley. The full range of the calibrated scale was divided into appropriate segments to allow calibrations of 20, 40, 60, 80, 100, 120, 140 and 160 percent of the expected maximum displacements. Where displacements were specified greater than one half the pulley circumference, the potentiometer rotated past the extreme point on its scale and began a second cycle. The steps on the calibration record for this situation ascended as the displacement became larger (in the positive direction) until the extreme point was reached and then dropped sharply to a position corresponding to the maximum negative displacement. From this point they continued to rise until the maximum displacement was reached. The slope of the shot record trace could be used to differentiate between negative displacements and those which had exceeded the first positive

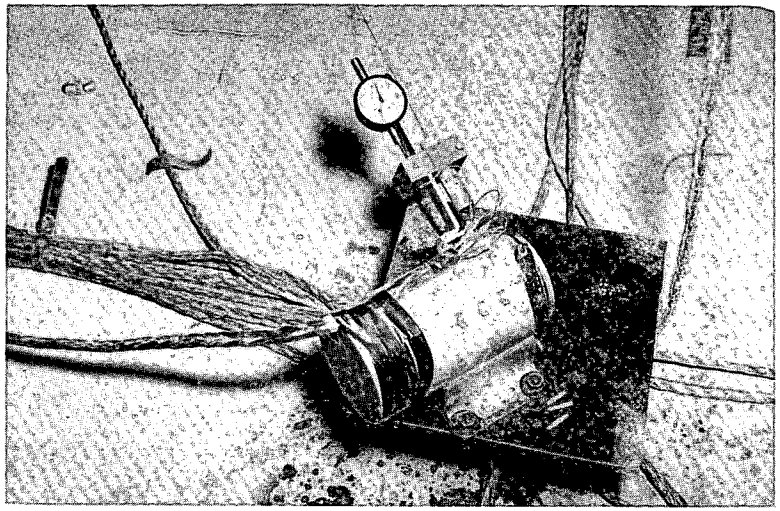

Figure B.7 Small deflection gage calibration.

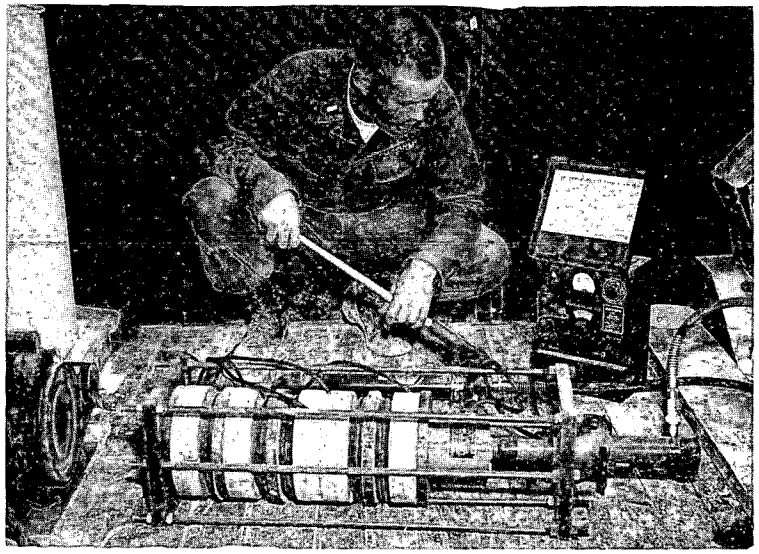

Figure B.9 Soil pressure gage calibration.

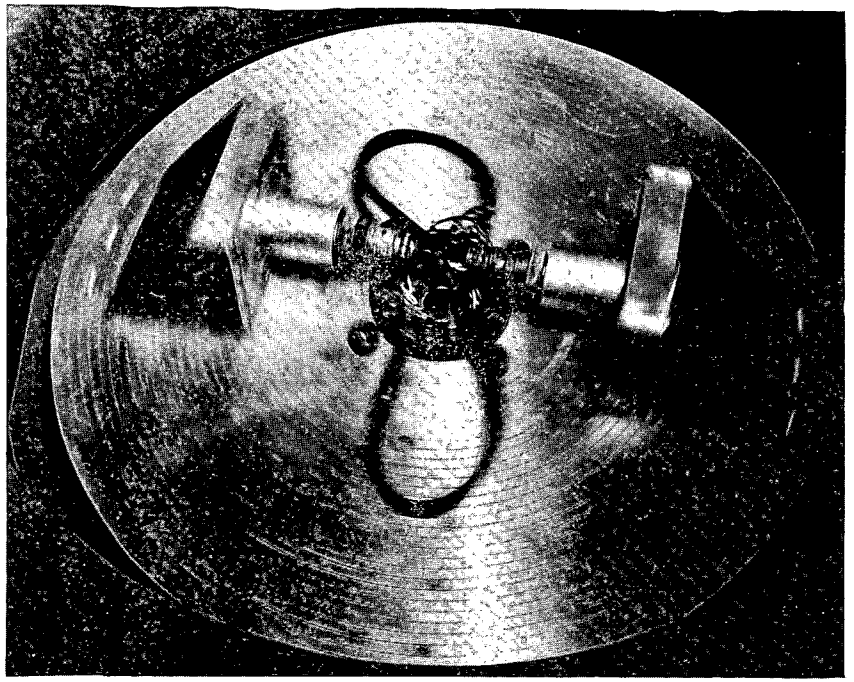

Figure B.8 Calibration of accelerometer.

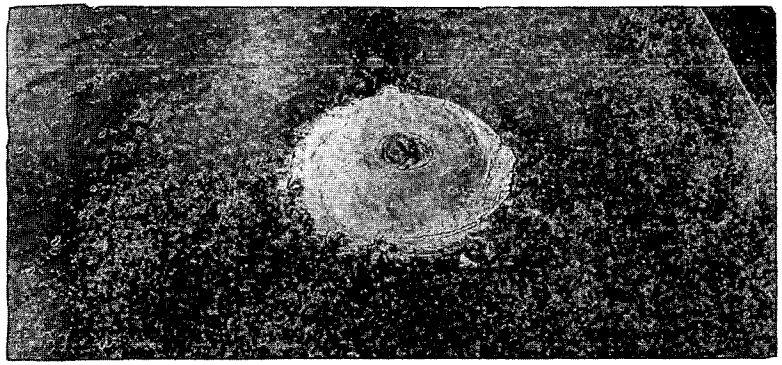

Figure B.10 Soil pressure gage in position at crown of Structure 3.1.b.

extreme point. Negative displacements were handled similarly.

The small-deflection gages were calibrated by using a dial micrometer as a standard to measure the motion of the coil relative to its support. After loosening the clamp which held the linearly variable differential transformer coil in place, a slotted block which held the micrometer was slipped over the coil-support bar (see Figure B.7) and locked in position. The coil was moved in a direction opposite to the actual deflection to produce calibration steps. Values, both positive and negative, of 20, 40, 60, 80, 100, 120 and 140 percent of the expected maximum were used.

B.4.4 Self-Recording Displacement Gages. These gages were calibrated before assembly by installing a disk, turning the recording mechanism shaft through one revolution, and measuring the height of the step produced on the disk. With the circumference of the pulley known, the displacement corresponding to this step height was readily deduced. The gage was linear, so that the slope of the curve of stylus motion versus displacement obtained in this manner could be extended over the full range of the gage.

B.4.5 Self-Recording Pressure Gages. Calibration of the pressure capsules was performed by the manufacturer. The calibrations were plotted using a Leeds-Northrup X-Y recorder. The output of a Statham strain-gage-type pressure transducer was fed through amplifiers to the pen (X-axis) of the recorder. Capsule deflection was measured by a micrometer head equipped with a null detector and servo system operating a slide-wire potentiometer which, in turn, controlled the chart drive (Y-axis). The resulting presentation gave a plot of capsule deflection as a function of applied pressure.

The disk drive motors were individually tested for start-up time and speed; these characteristics were recorded for each motor.

B.5 RESULTS

B.5.1 Performance. The operation of the gages and recording equipment is summarized in Table B.2. From a recording standpoint, 21 of the 48 records are considered excellent. The majority of the remaining records are beset with small zero shifts which make their interpretation slightly more difficult. Three traces appear with no visible record, and although the recording equipment gives every indication of having operated properly, it is difficult to conceive of negligible pressure existing at the corresponding gage positions. Calibration steps applied immediately before and after the test interval show proper operation of recording equipment, and the severe zero shift normally associated with faulty cables is missing. One record was lost completely apparently because of cable failure at detonation time.

B.5.2 Data Processing and Interpretation. The raw data was transcribed from the oscillograph traces into digital form on punched cards to facilitate processing. The punched cards were run through an electronic digital computer especially programmed to linearize the records. The linearized records of earth pressure, deflection, acceleration, and air overpressure were then replotted in final form for Structures 3.1.a, b, and c and are shown in Figures B.11, B.12, and B.13, respectively.

The interpretation of records having zero shifts at blast-arrival time leads to some difficulties, in that the exact course of the zero shift is often obscure. Experiments have shown, however, that when such shifts occur the calibration curve is generally not changed except that the zero value of the physical quantity being measured is shifted to a new position along the curve. To correctly interpret records of this type, it is necessary to determine from the calibration curve the size of the physical quantity represented by the zero shift and algebraically subtract this value from every physical quantity value on the calibration curve, and then to measure deflections on the shot record using the original system zero determined from the calibration record and relate these to physical quantity values using the revised calibration curve.

The estimates of calibration accuracy given in the sections on calibration cannot be applied directly to the test results because gages and equipment subjected to the severity of a nuclear detonation may not function just as they do under the tranquil conditions of a static calibration. For example, pressure gages may be affected by accelerations, and without elaborate instrumentation, the magnitude and effects of the acceleration cannot be known. Consequently, such instrumentation measurements made during nuclear tests are generally considered accurate to no better than 10 or 15 percent.

TABLE B.2 SUMMARY OF INSTRUMENTATION RESULTS

Structure	Gage	Comment
3.1.a	A5	Good record
	A6	Good record
	D15	Good record; large zero shift
	D16	Good record; small zero shift
	D17	Good record; small neg. zero shift
	E15	Good record
	P5	Peak pressure only
	P6	Good record
3.1.b	A3	Good record; zero shift
	A4	Good record
	D8	Good record
	D10	Good record
	D14	Good record except for regular pulse placed on record by system
	E14	Good record; negative shift
	E12	Good record
	E13	Good record
	E8	Good record; small zero shift
	E9	Good record
	E10	Good record
	E11	Good record
	E10.1	Usable record
	D9	Questionable record
	D11	Questionable record
	D13	Questionable record
	D12	Questionable record
	P3	Good record
	P4	Good record
3.1.c	A1	Good record
	A2	Good record
	D1	Good record
	D3	Good record
	D7	Noisy record; apparently good
	E7	No apparent record
	E5	Good record; small zero shift
	E6	Bad shift; no record
	E1	No apparent record; small neg. zero shift
	E2	No apparent record; no zero shift
	E3	Record saturated; pos. zero shift
	E4	Good record
	D2	Questionable record
	D4	Questionable record
	D5	Questionable record
	D6	Questionable record
	P1	Good record
	P2	Good record

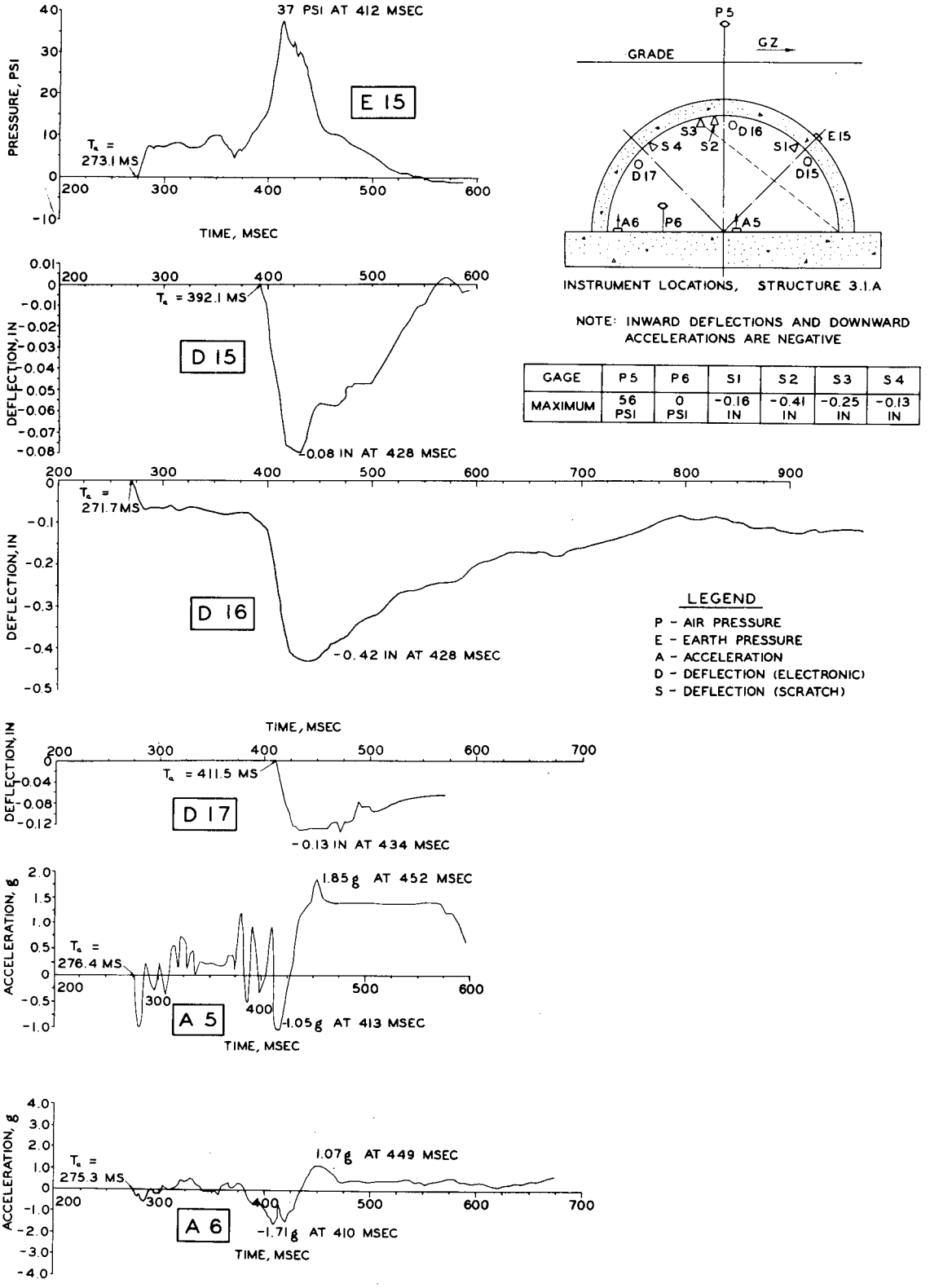

GAGE	P5	P6	S1	S2	S3	S4
MAXIMUM	56 PSI	0 PSI	-0.16 IN	-0.41 IN	-0.25 IN	-0.13 IN

Figure B.11 Transient records of earth pressure, deflection, and acceleration for Structure 3.1.a.

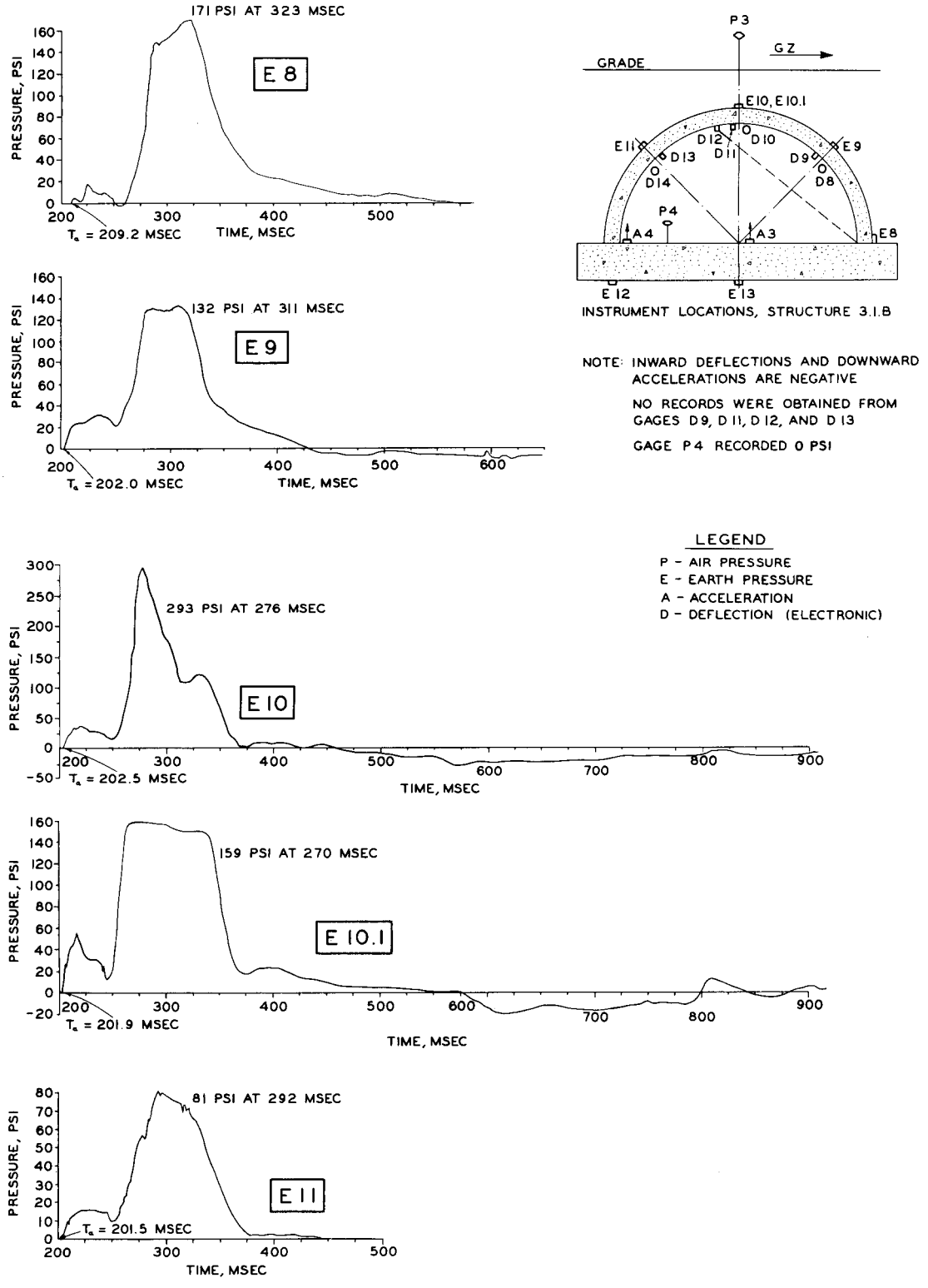

Figure B.12 Transient records of earth pressure, deflection, acceleration, and air overpressure for Structure 3.1.b.

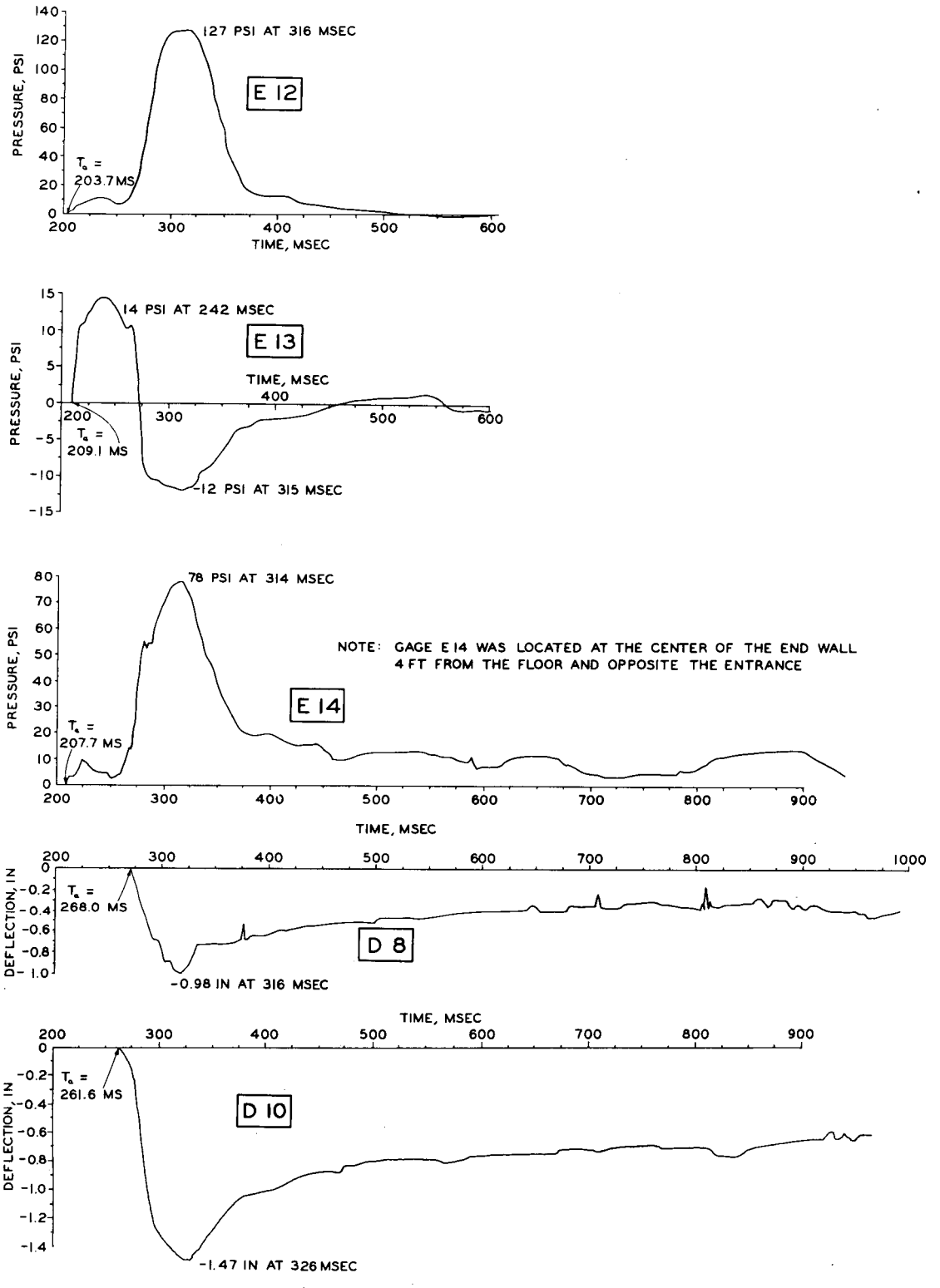

Figure B.12 Continued.

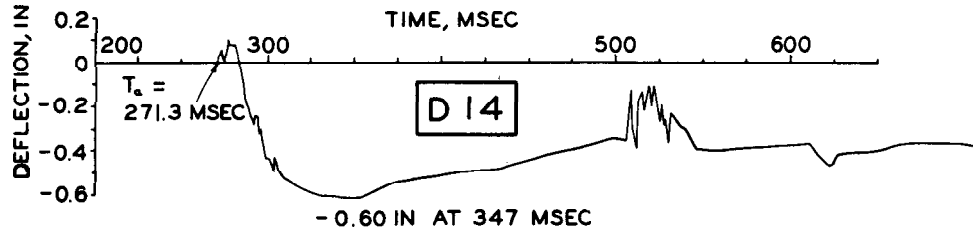

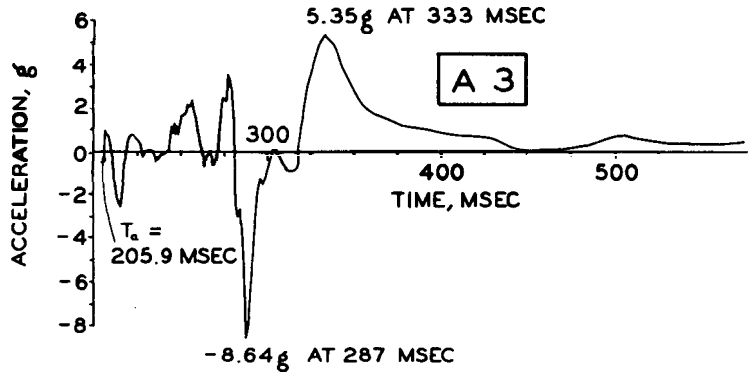

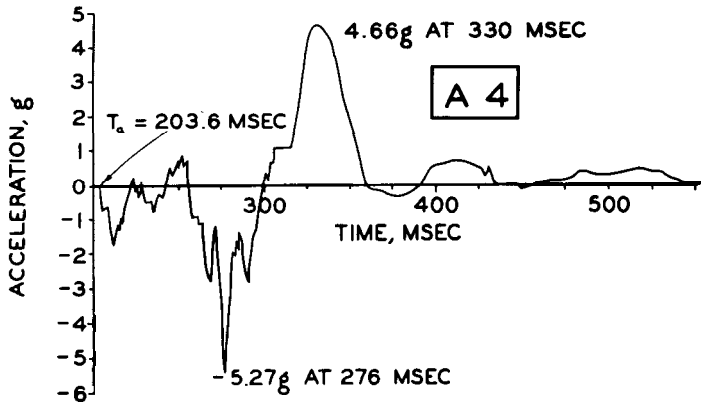

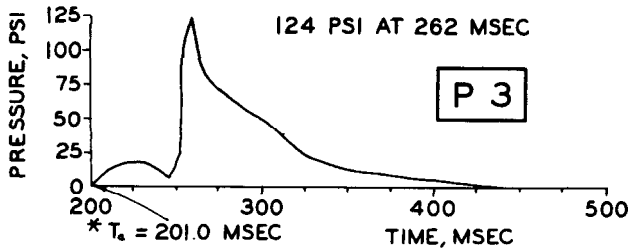

*NOTE: ARRIVAL TIME TAKEN FROM REFERENCES 12 AND 19

Figure B.12 Continued.

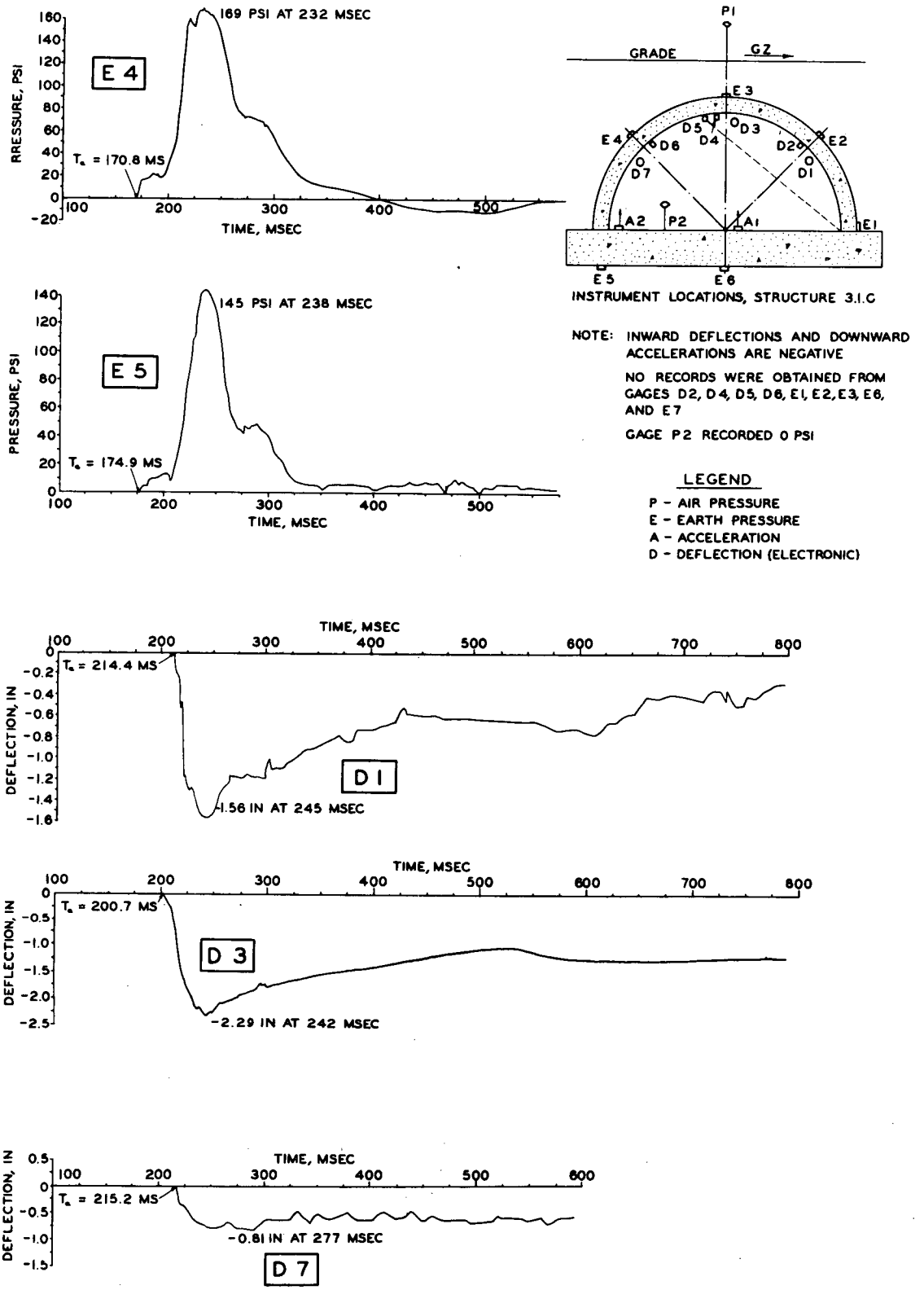

Figure B.13 Transient records of earth pressure, deflection, acceleration, and air overpressure for Structure 3.1.c.

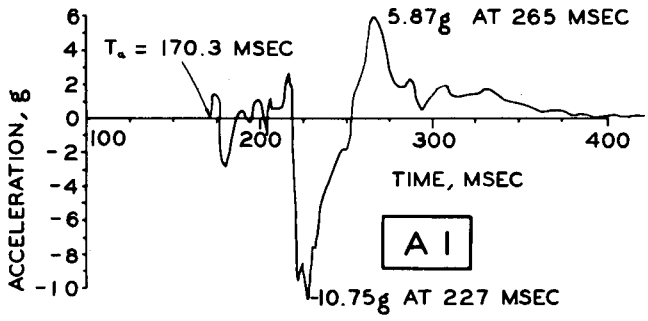

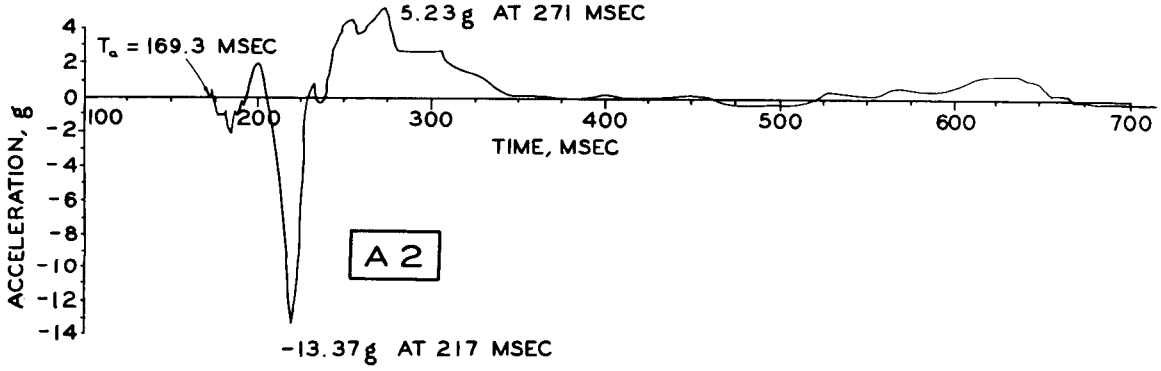

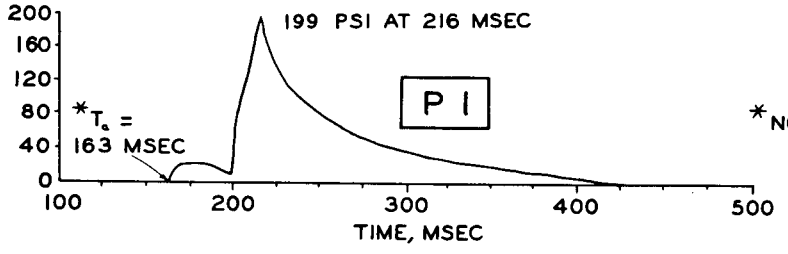

*NOTE: ARRIVAL TIME TAKEN FROM REFERENCES 12 AND 19

Figure B.13 Continued.

Appendix C
INSTRUMENTATION of STRUCTURE 3.1.n

C.1 QUANTITY AND LOCATION

The electronic instrumentation of Structure 3.1.n included 38 channels of transient information from the following gages and transducers: 16 electrical resistance strain gages, 11 soil-pressure gages, 8 deflection gages, 2 air-pressure gages, and 1 accelerometer. The output of 12 of the above electrical resistance strain gages was also recorded at larger attenuations to provide a backup in case the strains were so large as to exceed the range of the primary recording. Each of the eight electronic deflection gages was backed up by a self-recording deflection-versus-time gage. An additional eight self-recording deflection-versus-time gages were used to provide a more complete record of arch deflections than could be accomplished with the limited number of electronic channels available.

For the purpose of taking static readings, an additional 9 electrical resistance strain gages were installed, and 39 mechanical strain gage stations were established.

The location of all the instrumentation except the mechanical strain gage stations is shown in Figure 2.12. Note that each gage station "D" represents two gages. The location of the mechanical strain gage (Whittemore) stations is shown in Figure 3.11.

C.2 GAGES

C.2.1 Electrical Resistance Strain Gages. Standard SR-4 electrical resistance strain gages were used to measure the strain in the concrete and in the reinforcing steel. These gages were manufactured and calibrated by the Baldwin-Lima-Hamilton Corporation, Philadelphia, Pennsylvania. A 6-inch-long Type A-9 gage was selected for use on the surface of the concrete, since it would average out stress concentrations due to the nonhomogeneity of the concrete. Type AB-3 and A-12 gages were selected for use on the reinforcing bars.

Approximately one month after the concrete had been cast, the surface was prepared for application of the gages. The gage area was ground smooth and a thin layer of Epon resin cement was applied to the concrete surface and properly cured. The gages were then bonded to this surface with the same cement.

In order to mount the strain gages on the reinforcing bars, it was necessary to remove the bar deformations in the gage area. After cleaning the surface, the gages were bonded to the bars with Epon resin cement. All gages were completely waterproofed. Figures C.1 and C.2 show the installation of SR-4 strain gages on the extrados.

In order to protect the strain gages at zero time from the induction signal, a spark plug was placed between the shield in each cable and the local ground. The gap in the spark plug was set at 0.003 inch and would break down at approximately 800 volts dc. In this manner, a high voltage from the induction signal would be discharged through the spark gap to ground rather than flash over through the base of the gage, with accompanying destruction of the gage.

The calibration of each strain-gage channel was determined immediately prior to and immediately after the shot by connecting a resistor of selected magnitude in parallel with one arm of each strain-gage bridge. The electrical unbalance of the bridge was recorded on the oscillograph.

C.2.2 Soil-Pressure Gages. These gages were purchased from the Wiancko Engineering Company, Pasadena, California. They utilize the Carlson platter in conjunction with the Wiancko variable reluctance transducer and were designated as a Type P2303 pressure pickup. The completed gage had a 7 1/4-inch diameter and weighed 11 1/2 pounds. The gages were calibrated in the laboratory by applying static loads in a universal testing machine. The actual cables used in the field operation were used in the static calibration. The calibration of the gages was linear within 2 percent over the range of 0 to 100 psi and could withstand a 100-percent overload.

The soil-pressure gages were installed to measure the vertical and horizontal components of earth pressure. At the crown and springing lines of the arch, the gages were mounted on washer-shaped steel plates that were embedded in the concrete. At the 30- and 60-degree sections of the arch, the gages were mounted in precast Hydrostone blocks which were bolted to the arch. The top surface of each gage was mounted flush with the surface of the concrete or the Hydrostone block. Each gage was grouted in place with Hydrostone to assure intimate contact between gage and structure. Figures C.1 and C.2 illustrate the earth-pressure gages in place.

During the backfilling of Structure 3.1.n, the soil contiguous to each earth-pressure gage was carefully

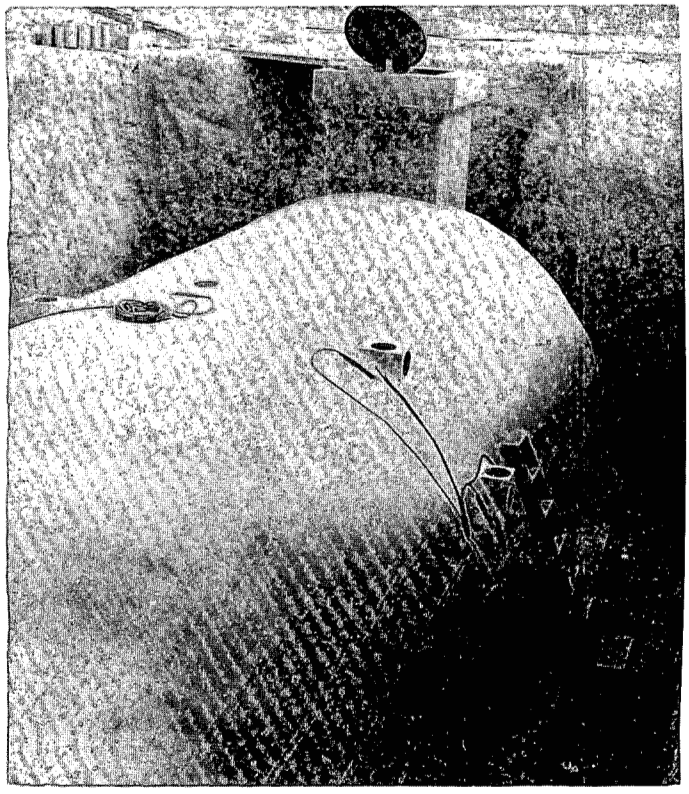

Figure C.1 Completed structure with earth-pressure gages and strain gages in place.

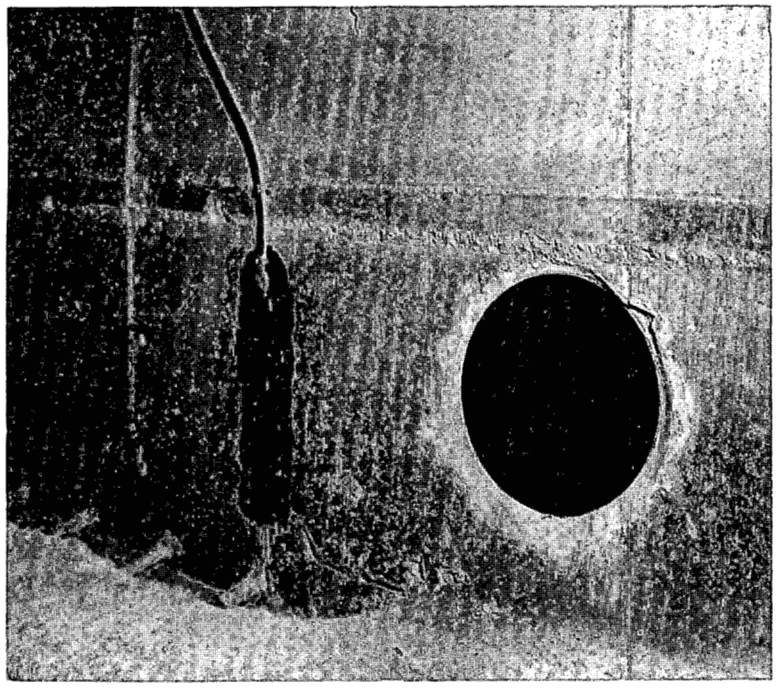

Figure C.2 Installation of an SR-4 strain gage and an earth-pressure gage at the springing line.

hand-tamped. For the vertically mounted gages, the soil was hand-tamped in 1- to 2-inch layers for a distance of approximately 4 inches from the face of the gage. For the horizontally mounted gages, the soil was hand-tamped to a depth of approximately 6 inches over the gages. The pneumatic tampers used in compacting the backfill material were carefully controlled in the immediate vicinity of the soil-pressure gages.

C.2.3 Deflection-versus-Time Gages. Two different types of deflection-versus-time gages were used: one electrical and one mechanical. The electrical gages were furnished by Ballistic Research Laboratories (BRL) and modified by the U.S. Naval Civil Engineering Laboratory (NCEL). They consisted of a spring-loaded shaft onto which a potentiometer and a pulley were secured. A wire was attached to the pulley and connected to the point on the structure where the deflection was desired. The gages were secured to the floor slab near the springing line of the arch.

One of the BRL gages was checked by comparing its output to that of other types of gages connected directly to a small beam which was subjected to dynamic loads. The BRL gage was connected to the beam with an 8-foot length of 0.024-inch-diameter music wire. These tests showed that the BRL gage had a delayed initial start of about 5 msec and a greater initial maximum deflection of about 0.2 inch, for beam accelerations of about 100 g and beam deflections of about $\frac{3}{4}$ inch. This error was probably due to the inertia of the BRL gage, which introduced an increase in force of about 27 pounds in the wire, thus causing an elastic elongation of the wire. In order to reduce this error in case of high accelerations, NCEL reduced the mass of the pulley and increased the size of the music wire to 0.033 inch. Also, in case of high accelerations, it was planned to perform postshot calibrations at the actual accelerations encountered.

The self-recording mechanical scratch gages were designed and fabricated by NCEL. They consisted of an 8-inch-long drum rotated by a constant-speed 27-volt-dc motor, and a scribe which was connected with 0.033-inch-diameter music wire to the point of desired deflection. Where the gage was used to back up a BRL gage, the scribe was secured to the same wire. Where the gage was used independently, a pulley and spring system similar to the BRL gage was used to spring load the wire. Figure C.3 shows a typical installation of the electronic and the mechanical deflection gages.

The motors for the self-recording gages operated at 60 ± 1 rpm, and the recording drums had a circumference of 10 inches. This made a very convenient time scale of 1 inch equal to 100 milliseconds.

C.2.4 Air-Pressure Gages. Wiancko Type P1412 transient air-pressure gages were used to measure the blast overpressures. These gages had a range of 0 to 100 psi and were installed in baffles furnished by the Stanford Research Institute. The gages were calibrated in the laboratory by applying static pressure loads by means of a pressure-calibrating unit. The actual cables used in the field operation were used in the static calibration. The response of the gages was linear within 2 percent over the full range of the gage.

C.2.5 Accelerometer. The accelerometer used (Model F-100-350) was manufactured by Statham Laboratories, Incorporated, and had a range of 0 to 100 g. It was calibrated on accelerometer calibration equipment at the U.S. Naval Air Missile Test Center (NAMTC), Point Mugu, California. Full-range calibration was performed at frequencies of 25, 50, 75, and 107 cps. The accelerometer was securely fastened to the inside crown at the center of the arch.

C.2.6 Mechanical Strain Gages. A 10-inch Whittemore strain gage was used for taking static strain readings at various stations located on the arch intrados. This instrument can be read to the nearest ± 10 μin/in. To use this instrument, small conical holes must be placed in the surface of the structure precisely 10 inches apart. For this purpose, $\frac{1}{2}$-inch-deep holes were drilled into the concrete and $\frac{1}{4}$-inch-diameter brass plugs were securely anchored in these holes with Hydrostone. The small conical holes were drilled into these plugs.

C.3 METHODS OF RECORDING AND PROCESSING DATA

The 48 channels of transient electronic instrumentation were recorded photographically on two Type 5-114-P3 oscillographs and one Type 5-114-P4 manufactured by Consolidated Electrodynamic Corporation (CEC). Type 809 photographic paper manufactured by Eastman Kodak Company was used as the recording medium in the oscillographs.

The carrier voltage for each channel was supplied by three CEC Type 2-105A oscillator-power supplies and two CEC Type 1-118 carrier amplifiers. The transient signals were amplified by CEC Type 1-113B amplifiers and the two Type 1-118 carrier amplifier units. In order to prevent cross-modulation of the various oscillators, it was necessary to disable the oscillator sections in two of the Type 2-105A power supplies and to drive the three power supplies from a single oscillator. It was also necessary to feed back a portion of the carrier voltage from the master power supply into the two Type 1-118 carrier amplifiers in order to lock in the oscillators of these units to the same frequency as that of the master power supply. The power supplies, carrier amplifiers, and the Type 5-114-P4 oscillograph operated on 115 volts ac at 60 cps provided by four converters manufactured by Carter Motor Company of Chicago, Illinois. The Type 5-114-P3 oscillographs and converters received power from six nickel-cadmium batteries having a total rat-

ing of 360 ampere-hours at 24 volts.

The BRL deflection gage bridges were operated at approximately 6.4 volts dc from the nickel-cadmium batteries. The actual voltage at shot time was to be indicated by the displacement of a galvanometer in one of the oscillographs. The deflection gage channels were balanced by means of a Century Model 1809 bridge control unit manufactured by Century Electronics and Instruments, Inc., of Tulsa, Oklahoma.

An electro-mechanical time-control unit contained (1) relays for unshorting the galvanometers connected to the dc bridge shortly after zero time, (2) stepping switches for calibration of the strain-gage channels, and (3) time-delay motors for starting the magazine drives of the oscillographs, preshot calibration, postshot calibration, and turning all equipment off. All relays in the time-control unit were of the mechanical latch type.

The recording instruments were located in an underground instrument shelter approximately 60 feet from Structure 3.1.n. The instrument shelter had reinforced-concrete walls and roof 27 inches thick, with the top of the shelter at ground level. An earth mound approximately 5 feet thick was placed over the shelter.

It was expected that the maximum total radiation inside the shelter would be less than 15 roentgens. This amount of radiation would not produce significant fogging of the Eastman Kodak Type 809 paper which was used as the recording medium in the three oscillographs. All equipment inside the instrument shelter was securely anchored to work benches by means of shock-mount connections.

Since the equipment could not be manually operated during the shot, it was necessary to rely on standard timing signals provided by Edgerton, Germeshausen and Grier (EG&G). A 30-minute signal activated a solenoid which released a heavy-duty knife switch, thereby providing power to the power supplies and oscillographs in order that the equipment would be warmed up by shot time. This signal was backed up by a minus-15-minute signal.

At minus 15 seconds, a signal initiated a time-delay motor of approximately 9 seconds, at which time the magazine drives of the oscillographs were started. Automatic stepping switches were also started which provided an electrical signal for calibration purposes to all strain gage channels in sequence. The last step of the stepping switch supplied a signal which was recorded on an extra channel on all oscillographs. This afforded a means of coordinating the records from the three oscillographs. A minus-5-second signal was used to back up the minus-15-second signal.

A minus-2 ½-second signal was used to start the rotating drum deflection gages. This signal also started two time-delay motors: one to initiate the postshot calibration of all strain-gage channels and one to shut off the electrical power to all equipment.

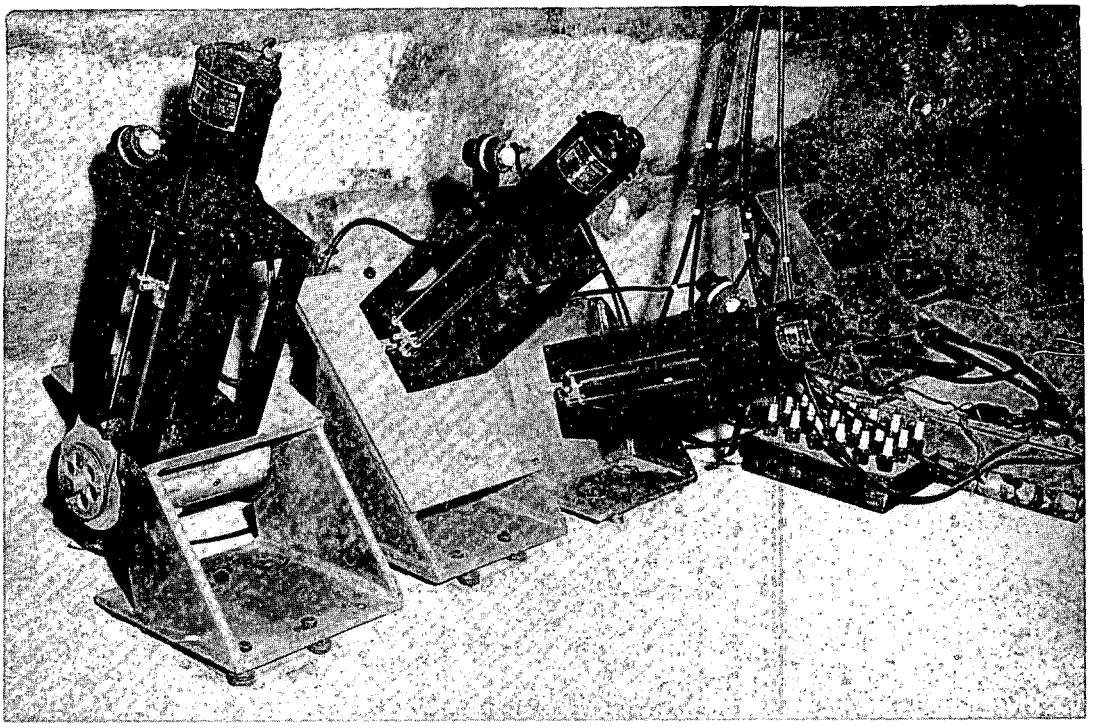

Figure C.3 Typical installation of the electronic and the mechanical deflection gages.

In the event of failure of both the minus-15-second and minus-5-second signals, the minus-2 ½-second signal would also start the record drives of the three oscillographs, although there would not be sufficient time for the preshot calibration of the strain-gage channels.

At zero time, thyratron tubes were used to backup the minus-2 ½-second signal and to supply a zero-time signal which was recorded on all of the oscillographs. These tubes, No. 5823, are sensitive to high light intensity, but will not be triggered by the light from the sun. Since the galvanometers connected to the dc bridges were shorted at zero time to protect them from the electro-magnetic propagation, these thyratron tubes were also used to unshort the galvanometers prior to arrival of the shock front.

At approximately 12 seconds after zero time, the stepping switches provided postshot calibration signals to the galvanometers connected to the strain gages. The power to all instrumentation equipment was shut off at approximately 17 seconds after zero time.

With the transducers and recording system used, all records which had a trace excursion of two inches or less were linear. This simplified the data reduction. However, because of the large volume of data, the oscillogram data reduction equipment of NAMTC was used. This equipment followed each trace, recorded the elapsed time, measured and recorded the trace excursions, applied the calibration constants, and produced a compilation of the information obtained. This data could now be plotted to a convenient scale.

The deflections of each instrumented point in Structure 3.1.n were measured with respect to both springing lines, thus giving two vectors which were resolved into horizontal and vertical components.

C.4 RESULTS

Because of the high intensity of the radioactive field in the vicinity of the instrumentation shelter, the oscillographic records were not recovered until a few days after the shot. A film badge which had been placed near the recorders indicated that the records had received a total dose of approximately 6 roentgens. This exposure produced records with a background only slightly darker than normal, and having an insignificant effect on the readability of the traces.

The three oscillographs and associated equipment operated very satisfactorily, electronically, during the shot; however, a slippage of the paper in one of the oscillographs resulted in a loss of those records. Several of these channels were backup, though, and the data recorded on other oscillographs. The information from only seven of the transducers was completely lost due to the slippage. A summary of the instrumentation results for Structure 3.1.n is given in Table C.1.

The SR-4 electrical resistance strain gages gave acceptable records. However, there was some drift due to a relatively low gage resistance to ground. This was probably caused by an electrical breakdown of the Epon resin used as a waterproof membrane between the gage and the concrete. In order to maintain a high gage resistance to ground, it is recommended that in future operations, metallic shim stock be used as the impervious membrane between the gage and the concrete surface. These records are given in Table C.2 and Figure C.4.

The earth pressure gages gave what appear to be good records, but the method of mounting the gages at the 30- and 60-degree positions produced questionable results, probably due to local earth arching. These records are given in Figure C.5.

The NCEL self-recording deflection-versus-time gages functioned exceptionally well. The scratches were so well defined that deflections could be read to the nearest 0.01 inch, and time could be read to the nearest millisecond. Acceleration records of other agencies indicated that these gages were not subjected to accelerations of a high enough magnitude to necessitate a postshot calibration (see Section C.2.3). One disadvantage of the NCEL self-recording deflection-versus-time gages was that there was no way by which zero time could be established and therefore no means by which their records could be coordinated time-wise. For future operations it is planned to modify these gages to provide a zero-time mark for this purpose. The records from these gages are reproduced in Figure C.6.

Records obtained from the electrical deflection-versus-time gages proved unsatisfactory. All of these records exhibited large zero shifts, and some had very high noise-to-signal ratios. These conditions did not exist during the preshot timing runs.

The differences between the preshot and postshot strain readings recorded by the mechanical (Whittemore) strain gages are shown in Figure 3.11.

TABLE C.1 SUMMARY OF INSTRUMENTATION RESULTS FOR STRUCTURE 3.1.n

Gage locations are given in Figure 2.10. Mechanical strain gages were used for static readings only. Results are given in Figure 3.5.

Gage	Comment	Figure	Gage	Comment	Figure
S1	Good Record	C.4	E16	Good Record	C.5
S2	Good Record	C.4	E17	Record Appears Good	C.5
S3	Good Record	C.4	E18	Beyond Range	C.5
S4	Static Readings Only	*	E19	No Record	—
S5	Good Record	C.4	E20	No Record	—
S6	Good Record	C.4	E21	Good Record	C.5
S7	Static Readings Only	*	E22	Questionable Record	C.5
S8	Backup Record Only	C.4	E23	Record Appears Good	C.5
S9	Good Record	C.4	E24	Beyond Range	C.5
S10	Good Record	C.4	E25	Record Appears Good	C.5
S11	Good Record	C.4	E26	No Record	—
S12	Static Readings Only	*			
S13	Static Readings Only	*	D18	No Record	—
S14	Static Readings Only	*	D19	Good Record	C.6
S15	Static Readings Only	*	D20	Good Record	C.6
S16	Static Readings Only	*	D21	No Record	—
S17	Static Readings Only	*	D22	Good Record	C.6
S18	Static Readings Only	*	D23	No Record	—
S19	Good Record	C.4	D24	Good Record	C.6
S20	Good Record	C.4	D25	Good Record	C.6
S21	No Record	—	D26	Good Record	C.6
S22	Good Record	C.4	D27	Unusable Record	—
S23	Good Record	C.4	D28	No Apparent Record	—
S24	No Record	—	D29	Good Record	C.6
S25	Good Record	C.4			
			P7	No Record	—
A7	No Record	—	P8	No Recordable Change	—

* See Table C.2 for results.

TABLE C.2 PERMANENT STRAINS, STRUCTURE 3.1.n

Refer to Figure 2.12 for gage location.

These values are the difference between readings taken two days before the shot and six days after the shot.

Gage Number	Permanent Strain	Gage Number	Permanent Strain
	10^{-6} in/in		10^{-6} in/in
S1	*	S13	*
S2	20 (C)	S14	10 (C)
S3	100 (C)	S15	70 (T)
S4	*	S16	*
S5	40 (T)	S17	20 (T)
S6	20 (T)	S18	120 (C)
S7	*	S19	*
S8	0	S20	0
S9	120 (T)	S21	140 (C)
S10	*	S22	40 (T)
S11	60 (T)	S23	320 (T)
S12	620 (T)	S24	40 (T)
		S25	60 (C)

* No record. (C) = Compression. (T) = Tension.

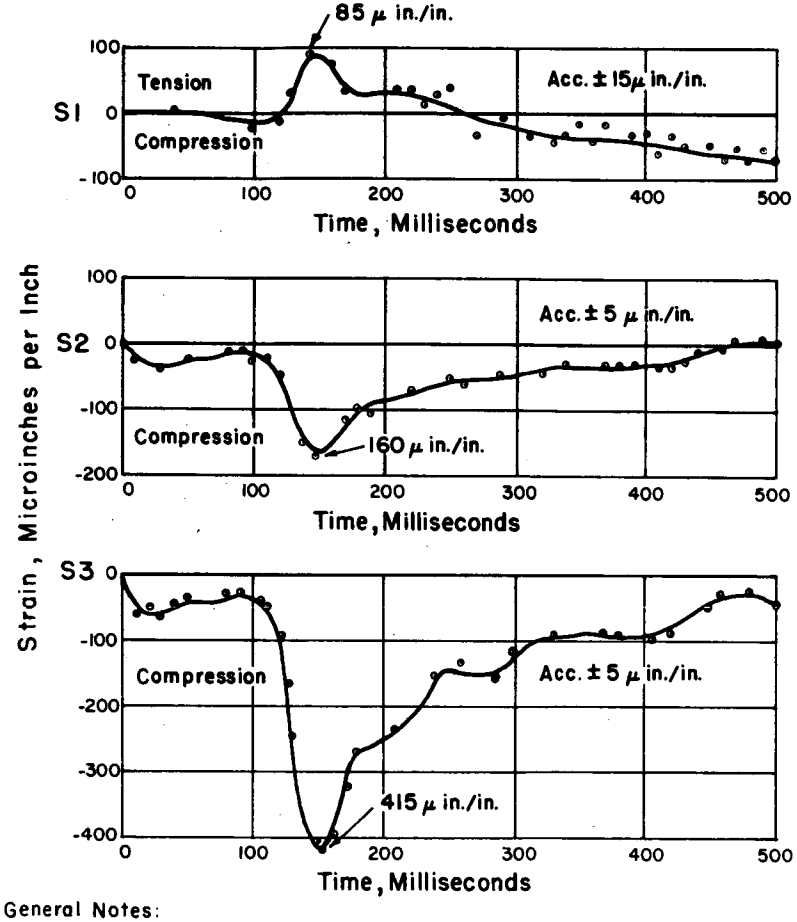

General Notes:

1. - is compression and + is tension.
2. Acc. is the accuracy to which the strain data could be obtained from the oscillograph records.
3. Curves start when blast wave first hit stucture 3.1.n, at zero + 274 milliseconds.

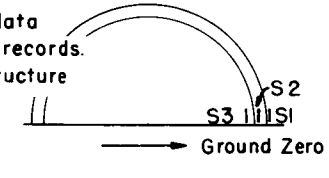

Figure C.4 (a) Strain versus time, Structure 3.1.n.

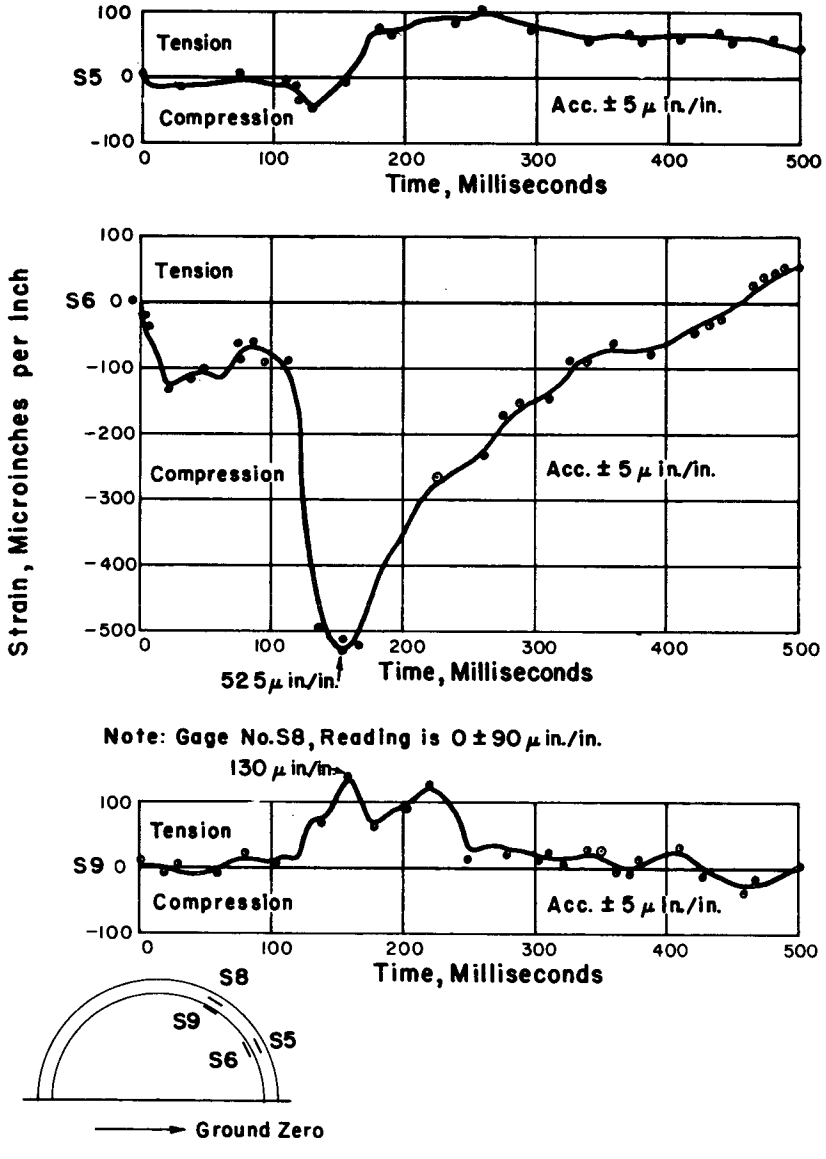

Figure C.4 (b) Strain versus time, Structure 3.1.n.

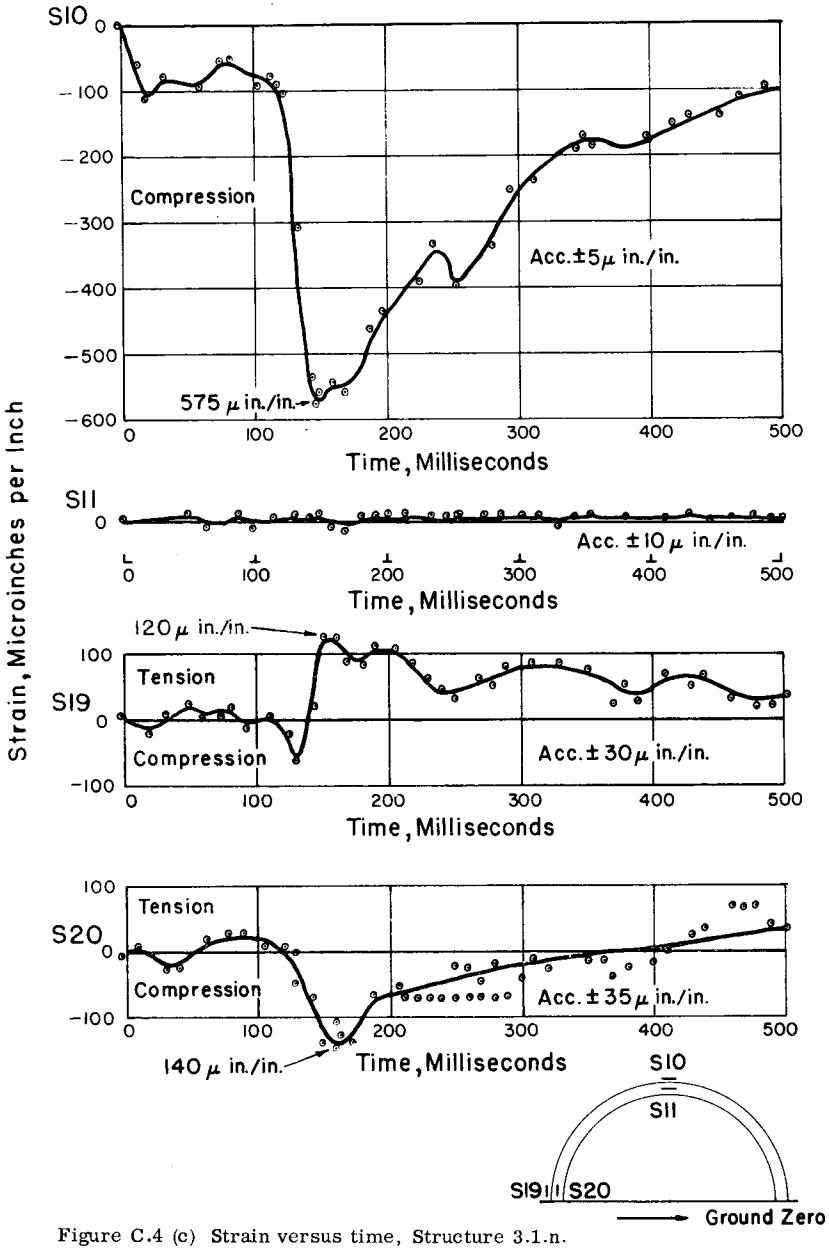

Figure C.4 (c) Strain versus time, Structure 3.1.n.

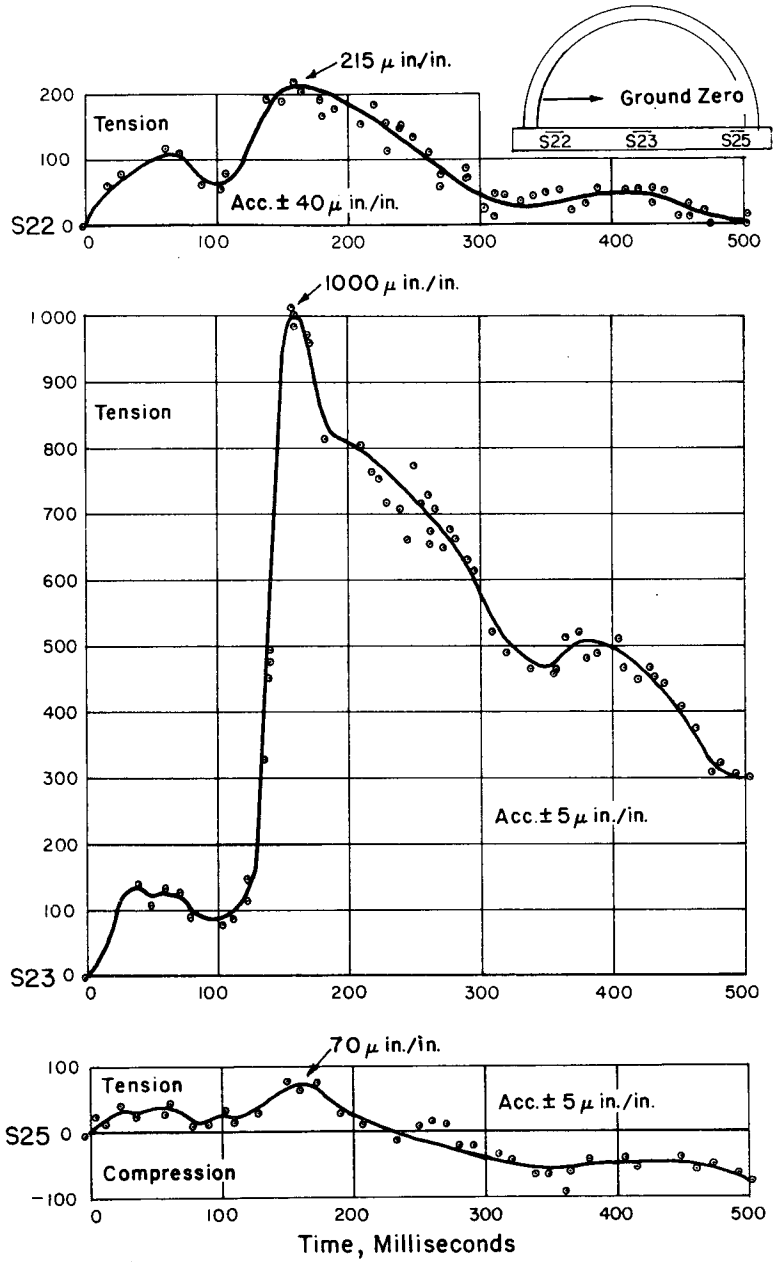

Figure C.4 (d) Strain versus time, Structure 3.1.n.

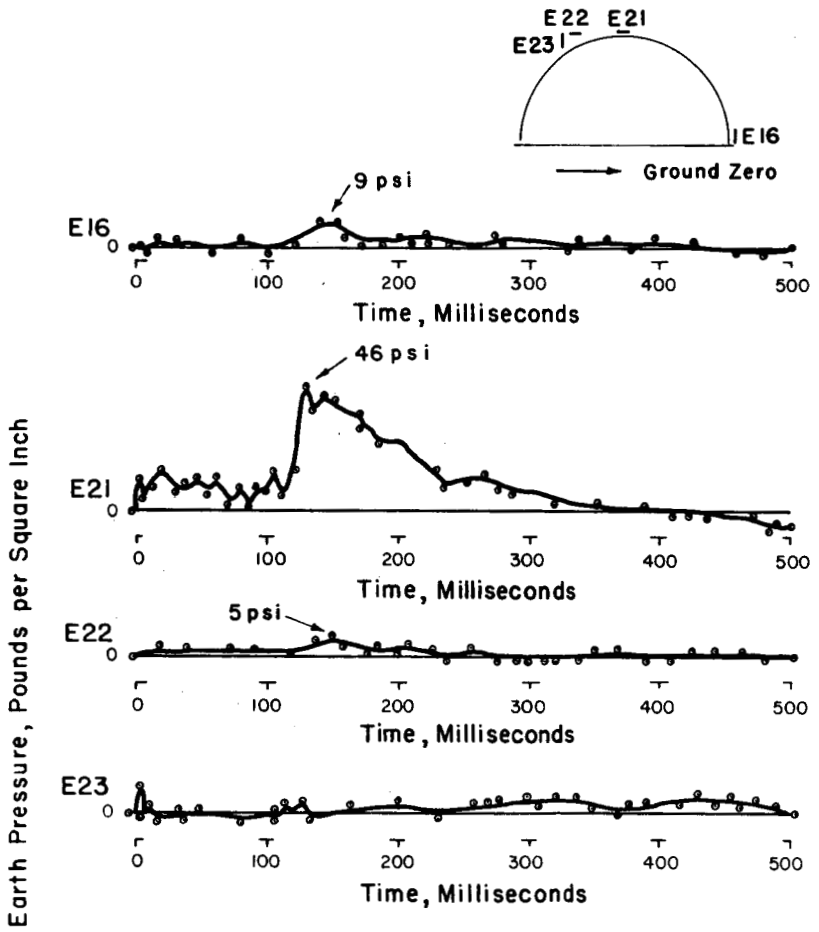

Note: 1. Earth pressure data could be obtained from the oscillograph records to the nearest 0.5 psi.

2. Curves start at zero plus 274 milliseconds (when blast wave first hit structure 3.1.n)

Figure C.5 (a) Earth pressure versus time, Structure 3.1.n.

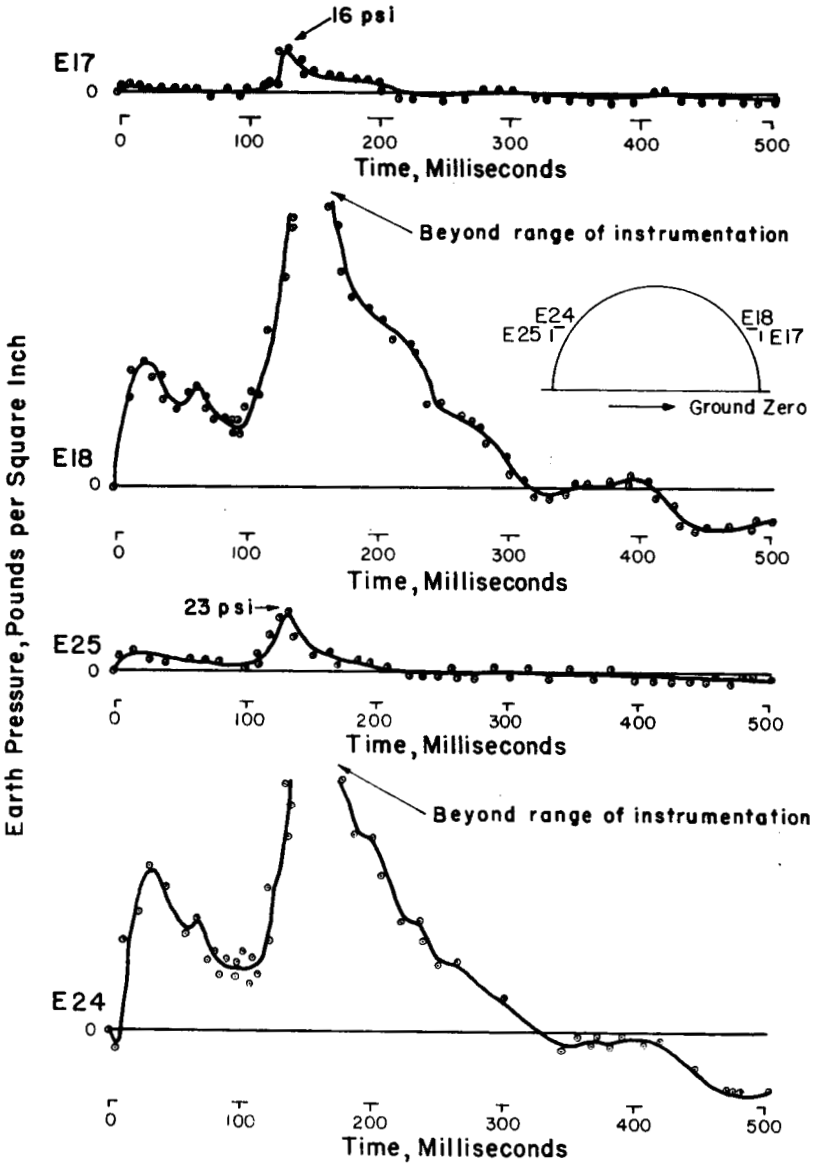

Figure C.5 (b) Earth pressure versus time, Structure 3.1.n.

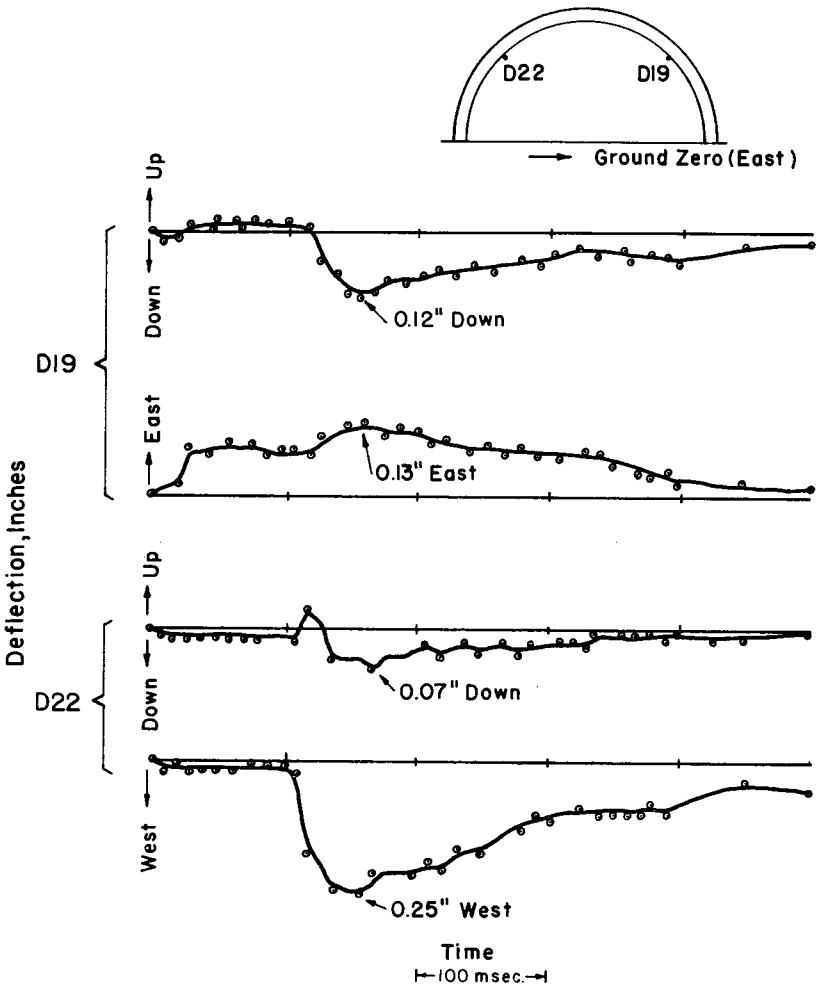

Figure C.6 (a) Deflection versus time, Structure 3.1.n.

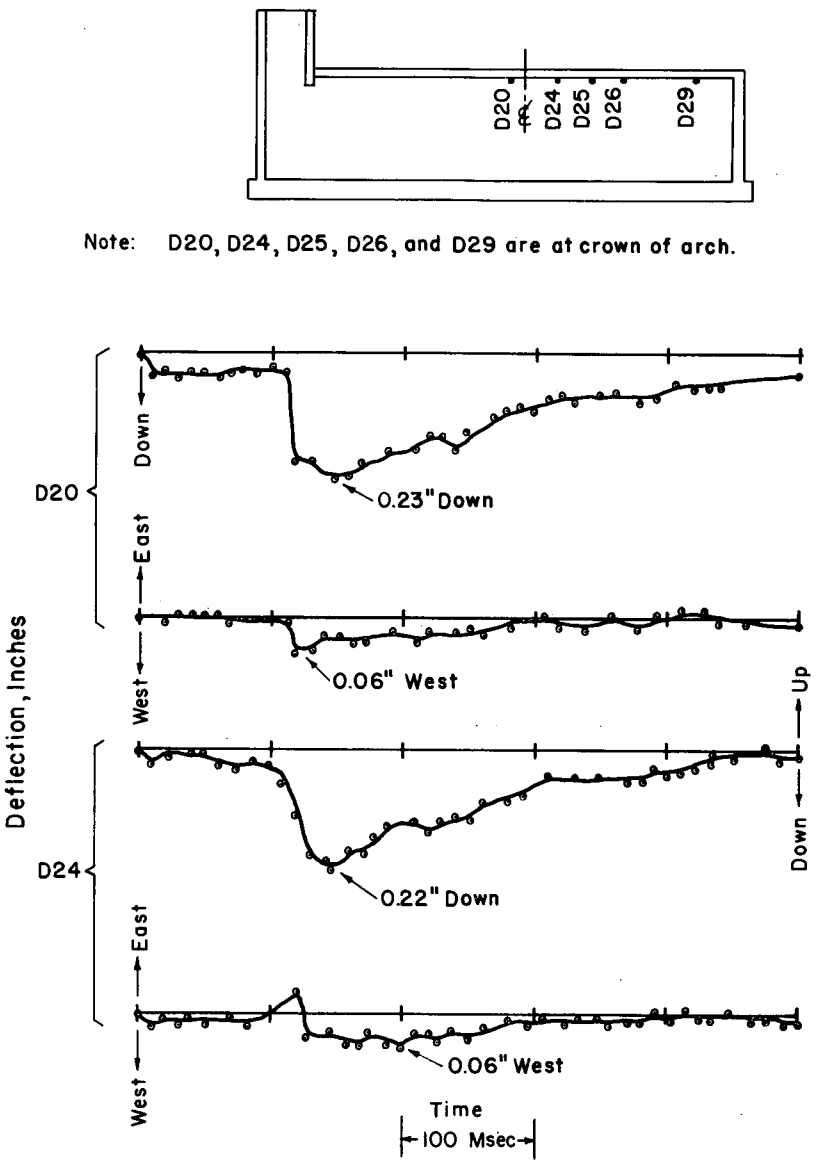

Figure C.6 (b) Deflection versus time, Structure 3.1.n.

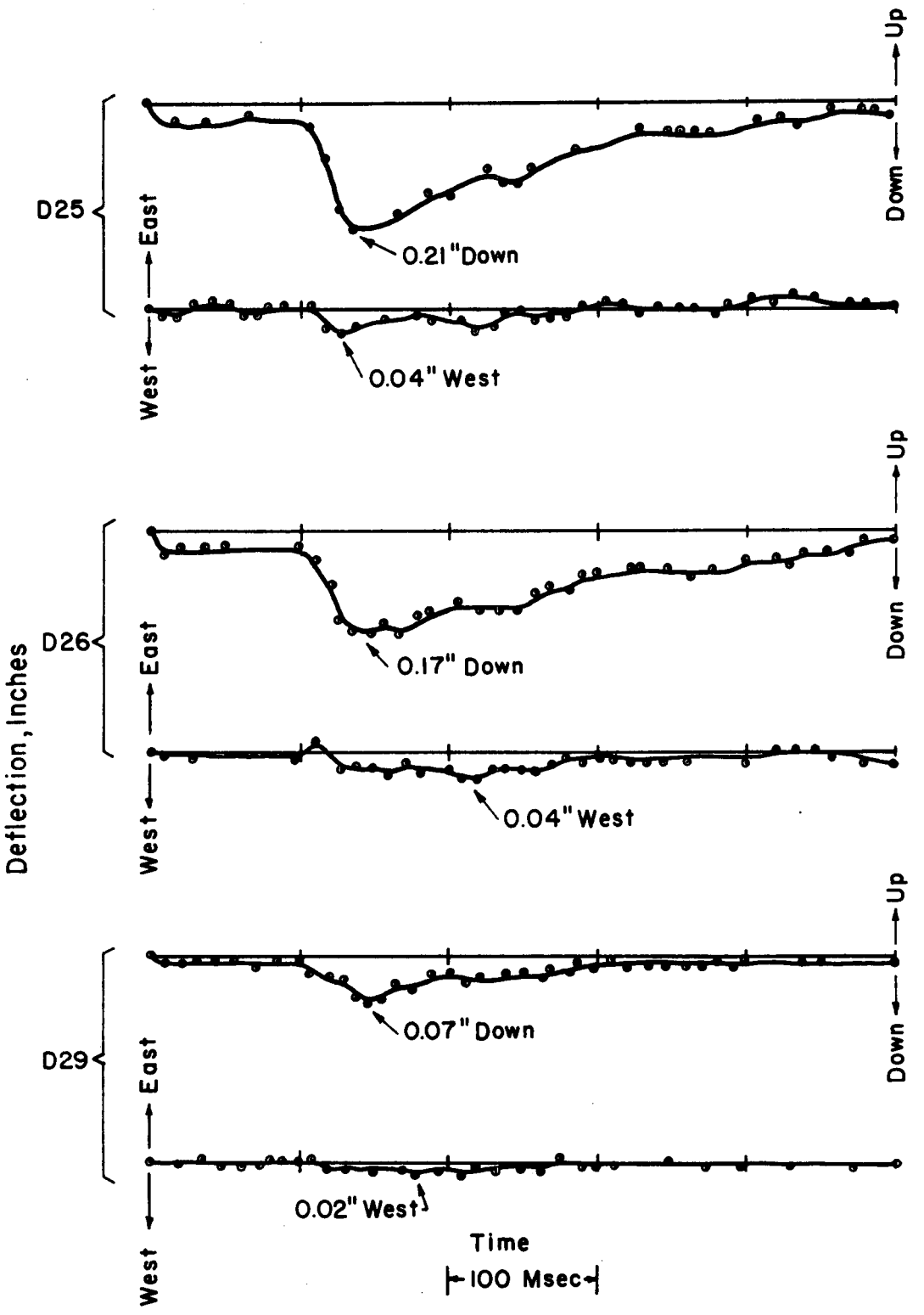

Figure C.6 (c) Deflection versus time, Structure 3.1.n.

Appendix D'
RADIATION INSTRUMENTATION

D.1 BACKGROUND AND THEORY

Tests prior to Operation Teapot have shown that below-grade shelters give 75 percent better gamma shielding than those shelters that are partially above grade (Reference 20). Teapot data illustrated that completely below-grade shelters with 4 feet of vertical earth cover gave an inside-to-outside gamma-dose ratio (to be defined herein as a gamma transmission factor) as low as 1.2×10^{-4} and a neutron transmission factor of 1.4×10^{-6} for the high-energy neutron flux which would be detected by sulfur threshold detectors (Reference 21). Detector stations nearer to the entranceways of the structures indicated much greater transmission factors and therefore received higher radiation dosages.

The shelters to be instrumented for radiation measurements during Operation Plumbbob were all underground. For this reason, the Teapot results in below-grade structures UK 3.8A, UK 3.8B, UK 3.8C, and UK 3.7 were particularly useful in predicting expected shielding by the shelters during Plumbbob (Reference 21). These results were augmented by empirical relations for neutron and gamma radiation passing through hollow cylinders as given in the "Reactor Shielding Design Manual" for evaluating the effect of various openings and baffles (Reference 22).

As a result of these analyses the only part of the Plumbbob 3.1 structures expected to have an adverse effect on shielding property was the entranceway. In regard to relative radiation dosages within such shelters, a consideration of the slant thickness (the line of sight cover) would indicate that the greater dose is to be expected in the portion of the shelter farthest from ground zero.

D.2 DESCRIPTION OF INSTRUMENTATION

D.2.1 Gamma Film Packets. Gamma dose was measured with the National Bureau of Standards–Evans Signal Laboratory (NBS-ESL) film packets (References 23, 24, and 25). In the exposure range from 1 to 50,000 r and in the energy range from 115 kev to 10 Mev the accuracy of the dosimeter is considered to be within ± 20 percent. The net photographic response is expected to be approximately energy independent. This is achieved by modifying the bare-emulsion energy response, which has peaks near the K-shell photoelectric absorption edges, absorber and bromine, by placing the entire emulsion in an 8.25-mm-thick bakelite case covered with 1.07 mm of tin and 0.3 mm of lead and surrounded by a $\frac{1}{32}$-inch lead strip over the open edges. The entire arrangement is placed in a plastic cigarette case.

Although the angular dependence of the gamma film packet when it is exposed to higher energy radiation is negligible, for lower energies it is important. An interpretation of the results obtained by Ehrlich (Reference 24) indicates that, for radiation isotropically incident on the packet, the dose value is about 5.5 percent lower for 1.2-Mev radiation than that obtained by an instrument having no angular dependence, about 32 percent low for 0.20-Mev radiation, and about 45 percent low for 0.11-Mev radiation. Although the film packets may show only ± 20-percent error in normal radiation fields, some consideration should be given to the fact that in a relatively isotropic and degraded energy field, such as might exist in structures with many feet of earth cover, the film packets may indicate low values.

D.2.2 Chemical Dosimeters. The chemical dosimeters utilized for instrumenting the structures were supplied by the United States Air Force School of Aviation Medicine (SAM).

The SAM chemical dosimeters include two main types of chemical systems.

The measurement of the neutron dose with the high-hydrogen-content dosimeter was accomplished by evaluation of the amount of stable acid produced in a mixed radiation field by one of the above techniques. Since the water-equivalent, high-hydrogen-content dosimeter is X- and gamma-ray energy-dependent and has a known neutron response, the total acid production can be considered as a combined function of the neutron and gamma radiations. Subtraction of the gamma-produced acids as measured by the fast neutron insensitive chemical dosimeter systems (Reference 26) left a given quantity of acid produced by the neutrons. Division of this neutron-produced acid by the acid yield per rep yielded a neutron dose in terms of reps.

Gamma measurements in the presence of neutrons were accomplished by using the hydrogen-free dosimeters. Since all chemical dosimeters are sensitive to thermal neutrons the thermal neutron dose was calculated independently from cadmium-gold difference

[1] Prepared by Project 2.4; Radiological Division, U.S. Army Chemical Warfare Laboratories, Robert C. Tompkins, Project Officer.

measurements. The data were then corrected by subtraction of 6.7 roentgen equivalents per thermal neutron rep (Reference 27).

D.2.3 Neutron Threshold Devices. A complete description of the neutron system used for instrumenting the structures can be found in Reference 28. Thermal and epithermal neutron flux was measured with gold foils by the cadmium difference method. This technique yields the flux of neutrons below the cadmium cutoff of about 0.3 electron volt. Intermediate energy neutrons were measured with a series of three boron-shielded fission-threshold detectors — Pu^{239} (>3.7 kev), Np^{237} (>0.7 Mev), and U^{238} (>1.5 Mev). High energy neutrons were measured with sulfur detectors having an effective threshold of 3 Mev. The cadmium cutoff and the various energy thresholds are not clearly defined points. For this reason neutron fluxes in this report will be identified with detectors rather than with energy ranges.

The accuracy of these detectors is approximately ±15 percent for doses greater than 25 rep. Measurements are unreliable below 25 rep and cannot be made below 5 rep. The detectors were calibrated and read by Project 2.3.

D.3 INSTRUMENTATION LAYOUT

The objective of the radiation instrumentation was to determine the effectiveness of the buried structures for providing radiation protection. Accordingly, the structures were instrumented to measure the gamma and neutron dose which would be received at a nominal height of 3 feet above the floor of the structure. Since the activities produced in the threshold detectors are relatively short-lived, the two structures, 3.1.a and 3.1.b, which were to be instrumented with these detectors were equipped with aluminum tubes from which the threshold devices could be withdrawn by means of a cable system a few minutes after shot time. The structural details of the cable systems are given in Appendix G, Figure G.3. Since none of the other dose detection systems require early recovery their locations were controlled only by the data that were desired. A film packet, a chemical dosimeter, and in some cases a thermal neutron detector were installed at each instrument station. Structure 3.1.n contained 6 such stations while the other 3 structures contained 3 stations each. The location of each instrumentation station is referenced in Tables D.2 and D.3, and in Figures D.1, D.2, and D.3, to a right-handed cartesian coordinate system with origin at the centroid of the floor of the structure proper. The X direction is taken as positive toward ground zero, Y is positive away from the entrance, and Z is positive upward. In order to calculate transmission factors it was necessary to obtain free-field readings. Neutron spectral data were obtained from the line of stations established by Project 2.3 at 100-yard intervals west from ground zero. In addition, chemical dosimeter and film packet free-field stations were located at ranges 287, 347, 383, and 453 yards.

D.4 RESULTS AND DISCUSSIONS

Free-field dosages are given in Table D.1, and gamma and neutron doses inside the shelters are listed in Tables D.2 and D.3, respectively. Results shown as less than a given figure indicate the lower limit for detector sensitivity in cases where the detectors gave no readings. It is evident from the decrease in dosages with distance from the entranceway that a large amount of radiation streamed through the entranceway.

TABLE D.1 FREE-FIELD INITIAL RADIATION DOSES: PRISCILLA SHOT, FRENCHMAN FLAT

The yield was 36.6 kt and the burst height, 700 ft.

Structure	Horizontal Range	Slant Range	Gamma Dose: Film Badge	Gamma Dose: Chemical Dosimeter	Neutron Dose: Foil Method	Neutron Dose: Chemical Dosimeter
	yd	yd	r	r	rep	rep
3.1.c	287	370	3.0×10^5	3.00×10^5	2.5×10^5	2.49×10^5
3.1.b	347	418	2.0×10^5	1.89×10^5	1.6×10^5	1.62×10^5
3.1.a and n	453	510	1.05×10^5	1.02×10^5	7.5×10^4	7.65×10^4

The effect of greater slant thickness of soil on the ground zero side of the structure is evident from a comparison of the D, E, and F positions in Structure 3.1.n.

D.5 CONCLUSIONS

The underground shelters constructed by Project 3.1 did not provide adequate protection throughout most of their areas against the initial gamma and neutron radiation from a 36.6-kt, moderately high-neutron-flux device at slant ranges from 370 to 510 yards. The gamma and neutron shielding could be improved considerably by suitable design of the entranceways.

TABLE D.2 GAMMA SHIELDING CHARACTERISTICS OF PROJECT 3.1 STRUCTURES: PRISCILLA SHOT, FRENCHMAN FLAT

Yield: 36.6 kt

Height of Burst: 700 ft						Coordinates of Position			Dose		Transmission Factor (Di/Do)	
Type		Earth Cover	Horizontal Range	Slant Range	Angle of Sight	X	Y	Z	Film Badge	Chemical Dosimeter	Film Badge	Chemical Dosimeter
Concrete arches		ft	yd	yd	deg	ft	ft	ft	r	r		
3.1.a	A	4	453	510	27	0	−12	3	$>10^3$	3.5×10^3	$>9 \times 10^{-3}$	3.4×10^{-2}
	B					0	−9	3	4.2×10^2	7.7×10^2	4×10^{-3}	7.6×10^{-3}
	C					−1.5	3.3	3	4.4×10^1	5.0×10^1	4.2×10^{-4}	4.9×10^{-4}
3.1.b	A	4	347	418	34	0	−12	3	$>10^3$	9.3×10^3	$>5 \times 10^{-3}$	4.9×10^{-4}
	B					0	−9	3	$>10^3$	3.5×10^3	$>5 \times 10^{-3}$	1.9×10^{-2}
	C					−1.5	3.3	3	1.25×10^2	1.35×10^2	6.2×10^{-4}	7.1×10^{-4}
3.1.c	A	4	287	370	39	0	−12	3	$>10^3$	1.5×10^4	$>3 \times 10^{-3}$	5.0×10^{-2}
	B					0	−9	3	$>10^3$	4.3×10^3	$>3 \times 10^{-3}$	1.4×10^{-2}
	C					−1.5	3.3	3	2.1×10^2	4.55×10^2	7.0×10^{-4}	1.5×10^{-3}
3.1.n	A	4	453	510	27	0	−18	3	$>10^3$	3.75×10^3	$>9 \times 10^{-3}$	3.7×10^{-2}
	B					0	−15	3	5.7×10^2	1.2×10^3	5.4×10^{-3}	1.2×10^{-2}
	C					0	15	3	1.65×10^2	<50	1.6×10^{-4}	$<5 \times 10^{-4}$
	D					6.5	0	3	3.3×10^1	8.4×10^1	3.1×10^{-4}	8.2×10^{-4}
	E					0	0	3	3.9×10^1	6.6×10^1	3.7×10^{-4}	6.5×10^{-4}
	F					−6.5	0	3	4.0×10^1	8.8×10^1	3.8×10^{-4}	8.6×10^{-4}

TABLE D.3 NEUTRON SHIELDING CHARACTERISTICS OF PROJECT 3.1 STRUCTURES: PRISCILLA SHOT, FRENCHMAN FLAT

Yield: 36.6 kt

Height of Burst: 700 ft						Coordinates of Position			Dose		Transmission Factor (Di/Do)	
Type		Earth Cover	Horizontal Range	Slant Range	Angle of Sight	X	Y	Z	Foil Method	Chemical Dosimeter	Foil Method	Chemical Dosimeter
Concrete arches		ft	yd	yd	deg	ft	ft	ft	rep	rep		
3.1.a	A	4	453	510	27	0	−12	3	*	7.0×10^3	*	8.0×10^{-2}
	B					0	−9	3	*	1.2×10^2	*	1.4×10^{-3}
	C					−1.5	3.3	3	<25	<50	$<3 \times 10^{-4}$	$<6 \times 10^{-4}$
3.1.b	A	4	347	418	34	0	−12	3	*	9.4×10^3	*	4.9×10^{-2}
	B					0	−9	3	*	†	*	†
	C					−1.5	3.3	3	5.7×10^2	9.0×10^1	3.6×10^{-3}	4.7×10^{-4}
3.1.c	A	4	287	370	39	0	−12	3	*	6.0×10^3	*	2.1×10^{-2}
	B					0	−9	3	*	6.6×10^3	*	2.3×10^{-2}
	C					−1.5	3.3	3	*	2.5×10^2	*	8.6×10^{-4}
3.1.n	A	4	453	510	27	0	−18	3	*	2.6×10^3	*	3.0×10^{-2}
	B					0	−15	3	*	7.0×10^2	*	8.0×10^{-3}
	C					0	15	3	*	<50	*	$<6 \times 10^{-4}$
	D					6.5	0	3	*	<50	*	$<6 \times 10^{-4}$
	E					0	0	3	*	<50	*	$<6 \times 10^{-4}$
	F					−6.5	0	3	*	<50	*	$<6 \times 10^{-4}$

* Not instrumented
† No data obtained

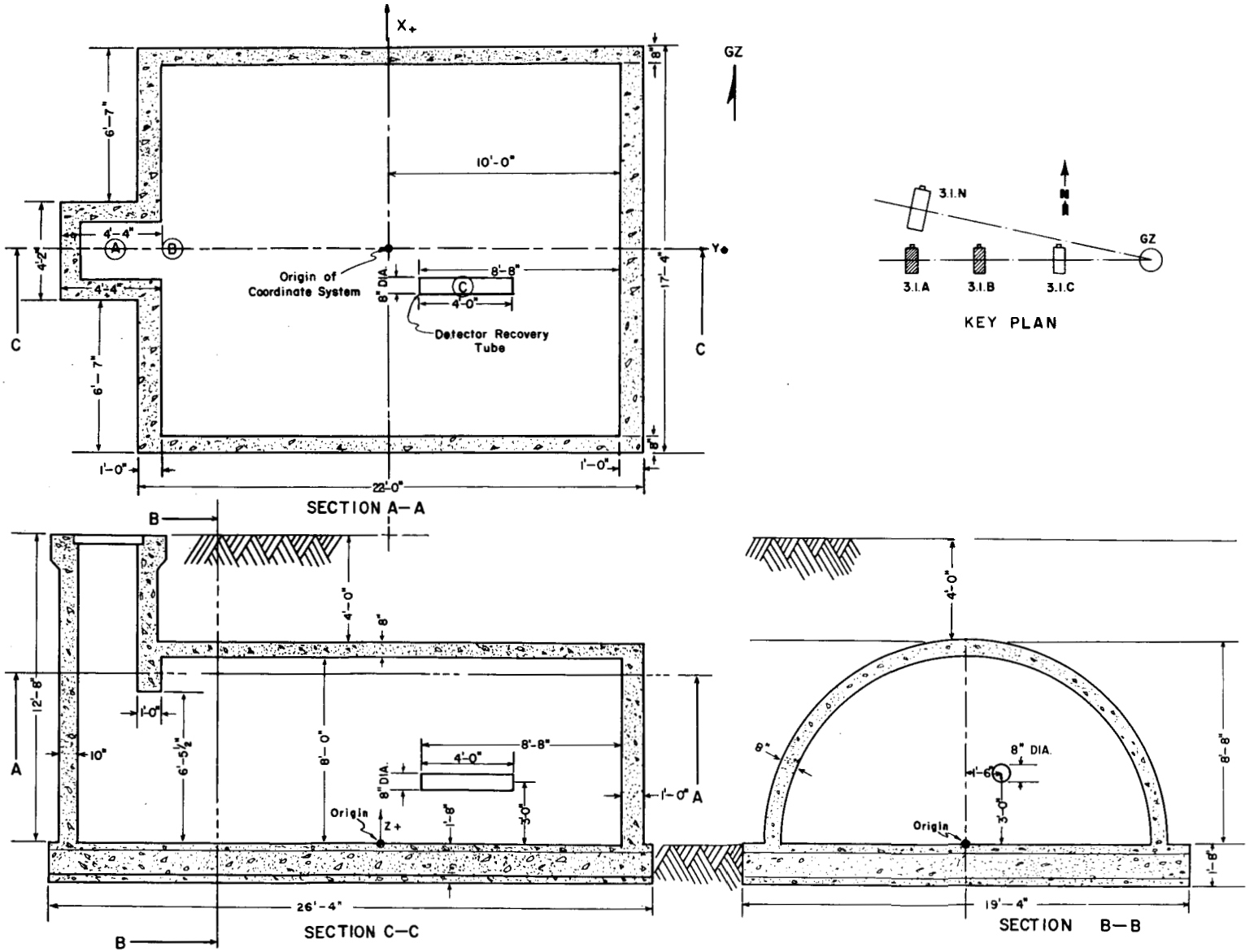

Figure D.1 Location of the detector coordinate system in Structures 3.1.a and b.

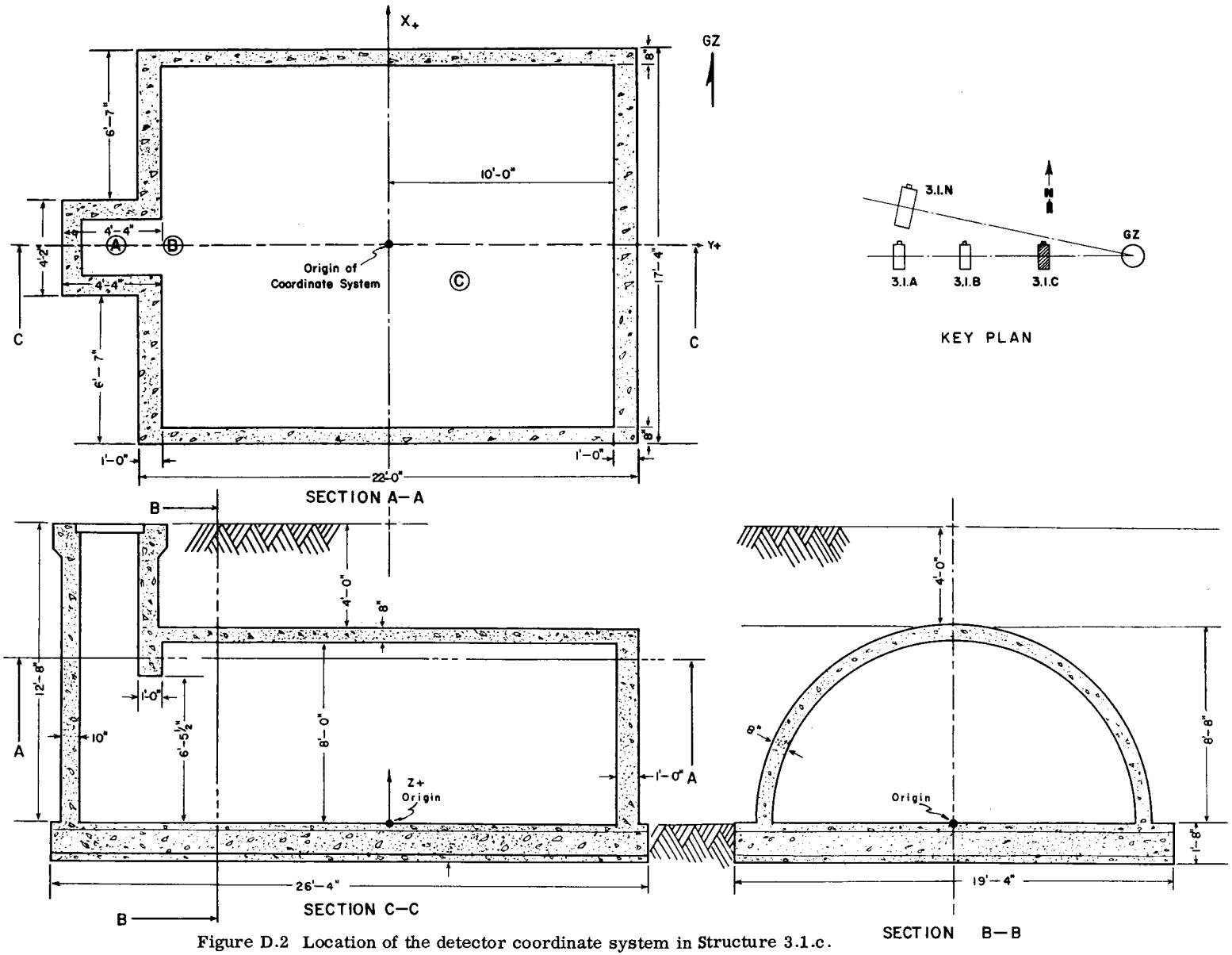

Figure D.2 Location of the detector coordinate system in Structure 3.1.c.

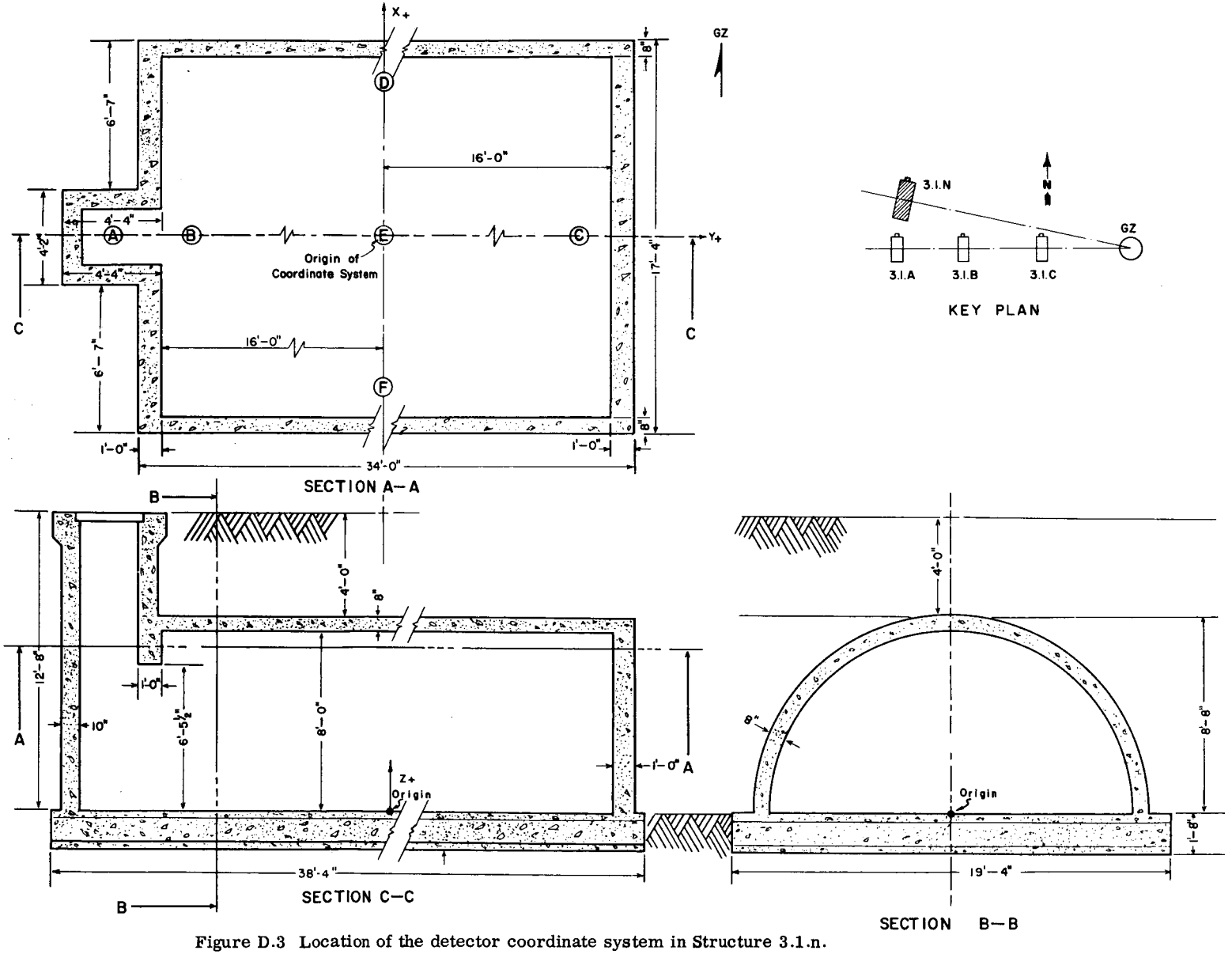

Figure D.3 Location of the detector coordinate system in Structure 3.1.n.

Appendix E[1]

INTERIOR MISSILE and DUST HAZARD

E.1 BACKGROUND

E.1.1 Missile Hazard. Although most of the recent work done in wound ballistics has been concerned with missiles having velocities between 600 and 9,000 ft/sec, it is also a fact that relatively slow velocity missiles which are secondary effects of large-scale explosions cause significant casualties. It is an important fact that missiles with velocities well below 500 ft/sec, in some instances even less than 90 ft/sec, penetrated the abdominal walls of experimental animals (dogs). From this, it is evident that slow-velocity missiles, the type that would be expected in underground concrete structures, possess wounding capabilities. (See also Reference 29.)

E.1.2 Interior Dust Hazard. Fatalities from the inhalation of dust among individuals who had entered structures to escape the effects of aerial bombardment are described in Reference 30. The sources of the dust (which often was in the particle size range to mechanically occlude the respiratory passages) were collapsed buildings and the ceilings and walls of structures near which bomb detonations occurred. Apparently, explosions can cause dust inside of nonpenetrated shelters not only because of mechanical factors but also by the spalling effect, a phenomenon which involves the transmission of a shock or pressure pulse through the walls of a structure, which upon reaching the air-structure interface at the inner surface is reflected as tension wave back into the wall. The consequence of the reflection is the spalling of portions of the wall and/or fine particles of different sizes which are kicked off the inner surface into the internal atmosphere. The existence of a potential hazard to occupants is a function of particle size, concentration in the inhaled air, and total time of exposure.

Since dust is a known environmental hazard and because no data exist referable to closed underground structures exposed to nuclear detonations, a decision was made to carry out field investigation to determine if a dust hazard actually existed in the structures of Project 3.1.

E.2 OBJECTIVES

The main objective of placing Styrofoam missile traps in the four structures was to determine whether or not a missile hazard (concrete fragments) actually existed, and to attempt a correlation of missile hazard with percent of structural damage. At the present time there exists no precise assay of casualties caused from missiles with respect to missile size and velocity.

The main objectives of the dust study were to document the particle sizes of preshot and postshot dust and to differentiate, if possible, the sources of the postshot dust; e.g., whether or not particles arose from the existing dirt on the floor of shelters or actually spalled from the floor, walls, or ceiling as a result of the explosion.

E.3 PROCEDURES

E.3.1 Missile Traps. Styrofoam 22 (made by the Dow Chemical Company, Midland, Michigan) has most of the required properties of a good absorber of missiles. The relatively low shear strength and the nonfibrous cellular structure of Styrofoam result in localized compressive deformation. The resistance of Styrofoam to deformation is low enough so that relatively slow velocity missiles penetrate sufficiently to be measured accurately. (See Reference 29).

The missile traps were constructed of $\frac{3}{4}$-inch-thick plywood and were 3 feet long, 1 foot wide, and 11 inches deep with Styrofoam filling the entire box. The traps were located near the center of each structure and secured to the floor by means of a chain anchored to Ramset fasteners. A typical trap in place is shown in Figure 2.14.

E.3.2 Dust Collectors. Two somewhat similar types of dust collectors were utilized. The first, taped to the floor of each shelter, consisted of an ordinary glass microscopic slide, one inch of which was covered with transparent scotch tape, sticky side up. The second, cemented to the floor of each structure, was the sticky-tray fallout collector: a $\frac{1}{16}$-inch-thick plate of galvanized sheet metal 9 $\frac{1}{2}$ by 10 $\frac{1}{2}$ inches was employed for rigidity, on top of which a transparent but sticky paper was fixed with masking tape. The top of the sticky tray (8 by 9 inches) was protected by two rectangular pieces of paper which ordinarily are stripped off just before exposure of the collector. Upon installation of each plate one of the protective papers was removed and the uncovered side of the collector was marked "C" for control. When the structures

[1] This appendix written by Clayton S. White, M.D., Project 33.2, Director of Research, The Lovelace Foundation, Albuquerque, New Mexico.

were closed up, the other protective paper was removed, thus exposing the other side of the collector marked "E" for experimental.

Thus the microscopic slides collected preshot and postshot dust, the control side of the fallout collector collected preshot and postshot dust, and the experimental side collected predominantly postshot dirt.

Two slides and two trays were placed in each structure. At the time of installation of the slides and trays, a sample of dirt was scraped from the floor of each structure and placed in a marked bottle.

E.4 RESULTS

The structures were closed up two days before the shot, at which time the protective covers were removed from the various missile traps. At the same time, the protective paper covering the experimental side of the dust collector trays was removed. The structures were initially re-entered four days after the shot, at which time the slides and trays were removed and returned to the laboratory for analysis.

E.4.1 Missile Traps. No evidence of concrete fragments (missiles) were found in the missile traps or on the floors of the various structures. There was one insignificant exception, however. Prior to the shot, a small hole in the end wall of Structure 3.1.c was patched with grout. The wall suffered some damage from the detonation in the form of cracks, one of which passed through the grout pocket, thus shaking loose some grout material. The cracked loose grout can be seen in Figure 3.21.

E.4.2 Dust Collectors. At the time of initial recovery, the tops of the microscopic slides were covered with transparent scotch tape. The fallout trays, after being pried loose from the floor, were placed face to face, care being taken to oppose the control side of one collector to the control side of the other taken from the same shelter. These measures served to protect each of the dust collectors from contamination after removal from the several structures.

After recovery, the two opposing sheets of the transparent sticky paper were stripped from the fallout trays. Inspection of the preparations revealed the following: The sticky paper from all of the shelters was successful in trapping debris; particle sizes varied from microscopic particles of dust to discrete pieces of mortar, wood, and small aggregates of dirt. None of the material on the slides was identified as originating from the interior surface of the arch. The dust particles on the slides matched the preshot dust samples taken from the floor of the structure.

E.5 CONCLUSIONS

E.5.1 Missile Hazards. The four concrete underground structures were free from concrete missiles. No interior missile hazard existed in the structures from the effects of a device of the yield tested in the Priscilla event beyond a range of 860 feet from ground zero.

E.5.2 Dust Hazard. It appears that no dust hazard was present in any of the structures.

Appendix F[1]

RADIATION EFFECTS on RECORDING PAPER

F.1 BACKGROUND

This study was made to determine the relative resistivity to fogging of various recording papers and film when exposed to nuclear radiation. In past operations, various laboratories have encountered difficulties in obtaining readable record traces on photographic-type recording papers exposed to radiation. Two methods currently employed to protect records from radiation effects are by using a tape recording system, or by shielding the instrumentation shelter to isolate the recording system from radiation effects.

Film fogging produced by radiation apparently has two sources: direct radiation effects and indirect effects which accrue from the removal of records through the high surface-radiation field.

F.2 PROCEDURE

The papers and film available at the Nevada Test Site for use in the tests were: Kodak 1127, Kodak Microfile Film Emulsion No. 1112, Kodak 809, Visicorder, and Lino Writ 3. Each paper was trace-exposed by conventional means with the exception of the Microfile, which was not exposed. Five-inch squares of each type of material were placed in twenty-seven lightproof, waterproof envelopes under dark-room conditions. **Envelopes, numbered 1 to 15,** were used in an experiment having a Co^{60} point source operated by Evans Signal Laboratory. The dosage rates varied from 100 mr to 1,000 r, with an accuracy of ± 5 percent of the indicated dosage.

The remaining envelopes, numbered 16 to 27, contained films that were placed in various structures to permit a direct effects comparison with the calibrated envelopes numbered 1 to 15. They were located in areas that would experience a significant variation of total radiation dosage. A film badge which is capable of measuring radiation exposure up to approximately 1,000 r was taped to each envelope.

After the shot, the envelopes placed in the field were removed between D-Day and D + 4. All of the recording papers were then developed at the Waterways Experiment Station under standard dark-room methods and in accordance with the manufacturers' specifications.

The film badges used to determine the field radiation dosages were analyzed by the Chemical Warfare Laboratory. Because the high energy radiation extended beyond the 1,000 r range of the film badges in some of the field positions, radiation exposure above this level is simply noted as being greater than 1,000 r. However, in two stations, F3.1 9014.01 (3.1.c) and 9014.02 (3.1.b), radiation values exceeding 1,000 r were recorded by Project 2.4 (see Appendix D) and are shown in Table F.1 under envelope Numbers 17 and 19. The dosage estimates have a possible variation of ± 20 percent.

F.3 RESULTS AND CONCLUSIONS

Table F.1 presents the results of the experiment. There were two recording papers that showed definite capabilities of resisting fogging from gamma radiation. The Visicorder paper received no apparent effects from values of gamma radiation up to 15,000 r. The Microfile film fogged out at some value greater than 200 r but less than 10,000 r; no other values between these two radiation ranges were available. Lino Writ 3 and K 1127 showed fogging effects in the range of 50 r, and became progressively darker with increased radiation until the traces on the records were no longer discernible at approximately 150 r. **Clear** traces were observed for the K 809 paper up to 30 r but at values greater than 50 r, the paper fogged to the extent that traces were no longer readable. It can be concluded that the Visicorder paper would require very little shielding from radiation while the other recording papers would require considerable shielding in order to obtain readable records.

[1] By J. D. Laarman, Sp 3, Project 3.1, and P. A. Shows, both from the U. S. Army Engineer Waterways Experiment Station, Vicksburg, Mississippi.

TABLE F.1 RADIATION EFFECTS ON RECORDING PAPER

Envelope Number	Envelope Contents	Station Placement	Radiation Dosage	Effects* Lino Writ 3 (L)	Visicorder (V)	K 809 (K)	K 1127 (K′)	K 1112 (M)
1	L, V, K, K′	Control	0 r	A	A	A	A	—
2	L, V, K, K′	Control	100 mr	A	A	A	A	—
3	L, V, K, K′	Control	500 mr	A	A	A	A	—
4	L, V, K, K′	Control	1 r	A	A	A	A	—
5	L, V, K, K′	Control	5 r	A	A	A	A	—
6	L, V, K, K′	Control	10 r	B	A	A	A	—
7	L, V, K, K′	Control	< 30 r	B	A	A	B	—
8	L, V, K, K′	Control	> 50 r	B	A	N.G.	B	—
9	L, V, K, K′	Control	70 r	B	A	N.G.	B	—
10	L, V, K, K′	Control	100 r	B	A	N.G.	C	—
11	L, V, K, K′	Control	150 r	C	A	N.G.	C	—
12	L, V, K, K′	Control	200 r	N.G.	A	N.G.	N.G.	—
13	L, V, K, K′	Control	300 r	N.G.	A	N.G.	N.G.	—
14	L, V, K, K′	Control	500 r	N.G.	A	N.G.	N.G.	—
15	L, V, K, K′	Control	1,000 r	N.G.	A	N.G.	N.G.	—
16	L, V, K, K′, M	F 3.1 9014.01	200 r	C	A	N.G.	C	A
17	L, V, K, K′, M	F 3.1 9014.01	15,000 r	N.G.	A	N.G.	N.G.	N.G.
18	L, V, K, K′, M	F 3.1 9014.02	150 r	C	A	N.G.	N.G.	A
19	L, V, K, K′, M	F 3.1 9014.02	10,000 r	N.G.	A	N.G.	N.G.	N.G.
20	L, V, M	F 3.1 9014.03	44 r	B	A	—	—	A
21	L, V, M	F 3.1 9015	16.5 r	B	A	—	—	A
22	L, V, M	F 733	6 r	A	A	—	—	A
23	L, V, M	F 733	8 r	A	A	—	—	A
24	L, V, K, M	F 713	> 1,000 r	N.G.	A	N.G.	—	N.G.
25	L, V, K, M	F 711	> 1,000 r	N.G.	A	N.G.	—	N.G.
26	L, V, K, M	F 223	1 r	A	A	A	—	A
27	L, V, K, M	Control	0 r	A	A	A	—	A

*A No fogging, excellent records obtainable.
B Slight fogging, fair records obtainable.
C Medium fogging, poor records obtainable.
N.G. Dense fogging, records not obtainable.

Appendix G
SPECIFICATIONS for ARCH STRUCTURES

Appendix G describes in detail the technical specifications as applied to the structures tested in Project 3.1. The applicable drawings referred to in the specifications are shown in Figures G.1, G.2, and G.3.

G.1 EXCAVATION, FILLING, AND BACKFILLING

The work covered by this section of the specifications consists in furnishing all plant, labor, equipment, appliances, and materials, and in performing all operations in connection with the excavation, filling, and backfilling, complete, in strict accordance with this section of the specifications and applicable drawings, and subject to the terms and conditions of the contract.

G.1.1 Applicable Standard. The following standard, of the issue listed below but referred to thereafter by basic designation only, forms a part of this specification:

American Association of State Highway Officials Standard Method: T 99-49. Standard Laboratory Method of Test for the Compaction and Density of Soil.

G.1.2 Excavation. The site indicated on the drawings shall be cleared of natural obstructions and existing foundations, pavements, utility lines, and other items that would interfere with the construction operations. The excavation shall conform to the dimensions and elevations indicated on the drawings for the structure, except as specified below, and all work incidental thereto. Excavation shall extend a minimum of 10 feet horizontally from footings, or to whatever distance is required to allow for placing and removal of forms, installation of services, and for inspection, except where the concrete for walls and footings is authorized to be deposited directly against excavated surfaces. Undercutting will not be permitted. Suitable excavated material required for fill under slabs shall be separately stockpiled as directed by the Contracting Officer. Excess material from excavation, not required for fill or backfill, shall be wasted. Wasted material shall be spread and leveled or graded as directed by the Contracting Officer.

G.1.3 Fill. Where concrete slabs are to be placed on earth, unsuitable material, as determined by the Contracting Officer, shall be removed. Fill, where required to raise the subgrade for concrete slabs to the elevations indicated on the drawings shall consist of crushed stone, sand, gravel, earth, or other material approved by the Contracting Officer. Fill shall be compacted in a manner approved by the Contracting Officer, and the subgrade brought to a reasonably true and even plane. Crushed stone, sand, or gravel used for fill shall be placed in layers not more than 8 inches thick. Earth used for fill shall be placed in layers not more than 8 inches thick. Each layer shall be uniformly spread.

G.1.4 Backfilling. After completion of foundation footings, foundation walls, and other construction below the elevation of the final grades, and prior to backfilling, forms shall be removed and the excavation shall be cleaned of trash and debris. Backfill shall consist of the excavation or borrow of sand, gravel, or other materials approved by the Contracting Officer, and shall be free of trash, lumber, or other debris. The backfill material shall conform to a moisture content determined by laboratory tests and compacted to a specified density. These values will be furnished to the contractor prior to the field operation. Backfill shall be placed in horizontal layers not more than 8 inches thick. Backfill shall be brought to a suitable elevation above grade to provide for anticipated settlement and shrinkage thereof. Backfill shall not be placed against the structure prior to 7 days after completion and then only after approval by the Contracting Officer. Backfill shall be brought up evenly on each side of the structure as far as practicable. In no case should the backfill on one side be carried more than 12 inches higher than on the opposite side. Heavy equipment for spreading and compacting backfill shall not be operated closer than 6 feet from the structure.

G.2 SUPPLEMENTAL BACKFILLING INSTRUCTIONS

The following supplemental instructions prepared by Project 3.8 were issued to the contractor to assure proper preparation and placement of the backfill material.

G.2.1 General Requirements and Conditions. The soil required to be excavated for all installations of Project 3.1 shall be stockpiled and used for backfilling the excavations around and over the completed installations to the specified grade. The backfill shall be compacted by means of mechanical tampers (pneumatic or power operated) to 100 percent standard AASHO density

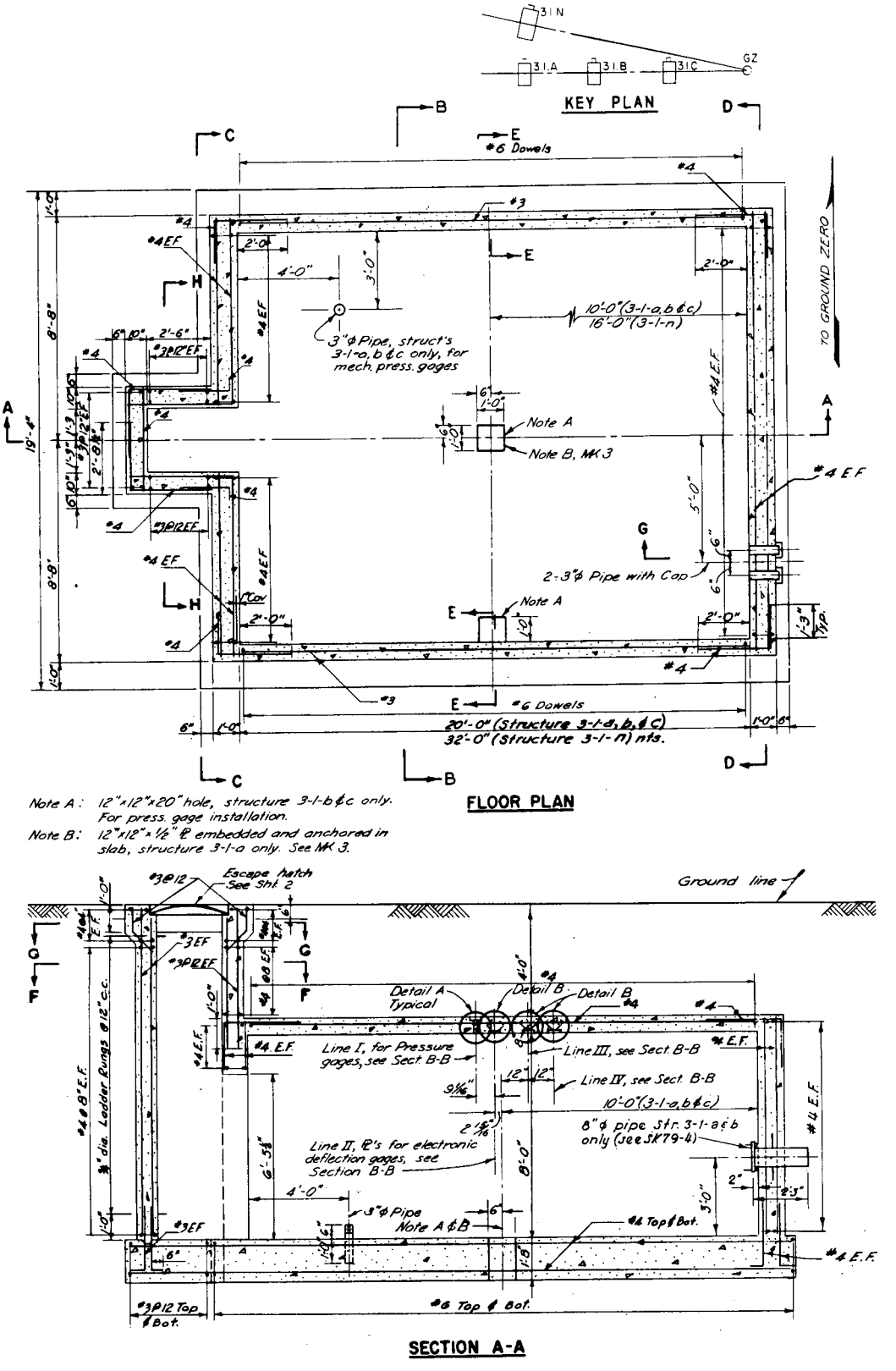

Figure G.1 Reinforced concrete arch structure, floor plan and sections.

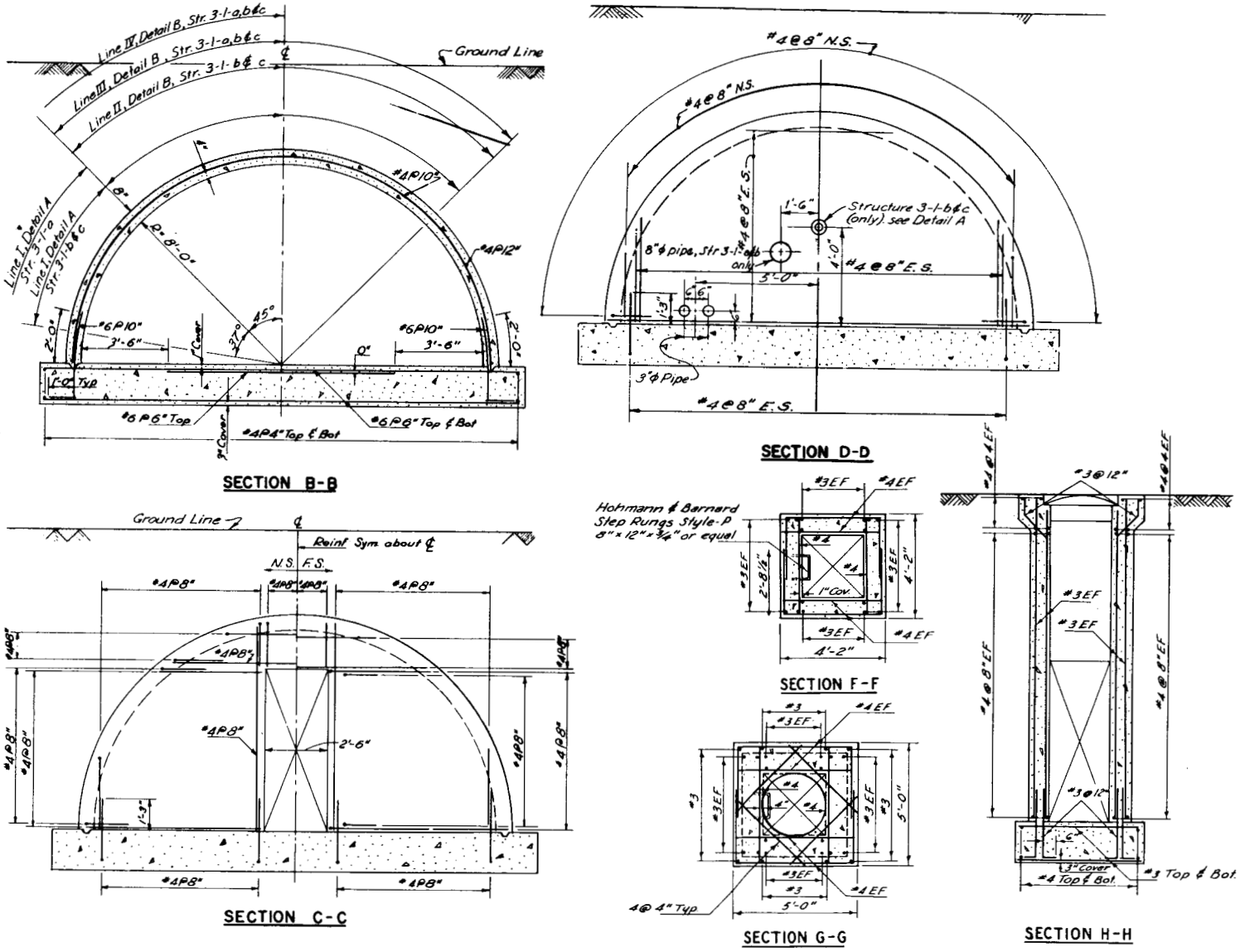

Figure G.1 Continued.

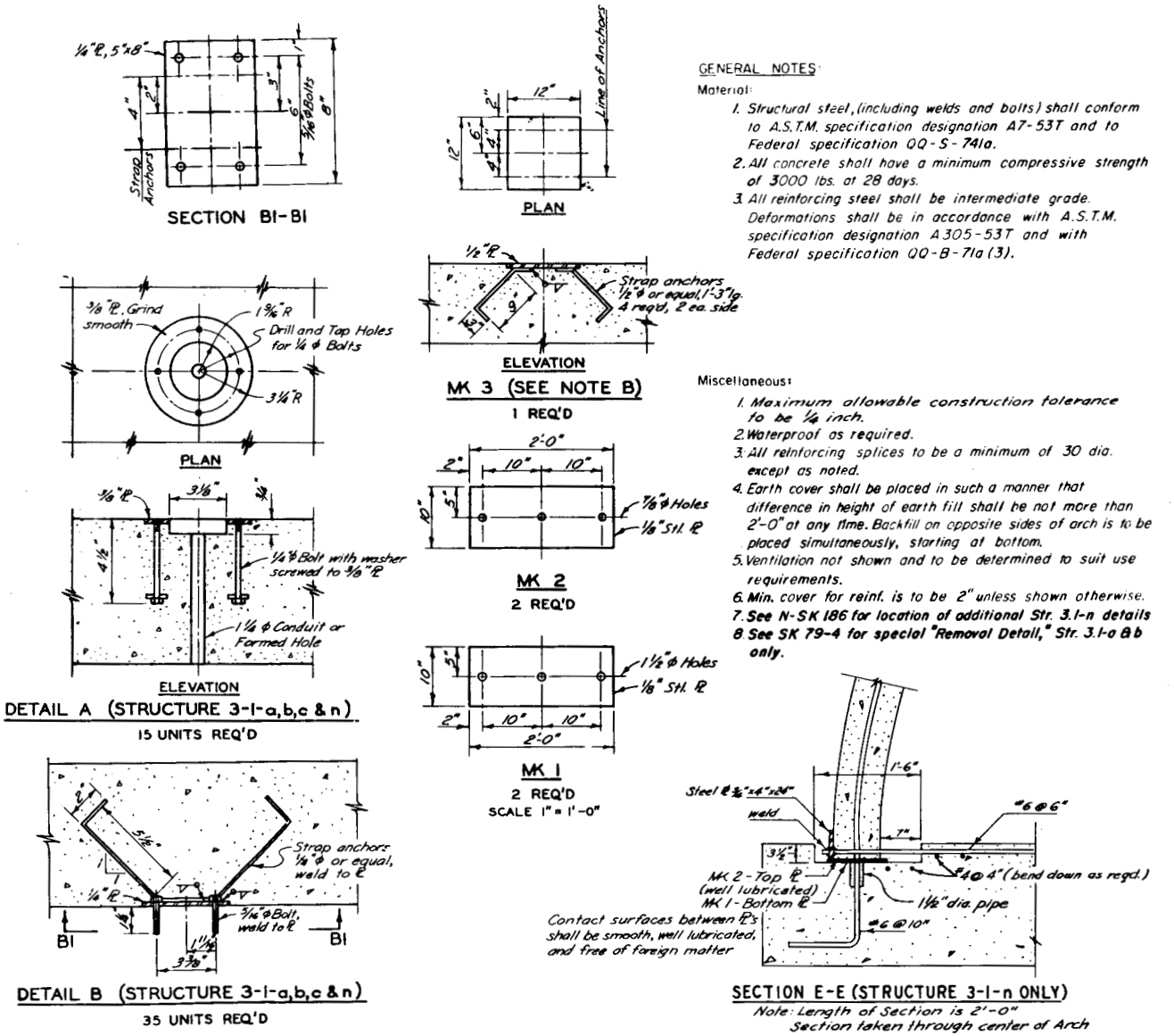

GENERAL NOTES:

Material:

1. Structural steel, (including welds and bolts) shall conform to A.S.T.M. specification designation A7-53T and to Federal specification QQ-S-741a.
2. All concrete shall have a minimum compressive strength of 3000 lbs. at 28 days.
3. All reinforcing steel shall be intermediate grade. Deformations shall be in accordance with A.S.T.M. specification designation A305-53T and with Federal specification QQ-B-71a (3).

Miscellaneous:

1. Maximum allowable construction tolerance to be ¼ inch.
2. Waterproof as required.
3. All reinforcing splices to be a minimum of 30 dia. except as noted.
4. Earth cover shall be placed in such a manner that difference in height of earth fill shall be not more than 2'-0" at any time. Backfill on opposite sides of arch is to be placed simultaneously, starting at bottom.
5. Ventilation not shown and to be determined to suit use requirements.
6. Min. cover for reinf. is to be 2" unless shown otherwise.
7. **See N-SK 186 for location of additional Str. 3.1-n details**
8. **See SK 79-4 for special "Removal Detail," Str. 3.1-a & b only.**

Figure G.1 Continued.

at a water content of 3 percent of the optimum water content for standard AASHO density. Sheepsfoot rollers will not be used for compaction of any backfill for Project 3.1 installations.

Soil from the stockpiles to be used for backfilling has been subjected to extensive compaction tests. The test results show relatively wide variations in the compaction characteristics of the soil in individual stockpiles, and that all of the soil is 8 to 15 percent dry of the water content required for compaction. As a result, the soil in individual stockpiles will have to be thoroughly mixed and sufficient water will have to be added to the soil to increase the water content to 3 percent dry of optimum before it is placed and compacted as backfill. **Otherwise, backfill with the required strength** characteristic cannot be constructed.

Equipment and procedures not covered in these instructions may be used if considered satisfactory by the Project Officer. Any additional detailed instructions, not covered by directives from higher authority, as to the equipment and procedures to be used in backfilling operations, will be issued to the appropriate contractor supervisory personnel by the Project Officer.

All soil sampling and testing required in connection with backfilling operations will be performed by Project 3.8 personnel. Results of completed tests may be obtained by both project and contractor personnel from the Project 3.8 field office located in the Frenchman Flat area.

Project 3.1 requires the backfilling of four structures which are identified as:

F-3.1-9014.01 (or 3.1.c)
F-3.1-9014.02 (or 3.1.b)
F-3.1-9014.03 (or 3.1.a)
F-3.1-9015 (or 3.1.n)

The backfill may start on any one of the four structures. Once started, the backfilling on each of all four structures shall be a continuous operation without intermittent delays.

There shall be no trash, lumber, debris, or uncontrolled soil contained in either the excavated holes or in any backfill soil.

The final grade of the earth fill for all four structures shall be the specified natural grade elevation. The final grade around the structure entrance shall be flush with the top of the structure entrance.

If floods or any similar act of God should be experienced before the backfilling is completed, all compacted and stockpiled backfill soil shall be protected from damage by the act.

At no time (i.e., during backfill mixing, placement, or compaction operations) shall any equipment come in contact with or otherwise endanger the soundness of the structures, instruments, instrument cables, or instrumentation piping.

At no time shall heavy equipment and/or earth-moving equipment operate closer to the structure than a vertical plane passing within 6 feet of any part of the foundation base of the structure.

The basic backfill procedures are to be identical for all four structures with the following exceptions: (a) Backfilling on Structure 3.1.n must cease for approximately one half hour to allow Project 3.1 personnel to make required instrumentation measurements when the backfill reaches a height of 6 feet above the top of the footings, and again when the backfill is level with the arch crown, and (b) Structures 3.1.a and 3.1.b have additional trench excavations with 8-inch-diameter pipes on their south ends. **Backfilling shall** include these trenches, with special precautions taken to protect the 8-inch-diameter pipes they contain.

Special precautions must also be taken to protect the instrumentation cables coming out of the structures into existing instrumentation trenches on the south end of all four structures. Controlled backfilling of these approximately 3-foot-deep trenches shall extend from the structure base slab for 15 feet.

After compaction is finished on all four structures, all waste soil shall be removed from the Project 3.1 area, and disposed of in a manner which shall not interfere with any other project test area.

The completion time for the backfill of all four structures shall be no later than 30 May 1957.

G.2.2 Backfill Construction Procedures.

G.2.2.1 Mixing backfill soil. Individual stockpiles of backfill soil shall be thoroughly mixed in order to achieve a uniform soil mixture before water is added to the soil. The required mixing shall be accomplished a minimum of 24 hours, and preferably longer, before water is added and the soil stockpiled for use as backfill.

Mixing of small stockpiles to be used for backfilling Project 3.1 installation shall be accomplished by casting the entire stockpile with a dragline or clamshell from its present location to a new location, then recasting the stockpile to another location convenient for adding water, mixing, and placing the prepared soil in the area to be backfilled.

G.2.2.2 Adding and Mixing Water into Backfill Soil. After backfill soil has been thoroughly mixed it shall be placed in windrows of convenient size, and sufficient water shall be added in increments and mixed into the soil by means of a pulvimixer and motor patrol to raise the water content to that specified by the Project Officer.

Immediately after the adding and mixing of water into the backfill soil has been completed, the soil windrow shall be stockpiled at a location convenient to the excavation to be backfilled. Stockpiling shall be accomplished by means of a dragline, clamshell, or endloader. Stockpiled soil to which water has been added shall be protected from drying by covering with tarpaulins, or sprinkling, as required or directed by the Project Officer. Also, stockpiles from which soil is being removed and placed for compaction shall be

maintained in a symmetrical cone shape, and shall not be permitted to become ragged, as this would result in excess evaporation of water.

G.2.2.3 Placement of Backfill Soil to be Compacted. All loose soil and debris shall be removed from excavations to be backfilled prior to the placement of the first lift of backfill soil, and thereafter as required or directed by the Project Officer.

The exposed surface of previously compacted backfill and the face of the excavation up to the top of successive lifts of backfill shall be sprinkled lightly with water to insure bonding of the backfill. Ponding of water on the surface of compacted lifts will not be permitted. Any surfaces of previously compacted lifts that appear too hard or glazed to insure bonding with the next lift to be placed shall be scarified if so directed by the Project Officer.

All soil placed as backfill shall be obtained from previously prepared stockpiles. The placing of soil directly from windrows into areas to be backfilled will not be permitted.

The soil will be placed in lifts of uniform thickness sufficient to result in compacted lifts of 4 inches. In order to insure uniformity of lift thickness the placement of successive lifts of loose backfill shall be controlled by grade stakes. Starting at the bottom of the excavation, grade stakes for placement of backfill will be set at successive heights of 4 inches above the bottom. In the event of undercompaction, or overcompaction, the Project Officer may order changes in the thickness of the lifts to be placed and compacted.

Loose soil that is permitted to become too wet, or too dry, from any cause whatsoever after it has been placed for compaction shall be removed and replaced with backfill of the proper water content, if so directed by the Project Officer.

The backfill shall be placed in alternate layers from both sides of the structures, maintaining as nearly as practicable a uniform height of backfill at all times. In no case shall the backfill on one side be carried more than 12 inches higher than on the opposite side of the structure.

Special care must be taken when backfilling and compacting within 2 feet of all instrumentation pressure gages (total 22 for all structures) mounted on the outside surface of the structures. Project 3.1 Project Officer will give explicit on-the-job instructions concerning hand-tamping over and around these instrumentation pressure cells on the Project 3.1 structures.

G.2.2.4 Compaction. Compaction by mechanical tampers shall be performed in a manner that will insure uniform application of compaction effort to the entire surface of each lift to be compacted. At the start of backfilling and compaction operations at each installation, each unit of surface area of each loose lift equal in area to the area of the tamping foot of the tampers shall be compacted by 25 blows of the tamper. It may be necessary to vary the compaction effort from time to time in order to achieve the required density in the backfill. In the event such changes are required, the Project Officer will issue instructions as to the compaction effort to be used.

The surface of all compacted lifts shall be protected so as to prevent undue drying out, or wetting from rainfall or otherwise, by covering with tarpaulins, or sprinkling as required or directed by the Project Officer.

G.3 CONCRETE

The work covered by this section of the specifications consists in furnishing all plant, labor, equipment, appliances, and materials, and in performing all operations in connection with the installation of concrete work, complete, in strict accordance with this section of the specifications and the applicable drawings, and subject to the terms and conditions of the contract. Full cooperation shall be given other trades to install embedded items. Suitable templates or instructions, or both, will be provided for setting items not placed in the forms. Embedded items shall have been inspected, and tests for concrete and other materials or for mechanical operations shall have been completed and approved, before concrete is placed.

G.3.1 Applicable Specifications. The following specifications, standards, and publications, of the issues listed below but referred to thereafter by basic designation only, form a part of this specification:

a. Federal Specifications:
P-O-361 (CRD-C 508) Oil, Floor; Mineral.
QQ-B-71a (CRD-C 500) Bars; Reinforcement for Concrete.
SS-C-158C (CRD-C 201) Cements, Hydraulic; General Specifications.
SS-A-281b (CRD-C 131) Aggregate; for Portland-Cement Concrete.
SS-C-192b (CRD-C 200) Cements, Portland.
O-C-106a (CRD-C 505) Calcium Chloride; Hydrated, Technical Grade.
SS-C-197 (CRD-C 251) Cement, Portland

SS-C-197 (CRD-C 251) Cement, Portland Blast Furnace Slag.

b. Corps of Engineers Specifications:
CRD-C-5-52 Slump of Portland Cement Concrete.
CRD-C-300-52 Pigmented Membrane-Forming Compounds for Curing Concrete.
CRD-C-16 Method of Testing for Flexural Strength of Concrete.

c. American Society for Testing Materials Standards:
A-305 (CRD-C 506) Minimum Requirements for the Deformation of Deformed Steel Bars

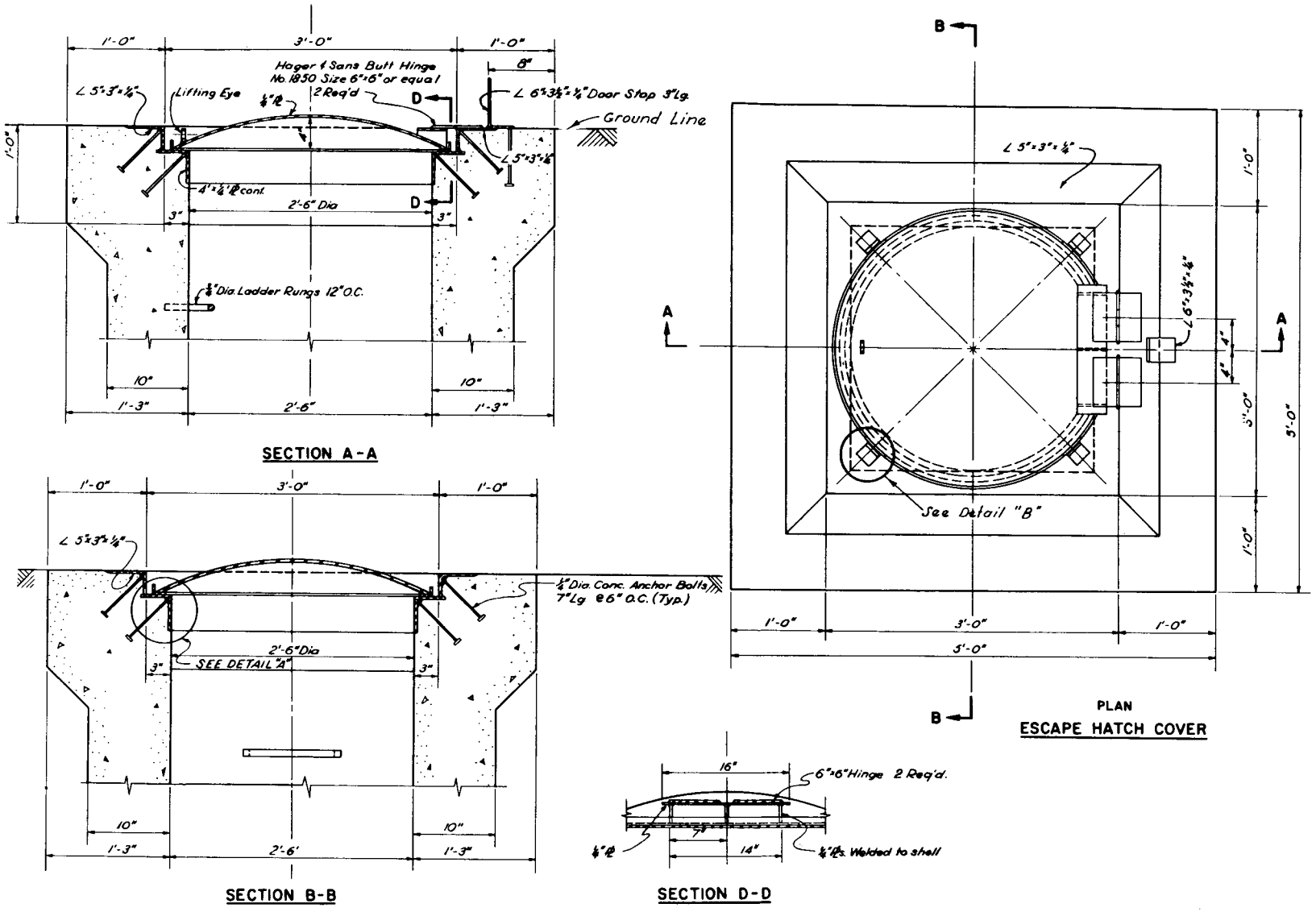

Figure G.2 Reinforced concrete arch structure, escape hatch cover.

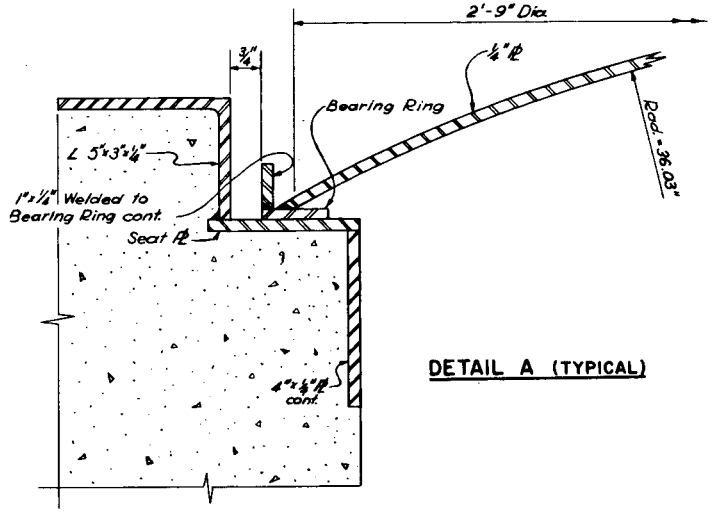

DETAIL A (TYPICAL)

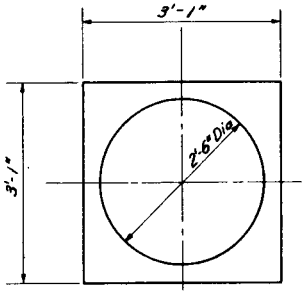

Note: Seat cut from 1/4" ℄

PLAN

SEAT PLATE

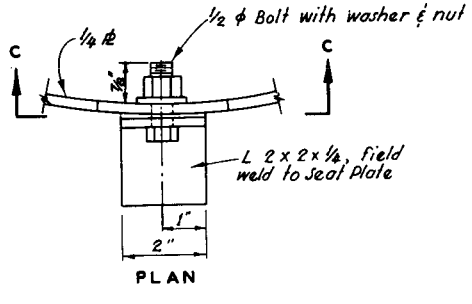

PLAN

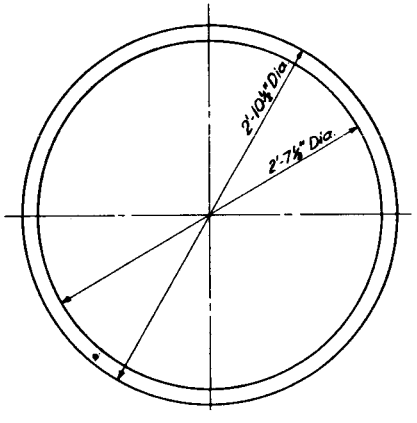

Note: Ring cut from 3/16" ℄

PLAN

BEARING RING

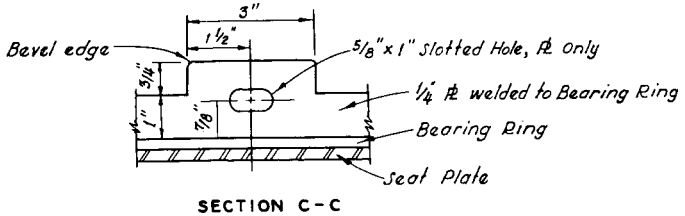

SECTION C-C

DETAIL B(TYPICAL)

Figure G.2 Continued.

for Concrete Reinforcement.

C-31 (CRD-C 11) Making and Curing Concrete Compression and Flexure Test Specimens in the Field.

C-39 (CRD-C 14) Compressive Strength of Molded Concrete Cylinders.

C-40 (CRD-C 121) Organic Impurities in Sands for Concrete.

C-42 (CRD-C 27) Securing, Preparing and Testing Specimens from Hardened Concrete for Compressive and Flexural Strengths.

C-94 (CRD-C 31) Ready Mixed Concrete.

C-192 (CRD-C 10) Making and Curing Concrete Compression and Flexure Test Specimens in the Laboratory.

C-171 (CRD-C 310) Paper, Concrete-Curing.

G.3.2 Materials.

a. Abrasives: Abrasive aggregate shall be aluminum oxide or emery graded from particles retained on a No. 50 sieve to particles passing a No. 8 sieve.

b. Accelerating agent shall be calcium chloride conforming to Federal Specification O-C-106 (CRD-C 505).

c. Aggregate: Both coarse and fine aggregate shall conform to Federal Specification SS-A-281 (CRD-C 131). Coarse aggregate shall be well graded from fine to coarse, within prescribed limits. The maximum size shall be 1 inch for class A concrete.

d. Cement: Only one brand of each type of cement shall be used for exposed concrete in any individual structure. Cement reclaimed from cleaning bags or leaking containers shall not be used. Cement shall be used in the sequence of receipt of shipments, unless otherwise directed by the Contracting Officer.

(1) Portland cement: Federal Specification SS-C-192 (CRD-C 200), Type I or Type II (Type I-A or Type II-A).

(2) High-early-strength Portland cement: Federal Specification SS-C-192, Type III) Type III-A).

(3) Portland blast-furnace slag cement: Federal Specification SS-C-197 (CRD-C 251).

e. Curing materials:

(1) Waterproof paper: ASTM Designation CRD-C 310.

(2) Mats: Commercial quality of type used for the purpose.

(3) Burlap: Commercial quality.

(4) Membrane curing compounds: Corps of Engineers Specification CRD-C 300.

f. Forms shall be of wood, metal, or other approved material and shall conform to the following requirements:

(1) Wood forms: No. 2 Common or better lumber.

(2) Plywood: Commercial-Standard Douglas fir, moisture-resistant, concrete-form plywood, not less than 5-ply and at least $^{9}/_{16}$-inch thick.

(3) Metal Forms of approved type that will produce surfaces equal to those specified for wood forms.

(4) Form oil: Federal Specification P-O-361 (CRD-C 508).

(5) Form ties shall be of approved design, fixed or adjustable in length, free of devices which will leave a hole larger than $^{7}/_{8}$ inch in diameter in surface of concrete.

g. Reinforcement:

(1) Bars: Federal Specification QQ-B-71 (CRD-C 500), type B, grade 2, intermediate billet. Deformations shall conform to ASTM Standard A-305 (CRD-C 506).

(2) Mill reports: Certified copies of mill reports shall accompany deliveries of reinforcing steel.

h. Water shall be clean, fresh, and free from injurious amounts of mineral and organic substances.

G.3.3 Admixtures. Admixtures shall be used only on written approval of the Contracting Officer. Tests of admixtures will be made by the Government in accordance with applicable Federal or ASTM specifications or as otherwise prescribed.

G.3.4 Samples and Testing. Testing of the aggregate and reinforcement shall be the responsibility of the contractor. The testing agency shall be approved. Testing of end items is the responsibility of the Government. Samples of concrete for strength tests and end items shall be provided and stored by the contractor when and as directed.

a. Cement shall be tested as prescribed in the applicable references specification under which it is furnished. Cement may be accepted on the basis of mill tests and the manufacturer's certification of compliance with the specifications, provided the cement is the product of a mill with a record of production of high-quality cement for the past 3 years. Certificates of compliance shall be furnished by the contractor, for each mill lot of cement furnished from different mills in mixed shipment and for each separate shipment from the same mill, prior to use of the cement in the work. This requirement is applicable to cement for job-mixed, ready-mixed, or transit-mixed concrete. Cement proposed for use where no certificate of compliance is furnished or where, in the opinion of the Contracting Officer, the cement furnished under certificate of compliance may have become damaged in transit, or deteriorated because of age or improper storage, will be sampled at the mixing site by representatives of the Government and tested for conformance to the specification at no expense to the contractor. Access to the cement and facilities for sampling shall be readily afforded the Government's agent. Cement being tested shall not be used in the work prior to receipt by the contractor of written notification from the Contracting Officer that the cement has satisfactorily passed the 7-day tests. Cement, for job-mixed concrete, failing to meet test requirements shall be removed from the site. Cement at batching plants for ready-mixed and transit-mixed concrete failing to meet test requirements shall not be used in Govern-

ment work.

b. Aggregate shall be tested as prescribed in Federal Specification SS-A-281b (CRD-C 131). In addition, fine aggregate shall be tested for organic impurities in conformance with ASTM Standard C-40 (CRD-C 121).

c. Reinforcement: Reinforcing bars shall be tested as prescribed in Federal Specification QQ-B-71 (CRD-C 500). Ten sample reinforcing bars of 18-inch length shall be taken from the structure for each of the following size groups: No. 5 or less, No. 5 to No. 8, and over No. 8. The ten samples shall be selected so as to represent a specimen from the wall reinforcement, the floor-slab reinforcement, and the arch reinforcement. Each sample shall be securely tagged so as to identify the source of the sample with respect to the structure and shall be forwarded to the testing laboratory, as directed by the Contracting Officer.

d. Concrete: The contractor shall provide for test purposes 30 compression test cylinders per structure and 10 beam specimens per structure taken during the pours. These samples shall be taken from pours designated by the Contracting Officer. Test specimens shall be made and cured in accordance with ASTM Standard C-31 (CRD-C 11). Specimens shall be cured under laboratory conditions except that the Contracting Officer may require curing under field conditions when he considers that there is a possibility of the air temperature falling below 40° F. Cylinders shall be tested in accordance with ASTM Standard C-39. Beams shall be tested in accordance with Corps of Engineers Specifications (CRD-C-16). The standard age of test for determining concrete strength shall be 28 days, but 7-day tests may be used with the permission of the Contracting Officer, provided that the relation between the 7-day and 28-day strength of the concrete is established by tests for the materials and properties used. Some specimens will be tested at an age designated by the Contracting Officer. If the average of the strength tests of the laboratory control specimens for any portion of the work falls below the minimum allowable compressive or flexural strength at 28 days required for the class of concrete used in that portion, the Contracting Officer shall have the right to order a change in the proportions or the water content of the concrete, or both, for the remaining portions of the work at the contractor's expense. If the average strength of the specimens cured on the job falls below the minimum allowable strength, the Contracting Officer may require changes in the conditions of temperature and moisture necessary to secure the required strength. Where there is question as to the quality of the concrete in the structure, the Contracting Officer may require tests in accordance with ASTM Standard C-42. In the event that tests indicate that concrete placed does not conform to the drawings and these specifications, measures prescribed by the Contracting Officer shall be taken to correct the deficiency at no additional expense to the Government.

G.3.5 Storage. Storage accommodations shall be subject to approval of the Contracting Officer and shall afford easy access for inspection and identification of each shipment in accordance with test reports.

a. Cement: Immediately upon receipt at site of work, cement shall be stored in a dry, weathertight, properly ventilated structure, with adequate provision for prevention of absorption of moisture.

b. Aggregate: Storage piles of aggregate shall afford good drainage, preclude inclusion of foreign matter, and preserve the gradation. Sufficient live storage shall be maintained to permit segregation of successive shipments, placement of concrete at required rate, and such procedures as heating, inspection, and testing.

G.3.6 Forms. Forms, complete with centering, cores, and molds, shall be constructed to conform to shape, form, line, and grade required, and shall be maintained sufficiently rigid to prevent deformation under load.

a. Design: Joints shall be leakproof and shall be arranged vertically or horizontally to conform to the pattern of the design. Forms placed on successive units for continuous surfaces shall be fitted to accurate alignment to assure a smooth completed surface free from irregularities. If adequate foundation for shores cannot be secured, trussed supports shall be provided. Temporary openings shall be arranged in wall forms and where otherwise required, to facilitate cleaning and inspection. Lumber once used in forms shall have nails withdrawn and surfaces to be exposed to concrete carefully cleaned before re-use. Forms shall be readily removable without hammering or prying against the concrete.

b. Form ties shall be of suitable design and adequate strength for the purpose. Bolts and rods which are to be completely withdrawn shall be coated with grease.

c. Joints: Corners and other exposed joints in more than one plane, unless otherwise indicated on the drawings or directed by the Contracting Officer, shall be beveled, rounded, or chamfered by moldings placed in the forms.

d. Coating: Forms for exposed surfaces shall be coated with oil before reinforcement is placed. Surplus oil on form surfaces and any oil on reinforcing steel shall be removed. Forms for surfaces not exposed to view may be thoroughly wet with water in lieu of oiling immediately before placing of concrete, except that in cold weather with probable freezing temperatures, oiling shall be mandatory.

e. Removal: Forms shall be removed only with approval of the Contracting Officer and in a manner to insure complete safety of the structure. Supporting forms or shoring shall not be removed until members have acquired sufficient strength to support safely their weight and any construction loads to which

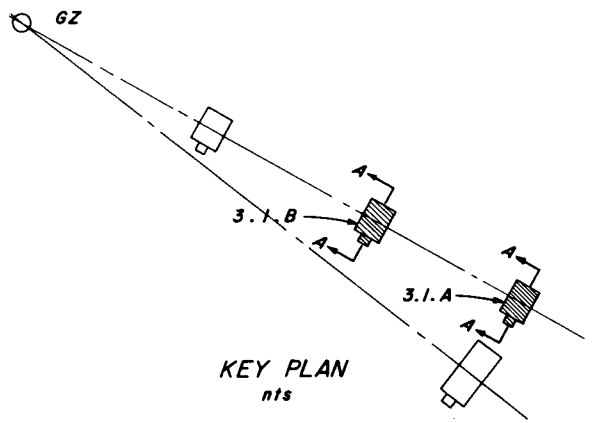

NOTES:
All pipe, 8" I.D.
All edges within pipe tract to be beveled.
Use thinnest wall section of Al. pipe deemed practical.
Responsibility of AE to finalize design and prepare construction drawings.
Contractor to provide bracing to support pipe during construction & backfill.
For additional details, Y&D drawing No. 774892 for Project 3.2 & 3.3.

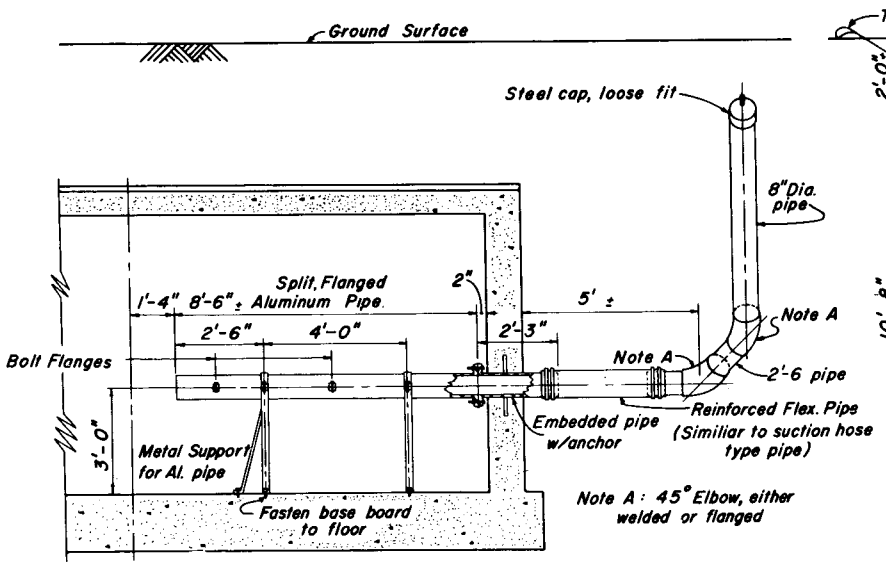

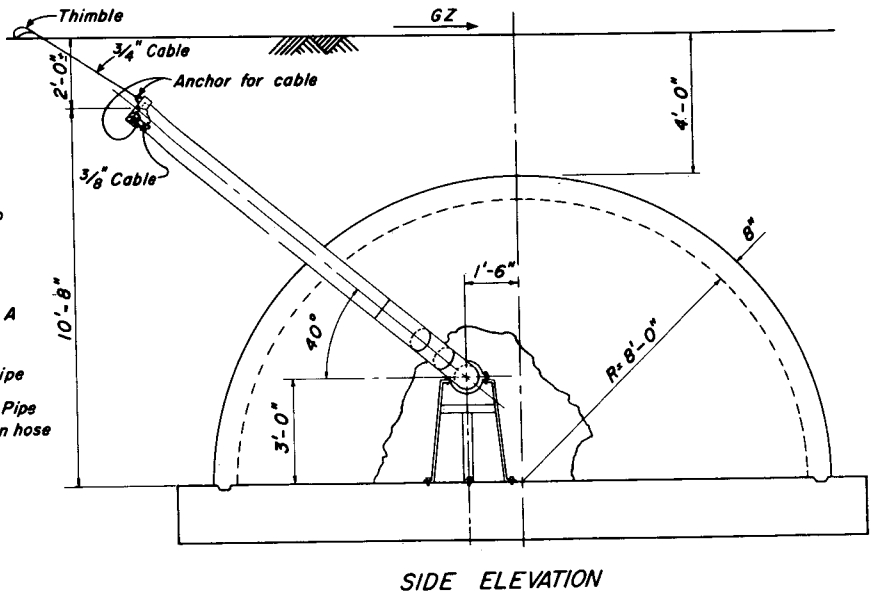

Scale 0 1 2 3 4 5 Feet

Figure G.3 Removal device for fission detector.

they may be subjected, but in no case shall they be removed in less than 6 days, nor shall forms used for curing be removed before expiration of curing period except as provided hereinafter under Section G.3.19, Curing. Care shall be taken to avoid spalling the concrete surface.

Results of suitable control tests will be used as evidence that concrete has attained sufficient strength to permit removal of supporting forms. Cylinders required for control tests shall be provided in addition to those otherwise required by this specification. Test specimens shall be removed from molds at end of 24 hours and stored in the structure as near points of sampling as possible, shall receive insofar as practicable the same protection from the elements during curing as is given those portions of the structure which they represent, and shall not be removed from the structures for transmittal to the laboratory prior to expiration of three fourths of the proposed period before removal of forms. In general, supporting forms or shoring shall not be removed until strength of control-test specimens has attained a value of at least 2,000 pounds. Care must be exercised to assure that the newly unsupported portions of the structure are not subjected to heavy construction or material loading.

Tie-rod clamps to be entirely removed from the wall shall be loosened 24 hours after concrete is placed, and form ties, except for a sufficient number to hold forms in place, may be removed at that time. Ties wholly withdrawn from wall shall be pulled toward inside face.

Holes left by bolts or tie rods shall be filled solid with cement mortar. Holes passing entirely through wall shall be filled from inside face with a device that will force the mortar through to outside face, using a stop held at the outside wall surface to insure complete filling. Holes which do not pass entirely through walls shall be packed full. Excess mortar at face of filled holes shall be struck off flush.

G.3.7 Reinforcing Steel. Reinforcing steel, fabricated to shapes and dimensions shown, shall be placed where indicated on drawings or required to carry out intent of drawings and specifications. Any changes shall be approved by the Contracting Officer and noted on the plans. Before being placed, reinforcement shall be thoroughly cleaned of rust, mill scale, or coating, including ice, that would reduce or destroy the bond. Reinforcement reduced in section shall not be used. Following any substantial delay in the work previously placed reinforcement left for future bonding shall be inspected and cleaned. Reinforcement shall not be bent or straightened in a manner injurious to the material. Bars with kinks or bends not shown on drawings shall not be placed. The heating of reinforcement for bending or straightening will be permitted only if entire operation is approved by the Contracting Officer. In slabs, beams, and girders, reinforcement shall be spliced only as shown on drawings except as approved by the Contracting Officer. At all points where bars lap or splice, including distribution reinforcement, a minimum lap of 30 bar diameters shall be provided, unless otherwise noted.

a. Design: Reinforcing details shown on the drawings shall govern the furnishing, fabrication, and placing of reinforcing steel. Except as otherwise shown on the drawings, or specified, construction shall conform to the following requirements:

(1) Concrete covering over steel reinforcement shall be not less than the following thickness:

Footings or other principal structural members in which concrete is deposited against the ground —3 inches between steel and ground.

Where concrete surfaces, after removal of forms, are exposed to weather or ground— 2 inches.

Where surfaces are not directly exposed to weather or ground— 1 inch.

(2) Steel in walls shall be as shown on the drawings. Splices shall be as shown, or shall be furnished for the approval of the Contracting Officer.

(3) Shop drawings: Shop detail and placing drawings for all reinforcing steel shall be furnished for approval of the Contracting Officer.

b. Supports: Reinforcement shall be accurately placed and securely tied at all intersections and splices with 18-gage black annealed wire, and shall be securely held in position during the placing of concrete by spacers, chairs, or other approved supports. Wire tie-ends shall point away from the form. Unless otherwise indicated on the drawings, or specified, the number, type, and spacing of supports shall conform to the ACI Detailing Manual (ACI 315). For slabs on grade (over earth or over drainage fill) and for footing reinforcement, bars shall be supported on precast concrete blocks, spaced at intervals required by size of reinforcement used, to keep reinforcement the minimum height specified above the underside of slab or footing.

G.3.8 Class of Concrete and Usage. Concrete shall be one class and shall be proportioned to provide a compressive strength at 28 days of 3,000 psi.

G.3.9 Proportioning of Concrete Mixes. Concrete shall be proportioned by weight.

a. Measurements: A one-cubic-foot bag of portland cement will be considered as 94 pounds in weight. One gallon of water will be considered as 8.33 pounds. Coarse aggregate shall be used in the greatest amount consistent with required workability, and shall be of the largest size suitable for the work and economically available.

b. Corrective additions to remedy deficiencies in aggregate gradations shall be used only with the written approval of the Contracting Officer. When such additions are permitted, the material shall be measured separately for each batch of concrete.

c. Control: The strength quality of the concrete proposed for use shall be established by tests made

in advance of the beginning of operations, using the consistencies suitable for the work. Trial design batches and testing shall be the responsibility of the contractor. Specimens shall be made and cured in accordance with ASTM Standard C-192 (CRD-C 10) and tests in accordance with ASTM Standard C-39 (CRD-C 14). A curve representing the relation between the water content and the average 28-day compressive strength, or earlier strength at which the concrete is to receive its full working load, shall be established for the compressive strength called for on the plans. The curve shall be established by at least three points, each point representing average values from at least four test specimens. The maximum allowable water content for the concrete for the structure shall be as determined from this curve and shall correspond to a strength 15 percent greater than indicated on the plans. The final proportions of the mix shall be determined by the Contracting Officer from the results of the trial mixes. The proportions so determined shall be adhered to unless otherwise directed by the Contracting Officer.

In the field, consistency shall be determined in accordance with CRD-C 5. The slump shall fall between 2 and 4 inches provided the required strength is obtained. The slump for nonvibrated concrete when approved by the Contracting Officer shall be from 3 to 6 inches. Should the specified strength not be obtained, the contractor will be required to vary the mixture sufficiently to meet the requirements but the maximum allowable water content specified shall not be exceeded.

G.3.10 Job-mixed Concrete, Batching and Mixing. Concrete shall be mixed by a mechanical batch-type mixing plant provided with adequate facilities for accurate measurement and control of each material entering the mixer and for changing the proportions to conform to varying conditions of the work. The mixing-plant assembly shall permit ready inspection of operations at all times. The plant and its location shall be subject to approval by the Contracting Officer.

a. Batching units shall be supplied with the following items:

(1) Weighing unit shall be provided for each type of material to indicate the scale load at convenient stages of the weighing operations. Weighing units shall be checked at times directed by and in the presence of the Contracting Officer, and required adjustments shall be made before further use.

(2) Water mechanism shall be tight, with the valves interlocked so that the discharge valves cannot be opened before the filling valve is fully closed, and shall be fitted with a graduated gage.

(3) Discharge gate shall control the mix to produce a ribboning and mixing of cement with aggregate. Delivery of materials from the batching equipment to the mixer shall be accurate within the following limits:

Material	Percentage by Weight	Material	Percentage by Weight
Cement	±1	Fine aggregate	±2
Water	±1	Coarse aggregate	±2

b. Mixing unit:

(1) Operation: Mixers shall not be charged in excess of rated capacity nor be operated in excess of rated speed. Excessive mixing, requiring addition of water to preserve required consistency, will not be permitted. The entire batch shall be discharged before recharging.

(2) Mixing time shall be measured from the instant water is introduced into the drum containing all solids. All mixing water shall be introduced before one fourth of the mixing time has elapsed. Mixing time for mixers of 1 yd^3 or less shall be $1\frac{1}{4}$ minutes; for mixers larger than 1 yd^3, mixing time shall be increased 15 seconds for each additional half cubic yard or fraction thereof.

(3) Discharge lock: Unless waived by the Contracting Officer, a device to lock the discharge mechanism until the required mixing time has elapsed shall be provided on each mixer.

G.3.11 Ready-mixed Concrete. Ready-mixed concrete may be used, unless disapproved by the Contracting Officer. Except for materials herein specified, ready-mixed concrete shall conform to ASTM Standard C 94 (CRD-C 31).

G.3.12 Construction Joints. Concrete shall be placed continuously so that the unit of operation will be monolithic in construction. At least 48 hours shall elapse between the casting of adjoining units, unless this requirement is waived by the Contracting Officer. Lifts shall terminate at such levels as are indicated on the drawings, or as conform to structural requirements, or as directed by the Contracting Officer. Special provision shall be made for jointing successive pours as detailed on drawings or required by the Contracting Officer.

G.3.13 Preparation for Placing. Water shall be removed from excavation before concrete is deposited. Any flow of water shall be diverted through proper side drains and shall be removed without washing over freshly deposited concrete. Hardened concrete, debris, and foreign materials shall be removed from interior of forms and from inner surfaces of mixing and conveying equipment. Reinforcement shall be secured in position, inspected, and approved by the Contracting Officer before pouring of concrete. Runways shall be provided for wheeled concrete-handling equipment; such equipment shall not be wheeled over reinforcement nor shall runways be supported on reinforcement.

G.3.14 Placing Concrete. The use of belt convey-

ors, chutes, or other similar equipment will not be permitted without written approval by the Contracting Officer. Concrete shall be handled from mixer or transport vehicle to place of final deposit in a continuous manner, as rapidly as practicable, and without segregation or loss of ingredients until the approved unit of operation is completed. Concrete that has attained its initial set or has contained its mixing water for more than 45 minutes shall not be placed in the work. Placing will not be permitted when, in the opinion of the Contracting Officer, the sun, heat, wind, or limitations of facilities furnished by the contractor prevent proper finishing and curing of the concrete. Forms or reinforcement shall not be splashed with concrete in advance of pouring. Concrete shall be placed in the forms as nearly as practicable in final position. Immediately after placing, concrete shall be compacted by thoroughly agitating in an approved manner. Tapping or other external vibration of forms will not be permitted. Concrete shall not be placed on concrete sufficiently hard to cause formation of seams and planes of weakness within the section. Concrete shall not be allowed to drop freely more than 5 feet in unexposed work nor more than 3 feet in exposed work; where greater drops are required, a tremie or other approved means shall be employed. The discharge of the tremies shall be controlled so that the concrete may be effectively compacted into horizontal layers not more than 12 inches thick, and the spacing of the tremies shall be such that segregation does not occur.

a. Placing temperature during cold weather: Concrete shall not be placed when the ambient temperature is below 35° F nor when the concrete without special protection is likely to be subjected to freezing temperature before final set has occurred. The temperature of the concrete when placed shall be not less than 40° F nor more than 60° F. Heating of the mixing water and/or aggregates will not be permitted until the temperature of the concrete has decreased to 45° F. Heated materials shall be free from ice, snow, and frozen lumps before entering the mixer. Methods and equipment for heating shall be subject to approval by the Contracting Officer. Suitable means shall also be provided for maintaining the concrete at a temperature of at least 40° F for not less than 72 hours after placing. Salt, chemicals, or other foreign materials shall not be mixed with the concrete to prevent freezing. Any concrete damaged by freezing shall be removed and replaced at the expense of the contractor.

b. Earth-foundation placement: Concrete footings shall be placed upon undisturbed clean surfaces, free from frost, ice, mud, and water. When the foundation is on dry soil or pervious material, waterproof sheathing paper shall be laid over earth surfaces to receive concrete.

c. Chute placement: When, upon written approval of the Contracting Officer, concrete is conveyed by chute, there shall be a continuous flow of concrete. The chute shall be of metal or metal-lined wood, with sections set at approximately the same slope; namely, not less than 1 vertical to 3 horizontal nor more than 1 vertical to 2 horizontal. The discharge end of the chute shall be provided with a baffle plate to prevent segregation. If the height of the discharge end of chute is more than 3 times the thickness of layer being deposited, but not more than 5 feet above surface of concrete in forms, a spout shall be used, and the lower end maintained as near surface of deposit as practicable. When pouring is intermittent, the chute shall discharge into a hopper. The chute shall be thoroughly cleaned before and after each run. Waste material and flushing water shall be discharged outside the forms.

d. Pump placement: Where concrete is conveyed and placed by pumping, the plant and equipment shall be approved by the Contracting Officer. Operation of pump shall be such that a continuous stream of concrete without air pockets is produced. When pumping is completed, concrete to be used remaining in pipeline shall be ejected without contamination of concrete or separation of ingredients. After each operation, equipment shall be thoroughly cleaned, and debris and flushing water shall be washed outside forms.

G.3.15 Compaction. Concrete shall be placed in layers not over 12 inches deep. Each layer shall be compacted by mechanical internal-vibrating equipment supplemented by hand spading, rodding, and tamping as directed by the Contracting Officer. Vibrators shall in no case be used to transport concrete inside forms. Use of form vibrators will not be permitted. Internal vibrators shall maintain a speed of not less than 6,000 impulses per minute when submerged in the concrete. Duration of vibration shall be limited to time necessary to produce satisfactory consolidation without causing objectionable segregation and shall be at least 20 seconds psf of exposed surface. The vibrator shall not be inserted into lower courses that have begun to set. Vibrators shall be applied at uniformly spaced points not farther apart than the visible effectiveness of the machine.

G.3.16 Bonding and Grouting. Before depositing new concrete on or against concrete that has set, existing surfaces shall be thoroughly roughened and cleaned of laitance, foreign matter, and loose particles. Forms shall be re-tightened and existing surfaces slushed with a grout coat consisting of cement and fine aggregate in the same proportions as concrete to be placed. New concrete shall be placed before the grout has attained initial set. Horizontal construction joints shall be given a brush coat of grout consisting of cement and fine aggregate in same proportion as concrete to be placed, followed by approximately 3 inches of concrete of regular mix except that the proportion of coarse aggregate shall be reduced 50 percent. Grout for setting metal items shall be composed of equal parts of sand and portland cement, with water sufficient to produce required

consistency.

G.3.17 Slabs on Grade. Any fill indicated or required to raise the subgrade shall be installed as specified under Section G.1, EXCAVATION, FILLING, AND BACKFILLING. Concrete shall be compacted, screeded to grade, and prepared for the specified finish.

G.3.18 Concrete Floor Finish. Concrete floor slabs shall be screeded and wood floated to the required level of the finished floors, as shown on the drawings.

G.3.19 Curing. Curing shall be accomplished by preventing loss of moisture, rapid temperature change, and mechanical injury or injury from rain or flowing water for a period of 7 days when normal portland cement has been used or 3 days when high-early-strength portland cement has been used. Curing shall be started as soon after placing and finishing as free water has disappeared from the surface of the concrete. Curing may be accomplished by any of the following methods or combination thereof, as approved by the Contracting Officer.

a. Moist curing: Unformed surfaces shall be covered with burlap, cotton, or other approved fabric mats, or with sand and shall be kept continually wet. Forms shall be kept continually wet and if removed before the end of the curing period, curing shall be continued as on unformed surfaces, using suitable materials. Burlap shall be used only on surfaces which will be unexposed in the finished work and shall be in two layers.

b. Waterproof-paper curing: Surfaces shall be covered with waterproof paper lapped 4 inches at edges and ends and sealed. Paper shall be weighted to prevent displacement, and tears or holes appearing during the curing period shall be immediately repaired by patching.

c. Membrane curing: Membrane curing compound shall be applied by power spraying equipment using a spray nozzle equipped with a wind guard. The compound shall be applied in a two-coat, continuous operation at a coverage of not more than 200 ft^2/gal for both coats. When application is made by hand sprayers, the second coat shall be applied in a direction approximately at right angles to the direction of the first coat. The compound shall form a uniform, continuous, adherent film that shall not check, crack, or peel, and shall be free from pinholes or other imperfections. Surfaces subjected to heavy rainfall within 3 hours after compound has been applied or surface damaged by subsequent construction operations within the curing period shall be resprayed at the rate specified above. Surfaces coated with curing compound shall be kept free of foot and vehicular traffic and other sources of abrasion during the curing period.

G.4 MISCELLANEOUS METALWORK

The work covered by this section of the specification consists in furnishing all plant, labor, equipment appliances, and materials, and in performing all operations in connection with the installation of miscellaneous metalwork, complete, including all shelf angles attached to the concrete, all steel hatches, all pipe sleeves, inserts, and anchor bolts, and miscellaneous bars, plates, and other accessories necessary for the completion of the work in strict accordance with this section of the specifications and the applicable drawings, and subject to the terms and conditions of the contract.

G.4.1 Applicable Specifications and Codes. The following specifications and codes form a part of this specification:

a. Federal Specifications:
QQ-S-741 and Am-3 Steel, Structural (including Welding) and Rivet; (for) Bridges and Buildings.
WW-P-406 and Am-1 Pipe; Steel and Ferrous-Alloy (for) Ordinary Uses (Iron-Pipe Size). (CRD-C 529).
TT-P-86A Type I and II Red Lead Primer.
TT-A-468A Type II Class B Aluminum Pigment.
TT-V-81B Type II Class B Varnish, Mixing.

b. American Institute of Steel Construction Publications:
Code of Standard Practice for Steel Buildings and Bridges.
Specification for the Design, Fabrication and Erection of Structural Steel for Buildings.

c. American Welding Society Code:
Arc and Gas Welding in Building Construction.

G.4.2 General.

a. Shop drawings: Shop drawings of all items of miscellaneous metalwork shall be submitted to the Contracting Officer for approval. Material fabricated or delivered to the site before the approved shop drawings have been received by the contractor shall be subject to rejection by the Contracting Officer.

b. Mill reports: The contractor shall furnish, without extra cost to the Government, two certified copies of all mill reports covering the chemical and physical properties of the steel used in the work under this specification.

c. Substitutions: Substitutions of sections, or modifications of details, or both, shall be made only when approved by the Contracting Officer providing, however, the strength and stiffness shall be at least equal to the original design.

d. Responsibility for errors: The contractor alone shall be responsible for all errors of fabrication and for the correct fitting of the structural members shown on the shop drawings.

G.4.3 Materials.

a. Structural steel: Structural steel shall conform to the requirements of Federal Specifications QQ-S-

741 and Am-3, Type I or II, Grade B, Class 1.

b. Anchor bolts: All anchor bolts shall conform to the requirements for structural steel.

c. Sleeves: Pipe sleeves for anchor bolts shall conform to the requirements of Federal Specification WW-P-406 and Am-1 (CRD-C 529).

d. Manhole rungs: Manhole rungs shall be Hohmann and Barnard, Inc., 204 East 33rd Street, New York City, Style P or equal.

G.4.4 Fabrication. Insofar as possible, work shall be fitted and shop assembled, ready for erection. Work shall conform to the drawings, details, and approved shop drawings. Shop and field connections shall be welded, attached with screws, and similar fastenings, all in accordance with a high standard of workmanship for the class of work concerned, and as approved by the Contracting Officer. Jointing and intersections shall be accurately made in true planes, tightly fitted and drawn up, welded, and dressed smooth.

a. Galvanizing: Wherever galvanizing is called for on the drawings the metal shall be hot-dip galvanized after fabrication, using not less than 2 ounces of zinc per square foot of surface area in conformance with the current ASTM Specification A-123. All parts to be galvanized shall be thoroughly cleaned and pickled before galvanizing.

b. Miscellaneous: Items not specifically referred to above shall be furnished, constructed, and installed as shown on the drawings or as approved by the Contracting Officer.

c. Escape hatch door: The escape hatch door and all miscellaneous accessories shall be fabricated and installed as shown on the design drawings.

G.4.5 Inspection and Tests. The material to be furnished under this specification shall be subject to inspection and tests in the mill, shop, and field by authorized Government inspectors. Inspection and tests will be conducted without expense to the contractor; however, inspection in the mill or shop shall not relieve the contractor of his responsibility to reject any material at any time before final acceptance of the building when, in the opinion of the Contracting Officer, the materials and workmanship do not conform to the specification requirements. Test specimens shall be made of sufficient number to determine the average yield point stress for the various structures.

G.4.6 Design. The design of members and connections for all portions of the structure are indicated on the drawings. In the event that it is deemed necessary to modify or change any member or connections such design drawings shall be submitted to the Contracting Officer for approval before any material is fabricated. Subsequent to approval by the Contracting Officer, no changes or modifications shall be made without his consent.

G.4.7 Painting. All iron and steelwork except that which is shown or specified as galvanized shall be cleaned of all dirt, scale, and rust and shall be given one shop coat of red lead in oil primer conforming to Federal Specification TT-P-86A Type I or II. After erection all abraded surfaces shall be touched up with shop paint.

REFERENCES

1. L.J. Vortman; "Effects of an Atomic Explosion on Group- and Family-type Personnel Shelters"; Projects 34.1 and 34.3, Operation Teapot, WT-1161, January 1957; Sandia Corporation, Albuquerque, New Mexico; Secret, Restricted Data.

2. C.L. Hayen; "U.S. Navy Structures"; Annex 3.2, Operation Greenhouse, WT-91, 8 April 1955; Bureau of Yards and Docks, Navy Department, Washington 25, D.C.; Secret, Security Information.

3. R.M. Longmire and L.D. Mills; "Navy Structures"; Projects 3.11-3.16, Operation Upshot-Knothole, WT-729, May 1955; Bureau of Yards and Docks, Department of the Navy, Washington 25, D.C.; Confidential, Restricted Data.

4. R.B. Vaile, Jr. and L.D. Mills; "Evaluation of Earth Cover as Protection to Aboveground Structures"; Project 3.6, Operation Teapot, WT-1128, December 1956; Bureau of Yards and Docks, Department of the Navy, Washington 25, D.C.; Confidential, Restricted Data.

5. "The Design of Structures to Resist the Effects of Atomic Weapons"; EM 1110-345-414 to 421, 15 March 1957; Massachusetts Institute of Technology, for Office of the Chief of Engineers, U.S. Army, Washington, D.C.; Unclassified.

6. N.M. Newmark, G.K. Sinnamon, and F. Matsuda; "Air Blast Effects on Underground Structures"; Project 3.4, Operation Teapot WT-1127, May 1955; for Office, Chief of Engineers, U.S. Army, Washington, D.C.; Confidential, Restricted Data.

7. N.M. Newmark and G.K. Sinnamon; "Air Blast Effects on Underground Structures"; Project 3.8, Operation Upshot-Knothole, WT-727, January 1954; for Office, Chief of Engineers, U.S. Army, Washington 25, D.C.; Confidential, Restricted Data.

8. D.T. Robbins; "Analysis Report for Basic Types of Underground Structures"; Contract No. DA-22-079-eng-196 with Holmes and Narver, Inc., October 1956; U.S. Army Engineers Waterways Experiment Station, Corps of Engineers, Vicksburg, Mississippi; Secret, Restricted Data.

9. N.M. Newmark; "Vulnerability of Arches - Preliminary Notes"; Revised 21 May 1956; University of Illinois; Unpublished; Unclassified.

10. E. Cohen; "Design Report for Three Basic Types of Underground Structures"; Contract No. DA-22-079-eng-195 with Ammann and Whitney, Consulting Engineers, August 1956; U.S. Army Engineers Waterways Experiment Station, Corps of Engineers, Vicksburg, Mississippi; Unclassified.

11. T.B. Goode and others; "Soil Survey and Backfill Control in Frenchman Flat"; Draft Manuscript, Project 3.8, Operation Plumbbob, WT-1427, 27 November 1957; U.S. Army Engineer Waterways Experiment Station, Corps of Engineers, Vicksburg, Mississippi; Unclassified.

12. J.W. Wistor and W.R. Perret; "Ground Motion Studies at High Incident Overpressure"; Project 1.5, Operation Plumbbob, ITR-1405, 11 October 1957; Sandia Corporation, Albuquerque, New Mexico; Confidential, Formerly Restricted Data.

13. W.J. Flathau and R.A. Cameron; "Damage to Existing EPG Structures"; Project 3.7, Operation Hardtack, ITR-1631, June 1958; U.S. Army Engineer Waterways Experiment Station, Corps of Engineers, Vicksburg, Mississippi, and Holmes and Narver, Inc., Los Angeles, California; Secret, Formerly Restricted Data.

14. "Capabilities of Atomic Weapons"; Department of the Army Technical Manual TM 23-200, Revised Edition, November 1957; Confidential.

15. D.T. Robbins and R.A. Williamson; "Post-Shot Analysis for Project 3.1, Operation Plumbbob"; Contract No. DA-22-079-eng-196, Modification No. 3, with Holmes and Narver, Inc., April 1958; U.S. Army Engineer Waterways Experiment Station, Corps of Engineers, Vicksburg, Mississippi; Confidential.

16. N. M. Newmark; "Recommended FCDA Specifications for Blast Resistant Structural Design - Method A"; Preliminary, 9 August 1957; Unclassified.

17. N. M. Newmark; "Designing for Atomic Blast Protection"; Proceedings of the Structural Engineers Association of California, Twenty-fifth Annual Convention, Reno, Nevada, October 1956; Unclassified.

18. J. J. Meszaros, H. S. Burden, and J. D. Day; "Instrumentation of Structures for Air-Blast and Ground-Shock Effects"; Project 3.7, Operation Plumbbob, ITR-1426, 6 December 1957; Ballistic Research Laboratories, Aberdeen Proving Ground, Maryland; Unclassified.

19. L. M. Swift, D. C. Sachs, and F. M. Sauer; "Ground Acceleration, Stress, and Strain at High Incident Overpressures"; Project 1.4, Operation Plumbbob, ITR-1404, 11 October 1957; Stanford Research Institute, Menlo Park, California; Confidential, Formerly Restricted Data.

20. A. P. Flynn; "FCDA Family Shelter Evaluation"; Project 9.1a, Operation Buster, WT-359, March 1952; Confidential, Formerly Restricted Data.

21. J. R. Hendrickson and others; "Shielding Studies"; Project 2.7, Operation Teapot, WT-1121, February 1957; Chemical Warfare Laboratories, Army Chemical Center, Maryland; Secret, Restricted Data.

22. Theodore Rockwell, III; "Reactor Shielding Design Manual"; AEC-TID 7004, USAEC, March 1956, page 261 ff; Unclassified.

23. R. G. Larrick and others; "Gamma Exposure versus Distance"; Project 2.1, Operation Teapot, ITR-1115, May 1955; Confidential, Formerly Restricted Data.

24. M. Ehrlich; "Photographic Dosimetry of X- and Gamma Rays"; Handbook 57, August 1954, page 10; U. S. Department of Commerce, National Bureau of Standards; Unclassified.

25. M. Ehrlich and S. H. Fitch; "Photographic X- and Gamma Ray Dosimetry"; Nucleonics, September 1951, Vol. 9, No. 3, pages 5-17; McGraw-Hill Publishing Company, Inc.; Unclassified.

26. S. C. Sigoloff; "Fast Neutron Insensitive Gamma Ray Dosimeters, the AC and ACTE Systems"; in Press; School of Aviation Medicine, USAF, San Antonio, Texas; Unclassified.

27. G. V. Taplin and others; "Measurement of Initial and Residual Radiations by Chemical Methods"; Project 39.6, Operation Teapot, ITR-1171; Secret, Restricted Data.

28. D. L. Rigotti, H. O. Funsten, and J. W. Kinch; "Neutron Flux from Selected Nuclear Devices"; Project 2.3, Operation Plumbbob, ITR-1412, March 1958; Secret, Restricted Data.

29. I. G. Bowen, A. F. Strehler, and M. B. Wetherbe; "Distribution and Density of Missiles from Nuclear Explosions"; Project 33.4, Operation Teapot, WT-1168, March 1956; Civil Effects Test Group, Washington, D. C.; Unclassified.

30. Hans Desega; "Experimental Investigations of the Action of Dust"; Chap. XIII-B, pages 1188-1203, German Aviation Medicine World War II, Vol. II, 1950; U. S. Government Printing Office, Washington, D. C.; Unclassified.

31. S. Ruff; "Brief Acceleration"; Chapter VI-C in German Aviation Medicine, World War II, pages 584-597, 1950; U. S. Government Printing Office, Washington, D. C.

DISTRIBUTION

Military Distribution Category 32

ARMY ACTIVITIES

1 Deputy Chief of Staff for Military Operations, D/A, Washington 25, D.C. ATTN: Dir. of SW&R
2 Chief of Research and Development, D/A, Washington 25, D.C. ATTN: Atomic Div.
3 Chief of Engineers, D/A, Washington 25, D.C. ATTN: ENGNB
4 Chief of Engineers, D/A, Washington 25, D.C. ATTN: ENGEB
5 Chief of Engineers, D/A, Washington 25, D.C. ATTN: ENGTB
6- 7 Office, Chief of Ordnance, D/A, Washington 25, D.C. ATTN: ORDTN
8 Chief of Transportation, D/A, Office of Planning and Int., Washington 25, D.C.
9- 11 Commanding General, U.S. Continental Army Command, Ft. Monroe, Va.
12 Director of Special Weapons Development Office, Headquarters CONARC, Ft. Bliss, Tex. ATTN: Capt. Chester I. Peterson
13 President, U.S. Army Artillery Board, U.S. Continental Army Command, Ft. Sill, Okla.
14 President, U.S. Army Air Defense Board, U.S. Continental Army Command, Ft. Bliss, Tex.
15 Commandant, U.S. Army Command & General Staff College, Ft. Leavenworth, Kansas. ATTN: ARCHIVES
16 Commandant, U.S. Army Air Defense School, Ft. Bliss, Tex. ATTN: Dept. of Tactics and Combined Arms
17 Commandant, U.S. Army Armored School, Ft. Knox, Ky.
18 Commandant, U.S. Army Artillery and Missile School, Ft. Sill, Okla. ATTN: Combat Development Department
19 Commandant, U.S. Army Aviation School, Ft. Rucker, Ala.
20 Commandant, U.S. Army Infantry School, Ft. Benning, Ga. ATTN: C.D.S.
21 Commanding General, Chemical Corps Training Comd., Ft. McClellan, Ala.
22 Commandant, USA Transport School, Ft. Eustis, Va. ATTN: Security and Info. Off.
23 Commanding General, The Engineer Center, Ft. Belvoir, Va. ATTN: Asst. Cmdt, Engr. School
24 Director, Armed Forces Institute of Pathology, Walter Reed Army Med. Center, 625 16th St., NW, Washington 25, D.C.
25 Commanding Officer, Army Medical Research Lab., Ft. Knox, Ky.
26 Commandant, Walter Reed Army Inst. of Res., Walter Reed Army Medical Center, Washington 25, D.C.
27- 28 Commanding Officer, Chemical Warfare Lab., Army Chemical Center, Md. ATTN: Tech. Library
29 Commanding General, Engineer Research and Dev. Lab., Ft. Belvoir, Va. ATTN: Chief, Tech. Support Branch
30 Director, Waterways Experiment Station, P.O. Box 631, Vicksburg, Miss. ATTN: Library
31- 32 Commanding General, Aberdeen Proving Grounds, Md. ATTN: Director, Ballistics Research Laboratory
33 Commanding General, Ordnance Ammunition Command, Joliet, Ill.
34 Director, Operations Research Office, Johns Hopkins University, 6935 Arlington Rd., Bethesda 14, Md.
35 Commander-in-Chief, U.S. Army Europe, APO 403, New York, N.Y. ATTN: Opot. Div., Weapons Br.

NAVY ACTIVITIES

36 Chief of Naval Operations, D/N, Washington 25, D.C. ATTN: OP-03EG
37 Chief of Naval Operations, D/N, Washington 25, D.C. ATTN: OP-36
38- 39 Chief of Naval Research, D/N, Washington 25, D.C. ATTN: Code 811
40 Chief, Bureau of Ordnance, D/N, Washington 25, D.C.
41 Chief, Bureau of Ships, D/N, Washington 25, D.C. ATTN: Code 423
42 Chief, Bureau of Yards and Docks, D/N, Washington 25, D.C. ATTN: D-440
43 Director, U.S. Naval Research Laboratory, Washington 25, D.C. ATTN: Mrs. Katherine H. Cass
44- 45 Commander, U.S. Naval Ordnance Laboratory, White Oak, Silver Spring 19, Md.
46- 47 Commanding Officer, U.S. Naval Radiological Defense Laboratory, San Francisco, Calif. ATTN: Tech. Info. Div.
48- 50 Officer-in-Charge, U.S. Naval Civil Engineering R&E Lab., U.S. Naval Construction Bn. Center, Port Hueneme, Calif. ATTN: Code 753
51 Commanding Officer, U.S. Naval Schools Command, U.S. Naval Station, Treasure Island, San Francisco, Calif.
52 Superintendent, U.S. Naval Postgraduate School, Monterey, Calif.
53 Officer-in-Charge, U.S. Naval School, CEC Officers, U.S. Naval Construction Bn. Center, Port Hueneme, Calif.
54 Commanding Officer, Nuclear Weapons Training Center, Atlantic, U.S. Naval Base, Norfolk 11, Va. ATTN: Nuclear Warfare Dept.
55 Commanding Officer, Nuclear Weapons Training Center, Pacific, Naval Station, San Diego, Calif.
56 Commanding Officer, U.S. Naval Damage Control Tng. Center, Naval Base, Philadelphia 12, Pa. ATTN: ABC Defense Course
57 Commanding Officer, U.S. Naval Medical Research Institute, National Naval Medical Center, Bethesda, Md.
58 Commanding Officer and Director, David W. Taylor Model Basin, Washington 7, D.C. ATTN: Library
59 Commander, Norfolk Naval Shipyard, Portsmouth, Va. ATTN: Underwater Explosions Research Division
60- 63 Commandant, U.S. Marine Corps, Washington 25, D.C. ATTN: Code A03H
64 Commanding Officer, U.S. Naval CIC School, U.S. Naval Air Station, Glynco, Brunswick, Ga.

AIR FORCE ACTIVITIES

65 Assistant for Atomic Energy, HQ, USAF, Washington 25, D.C. ATTN: DCS/O
66 Deputy Chief of Staff, Operations HQ. USAF, Washington 25, D.C. ATTN: Operations Analysis
67 Director of Civil Engineering, HQ. USAF, Washington 25, D.C. ATTN: AFOCE
68- 69 Assistant Chief of Staff, Intelligence, HQ. USAF, Washington 25, D.C. ATTN: AFCIN-IB2
70 Director of Research and Development, DCS/D, HQ. USAF, Washington 25, D.C. ATTN: Guidance and Weapons Div.
71 The Surgeon General, HQ. USAF, Washington 25, D.C. ATTN: Bio.-Def. Pre. Med. Division
72 Commander-in-Chief, Strategic Air Command, Offutt AFB, Neb. ATTN: OAWS
73 Commander, Tactical Air Command, Langley AFB, Va. ATTN: Doc. Security Branch
74 Commander, Air Defense Command, Ent AFB, Colorado. ATTN: Atomic Energy Div., ADLAN-A
75 Commander, Hq. Air Research and Development Command, Andrews AFB, Washington 25, D.C. ATTN: RDRWA
76 Commander, Air Force Ballistic Missile Div., HQ. ARDC, Air Force Unit Post Office, Los Angeles 45, Calif. ATTN: WDSOT
77- 78 Commander, AF Cambridge Research Center, L. G. Hanscom Field, Bedford, Mass. ATTN: CRQST-2
79- 83 Commander, Air Force Special Weapons Center, Kirtland AFB, Albuquerque, N. Mex. ATTN: Tech. Inf. & Intel. Div.
84- 85 Director, Air University Library, Maxwell AFB, Ala.
86 Commander, Lowry AFB, Denver, Colorado. ATTN: Dept. of Sp. Wpns. Tng.

87 Commandant, School of Aviation Medicine, USAF, Randolph AFB, Tex. ATTN: Research Secretariat
88 Commander, 1009th Sp. Wpns. Squadron, HQ. USAF, Washington 25, D.C.
89- 91 Commander, Wright Air Development Center, Wright-Patterson AFB, Dayton, Ohio. ATTN: WCOSI
92- 93 Director, USAF Project RAND, VIA: USAF Liaison Office, The RAND Corp., 1700 Main St., Santa Monica, Calif.
94 Commander, Rome Air Development Center, ARDC, Griffiss AFB, N. Y. ATTN: The Documents Library RCSSLD
95 Assistant Chief of Staff, Intelligence, HQ. USAFE, APO 633, New York, N.Y. ATTN: Directorate of Air Targets
96 Commander-in-Chief, Pacific Air Forces, APO 953, San Francisco, Calif. ATTN: PFCIE-MB, Base Recovery

OTHER DEPARTMENT OF DEFENSE ACTIVITIES

97 Director of Defense Research and Engineering, Washington 25, D.C. ATTN: Tech. Library
98 Chairman, Armed Services Explosives Safety Board, DOD, Building T-7, Gravelly Point, Washington 25, D.C.
99 Director, Weapons Systems Evaluation Group, Room 1E880, The Pentagon, Washington 25, D.C.
100-107 Chief, Armed Forces Special Weapons Project, Washington 25, D.C.
108 Commander, Field Command, AFSWP, Sandia Base, Albuquerque, N. Mex.
109 Commander, Field Command, AFSWP, Sandia Base, Albuquerque, N. Mex. ATTN: FCTG
110-114 Commander, Field Command, AFSWP, Sandia Base, Albuquerque, N. Mex. ATTN: FCWT
115 Administrator, National Aeronautics and Space Administration, 1520 "H" St., N.W., Washington 25, D.C. ATTN: Mr. R. V. Rhode
116 U.S. Documents Officer, Office of the United States National Military Representative - SHAPE, APO 55, New York, N.Y.

ATOMIC ENERGY COMMISSION ACTIVITIES

117-119 U.S. Atomic Energy Commission, Technical Library, Washington 25, D.C. ATTN: For DMA
120-121 Los Alamos Scientific Laboratory, Report Library, P.O. Box 1663, Los Alamos, N. Mex. ATTN: Helen Redman
122-126 Sandia Corporation, Classified Document Division, Sandia Base, Albuquerque, N. Mex. ATTN: H. J. Smyth, Jr.
127-129 University of California Radiation Laboratory, P.O. Box 808, Livermore, Calif. ATTN: Clovis G. Craig
130 Weapon Data Section, Technical Information Service Extension, Oak Ridge, Tenn.
131-165 Technical Information Service Extension, Oak Ridge, Tenn. (Surplus)